UNIVERSITY OF SOUTHAMPTON

Glial control of neurogenesis in rodent models of epilepsy

By
Matthew Paul Sadgrove

A thesis submitted for the degree of PhD

School of Medicine
Division of Clinical Neuroscience

October 2003

UNIVERSITY OF SOUTHAMPTON

ABSTRACT

FACULTY OF MEDICINE, HEALTH AND BIOLOGICAL SCIENCE

CLINICAL NEUROSCIENCE

Doctor of Philosophy

GLIAL CONTROL OF NEUROGENESIS IN RODENT MODELS OF EPILEPSY

By Matthew Paul Sadgrove

Epilepsy is a condition that affects about 1:200 people. Its cause is poorly understood and currently there are no drug therapies that modify disease progression. Mesial Temporal lobe epilepsy is the most common form of epilepsy where seizures arise from the hippocampus. The formation of new neurons (neurogenesis) from progenitor cells in the dentate gyrus of the hippocampus occurs throughout life, and is important for laying down memory. Seizures have been shown to increase this neurogenesis, although the functional role of this increase is unknown, it has been proposed as either a native repair mechanism or part of the progression to epilepsy.

The aim of this thesis is to investigate the control of dentate neurogenesis, especially after seizure, and to identify the principle cells involved in these processes. I have used a combination of in vivo and in vitro techniques to investigate the mechanisms and control of seizure induced dentate neurogenesis, chemoconvulsant kainate was used to induce seizures in all seizure models, maximizing the potential for comparison between experiments.

Initial in vitro work established conditions in which cell death and proliferation could be accurately and reproducibly quantified in organotypic hippocampal slice cultures. Subsequent experiments established that in immature tissue kainate induced cell death, followed by increased neurogenesis.

In vivo experiments in adult rats using a 'clonal' BrdU labelling technique, where a cohort of cells labelled prior to seizure induction were followed in recovery, found that the prelabelled cohort contributed less to seizure induced cell proliferation than the cohort of cells that were not dividing prior to seizures implying the recruitment of an additional dividing cell population by seizures.

Astrocytes with a radial glial like morphology are putative stem cells for dentate neurogenesis. To test our recruitment hypothesis, I used transgenic mice expressing enhanced green fluorescent protein under the hGFAP promoter to readily identify a subset of the radial glial like cells, and found their proliferation was selectively increased (10 fold vs. 2.5 fold overall increase in proliferation) in response to seizures.

The data obtained suggest that seizures result in either death or inactivation of a progenitor cell population with a consequent recruitment of either quiescent or slowly dividing stem cells, which divide to replenish the progenitor cell population and restore neurogenesis. This work also identifies GFAP expressing cells with a radial glial morphology as a quiescent stem cell population selectively recruited to divide by brain injury due to seizures, and is the first report of recruitment of an identified stem cell population in the dentate after brain injury.

Contents

Figures and tables

Acknowledgements

I would like to gratefully acknowledge the wit, patience and guidance of my supervisor Liam Gray in keeping me on the relatively straight and narrow. Owain and Chris for tolerating my incessant blithering. Ash for teaching me the organotypic technique, and Emma for 'surgical' instruction. Terry for being constantly enthused about science, suffering my odious presence for 4 years, and for staying in the UK to print the thesis when I disappeared. As its 7:30 pm and this is already late apologies to anyone (not that anyone will read this) not included individually, but thanks to the rest of Clinical Neurosciences for making another 4 years in Southampton at least tolerable (no small feat). And because they will read this, thanks to mummy and daddy, for … well being them.

Abbreviations

$5HT_{1A}$	Serotonin 1A receptor
abs	absorbance
AMPA	alpha-amino-3-hydroxy-5-methylisoxazole-4-propionic acid
ANOVA	analysis of variance
AP	anterior-posterior
AP-ABC	alkaline phosphatase conjugated Streptavidin-biotin complex
bFGF	basic fibroblast growth factor
BrdU	5-Bromo-2'-deoxyUridine
CA	Cornu Ammonis
c_{em}	number of cells derived using an exponential model
c_{ssm}	number of cells derived using a steady state model
C_t	number of cells generated in a given time
contra	contralateral
DAB	3,3-Diaminobenzene
DAPI	4',6-diamidino-2-phenyindole
Dcx	doublecortin
DG	dentate gyrus
DV	dorso-ventral
ECT	electroconvulsive therapy
EGFP	enhanced green fluorescent protein
em	emission
E*x*	embryonic day (where *x* is the day)
ex	excitation
FGF	fibroblast growth factor
FJB	Fluoro-Jade B
G-phase	gap phase of cell cycle
GABA	gamma-aminobutyric acid
GAP-43	growth-associated protein
GCL	granule cell layer
GFAP	glial fibrillary acidic protein
HBSS	Hank's balanced salt solution
HRP-ABC	Horseradish peroxidase conjugated Streptavidin-biotin complex
HS	horse serum based medium
HVC	higher vocal centre
ICV	intra cerebroventricular
IH	intra hippocampal
IP	intra peritoneal
ipsi	ipsilateral

LD	lethal dose
LTP	long term potentiation
M-phase	mitosis phase of cell cycle
MAG	myelin-associated glycoprotein
MAM	methylazoxymethanol
MAP-2	microtubule-associated protein-2
MEM	minimum essential medium
ML	midline
n	number of cell cycles
N	neuron
NB	Neurobasal™ based medium
N_B	number of BrdU positive cells
N_D	number of dividing cells
NeuN	neuronal nuclei
Neuro-D	neuronal determining factor
NMDA	N-methyl-D-aspartate
NSE	neuron-specific enolase
NSF	novelty-suppressed feeding
OHSC	organotypic hippocampal slice culture
P	progenitor
PBS	phosphate buffered saline
PBS-TS	PBS containing 0.1% triton and 0.05% Bovine Serum Albumin
PFA	paraformaldehyde
PI	propidium iodide
PSA-NCAM	polysialylated neural cell adhesion molecule
P*x*	postnatal day (where *x* is the day)
RG	radial glial
RG-EGFP	radial glial cells that are EGFP positive
RG-s100b	s100b positive cells, exhibiting a radial glial morphology
ROI	region of interest
S	stem cell
SD	standard deviation
SEM	standard error of mean
S-phase	synthesis phase of cell cycle
SGZ	sub granular zone
SSRI's	selective serotoinin reuptake inhibitors
SVZ	subventricular zone
t	time
T_B	duration of BrdU labelling pulse
TBI	traumatic brain injury
TBS	Tris-Buffered Saline

TBS-TS	TBS containing 0.1% triton and 0.05% Bovine Serum Albumin
T_C	cell cycle time
T_I	BrdU labelling time required before BrdU can be detected in a cell
T_S	length of S-phase of cell cycle
TUC-4	TOAD/Ulip/CRMP protein family
TUNEL	TdT-mediated dUTP-biotin nick end labelling
UOP	unoperated control group

Chapter 1

General Introduction

1 Introduction

'New neurons are continuously produced in the adult brain.' This is a statement that is only recently gaining widespread acceptance within the scientific community. Historically the brain was considered as a fully formed organ at birth, with subsequent experiences resulting in modification of the circuits within the brain and using up more capacity – presumably until the brain became 'full', with the loss of brain cells being permanent. However, over 35 years ago, Joseph Altman first demonstrated the existence of cells within the adult rat brain which are actively dividing and which subsequently become neurons (Altman and Das, 1965). In the last 10 years research in this field has expanded rapidly and adult neurogenesis has now been demonstrated in among others birds (Barnea and Nottebohm, 1994), new world primates (Gould, et al., 1998), old world primates (Kornack and Rakic, 1999) and humans (Eriksson, et al., 1998).

1.1 Stem cells, Progenitor cells and terminally differentiated cells

While adult neurogenesis has been observed in many species, this does not mean that all cells in the brain have the capacity to divide. In fact the cell types in the brain that can produce new cells are limited and relatively scarce (Temple and Alvarez-Buylla, 1999). Neurons themselves are considered terminally differentiated cells, that is they are unable to divide further and thus they cannot contribute directly to adult neurogenesis (they may however provide signals to other cells that neurogenesis is required). In terms of potential to divide embryonic stem cells are the extreme opposite to neurons; these cells can replicate themselves (proliferate) and form any other cell type (differentiate). Proliferation can be either symmetric producing two identical copies of the parent cell or asymmetric maintaining the parent cell and producing a different daughter cell. Cell division can be either proliferative or differentiative (Lukaszewicz, et al., 2002) with either expansion of the stem cell population or one or both daughter cells adopting a more mature phenotype. All stem cells can by definition both proliferate and differentiate and are often referred to as pluripotent cells. That is not to say that stem cells have to be permanently in the cell cycle, they may be able to remain quiescent or be removed from the brain by

programmed cell death (apoptosis). The latter pathway is the probable fate of most stem cells in the developing brain, however some stem cells persist in the mature brain (Palmer, et al., 1999). Between the extremes of stem cells and terminally differentiated cells there are populations of cells referred to as progenitor cells, these cells can proliferate and differentiate, however the number of cell types they can produce is limited. This results in there being populations of progenitor cells which can produce certain neurons, with other progenitor cells giving rise to different oligodendrocytes (Fig 1.1; Review Temple, 2001). Astrocytes maintain the ability to proliferate in the adult brain and they can be observed doing this in response to injury (Hailer, et al., 1999).

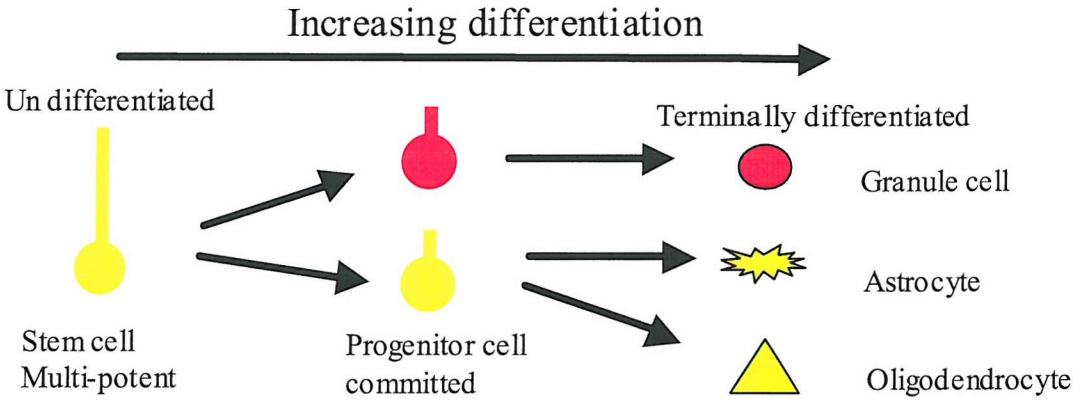

Fig 1.1: Stages in the generation of cells in the dentate gyrus. Showing stem cells capable of self-replicating (symmetric division) and forming many different cell types (asymmetric division), progenitor cells capable of self-replicating and differentiating to form a limited number of other cell types and terminally differentiated cells that are not thought capable of further division.

In addition to the types of cell that have the potential for neurogenesis being tightly regulated, the location of neurogenesis is not ubiquitous within the brain, but appears to occur in several restricted sites (Fig 1.2).

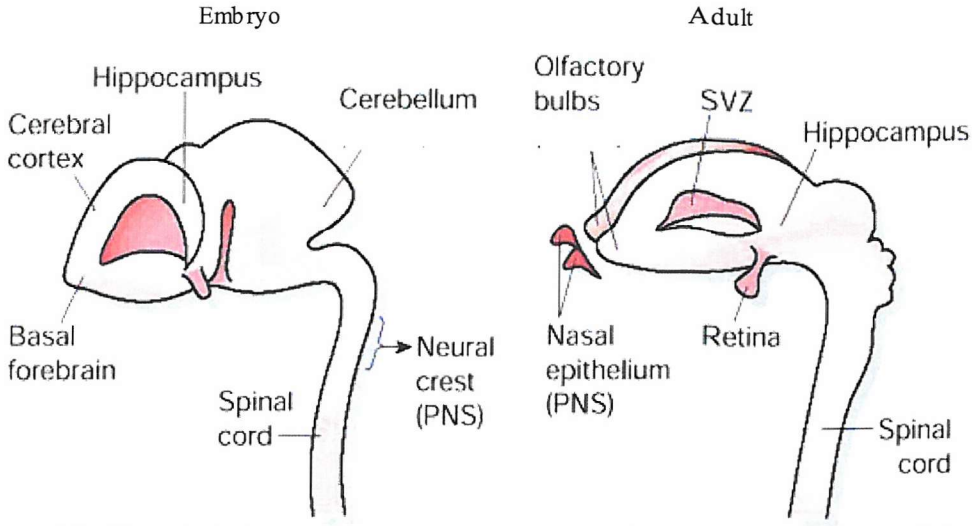

Figure 1.2: The principal regions of the embryonic and adult nervous system from which neural stem cells have been isolated. From *Nature* **414**, 112 - 117 (2001) Temple S. et al.

As the phenomenon of adult neurogenesis was shown to be common among mammals, studies also began to consider the possible functions these new cells could perform within the brain. Studies in songbirds were amongst the first to establish a functional role for the new neurons derived from adult neurogenesis; where a dividing population of cells in the sub-ventricular zone (SVZ) after migration contributes over 1% of the cells in the higher vocal center (HVC), daily (Hidalgo, et al., 1995). These neurons then become functional integrated neurons within the HVC (Goldman, 1998), a region of the songbird's brain involved in learning songs. However the brain of the songbird is structurally very different from humans and so understanding the functional significance of neurogenesis in other species is required. Within mammals there are two highly conserved regions of adult neurogenesis. One lies in the SVZ, cells generated in this region are destined for the olfactory bulb where they differentiate into neurons (Jin, et al., 2001; Noctor, et al., 2002) and integrate with existing cells in this region. The other is the sub granular zone (SGZ) of the dentate gyrus in the hippocampal formation.

1.2 Neurogenesis and the hippocampal formation

The hippocampal formation has its principle neurons arranged in a lamellar structure, resembling two interlocking "C" shapes (Fig 1.3). The first of these "C's" forms a

neuronal layer of granule cells, sandwiched between two layers of astrocytes and interneurons, and is called the granule cell layer of the dentate gyrus. Cells in this layer form synapses with pyramidal cells in the neuronal layer, again enclosed by a mixed layer of astrocytes and interneurons, of the second "C" – the hippocampus proper. The size of pyramidal cells in the hippocampus changes around the "C" and the cells in this layer are sub-divided into CA1 (Cornu Ammonis), CA2, CA3 and CA4 pyramidal cells. The neurogenesis that is observed in the hippocampal formation is largely restricted to the inside of the first of these "C's" that is the dentate gyrus, in a region referred to as the sub-granular zone. Neurogenesis also appears to occur within the hippocampus itself albeit at a much lower rate (Rietze, et al., 2000).

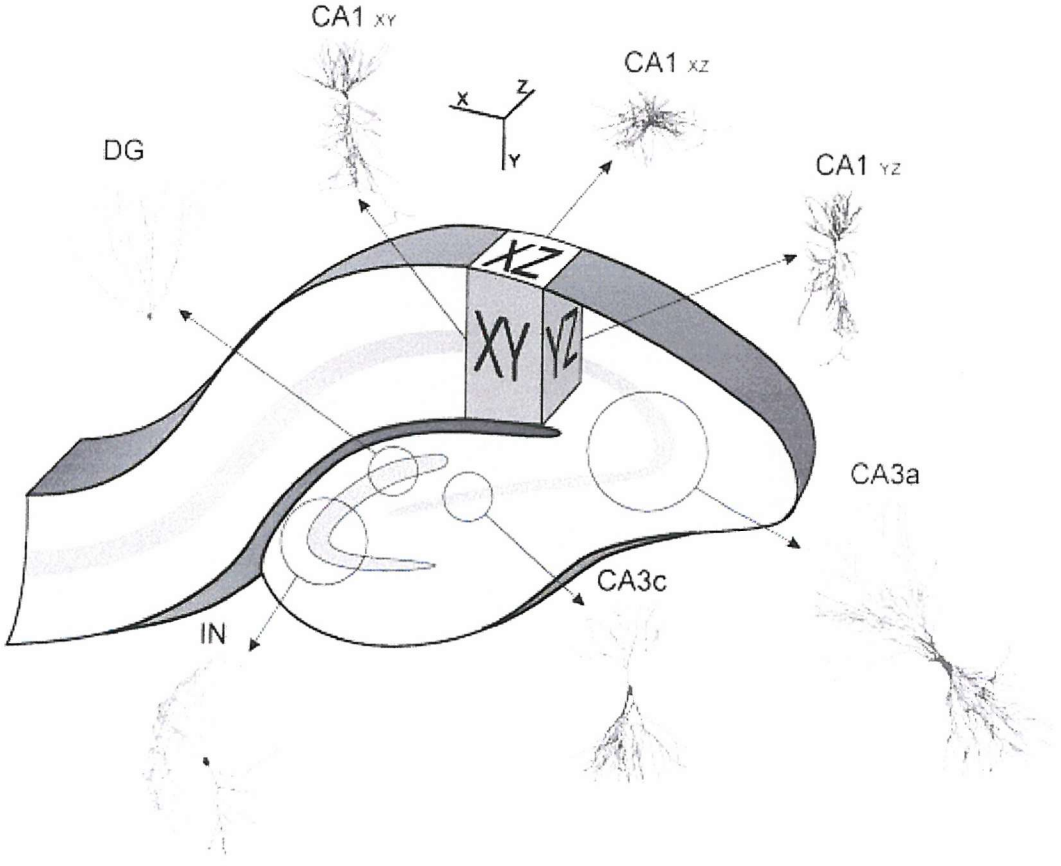

Fig. 1.3: Diagram of the hippocampus showing the principal cell layers: the dentate gyrus, CA3 and CA1 cell layers and the subiculum, beyond which is the entorhinal cortex. Examples of CA1 and CA3 pyramidal neurons are shown, as well as a dentate granule cell (DG) and an interneuron (IN). From Progress in Neurobiology (1998) 55 (6), 537-562. Turner, DA et al.

1.3 The sub-granular zone (SGZ)

The SGZ is an arbitrarily defined band of cells, two cells deep, on the border between the granule cell layer and the hilus. Consequently, unlike many of the other more formal structures in the hippocampus, the SGZ cannot be readily identified by the appearance of the cells from which it is formed. Indeed in addition to the presence of granule cell neurons, various different astrocytes, interneurons and the supporting vasculature, containing epithelial cells, can be found in this region. It is in this diverse environment that a large population of proliferating cells is located in the adult (Seaberg and van Der, 2002). The number of cells dividing in the SGZ is large with estimates of up to 250 000 new cells per month in the rat (Cameron and McKay, 2001), this is approximately one sixth of the maximal rate of proliferation during the formation of the dentate gyrus in the late embryonic and early postnatal period (Lewis, 1978; Nowakowski, et al., 1989). However, while the capacity of this region to proliferate is great, in adults, not all of these newly generated cells survive. Indeed the majority are not present 1 month after their birth (Cameron, et al., 1993; Gould, et al., 1999), but some survive and demonstrate many of the properties of mature granule cell neurons including the development of dendritic trees, axonal projection, expression of neuronal markers and electrophysiological responses (Cameron, et al., 1993; Hastings, et al., 2001; van Praag, et al., 2002). Recent studies suggest however that there may be some subtle differences in the responses of these cells to long-term potentiation (LTP) and to $GABA_A$ Receptor mediated inhibition (Wang, et al., 2000).

1.4 Control of neurogenesis

The mechanisms controlling postnatal SGZ neurogenesis are largely unclear. It is however well established that the environment modifies neurogenesis; both developmentally and in adults. Exercise, on a wheel in the cage, results in increased neurogenesis in mice (van Praag, et al., 1999). An enriched environment also results in increased adult neurogenesis compared with control mice kept in normal cages (Kempermann, et al., 1997; Young, et al., 1999). It has been known for some time that stress causes impaired neurogenesis during development (Lemaire, et al., 2000)with elevated levels of corticosteroids the probable cause. A decrease in adult neurogenesis is also seen after stress (Gould and Tanapat, 1999)or if exogenous

glucocorticoids are administered (Rodriguez, et al., 1998), the opposite response is observed if an adrenalectomy is performed (Montaron, et al., 1999; Park, et al., 2001). Similarly in aged animals there is a decrease in adult neurogenesis, which corresponds with an increase in corticoids concentrations in blood, and this can be abated either by environmental enrichment or by removal of the adrenal cortex (Kempermann, et al., 1998). Recently Gould's lab described these two phenomena in combination, where rats living in an enriched environment had differing levels of neurogenesis depending on their status within the colony. The dominant rat within the cage, which spent much of its time chasing the other rats out of a large central region of the cage, had increased neurogenesis. Whereas the more submissive rats, which had the stress of being chased showed decreased neurogenesis. This situation however was reversed if the group was formed from several more dominant rats, in which case the most dominant rat struggled to retain control and showed decreased neurogenesis (Gould, E. FENS abstract 2002). Stress is often a requisite factor for clinical depression, which can have associated hippocampal sclerosis and decreased neurogenesis (Duman, et al., 1997). Antidepressant drugs, including selective serotonin reuptake inhibitors (SSRI's) are known to increase neurogenesis (Malberg, et al., 2000). Recently, a study demonstrated that the time delay between initiation of antidepressant treatment and improvement in a test designed to assess antidepressant efficacy, novelty-suppressed feeding (NSF), correlated with an observed increase in neurogenesis. 5 days after antidepressant treatment no difference in responses or neurogenesis were present between placebo and drug treated mice, while by 28 days neurogenesis had increased and the latency of the feeding response had decreased in those animals receiving antidepressants, and that the latency response could be eliminated by irradiation significantly ablating neurogenesis (Santarelli, et al., 2003). Using $5HT_{1A}$ receptor knock-out mice the same group, demonstrated that both the antidepressive and neurogenic actions of Fluoxetine, an SSRI, were not present in the knock-out mice whereas imipramine and desipramine, which both have noradrenergic actions, retained their antidepressant and neurogenic potency (Santarelli, et al., 2003). This study demonstrates that potentially there are many signaling pathways that modulate neurogenesis, and that serotonin action on $5HT_{1A}$ receptors is among the proneurogenic signals. Fluctuations in the circulating concentration of the hormone estrogen can influence detected levels of neurogenesis (Tanapat, et al., 1999; Gould, et al., 2000), and this has been shown to also be mediated by serotonin (Banasr, et al.,

2001). Observations such as this are important when planning *in vivo* experiments as in mature female animals observations of neurogenesis may be complicated by fluctuations in estrogen concentrations dependent on the estrous cycle. Neurogenesis is also modified by seizures (Parent, et al., 1997; Gray and Sundstrom, 1998), ischaemia (stroke)(Liu, et al., 1998) and traumatic brain injury (Dash, et al., 2001; Chirumamilla, et al., 2002), and this will be explored in more depth later.

1.5 Possible functional roles for neurogenesis

The persistent adult neurogenesis described above in normal healthy animals is of such magnitude that it must have a purpose as there is no evolutionary benefit to expending the energy required for cell division if the new cells serve no purpose and the neurogenesis is preserved in so many species. Many studies have demonstrated that these new cells can integrate with the existing cells within the granule cell layer, and respond to electrical stimulation in a similar manner to granule cells (Snyder, et al., 2001; Song, et al., 2002; van Praag, et al., 2002). However, this does not indicate a function. For some time it has been suggested that the hippocampus is involved in learning and memory (Wagner, 2001; Rosenbaum, et al., 2001; Nestor, et al., 2002), this belief is based on human surgical evidence, where removal / deafferentation of all or parts of the hippocampus produces impaired learning/memory (Moscovitch and McAndrews, 2002). This property is thought to be linked to the ability of the neurons, in the hippocampus, to alter their responses to a stimulus or series of stimuli, reinforcing that stimulus the next time it is received – this property is referred to as long-term potentiation (Nakic, et al., 1998; Derrick, et al., 2000). Gould *et al.* indicated a link between learning and neurogenesis, by demonstrating that successful completion of hippocampal dependent learning tasks resulted in increased neurogenesis (Gould, et al., 1999). The importance of this neurogenesis in some memory formation was demonstrated by Shor *et al.* who gave adult rats methylazoxymethanol (MAM) for two weeks to significantly reduce neurogenesis. They then tested the rats' response to a hippocampal-dependent learning task (trace conditioning) and a hippocampal-independent learning task (delay conditioning), and compared these to saline treated controls. They found that hippocampal-independent learning was unaffected by MAM treatment. However conditioned responses in the

MAM treated group were significantly lower for the trace conditioned memory task. This effect that was not observed if the conditioning was performed 3 weeks after MAM administration, when proliferation was able to recover, indicating the MAM has not elicited its effect by causing damage to the hippocampus (Shors, et al., 2001). Another group (Kempermann and Gage, 2002) found a correlation between the basal level of neurogenesis in different mice strains and their ability to acquire spatial memory in the Morris water maze task, a hippocampal dependant task. Generally, a higher basal proliferation level resulted in faster spatial memory acquisition. This experiment also raises awkward questions about comparisons we make between the results of experiments, examining neurogenesis, carried out in not only in different species but also in different strains within the same species. Some of the factors known to influence neurogenesis are summarized in table 1.1.

Treatment	Effect on neurogenesis	References
Age	▼	Brezun & Daszuta (2000)
Enriched environment	▲	Kempermann, et al. (1997); Young, et al. (1999)
Exercise	▲	van Praag, et al. (1999)
Stress	▼	Gould & Tanapat (1999); Lemaire, et al. (2000)
Hippocampal-dependent learning	▲	Gould, et al. (1999)
Estrogen	▲ or ►	Banasr, et al. (2001)
Alcohol	▼	Pawlak, et al. (2002)
Nicotine	▼	Abrous, et al. (2002)
γ-irradiation	▼	Kee, et al. (2002)
Seizure	▲	Parent, et al.(1997); Gray & Sundstrom (1998)
Ischaemia	▲	Liu, et al. (1998)
Traumatic brain injury	▲	Dash, et al. (2001)
Corticosterone	▼	Rodriguez, et al. (1998)
Adrenalectomy	▲ or ►	Cameron & McKay (1999); Montaron, et al. (1999)
Glutamate	▼	Gould & Tanapat (1999)
NMDA	▼	Cameron, et al. (1995)
NMDA R antagonists	▲	Gould, et al. (1994); Nacher, et al. (2001)
Serotonin	▲	Brezun & Daszuta (2000)
Serotonin depletion	▲	Brezun & Daszuta (1999)

Table 1.1: Showing some of the factors that alter neurogenesis, their effect and experiments that demonstrate each effect.

1.6 Epilepsy and seizures

Epilepsy occurs in about 1-3% of the human population and is the most common acquired chronic neurological disorder (Shneker and Fountain, 2003). As with many disorders, there are numerous subdivisions to which individual cases can be ascribed,

one characteristic these cases all share is the occurrence of spontaneous seizures. Among the more common forms of epilepsy is temporal lobe epilepsy (TLE), and in many of these patients an initial precipitating event, such as brain infection, status epilepticus (an acute seizure), ischemia or TBI will result in later spontaneous seizures, characteristic of epilepsy. The period between the precipitating injury and the onset of the spontaneous seizures is referred to as the latent period during which epileptogenesis is thought to occur. This gap between a causative injury and symptomatic onset provides a window for potential preventative intervention. However, the changes that occur between injury and onset need to be understood, in order that specific interventions can be developed, as not every potential precipitating event will lead to onset, for example about 10% of the population will have at least one seizure, but the incidence of epilepsy is considerably lower than this, and includes cases derived from non-seizure precipitating events and epilepsies with a genetic basis (Shneker and Fountain, 2003).

Some studies into the pathology associated with epilepsy have been carried out in humans; these date back to the identification of hippocampal sclerosis in the early 19th century. From these studies localized neuronal cell death, gliosis (astrocytes proliferating into areas of localized neuronal death), axonal sprouting and changes in neurotransmitter release (During and Spencer, 1993) have all been detected in TLE. However, establishing mechanisms, and especially elaborating the processes of epileptogenesis are difficult in human tissue. This is because most studies are based on either postmortem tissue, or surgically resected tissue. In post mortem tissue it is difficult to establish whether pathology is cause or effect, and resected tissue is not a random sampling process, but based on the few patients considered suitable for surgery. More recently developed microdialysis techniques such as those used to establish the glutamate increase (During and Spencer, 1993) could shed more light on mechanisms, however it may have a greater value in helping to assess the validity and accuracy of animals models of epilepsy and seizures.

1.7 Neurogenesis and seizures

Increased adult neurogenesis as a consequence of brain injury was first observed in experimental models of seizure five years ago, in response to different chemoconvulsants (Parent, et al., 1997; Gray and Sundstrom, 1998) and repeated

electrical stimulation (kindling) (Bengzon, et al., 1997). As yet it has not been convincingly reported in human epilepsy, where increased expression of an immature neuronal marker has been described (Mikkonen, et al., 1998), and proliferation of neural precursors is reported to be increased in resected tissue from patients aged less than two years at time of surgery (Blumcke, et al., 2001). But proliferation is reported to be unchanged when the same proliferation marker Ki-67 is quantified in adult tissue (Del Bigio, 1999), and other studies report decreased neurogenesis after seizures in children (Mathern, et al., 2002). However as in other respects these models produce similar pathological and functional changes to those arising as a consequence of epilepsy, and humans retain a neurogenic potential in the dentate gyrus, it is not unreasonable to hypothesize that increased neurogenesis is a sequelae of human epilepsy. As such it may have a detrimental effect in the developing pathology of epilepsy through aberrant circuit formation, or it may be part of an internal repair mechanism attempting to attenuate the detrimental effects of seizures. While a detrimental effect arising from neurogenesis cannot be ruled out Parent demonstrated that the mossy fiber sprouting associated with seizures, a probable cause of aberrant network formation, occurs in the absence of seizure induced neurogenesis (Parent, et al., 1999), indicating neurogenesis is unlikely to be the sole cause of the progression from seizure events to epilepsy. Recently neurogenesis has been identified after ischaemic injury (Liu, et al., 1998; Zhang, et al., 2001) and traumatic brain injury (Dash, et al., 2001; Kernie, et al., 2001; Chirumamilla, et al., 2002). These observations of neurogenesis in other models of brain injury, which can involve an apparently similar cell loss in the hippocampal formation, adds credibility to the hypothesis of neurogenesis for repair purposes, since seizures are not an inevitable consequence of ischaemia and TBI, although they can develop after these injuries. With more detailed understanding of the mechanisms underlying seizure induced neurogenesis it may be possible to separate potentially beneficial neurogenesis from potentially detrimental neurogenesis.

1.8 Cell death resulting from brain injury

Cell death has been studied in considerably more detail than neurogenesis after seizures and other types of brain injury, and thus is a broad term that describes a number of processes. The most general classification of different types of cell death

has two classes, necrotic and apoptotic cell death. The precise definition of these processes and the methods for identifying which type of cell death is occurring, in an individual cell are still subject to considerable debate (reviewed in Dikranian, et al., 2001). However, these studies are focused on cell death during early development, and so have only limited relevance to this work, therefore the more simple and concise initial definitions where, apoptosis is a controlled process of 'self-induced' cell death, and necrosis is an uncontrolled, unregulated cell death are used as they are sufficient for the study of seizure induced cell death.

Necrosis is caused by a total energy failure of the cell, resulting in loss of the cells ability to maintain its ionic homeostasis, this failure induces cell swelling, and membrane rupture, with a subsequent loss of the cells contents to the extracellular milieu(Lipton and Nicotera, 1998; Nicotera and Lipton, 1999), one of the consequences of this cell lysis is an inflammatory response which tends to propagate the cell death.

Apoptosis is a more controlled process, where the cell recognizes it is damaged beyond repair and activates a sequence of cell death signaling cascades, these break down DNA, and cause the cell to shrink, becoming pyknotic in appearance, and then break into smaller fragments which retain intact membranes, and are phagocytosed (Lipton and Nicotera, 1998; Nicotera and Lipton, 1999). Apoptosis does not cause the same inflammatory response that follows necrotic death, however dying cells may be able to release signaling factors prior to death (Lipton and Nicotera, 1998; Nicotera and Lipton, 1999).

Some of the confusion pertaining to whether apoptosis or necrosis is occur in a cell may be caused by cells that begin to undergo apoptosis, activating the cell death signaling cascades which can then be detected. However, in some cells, before the apoptotic process can be completed total energy failure can lead to loss of cell membrane integrity and apparent necrosis (Covolan, et al., 2000). This concept is further supported by the observation that N-methyl-D-aspartate (NMDA) receptor mediated toxicity can induce either apoptotic or necrotic cell death depending on the severity of the insult (Bonfoco, et al., 1995).

The differences in detection techniques referred to above are important, only a few techniques are used to identify necrotic cell death, these typically use loss of cell membrane integrity to enter the necrotic cells and permit their identification, for example the fluorescent exclusion dye propidium iodide (PI). By contrast, there a

considerable number of methods for detecting cells proceeding through the process of apoptotic cell death exist. The breaks in the DNA that occur in apoptosis can be labeled, and many of the proteins activated in the process of apoptosis are thought to be specific to cell death, and so can be stained for, chief among these are the caspases (Reviewed in Earnshaw, et al., 1999). Additionally both types of cell death can be identified by their morphology.

In models of acute brain injury, such as ischemia, TBI and seizures, the process of cell death occurs through an excitotocic mechanism. The precise mechanisms of excitotoxic cell death are not fully understood, and changes, both intra and extracellular, resulting from excitotoxic injury are the subject of much research. However, the basic principle is well established, in normal conditions glutamate, the principle excitatory neurotransmitter in the brain, is released into the synapse. Activation of AMPA receptors, a glutamate receptor sub-type, in the synapse ensues, and Na^+ ions enter the cells producing a local depolarization of the cell. NMDA receptors require this cell depolarization in addition to glutamate binding to open their ion channels. Once the NMDA receptors are active more Na^+ ions and Ca^{2+} ions can enter the cell. Normally calcium is under tight homeostatic control in the cell, and each neuron expends large amounts of energy maintaining low intracellular calcium concentrations. A small influx of Ca^{2+} can significantly alter the local concentration of Ca^{2+} ions because the local Ca^{2+} concentration is initially very low. Increases in Ca^{2+} concentration elicit neurotransmitter release and thus a signal is propagated through the brain. Simultaneously the mechanisms in the cell that maintain homeostasis expend energy to remove the glutamate from the synapse and restore the Ca^{2+} and Na^+ ion concentrations to resting levels in the cell (reviewed in Kristian and Siesjo, 1998).

The cell death that occurs in seizures, ischaemia and traumatic brain injury (TBI) all result from failure of this homeostasis, as a prolonged elevation in Ca^{2+} concentration in the cell is toxic, although the mechanisms for this toxicity are not fully understood. In ischaemia the supply of oxygen and glucose to the neurons is greatly reduced and the efficiency with which glutamate is removed from the synapse and Ca^{2+} is eliminated from the cell is reduced. In seizure the glutamate release is uncontrolled, producing failure of the clearance mechanism. And in TBI initially the structure of the brain is disrupted, and this can then be followed by both localized ischaemia and

seizures (Vornov, et al., 1991; Albensi, 2001). Although this is a simplification of the events leading to cell death in brain injury and other functions are involved, for example K^+ homeostasis failure, increased Ca^{2+} ion concentration induced by glutamate is pivotal to cell death, as blocking its entry by preventing NMDA receptor activation is highly neuroprotective (Bennett, et al., 1990).

Initially it was thought that excitotocic cell death was entirely necrotic (van Lookeren, et al., 1995), however recent work has demonstrated that although an initial phase of cell death at the focus of the injury is probably necrotic, additional death occurring either later, or at a distance from the necrotic death, is apoptotic (Bengzon, et al., 1997; Fujikawa, et al., 2000; Liou, et al., 2003). When the mechanisms of the two types of death are considered this appears to be logical, closest to the energy failure cells are unable to undergo organized, controlled apoptotic death, whereas those cells that are not subjected to as severe an energy crisis are able to 'sacrifice' themselves. Although discussed as a result of seizure, this process is perhaps most clearly described in ischemia, where an initial infarct can be observed using magnetic resonance imaging, with a penumbra of cell death appearing later (Manabat, et al., 2003).

1.9 Cell death and neurogenesis

Since all the acute models of brain injury described produce an early phase of cell death it has been suggested that neurogenesis resulting from these injuries is driven by the cell death (Gould and Tanapat, 1997). This study used a bolus of saline as a mechanical injury, disrupting neuronal connections and ibotenic acid as an excitotoxic injury, and then quantified cell proliferation and cell death. 24 hours after the injury cell death was observed localized to the site of injection, and a similar localization of increased proliferation was observed, implying a possible link between the cell death and the neurogenesis. Although the coincidence of cell death and neurogenesis is repeated in other experiments this does not necessarily indicate that they are cause and effect.

Increased neurogenesis after ischaemia has been reported with no apparent cell death in the hippocampus (Arvidsson, et al., 2001) although other studies find this level of ischaemia produces hippocampal cell death. Perhaps more convincingly preconditioning with a brief non-lethal ischaemic insult is known to protect the

hippocampus from a second normally lethal insult. Neurogenesis has been observed after both the lethal insult and using the preconditioning insult with the subsequent normally lethal insult (Liu, et al., 1998).

Additionally electro-convulsive therapy (ECT) increases neurogenesis, but is not reported as producing cell death (Madsen, et al., 2000), and when applied before a kainate induced seizure significantly ameliorated apoptotic cell death, although necrotic death was not quantified (Kondratyev, et al., 2001). In a similar experiment to those described above, previous *in vitro* research in our laboratory showed that, a pre-treatment with a non-lethal kainate dose protects against a subsequent dose of kainate sufficient to cause cell death (Best, et al., 1996). However this model is not yet capable of quantifying neurogenesis.

1.10 Summary

Neurogenesis is a phenomenon that persists in the hippocampus of the adult brain and has a functional role in learning, and memory. Seizures increase hippocampal neurogenesis, an event that appears to coincide with significant cell loss. While there is some evidence to suggest that cell loss may induce neurogenesis, this has not been demonstrated as a response to seizures. Importantly the cells that generate the new neurons are as yet unidentified. Therefore, the aim of this thesis is to investigate the control of dentate neurogenesis, especially, after seizures, and to begin to identify the principle cells and events involved in these processes.

Chapter 2

Proliferating cell phenotypes in the Organotypic Hippocampal Slice Culture

2.1 Introduction

There are a number of *in vitro* techniques for considering the properties and interactions of neuronal tissue. Primary dissociated culture is a method that has been used for many years (Brewer, 1997) and is proving very useful in experiments investigating the properties of stem cells (Li, et al., 1998; Doetsch, et al., 1999; Seaberg and van Der, 2002), progenitor cells (Wolswijk and Noble, 1989; Noctor, et al., 2002), and factors which affect the division of these cells (Palmer, et al., 1999), their probability of survival or their eventual phenotypic fate (Shetty and Turner, 1998). Dissociated cultures also have some use when investigating the response of cells to both chemical and mechanical injury, and adding, for example, neurons to astrocytic dissociated cultures is widening our understanding of the ways in which different cell types interact with each other (Song, et al., 2002). However cells in these dissociated cultures, while they do form synapses with each other, do not form the highly organized network of synaptic connections observed *in vivo* - capable of controlling movement, breathing, thought, memory, learning – sentient life. The organotypic hippocampal slice culture (OHSC) is an *in vitro* model, which retains much of the circuitry present in the *in situ* hippocampus. The model of organotypic hippocampal slice cultures we use was established by Stoppini over 20 years ago and since then the method for culturing has been modified but not greatly changed (Stoppini, et al., 1991; Pringle, et al., 1996). Cultures are obtained by dissecting the hippocampal formation from neonatal rat brains and taking transverse sections that are subsequently grown on a semi-permeable membrane. The organotypic slice culture method of preparation results in the major circuitry of the hippocampal formation being retained, although afferents to the entorhinal cortex, the commissural pathways and some lateral connections are lost (Fig 2.1). It has also been suggested that some aberrant networks are also formed within the cultures after longer times in culture (Sakaguchi, et al., 1994) and a glial 'scar' or cap is formed over the cut face of the slice (Fig 2.2; from (Pringle, et al., 1997)) (Del Rio, et al., 1991). In spite of these minor defects the model responds to electrophysiological investigation in a manner similar to acute slices prepared from hippocampal tissue and used immediately (Gahwiler, et al., 1997).

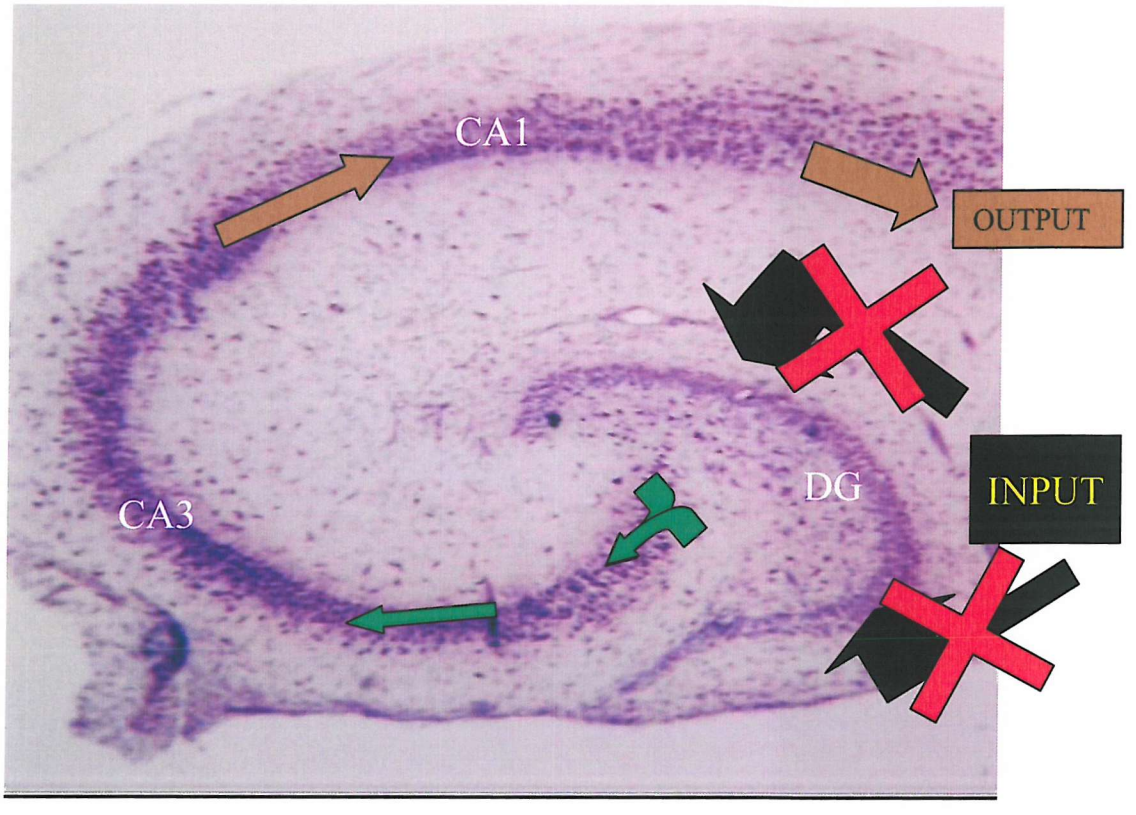

Fig 2.1: Structure of an organotypic hippocampal slice culture. Showing conservation of lamellar structure observed in vivo and indicating similarities and differences to the principle hippocampal circuitry. CA, cornu amonis and DG dentate gyrus.

One other obvious difference between organotypic cultures and the situation *in vivo* is the absence of a vascular system and the blood brain barrier (although the latter is not particularly defined in neonates). This is an advantage in simplifying the chemical influences on the neurons in the circuits. Coupled with the benefits of closely approximating many aspects of the real system (i.e. *in vivo* experimentation) OHSC's also retain the principle benefits of Primary dissociated cultures. Administration and the timing of removal of compounds of interest are simple. Manipulation of the tissues environment (i.e. temperature, pH, ion concentration, etc) is also easily possible.

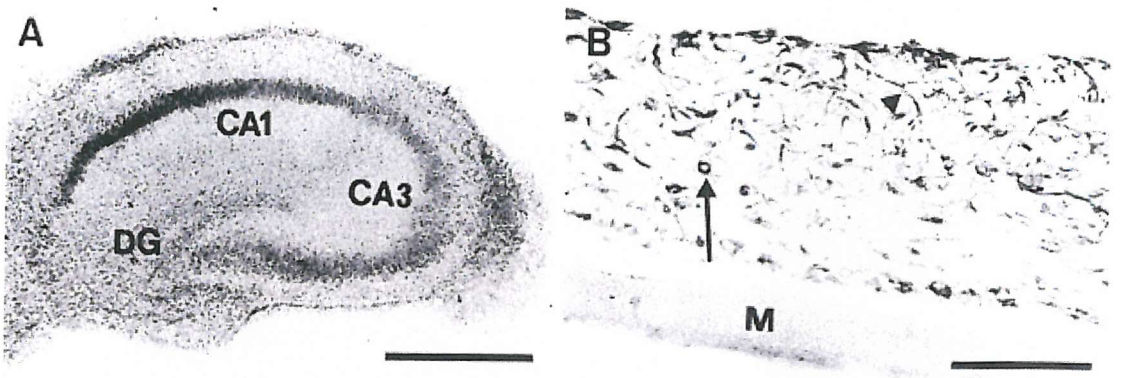

Fig. 2.2. Glial scar formation in organotypic hippocampal slice cultures. A) thionin-stained organotypic hippocampal slice culture after 2 weeks in vitro. The pyramidal cell fields (CA1, CA3) and dentate gyrus granule cells (DG) are clearly recognisable (scale bar = 1 mm). **B)** 5μm longitudinal section from a fixed paraffin-embedded culture stained for glial fibrillary acidophillic protein (GFAP). The membrane (M) is visible. GFAP positive cell bodies (arrow) and processes (arrow head) are visible throughout the culture (scale bar = 100μm). From Pringle et al., 1997.

2.1.1 Identifying neurogenesis

The dentate gyrus is the last part of the hippocampal formation to form and is derived from three distinct cell migrations. All the stem cells that produce the dentate gyrus originate in the primary dentate neuroepithelium, located on the surface of the lateral ventricle. The primary migration begins from the dentate neuroepithelium around embryonic day 16 (E16), these cells form the outer shell of the granule cell layer (closest to the hippocampal fissure and third ventricle). At about E18 a group of stem cells leave the primary matrix and form the secondary matrix, located close to the CA3 region of the hippocampus. Cells derived from this matrix then begin migrating to the granule cell layer around E22; these cells migrate inside the older cells from the primary migration. The primary migration finishes shortly after birth, postnatal day 1 (P1), and the secondary migration is complete by about P10. However on P2, the tertiary matrix begins to form, from cells in the secondary migration. This tertiary matrix is located between the blades of the dentate, in the hilus. The cells of the tertiary matrix move out into the subgranular zone (SGZ) of the dentate gyrus over the next 9 days until by about P13 most dividing cells are located in the SGZ, however this migration is not complete until P30 (Altman and Bayer, 1990a; Altman and Bayer, 1990b; Altman and Bayer, 1990c). This indicates that as the cultures are being set-up the processes of dentate formation are almost complete. Proteins that are vital to ensure neurogenesis during the formation of the dentate gyrus have been

demonstrated to also be vital in adult neurogenesis (Pleasure, et al., 2000). This suggests that although the tissue in the cultures is not mature, the signalling pathways that regulate neurogenesis appear to be conserved between immature and adult tissue, and thus the cultures are an acceptable model for examining adult neurogenesis. However, in order to establish that neurogenesis is occurring two facts need to be established. Firstly, cells have to be identified as dividing; and secondly, these new cells, or a fraction of them, need to be identified as neurons.

2.1.2 Proliferating cells

The process of cell replication is cyclic and is referred to as the cell cycle. Cells that are not dividing reside outside the cell cycle in a resting state (G_0, G is for gap). Cells that are likely to divide enter the cell cycle at G_1, and progress into the S (synthesis) phase, where replication of the DNA strands occurs, cells then progress to G_2 and finally the M phase – mitosis, when the cell divides (Fig 2.3). Progression through the cycle is tightly regulated and can be arrested at the end of the G_1, and G_2 phases. The fact that large amounts of DNA are synthesized in the S-phase of the cell cycle has been used to help identify dividing cells in the brain since the sixties (Altman and Das, 1965), when synthetic thymidine containing the radioactive ^3H isotope of hydrogen added to the diet of rats became incorporated into dividing cells. More recent experiments examining cell proliferation have generally used 5-Bromo-2'-deoxyUridine (BrdU) incorporation to measure cell proliferation. BrdU is a thymidine analogue and is incorporated into DNA during the S-phase of cell division (Nowakowski, et al., 1989). BrdU is now selected in preference to using ^3H-Thymidine because it can be detected in thicker tissue sections, is not a radiation hazard and is generally easier to use.

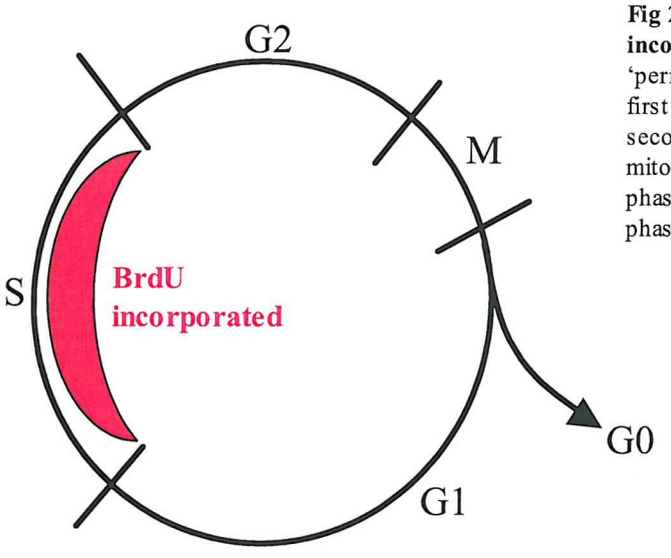

Fig 2.3: Cell cycle showing BrdU incorporation phase. **G0** represents a 'permanently' post mitotic state, **G1** the first gap phase of the cell cycle, **G2** the second gap phase of the cell cycle, **M** the mitotic phase and **S** the DNA-synthesis phase. BrdU is incorporated in the **S** phase.

2.1.3 Cell Phenotypes

There are a number of antibodies commonly used to identify mature neurons, including growth-associated protein (GAP-43), neuron-specific enolase (NSE), microtubule-associated protein-2 (MAP-2), and neuronal nuclei (NeuN). GAP-43 and NSE have been shown to be expressed in non-neuronal cells in certain conditions, including the presence of basic fibroblast growth factor (bFGF) (Sensenbrenner, et al., 1997), making them perhaps less suitable for use as neuronal markers. A similar problem has been identified with MAP-2, which may stain glial cells after brain injury (Lin and Matesic, 1994) and therefore may not be an appropriate general neuronal marker after seizures. In addition to these potential specificity problems, the experiments that are described here generate immature neurons that do not become mature neurons before the experiments are terminated and thus are unlikely to express mature neuronal markers, with the possible exception of MAP-2 some isoforms of which also mark immature neurons (Seki, 2002). The investigation of neurogenesis therefore requires a rapid identification of neuronal phenotype, and thus proteins that are present in the immature neuron are of interest. Class III β-tubulin is an early marker of immature neurons, it is expressed in neurons for about 4 weeks and thus will also label some mature neurons (Fig 2.4)(Lee, et al., 1990; Fanarraga, et al., 1999). Other markers of immature neurons are more transiently expressed; among these are TUC-4, polysialylated neural cell adhesion molecule (PSA-NCAM), neuronal determining factor (Neuro-D) and doublecortin. TUC-4's (from TOAD/Ulip/CRMP protein family) peak expression coincides with maximal cortical

neurogenesis in embryonic rats, after this its expression declines until in the adult it is only expressed in regions of neurogenesis (Quinn, et al., 1999). Normally NCAM is involved in maintaining cell-cell adhesion, however its polysialylation results in a reversal of this effect and is required for neural cell migration (Abrous, et al., 1997), PSA-NCAM's expression occurs rapidly in post-mitotic neurons permitting migration. Neuro-D is a member of the basic Helix-loop-helix family of proteins, and is required for normal dentate development. Mutant mice lacking Neuro-D fail to form a mature dentate granule cell layer implying a role for Neuro-D in cell fate determination (Schwab, et al., 2000; Liu, et al., 2000), making it a very early marker for granule cell neurons. Cortical malformation due to incorrect neuronal migration has been identified as a major cause of intractable epilepsy and one of the proteins implicated in some malformations is doublecortin (Dcx) (Des, et al., 1998). In Dcx deficient mice hippocampal development is also impaired, this is especially prominent in the migration of CA3 pyramidal neurons (Corbo, et al., 2002), the window of Dcx expression is probably similar to that of PSA-NCAM. The work of Seki has demonstrated that an estimate of the approximate age of an immature neuron can be determined by the markers expressed, Neuro-D expression occurs very early on, followed by both PSA-NCAM and TUC-4 expression a little later and finally TUC-4 stain alone (Seki, 2002).

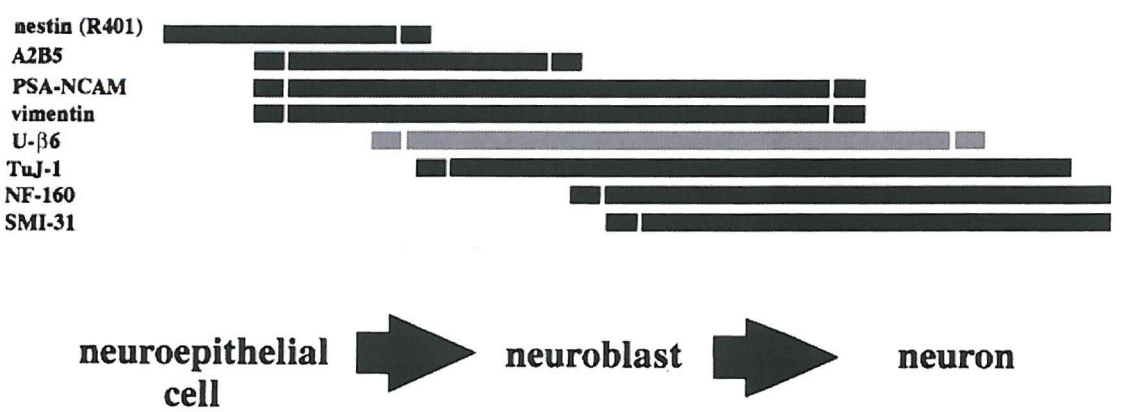

Fig 2.4: Expression profile of some common cell phenotype markers. PSA-NCAM, NF-160 (160 kDa Neurofilament), U-β6 and TuJ-1 (both Class III β-tubulin markers) are neuronal markers. Nestin stains progenitor cells, A2B5 stains oligodendrocyte precursors and vimentin is an astrocytic marker. From Fanarraga, M.L. et al. 1999.

Since gliosis accompanies lesions in brain tissue (Crespel, et al., 2002) astrocytic markers are also of interest. Glial fibrillary acidic protein (GFAP) and vimentin are

the most commonly used general astrocytic markers; they are both intermediate filament proteins (GFAP 52kD and vimentin 57kD) and as such like MAP-2, and class III β-tubulin show only weak staining in the cell body. Vimentin is less specific for astrocytes than GFAP as it also stains endothelial cells and fibroblasts, and so less useful as an astrocytic marker. S100b is another marker of astrocytes and its staining profile includes all parts of the cell, unlike GFAP and vimentin, making it easier to quantify. S100b is also known to be released by astrocytes and has both neurotropic and neurotrophic functions (Donato, 1999), and may have a role in responses to seizure (McAdory, et al., 1998).

2.1.4 Aims

In order to investigate the effect of seizures on neurogenesis in an *in vitro* system a method for identifying the cells involved needs to be developed. Thus, the aims of these experiments are threefold; to establish whether proliferation occurs under normal conditions in OHSCs as it does *in vivo*, to identify markers that can consistently label newly generated cells as neurons or other cell types, and to establish whether there is the potential to document these species quantitatively.

2.2 Methods

The method of culture preparation described below was followed for all the OHSC experiments detailed in this chapter and in chapters 3, 4 and 5. In all cases, preparation of OHSCs was carried out under home office licence 30/1639, and at all times effort was taken to minimize animal usage.

2.2.1 Preparing Organotypic hippocampal slice cultures

The method of culture preparation described here is based on the method originally described by Stoppini (Stoppini, et al., 1991), and modified by Pringle (Pringle, et al., 1996). Eight-day-old Wistar rat pups were killed by decapitation, without anaesthesia, and the hippocampi rapidly dissected out. The corpus callosum was bisected above the thalamus and the posterior margin of each cortical hemisphere rolled back. Each hippocampus was separated from the overlaying cortical white matter along the natural separating line of the alveus hippocampus. Transverse sections of hippocampus, 400 microns thick were cut on a McIlwain tissue chopper (Mickle Laboratory Engineering Ltd, Surrey, UK) and placed into cold Gey's balanced salt solution (4°C; Sigma) supplemented with 28mM glucose (Sigma). Slices were plated on Millicell-CM semi-porous membranes (0.4µm pore; Millipore, 4 cultures per insert, in six well culture plates (Nunc) using plastic paddles. All cultures were maintained *in vitro* at 37°C with 100% humidity and a 5% CO_2, 20% O_2, 75% N_2 atmosphere. Cultures were grown in 1.2ml of either horse serum based medium (HS) or Neurobasal™ based medium (NB). The horse serum based medium is comprised of minimum essential medium (MEM, 50%; Gibco), Hank's balanced salt solution (HBSS, 25%; ICN Biochemicals) and heat inactivated horse serum (25%; Gibco), supplemented with glutamine (1mM; Sigma) and D-glucose (4.5mg/ml; Sigma). The Neurobasal based medium is a completely defined medium, comprised of Neurobasal-A (98%; Gibco), and B27 (2%; Gibco) a combination of 27 essential salts and amino acids to aid culture growth (Brewer, Torricelli et al., 1993) supplemented with glutamine (0.5mM; Sigma). Every three days 1ml of medium was removed from each well and replaced with fresh medium.

2.2.2 Labelling of proliferation

After 14 days *in vitro*, BrdU (10μM) was added to the cultures and 2 hours later, they were fixed in 4% paraformaldehyde. Immunostaining was carried out 24 hours later.

2.2.3 Immunohistochemistry

Tissue processed for BrdU immunohistochemistry was exposed to 2N HCL at 37°C for 30 minutes and was subsequently washed in Boric acid (0.1M, pH 8.5) for 10 minutes. All tissue for immunohistochemistry then received multiple washes in Tris-Buffered Saline (TBS; 0.1M, pH7.4). Non-specific peroxidase staining was eliminated by incubating for 10 minutes with 3% H_2O_2 in distilled water. Multiple TBS washes were followed by overnight incubation with primary antibody to either BrdU (rat monoclonal, 1:1000; Oxford Biotech); class III beta tubulin (mouse monoclonal TUJ1 clone, 1:1000; BabCo); TUC-4 (rabbit polyclonal, 1:500; Chemicon); S100 beta (rabbit polyclonal, 1:2000; Swant) or GFAP (rabbit polyclonal, 1:1000; Mr P. Steers); PSA-NCAM (mouse, 1:500; gift of Dr G.Rougon, University of Marseilles, France) in TBS containing 0.1% triton and 0.05% Bovine Serum Albumin (TBS-TS) at 4°C, tissue processed for BrdU also had 1% Normal Goat Serum (Sigma) present with the primary antibody. Following multiple washes in TBS, tissue was incubated in TBS-TS with the appropriate biotinylated secondary antibody, raised against either rat (goat, 1:200; Vector); rabbit (swine, 1:500; DAKO); or mouse (sheep, 1:200; Amersham life sciences) for 1 hour. TBS washes were repeated and a Horseradish peroxidase conjugated Streptavidin-biotin complex (HRP-ABC, 1:200; DAKO) in TBS-TS was applied for 1 hour, further washing in TBS was followed by visualization with either 3,3-Diaminobenzene (DAB, brown; Vector) or VIP (purple, Vector) and a final set of washes. Cultures were mounted on gelatinised slides and where necessary received a light Thionine counter-stain to facilitate granule cell layer identification. Thionine staining was obtained by placing slides in distilled water containing 1% Thionine followed by differentiation in 90% Ethanol with 5% Acetic acid until a consistent staining intensity was observed. All cultures were dehydrated through 1 minute washes in alcohol (70%, 90% and 2x 100%) and then xylene before cover-slipping with DPX (Sigma).

For double antibody staining, cultures were initially treated for BrdU as described above and then incubated in a cocktail of primary antibodies combining BrdU with

either class III beta tubulin, TUC4 or S100 beta in TBS-TS containing 1% Goat serum overnight at 4°C. Stains were then sequentially developed using the biotinylated goat anti-rat and HRP-ABC steps as above and with Nickel-DAB (black, Vector) as the final substrate for visualization of the BrdU, and then repeating the process using the appropriate biotinylated secondary antibody and HRP-ABC with VIP as the final substrate for beta-tubulin, TUC-4 or S100 beta. Cultures were then mounted and cover-slipped as described above.

For triple antibody staining cultures were washed repeatedly in TBS followed by incubation in a cocktail of primary antibody containing GFAP (rabbit), doublecortin (Guinea pig polyclonal, 1:5000; Chemicon) and nestin (mouse monoclonal, 1:1000; BD Pharmingen).

2.3 Results

These initial experiments using whole cultures appeared to produce successful single immunostaining for the proliferation marker BrdU, with positive cells identified covering the entire culture (Fig 2.5). Single staining for the astrocytic markers GFAP and s100b, and early (TUC-4 and PSA-NCAM) and more general (class-III β-tubulin) neuronal markers was also achieved (Figs 2.5 and 2.6). It is interesting to note the absence of neuronal process staining at the edge of the cultures (Fig 2.5), possibly indicating part of the glial scar. Attempts at achieving double immunostaining, to identify the phenotypes of proliferating cells, markers were less successful, BrdU combined with s100b or β-tubulin labelling produced high background staining, combination with TUC-4 showed clearer staining but was difficult to achieve on a consistent basis (Fig 2.6). Subsequently multiple fluorescent dyes and confocal microscopy were used to clearly distinguish between cell types; this permitted clear identification of multiple cell phenotypes (Fig 2.7). The images generated using the confocal microscope also identified that the staining was limited to two bands approximately 20μm thick on either side of the cultures, with the middle of the cultures showing no fluorescence (Fig 2.7).

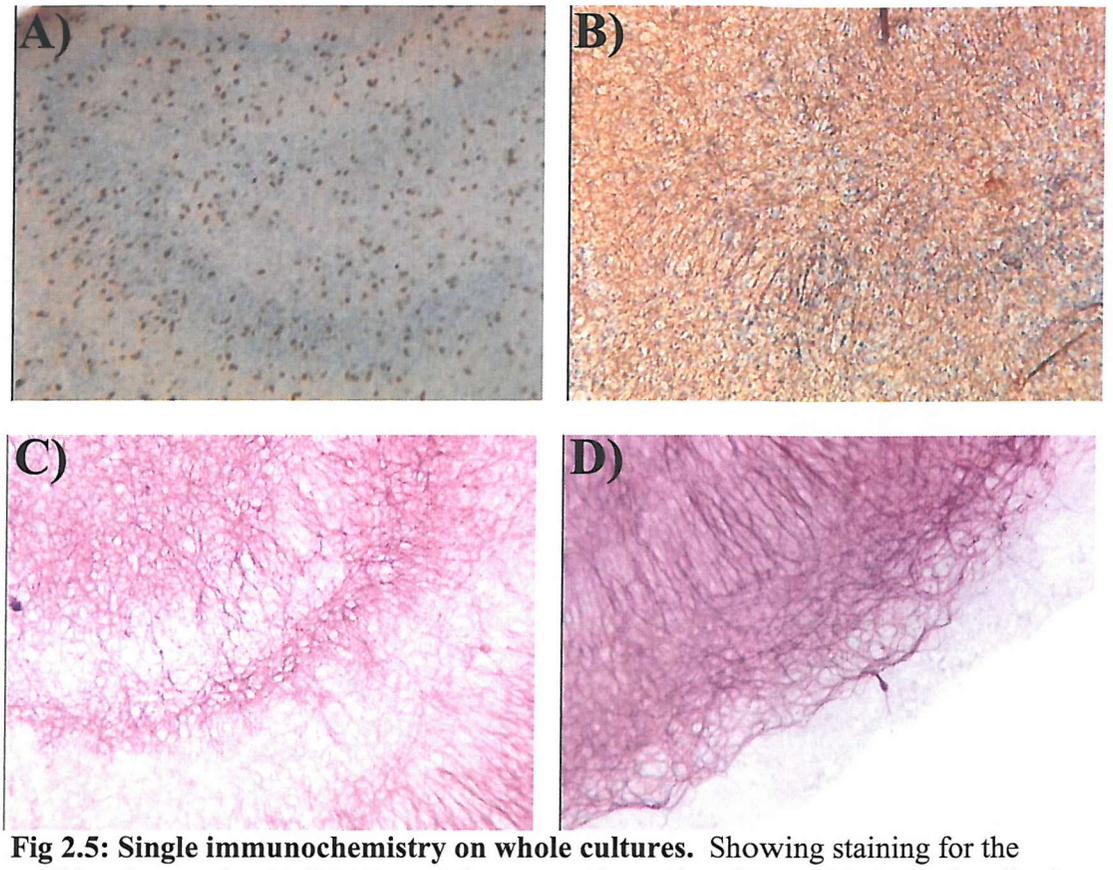

Fig 2.5: Single immunochemistry on whole cultures. Showing staining for the proliferation marker BrdU **(A)**, and the astrocytic marker GFAP **(B)**, both visualized with DAB (brown) and counterstained with thionine (blue) to reveal neuronal layers. **(C)** and **(D)** show staining for PSA-NCAM a marker for migrating neurons, visualized with VIP. In (D) it is clear that neuronal staining does not extend to the edge of the culture, possibly indicating the 'glial cap'. (A) is 10x magnification, all other images are 20x magnification.

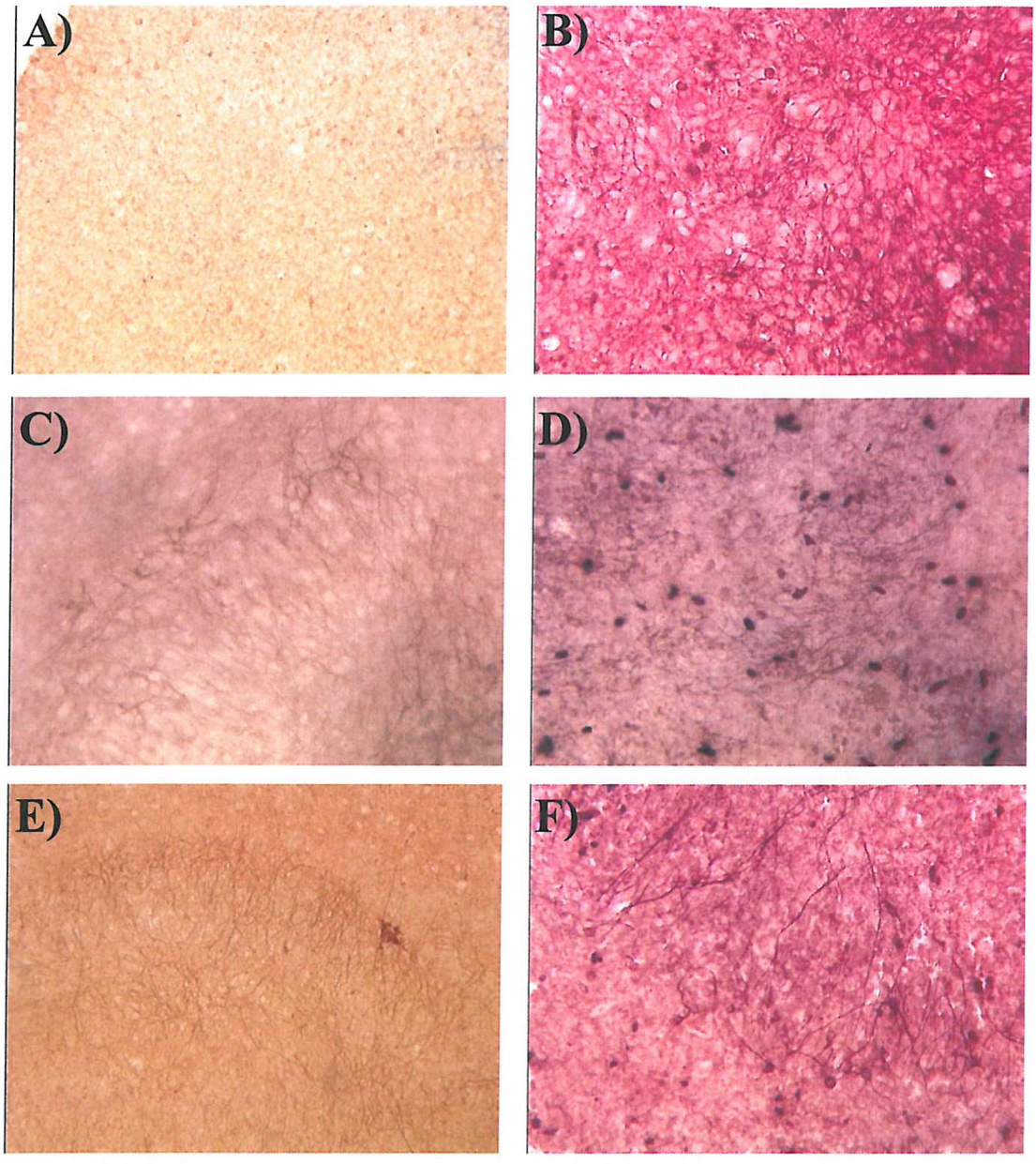

Fig 2.6: Single and double stain immunochemistry on whole cultures. Showing single staining for the astroglial marker s100b **(A)**, the early neuronal marker TUC-4 **(C)** and a marker for mature neurons class-III β-tubulin **(E)**, all antigens are visualized with DAB. Corresponding double stained cultures labelled with s100b **(B)**, TUC-4 **(D)** or class-III β-tubulin **(F)** all visualized with VIP (dark pink) and the proliferation marker BrdU (NDAB, Black). Images A and E are10x magnification, all other images are 20x magnification.

2.4 Discussion

Here we have examined the potential for identifying neurogenesis in OHSCs. Whilst the results obtained indicate that proliferating cells can be identified using BrdU, the identification of the phenotype of these proliferating cells is not so simple. Two factors combine to make this identification unfeasible. The organotypic cultures are produced from very young (P 8-10) rat pups and at the time of plating the hippocampus is only just formed, this means that early neuronal markers like β-tubulin are still expressed in virtually all neurons as they are mostly less than 4 weeks old. This produces a complex network of processes being labelled where identification of cells becomes difficult. While the clarity of the staining was sufficient with a single immunogen to permit accurate cell quantification using the double staining protocol produced a higher level of background staining and poor colour differentiation between the markers preventing accurate quantification. The problem of high background staining in the tissue stained for s100b is possibly due to detection of small quantities of the protein released from the astrocytes, since astrocytic s100b has been reported as influencing neurons (Donato, 1999). This is less of a problem when using in the fluorescent detection method, as there is less amplification with this technique than with the visible chromagen method.

In vivo the locations that are permissive for neurogenesis are tightly regulated; one of these sites is in the sub granular zone of the dentate gyrus. Similarly in the OHSCs it is this region that would be expected to produce the neurogenesis, unfortunately examination of the immunostained cultures revealed that the proliferating cells were not principally in the subgranular zone, or even the granule cell layer, but were ubiquitously distributed on the culture surface (Fig 2.5). As discussed previously confirmation of the phenotype of these proliferating cells was not possible due to difficulties in accurately identifying individual cells, but it is assumed that the majority of them are part of the glial scar that forms on the top of the cultures (Fig 2.2)(Del Rio, et al., 1991).

The confocal images obtained indicated a problem for quantifying changes in the cultures; if the antibodies are penetrating to different depths then counts of different cell markers become biased and are not based on the unit of a culture but on the fraction of that culture that has been stained. Variability of penetration depth between cultures could introduce even greater errors. Having seen this phenomenon in the

fluorescent tissue the cultures stained with DAB or VIP were re-examined, and the positive cells did appear to be concentrated in two focal planes, but this had not been considered as being of significance until the confocal analysis showed definitive proof that not all the culture was being stained. Because both fluorescent and non-fluorescent probes failed to penetrate deeply into the tissue, it was assumed that the problem lay with the depth that the primary antibodies could penetrate into the tissue. In order to continue using the whole culture experiments improved antibody penetration would be needed. Increasing antibody incubation time combined with reduced primary antibody concentrations have been shown to improve penetration (Best, et al., 1993). This improvement would probably come at the cost of higher background staining as increased incubation time typically increases background staining, something that is already a problem when using light microscopy. This would necessitate using confocal microscopy, where background staining was less of a problem, to image the cultures. This is both labour intensive and expensive, and combined with the fact that altering incubation times does not guarantee a sufficient increase in antibody penetration a different approach was adopted in subsequent experiments, with the cultures being cut in to 10μm thick sections. Cutting the cultures into thinner sections after they have been fixed has several advantages; the glial scar can be cut off the top of the tissue, the sections will not have antibody penetration problems and should have lower background, and this increase in staining clarity combined with the presence of fewer cells should permit easier quantification.

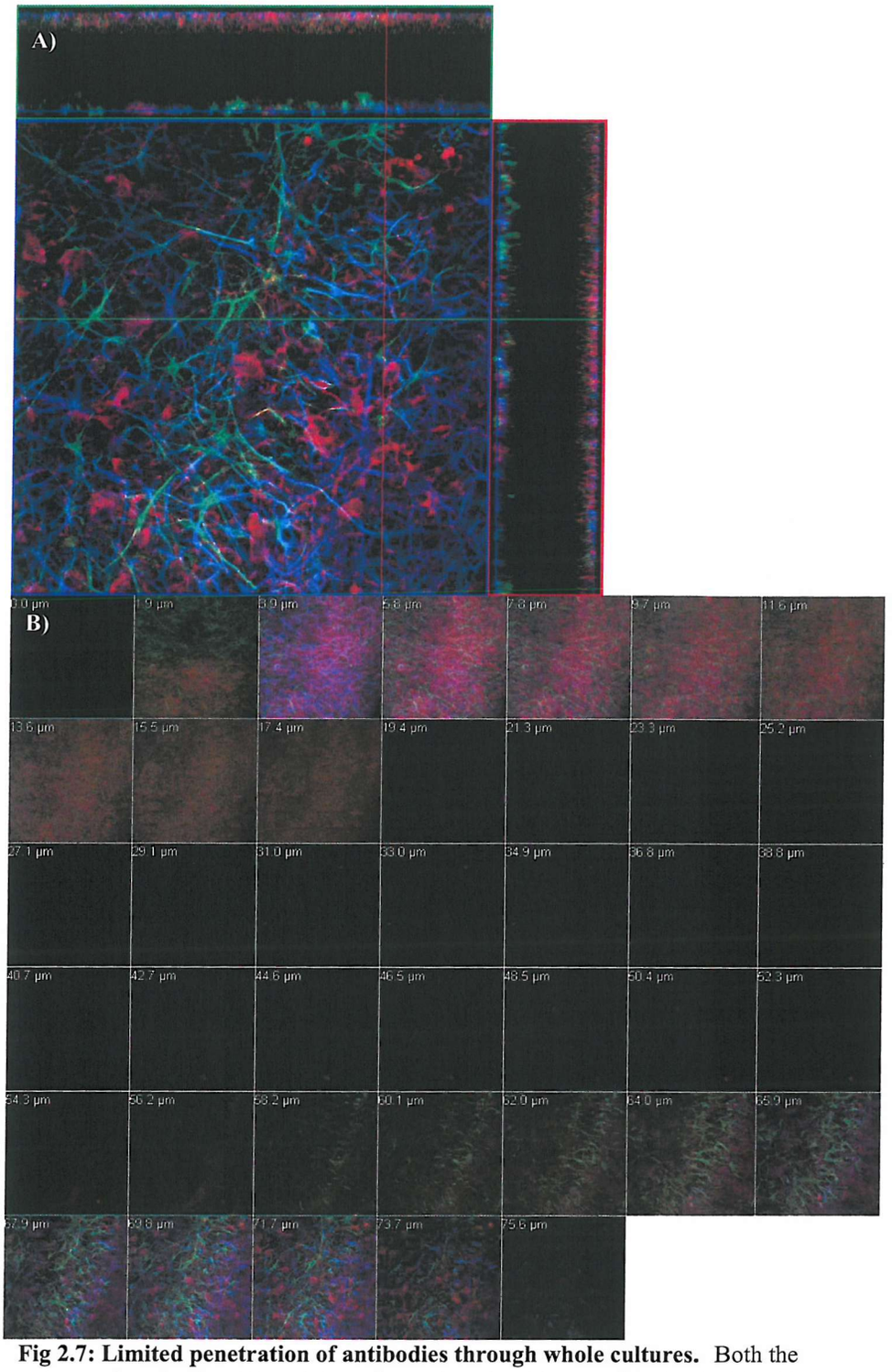

Fig 2.7: Limited penetration of antibodies through whole cultures. Both the orthogonal projection **(A)** and the gallery of confocal images **(B)** clearly identify staining at the top and bottom of the culture a distance of 15-20µm , with an unstained region in the middle. Staining is for the progenitor cell marker Nestin (Green), the immature neuronal marker doublecortin (Red), and the astrocytic marker GFAP (Blue). Imaged at 40x magnification using a confocal microscope.

Chapter 3

Measuring cell proliferation and death in the granule cell layer of Organotypic Hippocampal slice cultures

3.1 Introduction

In chapter 2, the potential for identifying neurogenesis in OHSCs was assessed. The results obtained indicated that proliferating cells could be identified, but at present neurogenesis could not. However, proliferation or 'cell birth' is not the only process occurring in the immature brain, cell death is also present (Kuan, et al., 2000). Cell death is an opposite effect to cell proliferation and thus, any model that we develop requires the ability to quantify both cell proliferation and cell death. This is because with any applied treatment three states for each of these parameters (cell proliferation and cell death) can arise – 1 an increase, 2 no change, and 3 a decrease. Some of these changes act synergistically on the overall population i.e. decreased proliferation and increased cell death would both act to decrease the overall population. Alternatively, other changes could cancel each other's effect i.e. increased proliferation and increased cell death, which would tend to produce no change in the overall population. In all of these examples, knowledge of the total granule cell population per section would help to add context to the changes being observed. Thus in order to improve the value of the model in addition to quantifying proliferation, which is already feasible, quantification of both granule cell numbers and cell death are desirable.

The results of the previous chapter also indicated that proliferation was ubiquitously distributed on the surface of the cultures (Fig 2.2), where a glial scar has been reported (Del Rio, et al., 1991). This is markedly different from the situation *in vivo* at this time, where proliferation is principally restricted to the SGZ and what remains of the tertiary matrix in the hilus, possibly with a few isolated cells dividing in the rest of the hippocampus (Altman and Bayer, 1990). In order to try and eliminate this 'un-organotypic' proliferation from the analysis of the experiments it was decided to section the cultures, an approach that has also recently been described elsewhere (Haydar, et al., 1999). This approach will result in the initial sections of the cultures containing the glial cap, which can be discarded, and then subsequent sections should be representative hippocampal tissue. Sectioning the cultures will also overcome the problem described in the previous chapter of antibody penetration, as the antibodies used thus far have penetrated at least 20microns into the culture tissue. In addition to solving the technical problems associated with quantifying proliferation that have

already been identified sectioning should fit with the requirements of the model we are developing, namely, quantification of cell proliferation, cell death and total granule cell number. Each of these parameters can be quantified on adjacent sections from the cultures, permitting all three parameters to be estimated in each culture.

3.1.1 Stereology as a tool for quantifying cells

One of the problems of quantitative analysis in the brain is the sheer number of cells present in each structure. Actual cell counts are impossible, as estimates of the number of granule cells in a 30 day old male Wister rat hippocampus range from 890 thousand to 1.2 million cells (West, et al., 1991), another study estimates there to be approximately 15 million granule cells in the human hippocampus (Rosenbaum, et al., 2001). All these estimates were obtained using stereological techniques or 'probes'; the cell counts obtained using two different probes in the hippocampus of rats in both cases of the same age, sex and strain clearly demonstrate that cell counting is highly variable (West, et al., 1991). Calculating the total volume of all the nuclei in the granule cell layer and dividing this by the mean volume of a granule cell nuclei obtained the lower estimate in the studies above. The larger estimate used an Optical fractionator probe to estimate cell numbers. The optical fractionator combines two sampling methods, the optical dissector and the fractionator.

The fractionator is a systematic uniform random sampling scheme for counting objects in two-dimensions, it distributes counting frames across a region of interest (ROI) and objects within the counting frames are noted. The object count is then scaled by the fraction of the ROI sampled, giving an estimate of the number of objects within the region of interest. The optical dissector counts objects in three dimensions; a depth of focus is defined within the counting frame (typically 20 microns), any object that comes into focus in those 20 microns is counted. Combining the two methods into the optical fractionator permits a random sampling of cells from a large ROI (the fractionator part) combined with an accurate count of cells due to tissue thickness (the optical dissector part). For estimating cell counts per hippocampus, the accurate identification of a cells location is important. When tissue is cut into sections inevitably some of the cells are cut in half, and can therefore appear in two adjacent sections. If a fractionator probe is used all cell's appearing in the counting frame are counted, and when counts from all sections are added the cells that are cut in half will all have been counted twice, overestimating the number of cells present.

However the addition of the optical dissector to this probe produces a more accurate estimate because in one of the two sections cells that have been cut in half will start in focus and so will not be counted, in the other section the cell will not start in focus but appear in the section and so will be counted. All cells are now only counted once. It is important to select an appropriate stereological technique, as many stereological methods are labour intensive and may eventually produce experimental errors that are larger than the expected change (Guillery and Herrup, 1997). The Optical fractionator is ideal for estimating total cell numbers in a large 3D structure. However, the fractionator method is simpler and can be considered adequate for comparing cell counts between single sections in different treatment conditions (Guillery and Herrup, 1997). This requires a less robust sampling as no estimate of the total population, from multiple sections, is being made. Instead, comparisons are between sections, and providing all groups are prepared for analysis in the same way the tissue should be comparable. The granule cell count in the dentate gyrus can be estimated using this technique as they are roughly evenly distributed and at a high density, but proliferating or dying cell numbers cannot be accurately estimated as their frequency is low and their distribution is variable.

3.1.2 Quantifying cell death

Cell death has been more extensively studied in the culture model than cell proliferation, our lab and others have established methods for quantifying cell death in the principle neuronal layers of OHSCs these typically use the fluorescent exclusion dye propidium iodide. The propidium iodide is usually added to the culture medium during and after an insult, where it becomes incorporated into the nucleus of cells whose membranes have become compromised (Wilde, et al., 1994). Cell death is measured as the area of the ROI exhibiting fluorescence, typically at 24 or 48 hours after insult, as a fraction of the area of the ROI measured from a transmission image captured before the insult (Pringle, et al., 1996). This method has been used to investigate cell death in mature (14 day old) cultures treated with excitotoxic chemicals, for example, glutamate (Vornov, et al., 1991), NMDA (Vornov, et al., 1991) and kainate (Vornov, et al., 1991; Best, et al., 1996), hypoxia (oxygen deprivation) (Pringle, et al., 1996), hypoglycemia (glucose deprivation) (Cater, et al., 2001), ischaemia (oxygen and glucose deprivation)(Pringle, et al., 1997); and mechanical stress or traumatic brain injury (Adamchik, et al., 2000). In addition to

the propidium iodide method, other markers of cell death have been used, the simplest of these are stains such as 4',6-diamidino-2-phenyindole (DAPI) and bisbenzimide (Hoescht33342), these stain the nucleus of cells and dead cells can then be identified by their morphology, the nuclei being shrunken and condensed (pyknotic) or fragmented (blebbing). Another technique, TdT-mediated dUTP-biotin nick end labelling (TUNEL), involves labelling the breaks in the DNA strands that form when cell undergo apoptotic death (Nijhawan, et al., 2000). Apoptotic death is by definition an instructed and controlled process, and as such has many potential markers; the proteins that are up regulated or activated in the signalling cascade that ends in cell death. Activated Caspase-3 is one such marker; a member of the effector caspases, caspase-3 is activated by cleavage of aspartate residues a process that normally leads to cell death (Earnshaw, et al., 1999). These markers of cell death are not all appropriate for this model; the PI stain intensity is partly dependent on the thickness of the cultures and this changes over time. TUNEL stain identifies strand breaks in DNA and BrdU incorporation leads to a weakening of the DNA, possibly leading to fragmentation and thus false positive staining. Finally, counting pyknotic cells located amongst densely packed healthy cells is labour intensive, so although activated caspase-3 is only an indirect marker of cell death it is the preferred marker in these experiments.

3.1.3 Culture variability

The techniques for quantifying cell proliferation, cell death and total cell number described above should permit the model we are developing to identify changes in the dentates of cultures arising from an applied treatment. However, before using the model other factors need to be considered, *in vivo* the dentate gyrus does not develop in exactly the same manner along its entire length. The septal and temporal extremes of the dentate gyrus form earlier than the mid dentate, this is associated with an earlier decrease in proliferation observed in sections of the dentate taken from the extremities (Bayer, 1980). This work does not attempt to quantify cell death across the septo-temporal axis and to the best of my knowledge, nor does any other literature. The difference in proliferation alone may be enough to induce increased variability (or error) into the measurements obtained, potentially limiting the value of the model for assessing changes induced by any treatment. Thus, a quantification of cell

proliferation, cell death and total granule cell count across the entire septo-temporal axis of the hippocampal formation is an important step in establishing and defining the proposed model.

3.1.4 Growth media

Another factor that could affect the state of the cultures is the medium they are grown in, different media types with different supplements are well documented as altering the types of cell and the levels of proliferation and death observed in primary cell cultures (Brewer, 1995; Lowenstein and Arsenault, 1996; Brewer, 1997).
The medium used when the OHSC method was established had a horse serum base supplying many of the factors necessary for survival of the cultures (Pringle, et al., 1996), and this is the media that previous experiments in our lab have used (Best, et al., 1996; Gatherer and Sundstrom, 1998; Cater, et al., 2001). The chemical constituents of horse serum have not all been identified, and the concentrations of those growth factors, etc. that have been identified are not standardized across all batches of the serum. Serum based growth media produces consistent levels of cell death in injury models, where serum free medium is used for short periods of injury induction without causing additional cell damaged medium. However, the effect of potentially variable growth factor concentration on proliferation has not yet been quantified. More recently a chemically defined medium has been developed for growing primary dissociated cultures (Brewer, et al., 1993). This medium differs from the horse serum based media in two ways; it is chemically defined and so the variability between batches is minimized and quantified, and whilst Horse serum has been suggested as inducing astrocytic differentiation (Brewer, et al., 1993), the defined medium (Neurobasal/B27) is more permissive to neurogenesis (Delatour and Witter, 2002). A comparison of these two types of medium is an opportunity to investigate the potential of this model to measure granule cell number, cell proliferation and cell death in the dentate gyrus. This is an important process as currently experiments in our lab using the horse serum based medium only take cultures from the septal hippocampus because those cultures from the temporal hippocampus can produce variable cell death (unpublished observations). Cultures grown in Neurobasal based medium might be viable along the entire extent of the hippocampus, and thus fewer animals would be needed to perform subsequent experiments, which is always an important consideration.

3.1.5 Questions to be addressed using OHSCs

The aim is to establish a model in OHSCs, where granule cell number, cell proliferation, and cell death can be quantified in the dentate gyrus. To achieve this a pulse of BrdU labelling is going to be used as a proliferative marker, activated caspase-3 will be used to identify apoptotic cells and a stereological technique, the fractionator, will estimate granule cell number in thionine stained tissue. To further the general aim of establishing this model the factors that can alter the homogeneity of both cell proliferation and cell death in the cultures under control conditions need standardizing. The principle factors that could affect these responses are the growth media type, the part of the hippocampus from which the culture is taken. Therefore, these experiments are designed at quantifying cell proliferation, cell death and total cell number in two different growth media and at many different hippocampal loci. To this end, matched cultures from all parts of the two hippocampi in a rat were taken and place in two media types. Data from four basic parameters was obtained; granule cell layer area, granule cell number, BrdU positive cells, and activated caspase-3 positive cells. The influence of these parameters on each other was also considered in three 1st order derivatives; granule cell layer density, and the proportion of granule cells that are BrdU positive or activated caspase-3 positive.

3.2 Methods

In all the experiments in this chapter, cultures were prepared as described in chapter 2.2.1, with the method of selecting cultures for each well and the treatment the cultures subsequently received until fixation detailed in section 3.2.1. The processing of all the cultures after fixation is subsequently described in sections 3.2.2 – 3.2.5.

3.2.1 Septo-temporal analysis of cell proliferation and death in 10-micron sections from Organotypic Hippocampal slice cultures.

Cultures were prepared as described in chapter 2.2.1; placing cultures into the inserts was carried out in a systematic manner such that the septo-temporal position of each culture is known and cultures are paired between the two media types. Slices from one hippocampus per animal are placed in NB medium and slices from the other are placed in HS medium, effectively matching the cultures between groups for septo-temporal position. BrdU (10μM) was added to the culture media after 5 days *in vitro* and the cultures fixed in 4% Paraformaldehyde (PFA) 2 hours later (Fig 3.1). Six 8-day-old Wistar rats were used in this experiment, with each hippocampus from the eight-day-old Wistar rats used in these experiments cut into sixteen 400μm sections containing dentate gyrus, and every other culture was analysed. The cultures are referred to by their position on the septo-temporal axis, with position 1 being the most temporal (position 2 was the most temporal culture analysed as a result of the sampling pattern) and position 16 being at the septal extreme.

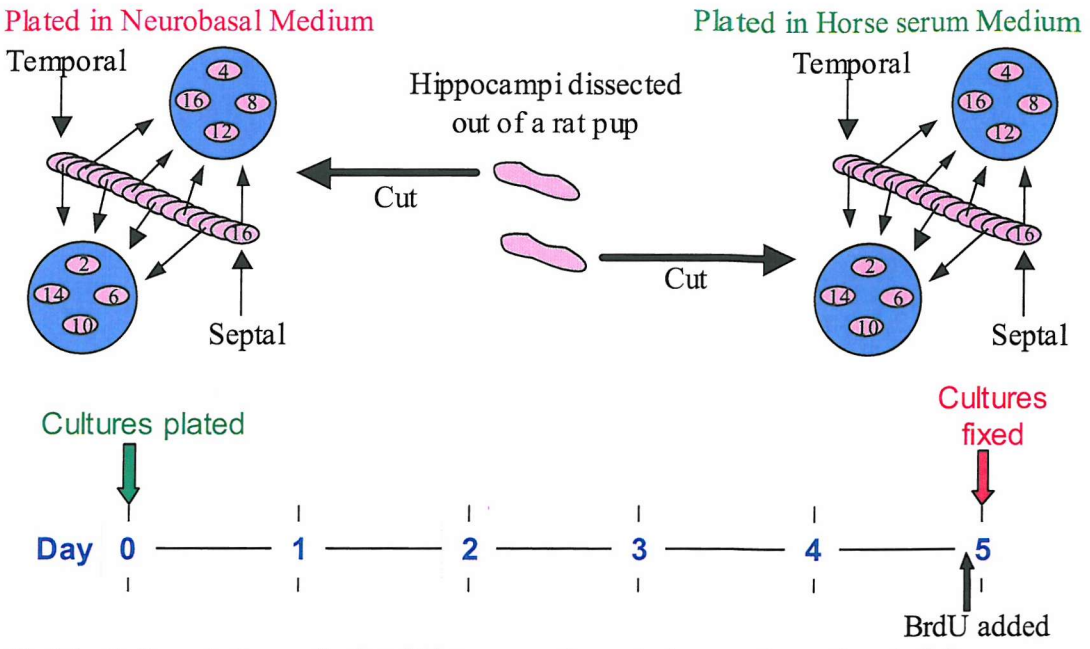

Fig 3.1: Culture plating method and Time course for septo-temporal experiment. Cultures were either grown in Neurobasal based medium or Horse serum based medium, and BrdU (10μM) was added to all cultures 2 hours before fixation in 4% PFA, after 5 days *in vitro*.

3.2.2 Cryosectioning

Following 24 hours in 4% PFA cultures are transferred to a 30% sucrose solution for 24 hours to protect cells from lysing during the freezing process. Single cultures were placed on the flat base of a metal dish, and the excess liquid removed, the culture was then covered in a drop of OCT (RA Lamb) and the dish containing the culture placed in liquid nitrogen, until the OCT became frozen. The dish was quickly transferred to the cold block (-30˚C) in the cryostat, with the chamber temperature maintained below –23˚C, and the culture in OCT removed using a scalpel. A covering of about 5mm of OCT was applied to an orientating chuck that had been pre-cooled on the cryostat's cold block. The culture in frozen OCT was then placed, flat surface up, on the chuck and the OCT allowed to freeze. With the culture frozen onto it, the chuck was placed in the microtome and aligned by eye with the cutting blade. Careful approach sections were taken, correcting the orientation of the culture until cutting blade and culture lay in parallel planes. The initial two sections were discarded as they generally do not contain complete hippocampi and the topmost part of the cultures has the glial scar. The next four 10μm sections were collected on separate gelatinised slides, this process was repeated collecting another section on each slide, and the sections stored at –74˚C until needed.

3.2.3 Immunostaining

Adjacent sections from each culture were stained with thionine, BrdU and activated caspase-3; allowing estimation of total granule cell number, and counts of proliferating cells and apoptotic cells respectively.

Tissue processed for BrdU immunohistochemistry was exposed to 2N HCl at 37°C for 20 minutes. All tissue processed for immunohistochemistry received multiple washes in Tris-Buffered Saline (TBS; 0.1M, pH7.4), followed by incubation with 3% H_2O_2 in distilled water for 10 minutes to eliminate non-specific peroxidase activity. Further TBS washes were followed by overnight incubation with primary antibody to either BrdU (rat monoclonal, 1:1000; Oxford Biotech) or activated caspase-3 (New England Biolabs.) in TBS containing 0.1% triton and 0.05% Bovine Serum Albumin (TBS-TS) at 4°C, tissue processed for BrdU also had 1% Normal Goat Serum (Sigma) present with the primary antibody. Following multiple washes in TBS, tissue was incubated in TBS-TS with the appropriate biotinylated secondary antibody, raised against either rat (goat, 1:200; Vector) or rabbit (swine, 1:500; DAKO) for 1 hour. TBS washes were repeated and a Horseradish peroxidase conjugated Streptavidin-biotin complex (HRP-ABC, 1:200; DAKO) in TBS-TS was applied for 1 hour, further washing in TBS was followed by visualization with 3,3-Diaminobenzene (DAB, brown; Vector) and a final set of washes. Cultures were mounted on gelatinised slides and where necessary received a light Thionine counter-stain to facilitate granule cell layer identification. Thionine staining was obtained by placing slides in distilled water containing 1% Thionine followed by differentiation in 90% Ethanol with 5% Acetic acid until a consistent staining intensity was observed. All cultures were dehydrated through 1 minute washes in alcohol (70%, 90% and 2x 100%) and then xylene before cover-slipping with DPX (Sigma).

3.2.4 Cell counting and stereology

For all quantification, slides were coded and counts carried out with the examiner blind to the experimental condition of each section. A mask of the granule cell layer was generated with the contour tool in StereoInvestigator™ (Ver. 5.0; Microbrightfield) software package; using the thionine stained section as a template

(Fig 3.2 A and B). The mask was then superimposed onto adjacent sections from the same OHSC, which had been immunostained for either BrdU or activated caspase-3 and exhaustive counts carried out within the area defined by the mask. Estimation of total cell number was carried out using the fractionator probe in StereoInvestigator™; the software controlled a motorized stage (LEP) attached to a light microscope (Dialux 22, Leitz), live video images obtained with a Flashpoint3D graphics card (Ver. 1.54; Integral Technologies), through a CCU, DEI-750D digital camera and controller (Optronics).

Examination of the thionine-stained section, under low magnification (10x; Fig 3.2), allowed the granule cell layer to be outlined using the contour feature in StereoInvestigator, this became the region of interest (ROI). A virtual grid with spacing of 100μm x 100μm was thrown over the ROI, with a randomised orientation and starting location, this grid contained counting frame 25μm x 25μm located in the upper left corner of each square (Fig 3.2).

Counting frames within the ROI were then examined under higher magnification (63x) and cell bodies, which lay within the counting frame or touched the green lines of the counting frame were marked on the virtual grid, any cell which touched a red line was not counted (Fig 3.2). The software then generated an estimate of cell numbers and the associated error (Scheaffer coefficient of error) for the whole ROI. Estimated cell counts obtained from multiple cultures were then expressed as a mean and the associated error of sampling calculated using both the Scheaffer coefficient of error, a value heavily dependant on variation between counting frame counts, and the Gunderson coefficient of error, a value principally governed by variation between cultures. A coefficient of error of less than 0.15 was considered acceptable.

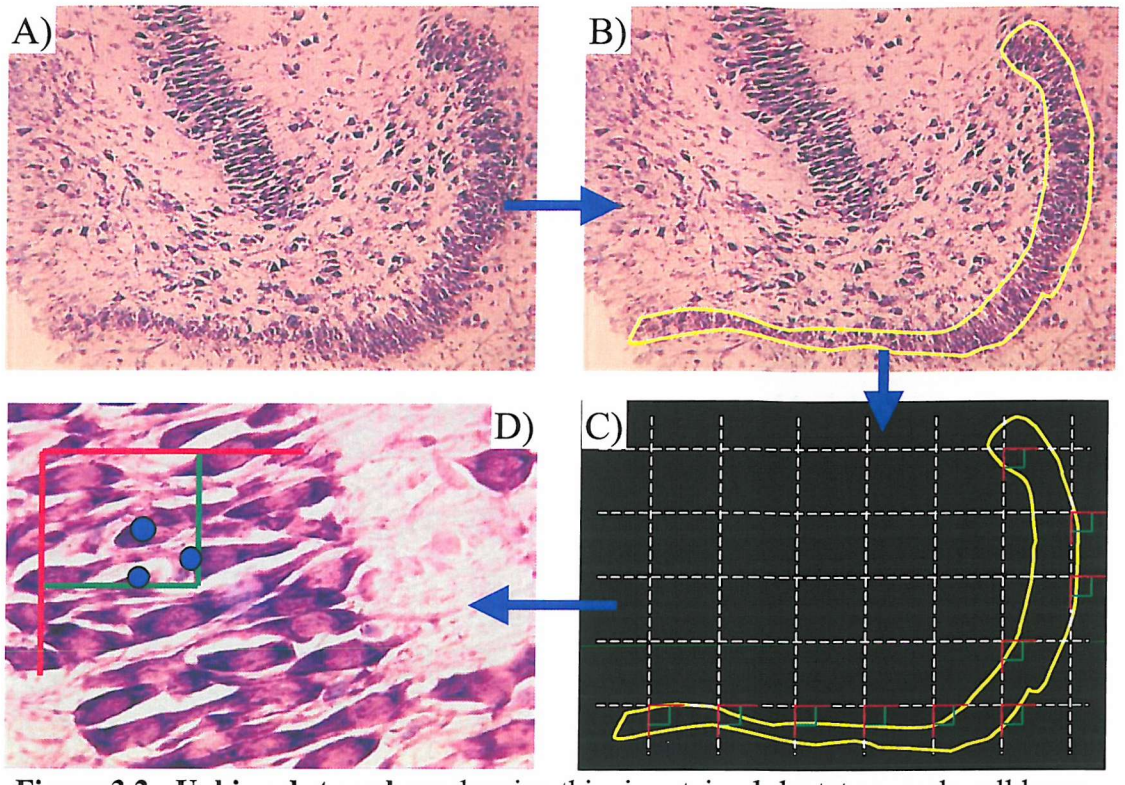

Figure 3.2: Unbiased stereology showing thionine stained dentate granule cell layer and hilus at low (10x) magnification **(A)**, with the region of interest marked **(B)**, a computer generated randomly positioned and orientated 100µm x 100µm grid containing 25µm x 25µm sampling frames **(C)** and a high (63x) magnification image of a counting frame placed over the granule cell layer with 3 counted cells marked **(D)** Note; overlays on images are for demonstration and not necessarily to scale.

3.2.5 Statistical analysis

Statistical analysis was used to investigate each of the seven factors; Area, cell count, cell density, BrdU positive cells, activated capsase-3 positive cells and the proportion of the granule cells that were either BrdU or activated caspase-3 positive. Two-way ANOVA was used to investigate the overall contributions of media type (column factor), septo-temporal position (row factor) and interaction between row and column factors on data variance; Bonferroni post hoc test compared media types at each position where the cultures are paired between with one hippocampus per animal contributing cultures to each media type. Comparison between sections of different position in the same medium was by one-way ANOVA with Bonferroni post hoc test; these cultures were not matched to the same extent as comparisons between media types at each position. Statistical significance is expressed at the 0.05, 0.01 and 0.001 levels. Two of the factors investigated are ratios with a range limited to between 0

and 1. These factors were subjected to a Kolmogorov-Smirnov test to ensure that they approximated to a Gaussian distribution prior to ANOVA analysis.

3.3 Results

Cultures in this experiment are paired between media types, so at each position the number of cultures analysed is the same for each medium; if one of the pair of sections was incomplete then both of the sections were excluded from the results. The exception to this is at position 8 in tissue stained for activated caspase-3 where only cultures grown in Neurobasal medium are analysed, as all the remaining sections (after cell counts and BrdU counts had been completed) of cultures grown in horse serum medium were incomplete. Culture area, cell count and density are averages of 4 cultures (positions 4, 6, 8, 14 and 16), except at position 2 and position 10 (both 3 cultures) and position 12 (5 cultures). BrdU cell counts and proportions are taken from a subset of these cultures, typically with an average of 3 cultures (positions 2, 6, 8, 12, 14 and 16), with position 10 (2 cultures) and position 4 (4 cultures) being exceptions. Similarly, activated caspase-3 cell counts and proportions are taken from a subset of the cultures used for total cell counting, typically with an average of 2 cultures (positions 2, 4, 10, 12, and 14), with position 10 (3 cultures) and positions 6 and 8 (4 cultures) the exceptions.

3.3.1 Area and cell counts increase in a temporal to septal direction but density is unchanged in the cultures grown in horse serum

There is a trend for increasing granule cell layer area and granule cell number as cultures become more septal when they are maintained in HS medium. The GCL of cultures from positions 12 and 14 ($0.158\pm0.022mm^2$ and $0.163\pm0.088mm^2$) have a significantly larger area than those in position 2 ($0.069\pm0.013mm^2$), the mean GCL area of cultures from position 14 is also significantly larger than that at position 6 ($0.075\pm0.024mm^2$). Significantly, fewer cells were observed in temporal horse serum cultures than in cultures taken from the septal hippocampus and a trend for increasing granule cell numbers as cultures became more septal was also evident. Position 2 had significantly fewer cells (555±88 cells) than positions 12 and 14 (1862±356 cells and 1884±1242 cells; Fig 3.3). The combination of these parallel trends resulted in a density of cells in the GCL that did not change significantly depending on the position sampled ($p=0.47$; One-way ANOVA; Fig 3.3).

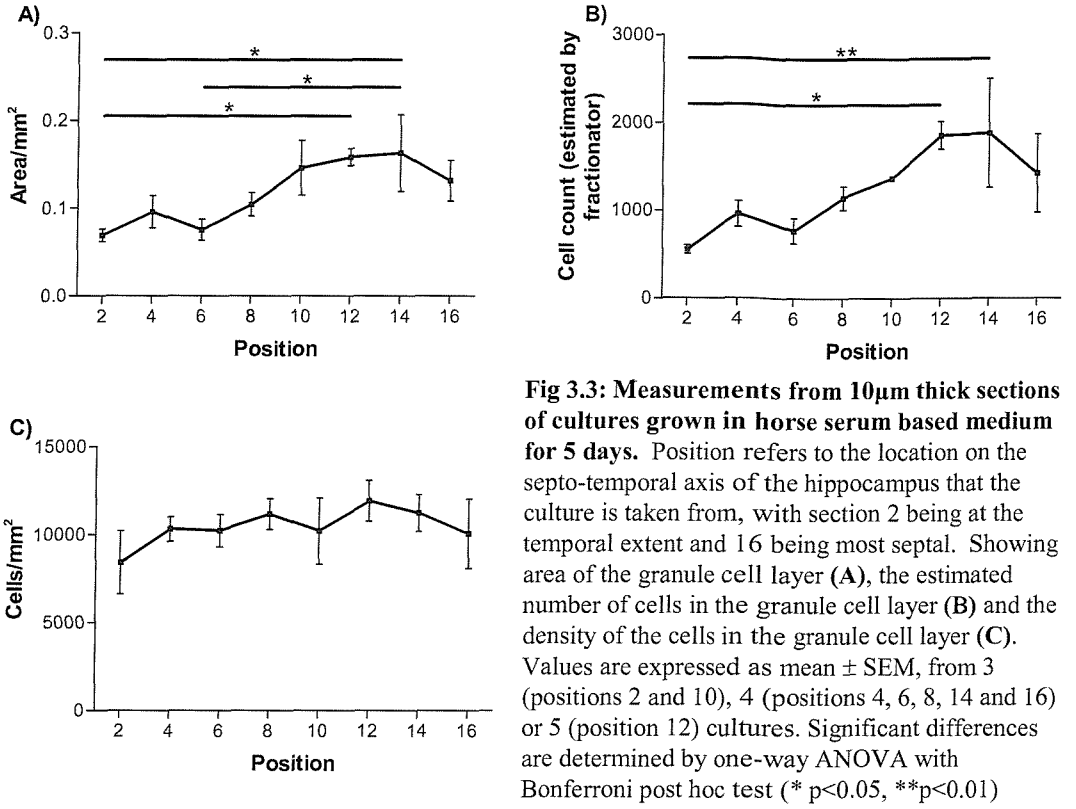

Fig 3.3: Measurements from 10μm thick sections of cultures grown in horse serum based medium for 5 days. Position refers to the location on the septo-temporal axis of the hippocampus that the culture is taken from, with section 2 being at the temporal extent and 16 being most septal. Showing area of the granule cell layer **(A)**, the estimated number of cells in the granule cell layer **(B)** and the density of the cells in the granule cell layer **(C)**. Values are expressed as mean ± SEM, from 3 (positions 2 and 10), 4 (positions 4, 6, 8, 14 and 16) or 5 (position 12) cultures. Significant differences are determined by one-way ANOVA with Bonferroni post hoc test (* $p<0.05$, ** $p<0.01$)

3.3.2 BrdU and the proportion of BrdU positive cells are highly variable in cultures of different septo-temporal loci grown in horse serum medium

The septo-temporal BrdU profile of cultures grown in horse serum was much more varied than area or cell count; significantly more BrdU positive cells were observed at position 12 (57.7±11.0 cells) than at positions 2 (27.3±6.7 cells; $p<0.05$), 4 (18.8±2.5 cells; $p<0.01$), 6 (24.7±4.0 cells; $p<0.05$), 10 (24.0±1.4 cells; $p<0.01$) and 14 (14.3±8.0 cells; $p<0.001$). In addition to having significantly fewer cells than the cultures from position 12, cultures from position 14 also had fewer cells than cultures from position 8 (44.0±26.2 cells; $p<0.05$) and position 16 (47.7±28.0 cells; $p<0.01$). Unlike the results for area and cell count, which demonstrated a tendency for larger values in septal cultures, BrdU positive cell counts showed no trend relative to septo-temporal position (Fig 3.4).

Another way of examining changes in BrdU labelling is to consider the fraction of the whole granule cell population, which is BrdU positive. This measure minimizes differences between the cultures caused by changes in granule cell number; the value of this effect is discussed in section 3.4. In the HS cultures, the proportion of cells labelled with BrdU varies quite considerably. Cultures from position 2 (5.06±1.7% of cells) have a significantly higher proportion of BrdU positive cells than those from position 4 (2.17±1.0% of cells; $p<0.05$), position 10 (1.76±0.1% of cells; $p<0.01$), and

position 14 (1.05±0.3% of cells; $p<0.001$), cultures from position 14 also have a significantly lower proportion of BrdU positive cells than cultures from position 8 (4.03±2.2% of cells; $p<0.01$; Fig 3.4).

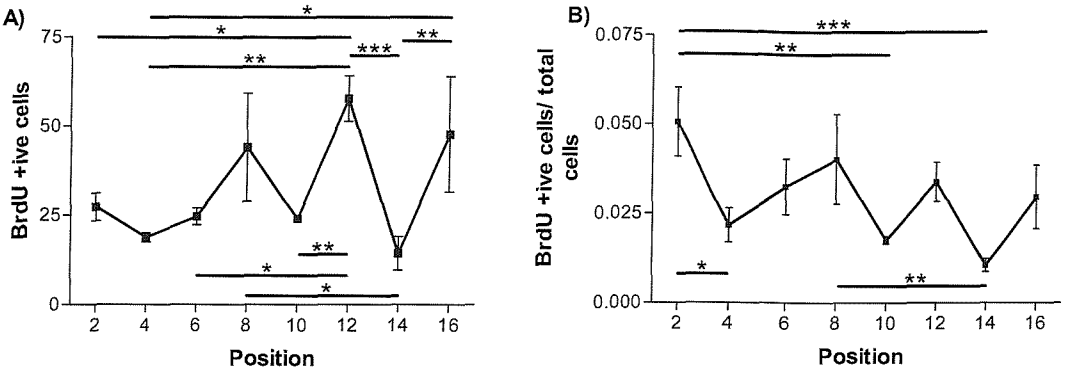

Fig 3.4: BrdU measurements from 10µm thick sections of cultures grown in horse serum based medium for 5 days. Position refers to the location on the septo-temporal axis of the hippocampus that the culture is taken from, with section 2 being at the temporal extent and 16 being most septal. Showing mitotic activity in the granule cell layer identified by BrdU immunochemistry, as absolute cell counts **(A)** and as a proportion of the cells present **(B)**. Values are expressed as mean ± SEM, from 2 (position 10), 3 (positions 2, 6, 8, 12, 14 and 16) or 4 (position 4) cultures. *Asterisks* denote significant differences determined by One-way ANOVA with Bonferroni post hoc test (* $p<0.05$, ** $p<0.01$, *** $p<0.001$).

3.3.3 Caspase-3 activation is not changed by hippocampal locus in cultures grown in horse serum medium

Levels of caspase-3 activation in the cultures grown in HS medium were not greatly altered by septo-temporal position. There are no significant differences between the numbers of activated caspase-3 positive cells at any position and the only significant change in the proportion of activated caspase-3 positive cells is between position 4 (0.6±0.9% of cells) and position 16 (3.9±4.4% of cells; $p<0.05$). No analysis could be performed on sections from position 8 as none of the sections in this group had complete dentate granule cell layers (Fig 3.5).

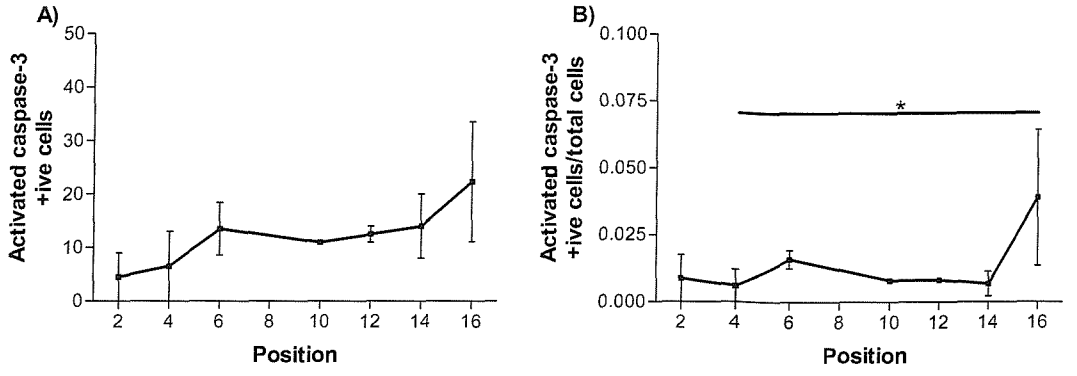

Fig 3.5: Activated caspase-3 measurements from 10μm thick sections of cultures grown in horse serum based medium for 5 days. Position refers to the location on the septo-temporal axis of the hippocampus that the culture is taken from, with section 2 being at the temporal extent and 16 being most septal. Showing apoptotic cell death identified by activated caspase-3 immunochemistry, as absolute cell counts **(A)** and as a proportion of the cells present **(B)**. Values are expressed as mean ± SEM, from 2 (positions 2, 4, 10, 12 and 14), 3 (position 10) or 4 (position 6) cultures, no cultures from position 8 were assessed. *Asterisks* denote significant differences determined by One-way ANOVA with Bonferroni post hoc test (* $p<0.05$, ** $p<0.01$, *** $p<0.001$).

3.3.4 Area and cell counts and density are lower in temporal cultures grown in Neurobasal medium

Cultures grown in NB medium, like those grown in HS medium, have a trend for increasing granule cell layer area and granule cell number as they become more septal. The GCLs of cultures from positions 2 and 4 ($0.130\pm0.049mm^2$ and $0.136\pm0.036mm^2$) are significantly smaller than those in positions 12, 14 and 16 ($0.340\pm0.111mm^2$, $0.310\pm0.138mm^2$ and $0.300\pm0.123mm^2$ respectively). Similarly significantly fewer cells were observed in cultures from positions 2, 4 and 6 (933±587 cells, 1372±376 cells and 1708±288 cells respectively) than position 12 (3933±1559 cells); cultures from positions 2 and 4 also had fewer cells than position 14 (3468±1825 cells) and counts from position 2 and 16 (3276±1121 cells) are also significantly different (Fig 3.6). This suggests the septo-temporal change in these cultures is quite dramatic, both for area and especially for granule cell counts.

The density of cells also changed significantly across the granule cell layer ($p<0.01$; one-way ANOVA). The most temporal cultures (position 2, 6503±2617 cells/mm^2) had significantly lower granule cell densities than cultures from positions 8 and 12 (12966±3901 cells/mm^2 and 11530±2724 cells/mm^2) when grown in Neurobasal medium. The cell densities in all the other cultures are similar to those and day 12

(ranging between 10 and 12 thousand cells/mm^2), indicating that although there are differences between some sections the general trend is for a consistent density across cultures grown in NB medium (Fig 3.6).

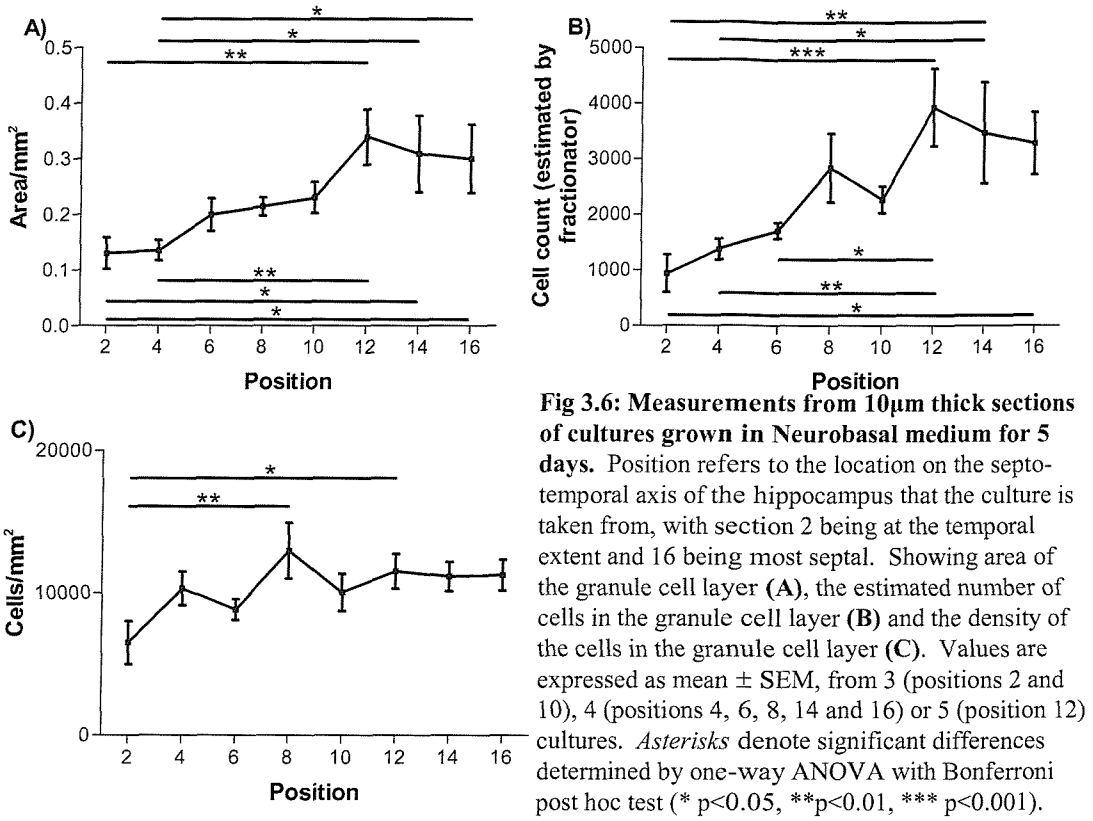

Fig 3.6: Measurements from 10µm thick sections of cultures grown in Neurobasal medium for 5 days. Position refers to the location on the septo-temporal axis of the hippocampus that the culture is taken from, with section 2 being at the temporal extent and 16 being most septal. Showing area of the granule cell layer **(A)**, the estimated number of cells in the granule cell layer **(B)** and the density of the cells in the granule cell layer **(C)**. Values are expressed as mean ± SEM, from 3 (positions 2 and 10), 4 (positions 4, 6, 8, 14 and 16) or 5 (position 12) cultures. *Asterisks* denote significant differences determined by one-way ANOVA with Bonferroni post hoc test (* $p<0.05$, **$p<0.01$, *** $p<0.001$).

3.3.5 BrdU cell counts increase in a temporal to septal direction but the proportion of cells incorporating BrdU is unchanged in the cultures grown in Neurobasal medium

The profile of BrdU incorporation across the septo-temporal axis in NB cultures shows significantly fewer BrdU positive cells were detected at position 2 (32.0±1.0 cells) than position 10 (63.5±20.5 cells; $p<0.05$) and position 16 (69.0±13.9 cells; $p<0.01$). Additionally as with the granule cell count data there was also a trend for increased BrdU positive cell counts as cultures became more septal. However, the position a culture grown in Neurobasal medium is taken from does not significantly alter the proportion of BrdU positive cells observed (Fig 3.7).

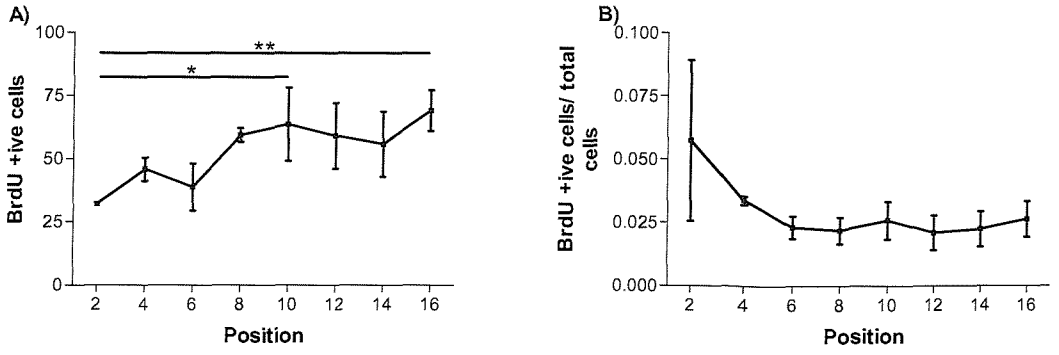

Fig 3.7: BrdU measurements from 10μm thick sections of cultures grown in Neurobasal medium for 5 days. Position refers to the location on the septo-temporal axis of the hippocampus that the culture is taken from, with section 2 being at the temporal extent and 16 being most septal. Showing mitotic activity in the granule cell layer identified by BrdU immunochemistry, as absolute cell counts **(A)** and as a proportion of the cells present **(B)**. Values are expressed as mean ± SEM from 2 (position 10), 3 (positions 2, 6, 8, 12, 14 and 16) or 4 (position 4) cultures. *Asterisks* denote significant differences determined by One-way ANOVA with Bonferroni post hoc test (* $p<0.05$, ** $p<0.01$, *** $p<0.001$).

3.3.6 Cultures from both extremes of the hippocampus had significantly higher caspase-3 activation than those in the centre when grown in Neurobasal medium

The cultures grown in NB medium have significantly more activated caspase-3 positive cells at both extremes of the septo-temporal axis than in the centre. The most temporal cultures examined, position 2, had significantly more activated caspase-3 positive cells than any of the other sections (position 2, 100.0±33.9 cells vs. position 4, 18.5±7.8 cells; position 6, 30.5±6.8 cells; position 8, 25.5±10.0 cells; position 10, 18.5±4.9 cells; position 12, 9.5±4.9 cells; position 14, 17.5±7.8 cells, all $p<0.001$; and position 16, 69.7±19.6 cells, $p<0.05$). Cultures from the septal extreme, position 16, in addition to having significantly fewer activated Caspase-3 positive cells than position 2, have significantly more positive cells than all the other positions (all $p<0.001$, except position 6, $p<0.01$; Fig 3.8). When the proportion of cells expressing activated caspase-3 is considered cultures from the septal extreme (position 16) are not significantly different from the bulk of the cultures, however cultures from position 2 retain a significantly higher proportion of activated caspase-3 positive cells (19.6±14.2% of cells) than cultures from any other position (4, 1.7±1.1% of cells; 6, 1.8±0.7% of cells; 8, 0.9±0.3% of cells; 10, 0.7±0.1% of cells; 12, 0.4±0.2% of cells; 14, 0.5±0.1% of cells; and 16, 1.9±0.2% of cells; all $p<0.001$; Fig 3.8).

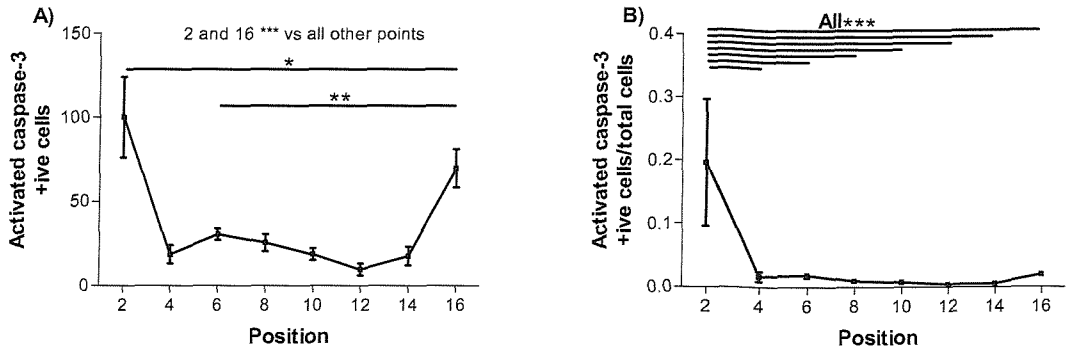

Fig 3.8: Activated caspase-3 measurements from 10μm thick sections of cultures grown in Neurobasal medium for 5 days. Position refers to the location on the septo-temporal axis of the hippocampus that the culture is taken from, with section 2 being at the temporal extent and 16 being most septal. Showing apoptotic cell death identified by activated caspase-3 immunochemistry, as absolute cell counts **(A)** and as a proportion of the cells present **(B).** Values are expressed as mean ± SEM, from 2 (positions 2, 4, 10, 12 and 14), 3 (position 10) or 4 (positions 6 and 8) cultures. *Asterisks* denote significant differences determined by One-way ANOVA with Bonferroni post hoc test (* $p<0.05$, ** $p<0.01$, *** $p<0.001$). In **(A)** sections 2 and 16 are *** compared with all other sections.

3.3.7 What does a two-way ANOVA do?

Analysis up until now has been by one-way ANOVA with Bonferroni post testing, the one-way ANOVA requires at least three groups and considers the question: If the means of these groups are equal what is the probability of observing the experimental result obtained? The post hoc test compares the means of each group and can identify those groups where the means have a low probability (less than 5%) of being the same. In the above analysis these groups are the septo-temporal position of the cultures (8 groups), however the effects of media type cannot be considered in the same manner as septo-temporal position, as only 2 types of medium were used.

So comparisons between media were made by two-way ANOVA with Bonferroni post hoc testing; the two-way ANOVA can be used to determine how a response is affected by two factors. In these experiments, the responses tested are area, cell count, BrdU count, etc. and the two factors being investigated are the media type, and the septo-temporal position. The two-way ANOVA simultaneously asks 3 questions of this data, does the media type affect the means? Does the position affect the means? And do media type and position interact? Interaction tests for consistency between the differences arising from media type at each position, i.e. interaction becomes significant when the difference between media types changes at different positions. When interaction is statistically significant, it becomes difficult to interpret any effect on media type or position.

3.3.8 Area and cell counts are greater when cultures are grown in Neurobasal medium but density is unchanged by media type

The mean GCL areas and mean granule cells counts for cultures grown in NB and HS medium differ significantly (both $p<0.001$); two-way ANOVA). The difference in the areas is significant at positions 12, 14 and 16, at all these loci growth in NB medium results in cultures with larger GCL areas; position 12 (NB, $0.340\pm0.111mm^2$ and HS, $0.158\pm0.022mm^2$; $p<0.01$), position 14 (NB, $0.310\pm0.138mm^2$ and HS, $0.163\pm0.088mm^2$; $p<0.05$), and position 16 (NB, $0.300\pm0.123mm^2$ and HS, $0.131\pm0.046mm^2$; $p<0.05$). Similarly, the number of granule cells present in each dentate gyrus is also significantly greater in cultures grown in NB medium at positions 12 (NB, 3933±1559 cells vs. HS, 1862±356 cells; $p<0.01$) and 16 (NB, 3276±1121 cells vs. HS, 1424±895 cells; $p<0.05$) than those grown in HS medium (Fig 3.9). The significant increases in GCL area (positions 12, 14 and 16) and cell count (positions 12 and 16) in cultures grown Neurobasal medium are reflected in the trends of all the other positions sampled along the septo-temporal axis (Figs 3.9A and B). A consequence of the matching of these trends in area and cell count is that the densities of the cells in the dentate gyrus are not significantly different between the media ($p=0.85$ two-way ANOVA; Fig 3.9C).

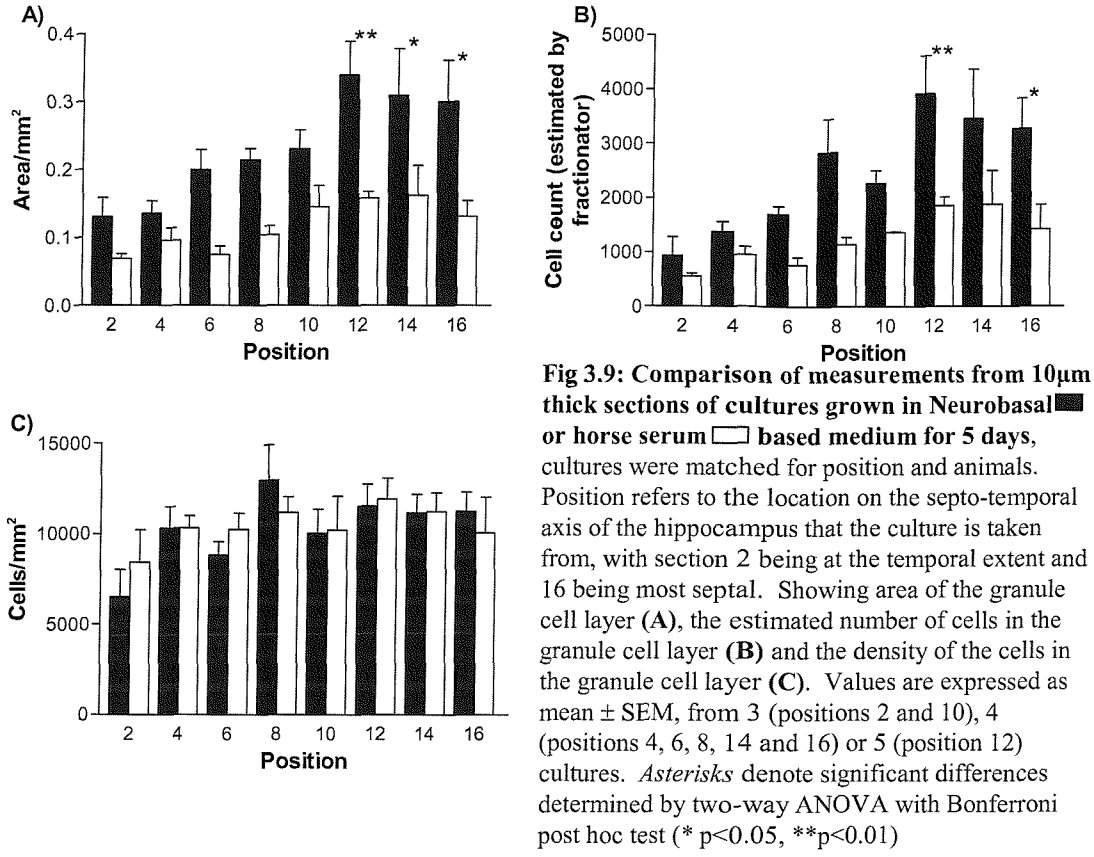

Fig 3.9: Comparison of measurements from 10μm thick sections of cultures grown in Neurobasal■ or horse serum□ based medium for 5 days, cultures were matched for position and animals. Position refers to the location on the septo-temporal axis of the hippocampus that the culture is taken from, with section 2 being at the temporal extent and 16 being most septal. Showing area of the granule cell layer **(A)**, the estimated number of cells in the granule cell layer **(B)** and the density of the cells in the granule cell layer **(C)**. Values are expressed as mean ± SEM, from 3 (positions 2 and 10), 4 (positions 4, 6, 8, 14 and 16) or 5 (position 12) cultures. *Asterisks* denote significant differences determined by two-way ANOVA with Bonferroni post hoc test (* $p<0.05$, ** $p<0.01$)

3.3.9 BrdU cell counts differ significantly but the proportion of cells incorporating BrdU is unchanged in the cultures grown in the different media types

The average number of BrdU positive cells observed in cultures grown in each media type differs significantly ($p<0.001$), and at position 14 cultures grown in NB have significantly more BrdU positive cells (NB, 55.7±22.3 cells vs. HS, 14.3±8.0 cells; $p<0.05$). However, the growth medium used does not significantly affect the mean proportion of cells that are BrdU positive ($p=0.916$; two-way ANOVA; Fig 3.10).

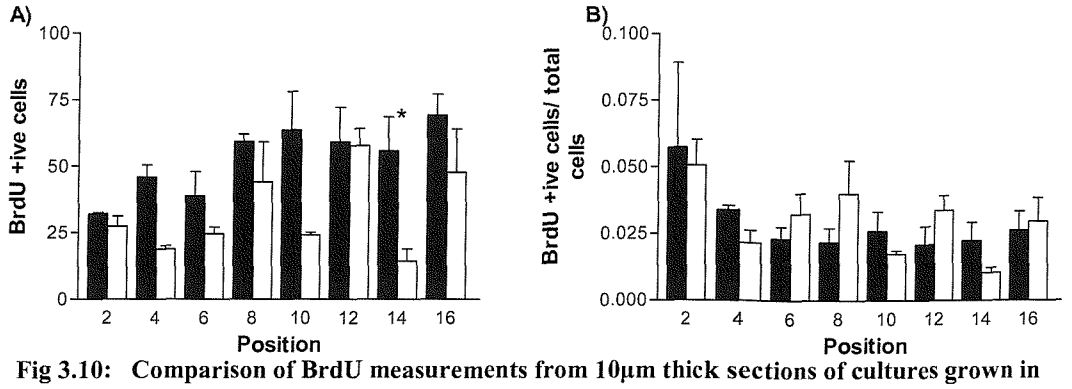

Fig 3.10: Comparison of BrdU measurements from 10μm thick sections of cultures grown in Neurobasal ■ or horse serum □ based medium for 5 days, cultures were matched for position and animals. Position refers to the location on the septo-temporal axis of the hippocampus that the culture is taken from, with section 2 being at the temporal extent and 16 being most septal. Showing mitotic activity in the granule cell layer identified by BrdU immunochemistry, as absolute cell counts **(A)** and as a proportion of the cells present **(B)**. Values are expressed as mean ± SEM from 2 (position 10), 3 (positions 2, 6, 8, 12, 14 and 16) or 4 (position 4) cultures. *Asterisks* denote significant differences between groups determined by two-way ANOVA with Bonferroni post hoc test (* $p<0.05$, ** $p<0.01$).

3.3.10 Cultures take from the hippocampal extremities have significantly higher caspase-3 activation when grown in Neurobasal medium

Comparison of overall differences between activated caspase-3 positive cells between media type was not possible as significant interaction between the growth media and hippocampal locus ($p<0.001$) was observed, i.e. the quantity of immunostaining observed at different hippocampal loci was not consistent for each media and the number of positive cells observed for each media type was not consistent at each locus. When the two factors in the two-way ANOVA interact the results for the individual factors can be misleading, however the post hoc tests are still valid. Cultures that were taken from position 2 (NB, 100±33.9 cells and HS, 4.5±6.4 cells; $p<0.001$) and position 16 (NB, 69.7±19.6 cells and HS, 22.3±19.4 cells; $p<0.01$) had significantly more activated caspase-3 positive cells when grown in Neurobasal medium (Fig 3.11).

Two-way ANOVA analysis of the proportion of cells that are activated caspase-3 positive also showed significant interaction between growth media and hippocampal location ($p<0.01$). Post hoc analysis demonstrated that cultures from the most temporal position (2) grown in Neurobasal medium have a significantly higher proportion of activated caspase-3 positive cells than cultures from the same position grown in horse serum medium (NB, 19.6±14.2% of cells and HS, 0.9±1.2% of cells; $p<0.001$; Fig 3.11). All cultures from position 8 were excluded from the two-way

ANOVAs involving activated caspase-3 because there were no complete sections from cultures grown in HS medium in this group.

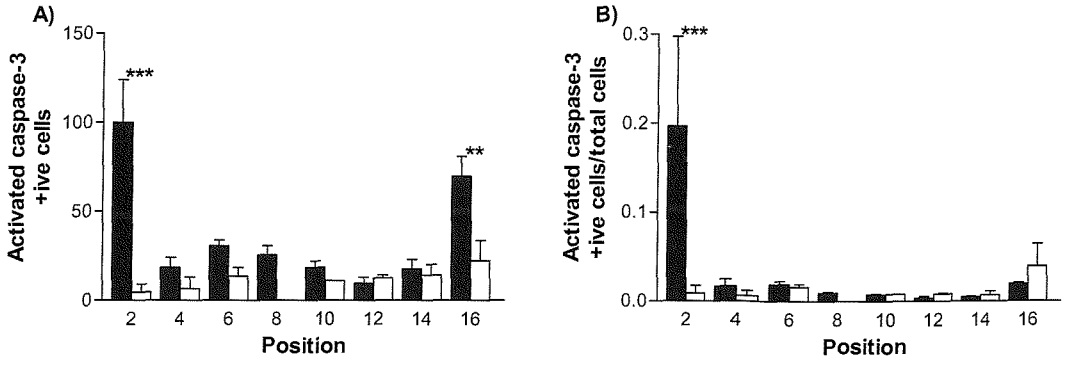

Fig 3.11: Comparison of activated caspase-3 measurements from 10μm thick sections of cultures grown in Neurobasal ■ or horse serum □ based medium for 5 days, cultures were matched for position and animals. Position refers to the location on the septo-temporal axis of the hippocampus that the culture is taken from, with section 2 being at the temporal extent and 16 being most septal. Showing apoptotic cell death identified by activated caspase-3 immunochemistry, as absolute cell counts **(A)** and as a proportion of the cells present **(B)**. Values are expressed as mean ± SEM , from 2 (positions 2, 4, 10, 12 and 14), 3 (position 10) or 4 (positions 6 and 8 (NB only)) cultures. *Asterisks* denote significant differences between groups determined by two-way ANOVA with Bonferroni post hoc test (* $p<0.05$, ** $p<0.01$).

3.3.11 Identifying a stable culture population

The mid-septal cultures (sampled positions 8,10,12 and 14) appear to be the most consistent in both media types, and so were re-analysed using the two-way ANOVA. In cultures from these 4 positions the mean does not change significantly due to a cultures position in any of the parameter considered (area, $p=0.094$; cell count, $p=0.193$; density, $p=0.560$, BrdU positive cells, $p=0.162$; activated caspase-3 positive cells, $p=0.489$; and the proportion of cells that are BrdU or activated caspase-3 positive, $p=0.209$ and $p=0.499$ respectively; note: only positions 10, 12 and 14 were considered for activated caspase-3 cell count and the proportion of activated caspase-3 cells as there were no complete dentates in the cultures grown in horse serum at position 8).

Culture growth in the different media types still produces significant changes in the means area ($p<0.001$), cell count ($p<0.001$) and BrdU count ($p<0.01$; all two-way ANOVAs), but importantly density, and the proportions of cells that are BrdU or activated caspase-3 positive are not affected by media type in these cultures.

3.4 Discussion

Cultures taken from different positions on the septo-temporal axis of the hippocampus show considerable variability, independent of the media they are grown in. There are also significant differences between cultures from the same locus grown in the different media. However, it is possible to minimize the variability between septo-temporal positions by selection of cultures from a smaller a region of the hippocampus and the use of 1st order derivatives in addition to raw data can allow direct comparison between media types.

3.4.1 Septo-temporal effects

We found that independent of the growth medium, the dentate gyrus gets larger both in area and in cell number, as it becomes more septal. This is also observed in the mature animal *in vivo*. When the cultures are prepared, the whole hippocampus is removed and then sectioned flat, perpendicular to the septo-temporal axis. A different procedure is generally used when fixed brains from in vivo experiments are analysed; where the whole brain is sectioned coronally, sagitally or horizontally. The hippocampus, when *in situ*, curves around the mid brain and can be divided into two halves, ventral and dorsal. Cultures (and sections thereof) taken from the temporal end are in the ventral hippocampus and are effectively cut in a horizontal plane, whereas cultures taken from the septal end are in the dorsal hippocampus and are effectively cut in a sagital plane. Comparison of the dorsal sagitally sectioned septal dentate (plates 49-51, from Paxinos and Watson, 1982) and the ventral horizontally sectioned temporal dentate (plates 57-62, from Paxinos and Watson, 1982) clearly show the septal granule cell layer area is larger *in vivo*.

One of the concerns this experiments was designed to address was the *in vivo* observation that different parts of the dentate gyrus develop at different times, with one report describing a temporal to septal development (Schlessinger, et al., 1975), and another describing development from both extremes to the middle (Bayer, 1980). Both these studies considered proliferation at various perinatal and postnatal times, and evaluated time points close to the age of our cultures (equivalent to P15). They found that by P15 proliferation was lower at the temporal extreme than in the mid-dentate, this agrees well with our in vitro results where numbers of BrdU positive

cells were generally lower in the more temporal cultures. This would seem to indicate that the cultures continue to develop in a similar manner to tissue examined from a similar position in the intact brain.

3.4.2 Media effects

While the observed differences in cell number and area along the septo-temporal axis could be expected based on *in vivo* observations (Paxinos and Watson, 1982), when cultures were initially prepared and in the subsequent analysis of the experiment everything possible was done to ensure that the cultures grown in each medium group at any position are as similar as possible. The cultures were initially plated in a systematic manner so they were paired between the two media types, with slices from one hippocampus per animal placed in NB medium and slices from the other in HS medium, effectively matching the cultures between groups for septo-temporal position. This matching was then carried through to the analysis where only pairs of cultures were included, if in either medium at a particular position analysis of one sections was not possible both that section and the matched section grown in the other media type were excluded. Bearing this in mind it is therefore interesting to note that both the cell count and GCL area of cultures grown in NB medium are larger than those grown in HS medium. Thus, growth medium must alter the properties of the cultures, and further to this, evaluation of density, which is unchanged between media types, demonstrates that the medium does not change the distribution of the cells in the GCL. Horse serum medium is reported as driving astrocytic proliferation and Neurobasal medium is reported to be neuro-proliferative (Brewer, et al., 1993), these different responses might cause the significant change in granule cell number observed.

In these experiments a short pulse of BrdU was used to label dividing cells, only identifies cells that are in the S-phase of the cell cycle for at least part of the 2 hours during which the BrdU was applied. As cultures were fixed at the end of this time BrdU labelled cells have not had time to complete mitosis and are all still in the cell cycle, and assumed to be undergoing division, at the end of the experiment. This method does not label all dividing cells. A complete cell cycle has been reported as taking between 16 and 25 hours in rats depending on their age (Lewis, 1978; Cameron and McKay, 2001), and the S-phase of this process takes roughly 8 hours, indicating that probably between a third and half of the total number of cells in the cycle are

labelled. If in one medium the cell cycle is about 16 hours and in the other it is about 24 hours, both values within the *in vivo* biological range, then BrdU would label about half of the proliferating cells in the first medium and a third of the cells in the second medium. Thus, similar levels of BrdU incorporation could be observed in cultures where actual cell proliferation differs by 50%, although a difference of this magnitude is unlikely, as extreme values have been used here to illustrate the point. Therefore, the results of this experiment are not sufficient to establish whether media effects on proliferation or cell death are sufficient to produce the observed differences in cell number in this experiment, as both the proliferation and death are 'snapshot' measurements and cannot identify changes that have occurred in the preceding 5 days *in vitro*. The levels of proliferation, or death, at earlier times may differ dramatically between media types or alternatively, the cultures could thin and spread out at different rates. Thinning out of cultures over time has been described previously (Gahwiler, et al., 1997), and cultures in our lab which are prepared at 400μm thick are estimated to shrink to about 100-150μm thick by 14 days *in vitro*; however an actual profile of culture thickness over time or between media types has not been reported. A time course experiment is required to try to identify which of these possible changes is the cause of the differences between media types.

Chapter 4

Time course experiments in OHSCs

4.1 Introduction

The previous chapter demonstrated that the model we are developing is capable of quantifying BrdU positive cells, activated caspase-3 positive cells and the total number of granule cells present in the sections of cultures. Although not absolute measures of cell proliferation and death, these observations were sufficient to determine similarities, between *in vitro* tissue and previous *in vivo* studies (Schlessinger, et al., 1975; Bayer, 1980), related to the position on the septo-temporal axis of the hippocampus. The experiments also identified a region of the hippocampus comprising cultures 8-15 (mid-septal) of the 16 loci considered in which area, cell count, cell density, BrdU positive cells, activated caspase-3 positive cells and the proportion of cells expressing either BrdU or activated caspase-3 were stable. However, the comparison of media types undertaken in that experiment clearly indicated that, after 5 days *in vitro*, growth media significantly changed the number of granule cells and cross-sectional area of the dentate gyrus. There are three possible reasons for this observed difference, different numbers of proliferating and dying cells between the two media types, different cell cycle times and differing structural stability. These three possibilities are all time dependent and so changes in the cultures over time need to be considered.

4.1.1 Postnatal dentate gyrus development

A consideration of the changes occurring over time in the cultures is important for defining the control conditions in the model. Any experiment investigating the effects of a treatment on cell numbers, proliferation, and death will need to consider more than one time point. Changes in cell proliferation and cell death are likely to occur at different rates, possibly in an ordered or sequential manner (Liu, et al., 1998; Nakagawa, et al., 2000; Nacher, et al., 2001). It is also important to examine the behaviour of the cultures over time as the dentate gyrus has been shown to develop largely postnatally (Altman and Bayer, 1990). Although this development is almost complete by around P10 (when the cultures are prepared), it has been variously reported to persist to the end of the second postnatal week (Schlessinger, et al., 1975), into the third postnatal week (Bayer, 1980) and even beyond (Altman and Bayer, 1990). Some of these differences arise from the fact that neurogenesis persists in the SGZ of the dentate gyrus throughout adult life (Hastings, et al., 2001), and so

identifying when dentate development becomes on going neurogenesis is not a finite point. It is important for our model, however, to be aware of any differences over these times.

4.1.2 Modelling the effects of different cell cycles on granule cell number

Factors that affect the cell cycle potentially significantly influence how the cultures change over time, by altering the rate at which cells are added to the granule cell layer. It is possible to estimate the maximum increase in granule cell number that could arise in a period (for example 24 hours), as a direct consequence of cell division. This estimate is of course dependent upon some assumptions, which are detailed and explained below.

i) Organisation of cell division

In the embryo each round of cell division is tightly regulated, all cells divide simultaneously, this means that all the cells complete the M-phase of the cell cycle together and all the dividing cells start a new cell cycle simultaneously, and enter the S-phase simultaneously (O'Farrell, et al., 1989). Many of the factors responsible for regulating these steps have been identified and all the embryonic cells respond in the same manner because they all share the same microenvironment. It might be possible for partial simultaneous or synchronous cell division to occur in the organotypic cultures, however it is unlikely that completely synchronised cell division could occur. This can be inferred from the fact that in all the previous experiments described in chapters 2 and 3, where a two hour pulse of BrdU was used to label cells in the S-phase, labelling was always observed. If all the cells entered and exited S-phase in a synchronised fashion then BrdU addition would either label all dividing cells (as all are in S-phase) or no dividing cells would be detected (all cells are in G1, G2 or M-phase). Partial synchronisation of cell division could occur where clusters of dividing cells share the same microenvironment and so division is synchronised within the cluster but is not synchronised with the rest of the culture. The other possibility is there is no synchronisation of cell division; all cells are at random points in the cell cycle relative to each other. The most likely of these is probably the partial synchronisation model but this is difficult to describe mathematically. However, as the number of sites with clusters of synchronously dividing cells gets larger the partial

synchronisation model approaches that of the random model. Therefore, we have assumed that cell division occurs in a random fashion.

ii) Cell cycle length

The minimum reported *in vivo* cell cycle time in the rat dentate gyrus occurs during formation and is 16 hours (Lewis, 1978) and this declines to about 25 hours in young adult rats (9-10 weeks) (Cameron and McKay, 2001). This demonstrates that the total cell cycle time can be modulated, and potentially could be affected by factors in the growth media. Our cultures are taken from just after the time when cell cycle length is shortest, and so probably still have a cycle time (T_C) close to 16 hours, but again this could change over time. Unfortunately, estimation of cell cycle time is a complex and time-consuming process. Lewis used pulses of BrdU administered every 2 hours for 12 hours; animals were also sacrificed at two hour intervals, 30 minutes after each of the BrdU injections. They then measured the proportion of cells labelled as proliferating at each time point, and demonstrated that the gradient of this increase in the proportion of labelled cells is equal to the inverse of cell cycle time (Lewis, 1978). To estimate the maximum increase in granule cell number that could arise in a period (for example 24 hours), as a direct consequence of cell division it is necessary to assume that the cell cycle is of a length that results in the maximum number of new cells. This is dependant on two factors described below.

iii) Dynamics of BrdU labelling

The protocol used by Lewis can also be used to estimate the length of the S-phase of the cell cycle (T_S); the period during which BrdU is incorporated. Although Lewis and Cameron reported different cell cycle times, between the age groups, the length of S-phase was unchanged at 8-10 hours. Having assumed that cell division occurs randomly the relationship between TC and TS becomes valuable, as the number of BrdU positive cells (N_B) can be related to the total number of dividing cells (N_D), *Equation 1*.

Equation 1: $N_D = N_B * T_C / T_S$

The above equation assumes an instantaneous pulse of BrdU will label all of the cells in the S-phase at that moment. However an instant pulse is not possible as cells need

time for BrdU uptake and incorporation into DNA to occur, thus longer pulses are used this adds another variable to Equation 1, the length of the BrdU pulse (T_B), this can be seen in *Equation 2*.

Equation 2: $N_D = N_B * T_C / (T_S + T_B)$

Unfortunately, this does not fully describe the labelling dynamics, because a pulse of BrdU has to be used in order that cells are detected since cell labelling is not instant. This value is the time required for BrdU to be present before it can be detected in a cell (T_I), and produces adds a further variable to number of dividing cells, *Equation 3*. T_I appears twice in this equation because those cells leaving the S-phase during T_I will not be labelled and those cells entering the S-phase for less than T_I will not be labelled.

Equation 3: $N_D = N_B * T_C / (T_S + T_B - 2T_I)$

T_I must lie within a range of values, bounded at a minimum by instant labelling (T_I=0) and at a maximum by the length of the applied BrdU pulse (T_I=T_B), as otherwise no cells would be detected, therefore the number of dividing cells lies in the range.

$$N_B * T_C / (T_S + T_B) \leq N_D \leq N_B * T_C / (T_S - T_B)$$

A pulse of X hours has been reported to result in BrdU positive cells defining an upper limit for T_I, we shall assume that this is the actual value of T_I, which means that the range described above can be resolved, *Equation 4*.

Equation 4: $N_D = N_B * T_C / (T_S + T_B - 2X)$

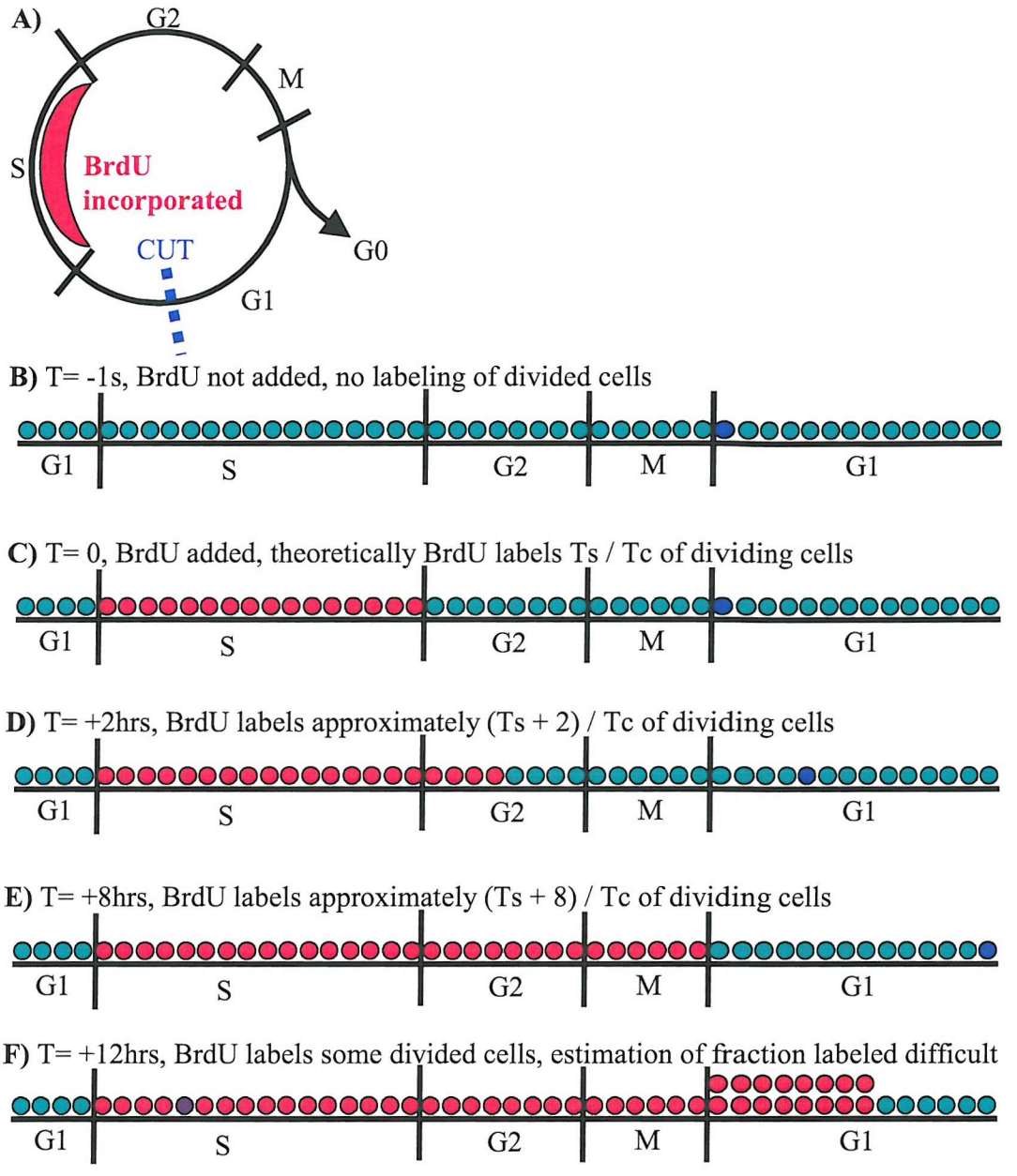

Fig 4.1: The duration of BrdU incubation of time affects the number of dividing cells labeled. The cell cycle (A), is cut in the G1-phase and represented in a linear fashion (B), with cells● residing at all possible points of the cell cycle, a cell that has just completed mitosis is marked● so its progress can be followed over time. Addition of BrdU theoretically labels all cells in the S-phase● at that time (C). Continued incubation results in BrdU labeled cells from the S-phase moving into G2 and new unlabeled cells entering from G1 and becoming labeled (D) and (E). Once labeled cells complete division (exit M-phase) it is not possible to calculate the fraction of the total dividing population that is labeled, as some labeled cells could have left the cell cycle and become post mitotic (G0).

iv) Mechanisms of cell division

There are a number of possible outcomes from a cell division. At the most simple level 3 permutations are possible from the division of a single stem cell undergoing one division.

1) The stem cell divides asymmetrically maintaining itself and producing a terminally differentiated neuron as a daughter cell.
2) The stem cell divides symmetrically producing two identical stem cells.
3) The stem cell divides symmetrically producing two identical terminally differentiated neurons.

Combining many sequential cell divisions of the first type results in a steady state model of proliferation (Fig 4.2A) the number of new cells (c_{ssm}) generated is equal to the number of cell cycles (n) completed; $c_{ssm} = n$.

Combining many sequential cell divisions of the second type results in an exponential model of proliferation (Fig 4.2B), the number of new cells (c_{em}) = 2^n-1.

It is not possible to obtain sequential divisions of third type as this division eliminates the dividing cell type.

If only one cell division is considered these models will appear to generate the same number of cells since if n=1, 2^n-1=1. However, if more than 1 cell cycle is completed then the steady state model produces fewer cells than the exponential model. For example, with 3 cell cycles n=3, therefore, c_{ssm}= 3 and c_{em}=2^3-1 = 7.

Thus, we will assume an exponential model of cell division for estimating the maximum increase in cell number that could arise in a period (for example 24 hours), as a direct consequence of cell division.

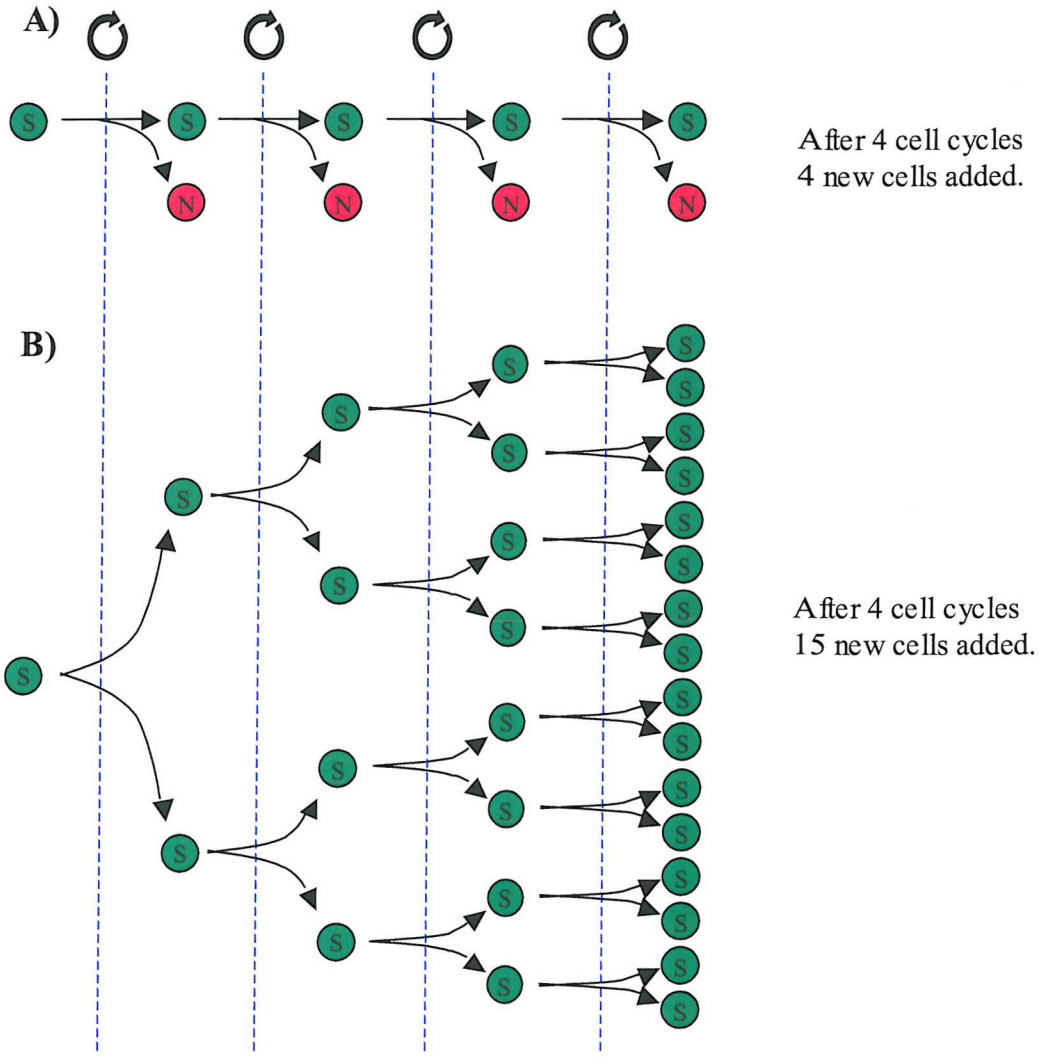

Fig 4.2: Simple models of cell proliferation. A stem cell (S) dividing asymmetrically adds one neuron (N) per cell cycle to the granule cell layer **(A)**, this is the steady state model of proliferation described by Nowakowski et al.(1989). The model at the opposite extreme is exponential division **(B)**, where stem cells undergo symmetrical divisions generating up to $(2^n - 1)/n$ new stem cells per cell cycle (where n is the number of cell cycles occurring).

v) Combining effects to generate a model of maximal proliferation, with defined assumptions

So far we have established that the number of cells dividing at any point $N_D = N_B * T_C / (T_S + T_B - 2X)$ and that the number of new cells generated per cell cycle, $c_{em} = 2^n-1$. In order to determine the maximal increase in cell numbers resulting from cell proliferation a few more calculations are required.

In any given length of time (t) the number of new cells generated (C_t) is dependent on the number of dividing cells per cell cycle (N_D) and the length of the cell cycle (T_C), such that:

$$C_t = N_D * t / T_C$$

In the same length of time (t) the number of cell cycles complete (n) is also dependent on the length of the cell cycle (T_C), thus the number of newly generated cells per dividing cell (c_{em}) is also dependent on T_C, such that:

$$c_{em} = 2^{(t/ Tc)} - 1$$

And the number cells generated from each BrdU positive cell N_B is equivalent c_{em}. These generate the equation:

$$Ct = (2^{(t/ Tc)} - 1)* T_C / (T_S + T_B - 2X)$$

By considering the number of cells added in a 24 hour period (i.e. t = 24hrs), with a 2 hour pulse of BrdU, and the time required for the label to be detected (X) is 1 hour, the cell cycle times identified by Lewis and Cameron (about 16 and 24 hours) can be compared, since both experiments found similar S-phase durations (T_S = 8 hours).

If T_C =16 hours

$C_{24} = (2^{(24/16)} * 24 - 24) / (8 + 2 - 2*1)$ cells

C_{24} = 5.5 cells per BrdU cell labelled (4.4)

And if Tc = 24 hours

$C_{24} = (2^{(24/24)} * 24 - 24) / (8 + 2 - 2*1)$ cells

C_{24} = 3 cells per BrdU cell labelled (2.4)

Therefore the assessment of the maximum number of cells that can be added to the granule cell layer 24 hours after a two hour pulse of BrdU was begun will use the following assumptions.

1) The initial position of all dividing cells within the cell cycle is random.
2) Cell division follows an exponential model.
3) The length of the cell cycle is 16 hours.
4) Dividing cells require at least 1 hour in the S-phase with BrdU present to be detected.

It is important to note that this is not being proposed as an actual model of cell proliferation in the cultures; rather it describes the largest possible increase in cell numbers within the granule cell layer if proliferation is the only factor that changes.

The final assumption in the above model is that no cell death occurs. However inaccurate this assumption is, it is in keeping with the aim of discovering what the maximum change in cell numbers due to proliferation is, because any cell death would reduce the number of cells added. Unfortunately the markers of cell death available do not have known expression times, so unlike with BrdU it is not possible to calculate the total number of cells dying in a 24 hour period from the number of cells expressing activated caspase-3 at any one time.

4.1.3 Structural changes in cultures

The third factor that could be a major influence on the size of the granule cell layer, arises from the fact that the cultures are well documented as thinning over time (Gahwiler, et al., 1997). The cultures are prepared as 400μm thick slices, after 14 days in vitro cultures grown in horse serum medium are approximately 150μm thick when grown on semi-porous membranes and 50μm thick when grown using the roller method developed by Gahwiler (Gahwiler, et al., 1997). Cultures may also spread out in the x-y plane at different rates i.e. their density can change because of dispersion of the granule cell layer, (experiments in our labs growing cultures on different membranes noted that cultures spread out differently (Cater, unpublished observation)). Both of these changes, and the way that they interact, could affect the area, cell count and density of granule cells observed in the cultures (Fig 4.3).

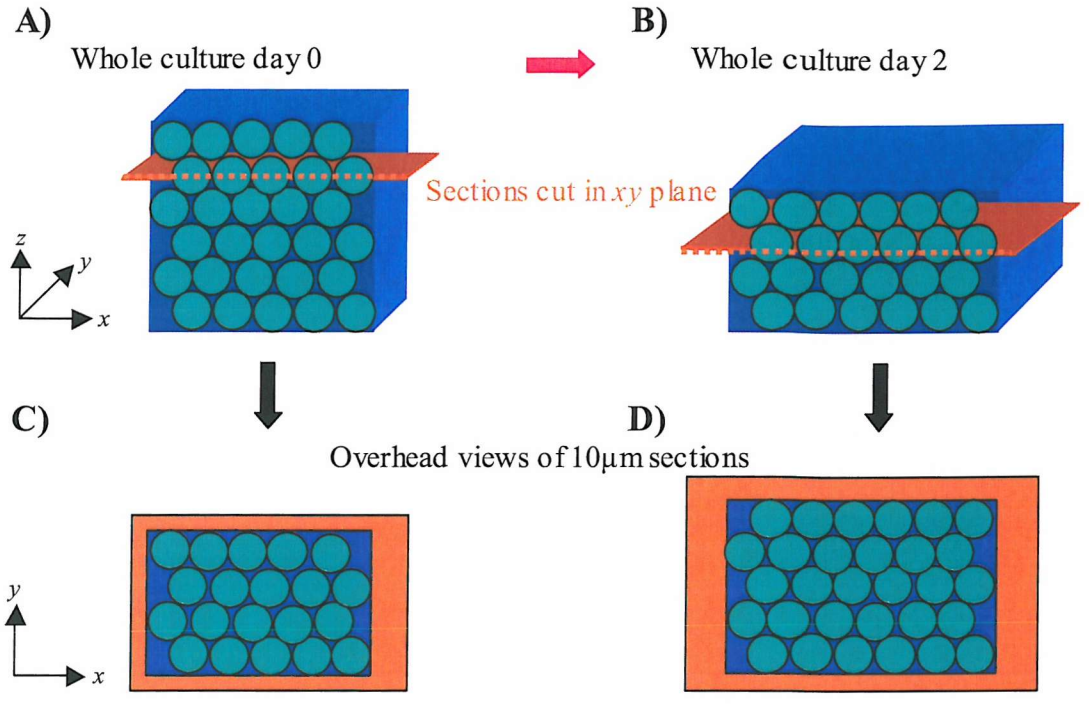

Fig 4.3: Changes in section area and cell count, without a change in density, as a result of culture thinning. Cultures when initially prepared are 400µm thick **(A)** and have certain dimensions in the *xy* plane **(C)**, with time these cultures become thinner **(B)** and also expand in the *xy* plane **(D)**. In the example here, the number of cells in the whole culture is unchanged, on day 0 x=5, y=4 and z=6; total 120 cells, and on day 2 x=6, y=5 and z=4; total 120 cells. The cells all remain the same size so density is unchanged. This could be inaccurately interpreted as an increase in cell number and area over time due to cell proliferation.

4.1.4 Questions to be addressed

The aim is to establish a model in OHSCs, where granule cell number, cell proliferation, and cell death can be quantified in the dentate gyrus. To achieve this a pulse of BrdU labelling is going to be used as a proliferative marker, activated caspase-3 will be used to identify apoptotic cells and a stereological technique, the fractionator, will estimate granule cell number in thionine stained tissue. To further the general aim of establishing this model the factors that can alter the homogeneity of both cell proliferation and cell death in the cultures under control conditions need standardizing. Some of the factors that could affect these responses have already been investigated, in the previous chapter, a part of the hippocampus which produces consistent cultures was identified, but the influence of media type on the model could

not be fully characterized without considering what happened in the time between plating and examination. Therefore, these experiments are designed at quantifying cell proliferation, cell death and total cell number in two different growth media and at different times. To this end, matched cultures from the mid-septal part of the two hippocampi in a rat were taken and placed in different media types. Data from four basic parameters was obtained; granule cell layer area, granule cell number, BrdU positive cells, and activated caspase-3 positive cells. The influence of these parameters on each other was also considered in three 1st order derivatives; granule cell layer density, and the proportion of granule cells that are BrdU positive or activated caspase-3 positive.

4.2 Methods

In all the experiments in this chapter, cultures were prepared as described in chapter 2.2.1, with the method of selecting cultures for each well and the treatment the cultures subsequently received until fixation detailed in sections 4.2.1. The processing of all the cultures after fixation is subsequently described in sections 3.2.2 – 3.2.5.

4.2.1 Analysis of cell proliferation and death as a function of age in 10-micron sections from Organotypic Hippocampal slice cultures.

Cultures were prepared as described in chapter 2, and systematically placed into the inserts such that cultures were paired between the two media types, with slices from one hippocampus per animal placed in NB medium and slices from the other in HS medium. Cultures from the mid-septal hippocampus (positions 8-15 in the previous chapter) were used and contributed equally to each experimental time point. The two experiments differed only in the time points examined. In the first BrdU (10μM) was added to the culture media 2 hours prior to fixation in 4% PFA on days 1,3,5,7 and 14 *in vitro*. In the second experiment, BrdU (10μM) was added to the culture media 2 hours before fixation in 4% PFA after1, 2, 3 and 5 days *in vitro*. Additionally, in this second experiment a group of slices were not plated or exposed to BrdU but were fixed immediately as time 0 controls (**Fig 4.4**), this group was compared with all other points with a one-way ANOVA and Dunnett's post hoc test.

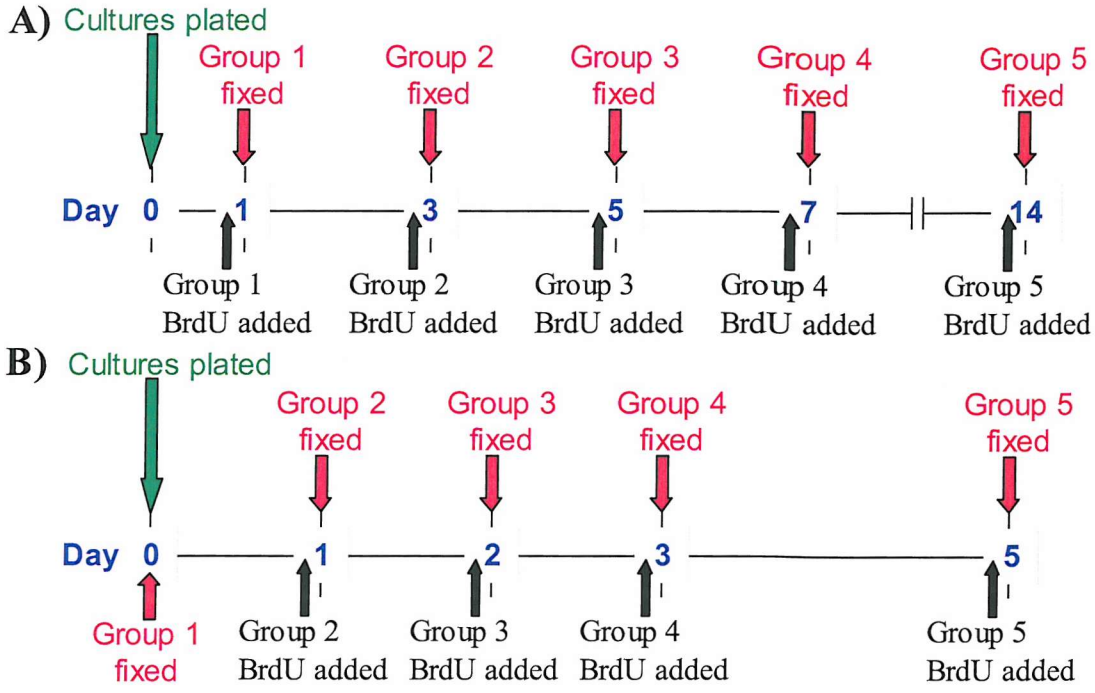

Fig 4.4: Time courses for comparision of Neurobasal and Horse serum based media. Showing the times that cultures were fixed in the long survival **(A)**, and short survival **(B)** experiments. Cultures were either grown in Neurobasal based medium or Horse serum based medium, and BrdU (10μM) was added to all cultures 2 hours before fixation in 4% PFA, with the exception of cultures fixed at 0 hours in the short survival experiment **(B)** which did not receive any BrdU.

4.3 Results

4.3.1 Changes in the dentate granule cell layer over time

In two separate experiments cell number, cell proliferation and cell death were quantified. In the first the time points considered were 1,3,5,7 and 14 days after plating and in the second 1,2,3 and 5 days were examined, additionally in this experiment cell number and cell death were examined immediately after preparation, proliferation at this time could not be calculated as this requires exposure to BrdU for 2 hours prior to fixation. The approach used in the previous chapter, to describe the dentate gyrus is taken, with a combination of area, cell count and density describing the physical state of the cultures. BrdU cell counts and the proportion of cells incorporating BrdU describe the proliferative state of the cultures, and activated caspase-3 cell counts and the proportion of cells expressing activated caspase-3 describe some of the facets of cell death in the cultures. As the cultures in both these experiments are sampled using the same method and there are three time points common to both experiments, these time points were also used to assess the reproducibility of individual results between experimental repeats.

4.3.2 Long time course experiment considering up to 14 days *in vitro* in cultures grown in horse serum

i) Area and cell counts are variable over time in cultures grown in horse serum medium, density decreases after the first week.

The general profile of granule cell number in cultures grown in HS medium was a rise from day 1 to day 5 and then a fall to day 14, with the initial and final cell counts being similar. This profile resulted in several significant changes in cell counts with cultures fixed on days 3 and 5 (1880±869 cells and 2432±68 cells respectively) having significantly more cells in a section than those on day 1 (960±430 cells; $p<0.05$ vs. day 3 and $p<0.001$ vs. day 5) and those on day 14 (888±57; $p<0.01$ vs. day 3 and $p<0.001$ vs. day 14), cultures from day 5 also had significantly more cells than those from day 7 (1232±563 cells; $p<0.01$; **Fig 4.5B**).

Initially area follows a similar temporal profile to the cell count; an increase in area to day 5 followed by a decline. Cultures on day 1 have significantly smaller GCLs ($0.093\pm0.028mm^2$) than day 3 ($0.150\pm0.040mm^2$; $p<0.05$) and day 5 ($0.179\pm0.001mm^2$;$p<0.001$); day 5 cultures also have significantly larger GCL areas

than those from day 7 (0.120±0.026mm^2; $p<0.05$). However, the pattern by day 14 is different from that seen in with cell counts, instead of a continued decrease in area the granule cell layer appears to get bigger and at day 14 is significantly larger than on day 1 (day 14, 0.154±0.044mm^2; $p<0.05$ vs. day 1; **Fig 4.5A**).

These two factors combine with the resultant cell density relatively constant from day 1 to day 7, although it rises slightly to day 5 and then falls none of these changes are significant, however subsequently density falls significantly by day 14 compared with all other cultures (day 14, 5951±1347 cells/mm^2 vs. day 1, 10123±2019 cells/mm^2, $p<0.05$; day 3, 12329±3625 cells/mm^2, $p<0.001$; day 5, 13553±402 cells/mm^2, $p<0.001$; and day 7, 9970±2358 cells/mm^2, $p<0.05$; **Fig. 4.5C**).

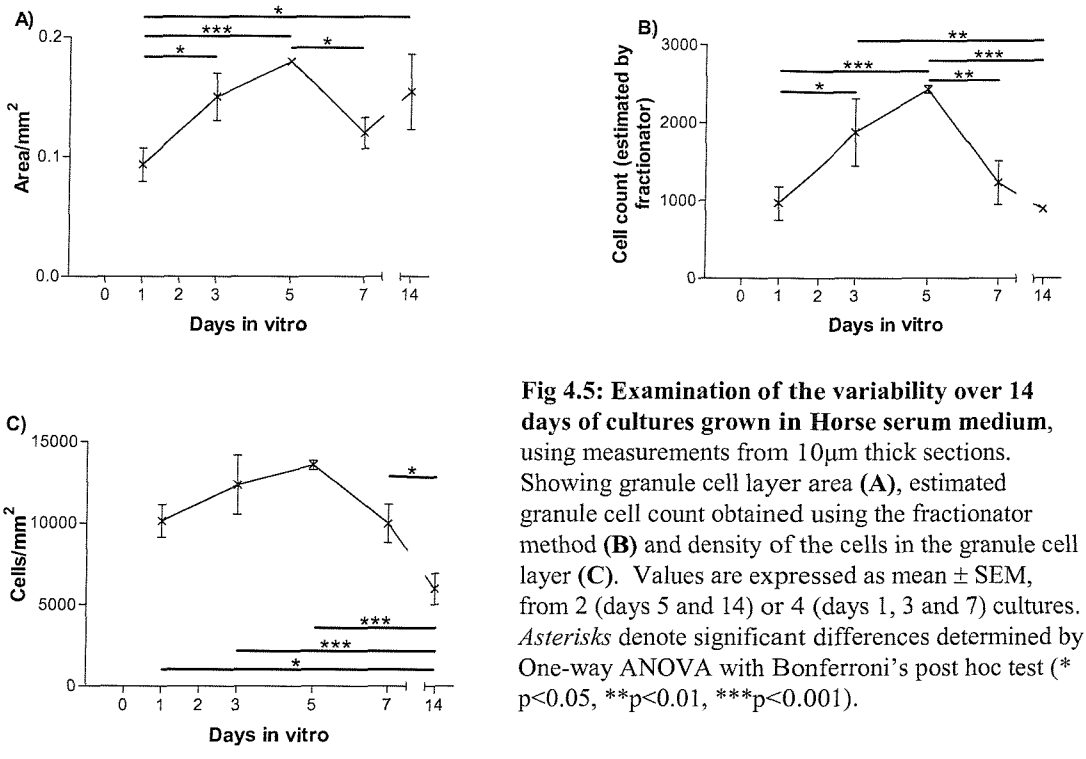

Fig 4.5: Examination of the variability over 14 days of cultures grown in Horse serum medium, using measurements from 10μm thick sections. Showing granule cell layer area **(A)**, estimated granule cell count obtained using the fractionator method **(B)** and density of the cells in the granule cell layer **(C)**. Values are expressed as mean ± SEM, from 2 (days 5 and 14) or 4 (days 1, 3 and 7) cultures. *Asterisks* denote significant differences determined by One-way ANOVA with Bonferroni's post hoc test (* $p<0.05$, ** $p<0.01$, *** $p<0.001$).

ii) In horse serum cultures BrdU counts and the proportion of BrdU positive cells decreased during the first 5 days the absolute count then stabilised and the proportion increased.

In cultures grown in HS medium the number of BrdU positive cells declines from day 1 to day 5 and then remains fairly stable until day 14. This decrease is significant on both day 5 and day 7 (day 1, 68.3±45.4 cells vs. day 5, 25.0±9.9 cells and day 7, 27.0±2.2 cells; both $p<0.01$; **Fig 4.6A**). The profile obtained for the proportion of cells incorporating BrdU is initially similar to that of the BrdU cell counts. A

decrease from day 1 to day 5, but then due to the smaller cell counts on days 7 and 14 the proportion of BrdU positive cells tends to increase again, although only the initial decline is of statistical significance. The result of this is that the proportion of BrdU positive cells is significantly greater on day 1 (7.0±3.9 % of cells) than on day 3 (3.0±1.4 % of cells; $p<0.01$), day 5 (1.0±0.4 % of cells; $p<0.001$) and day 7 (2.5±0.4 % of cells; $p<0.01$; **Fig 4.6B**).

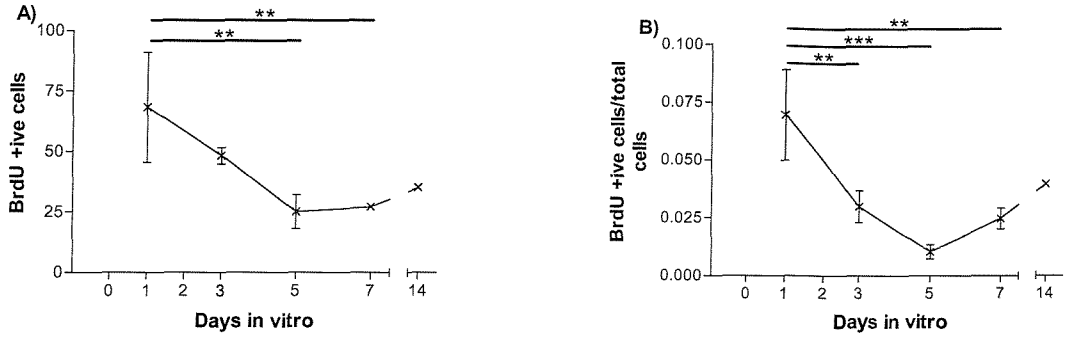

Fig 4.6: 14 day proliferation profile of cultures grown in horse serum medium, using measurements from 10μm thick sections. Showing absolute numbers of BrdU positive cells **(A)**, and the proportion of granule cells detected as also incorporating BrdU **(B)**. Values are expressed as mean ± SEM, from 2 (days 5 and 14) or 4 (days 1, 3 and 7) cultures. *Asterisks* denote significant differences determined by One-way ANOVA with Bonferroni's post hoc test, (* $p<0.05$, ** $p<0.01$, *** $p<0.001$).

iii) Caspase-3 activation decreased over the first 5 days and then increased in cultures grown in horse serum.

HS cultures show a general trend for declining caspase-3 activation from day 1 to day 14, with the exception of day 7 in which the number of activated caspase-3 cells observed was high. However none of these changes were significant, and overall day did not significantly affect caspase-3 activation ($p=0.084$; one-way ANOVA; **Fig 4.7A**).

While the number of activated caspase-3 positive cells detected in cultures grown in HS medium were unchanged over time the proportion of cells showing caspase-3 activation did change significantly; initial declining from day 1 (8.4±4.2 % of cells) to day 3 (3.6±1.3 % of cells; $p<0.05$) and day 5 (1.6±0.5 % of cells; $p<0.001$) and then increased at day 7 (6.8±2.1 % of cells; $p<0.01$ vs. day 5; **Fig 4.7B**).

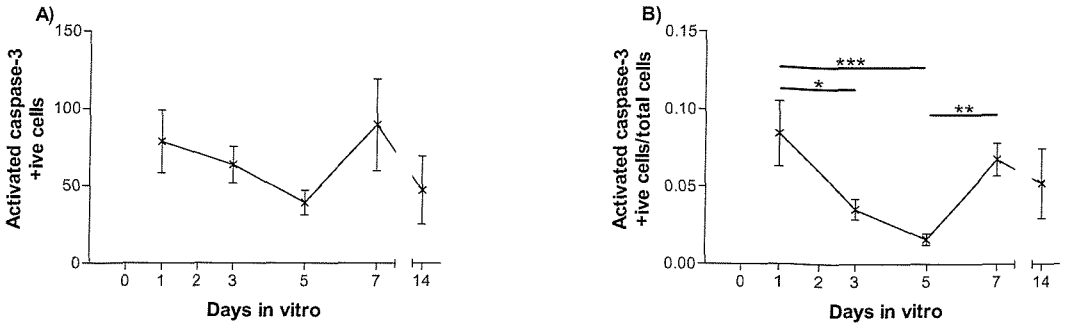

Fig 4.7: 14 day activated caspase-3 profile of cultures grown in horse serum medium, using measurements from 10μm thick sections. Showing absolute numbers of activated caspase-3 positive cells **(A)**, and the proportion of granule cells that expressed activated caspase-3 **(B)**. Values are expressed as mean ± SEM, from 2 (days 5 and 14) or 4 (days 1, 3 and 7) cultures. *Asterisks* denote significant differences determined by One-way ANOVA with Bonferroni's post hoc test, (* $p<0.05$, ** $p<0.01$, *** $p<0.001$).

4.3.3 Long time course experiment considering up to 14 days *in vitro* in cultures grown in Neurobasal medium

i) Area and cell counts are variable over time in cultures grown in Neurobasal medium, but density decreases after the first week.

The number of granule cells in sections from cultures grown in NB medium did not change significantly over time and remained relatively constant over time (**Fig 4.8B**). Similarly, the area of the GCL does not vary significantly between individual times. However, the profile is of decreased area between day 1 and days 3 and 5 followed by increased area from day 5 to day 14 results in significant variance in the means over time ($p<0.05$; one-way ANOVA), although no individual difference is significant (**Fig 4.8A**). Density in the NB cultures remains relatively constant until day 5, then beings to decline. It is significantly lower on day 7 (10191±1960 cells/mm^2) than on day 3 (16267±3111 cells/mm^2; $p<0.05$) and significantly lower on day 14 (7081±3846 cells/mm^2) than on day 1 (12974±2221 cells/mm^2; $p<0.05$), day 3 ($p<0.001$), and day 5 (14276±5381 cells/mm^2; $p<0.01$; **Fig 4.8C**).

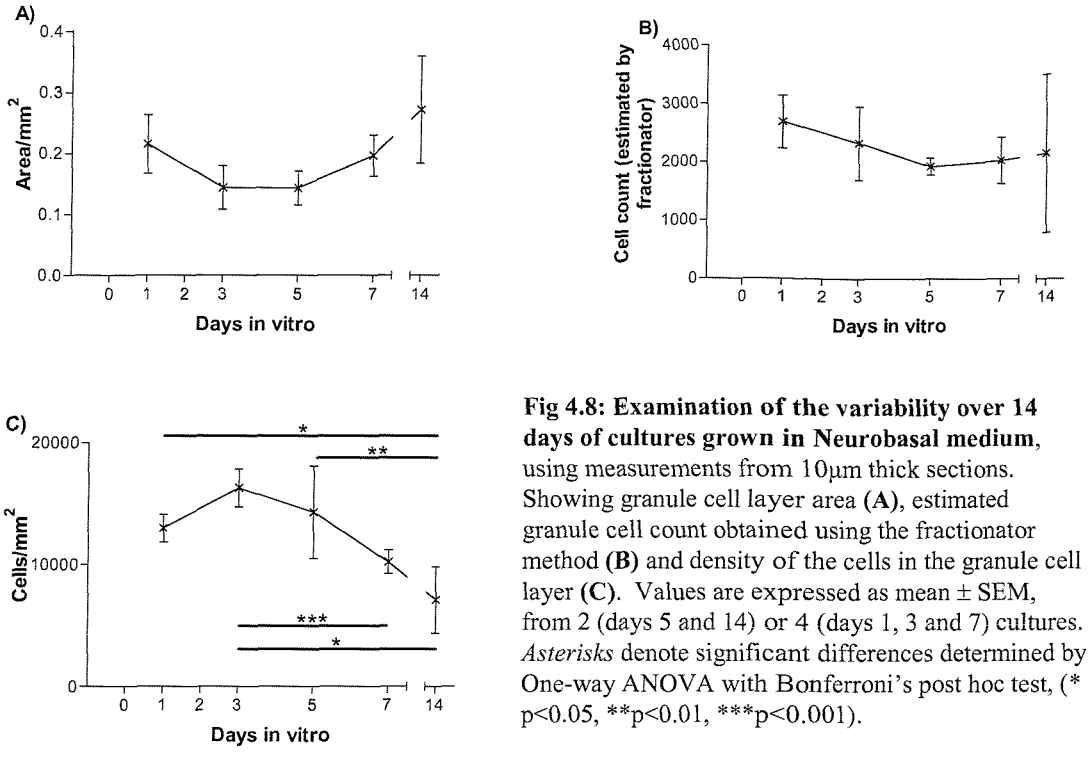

Fig 4.8: Examination of the variability over 14 days of cultures grown in Neurobasal medium, using measurements from 10μm thick sections. Showing granule cell layer area **(A)**, estimated granule cell count obtained using the fractionator method **(B)** and density of the cells in the granule cell layer **(C)**. Values are expressed as mean ± SEM, from 2 (days 5 and 14) or 4 (days 1, 3 and 7) cultures. *Asterisks* denote significant differences determined by One-way ANOVA with Bonferroni's post hoc test, (* $p<0.05$, ** $p<0.01$, *** $p<0.001$).

ii) BrdU incorporation is unchanged over 14 days in cultures grown in Neurobasal medium.

NB cultures show a general trend for declining BrdU incorporation from day 1 to day 14, with the exception of day 7 in which the number of BrdU positive cells observed was high. None of these individual means were significantly different, but overall the means did vary significantly ($p<0.05$; one-way ANOVA; **Fig 4.9A**).

The proportion of cells incorporating BrdU was slightly, but not significantly, decreasing from day 1 (2.8±1.7 % of cells) to day 5 (1.66± 0.4 % of cells), and then as with the absolute number of BrdU positive cells on day 7 an increase was observed (4.0±2.8 % of cells), and the proportion finished on day 14 (2.7±3.0 % of cells) at a similar level to day 1 (**Fig 4.9B**). It is important to note that while none of these changes are statistically significant, and indeed overall the means do not differ significantly ($p=0.28$; one-way ANOVA), this is probably due to the increase in the variability of the cultures responses at day 7 and especially day 14. On day 14 the standard deviation is approximately 110% of the mean making a Gaussian distribution unlikely, despite the data passing the Kolmogorov-Smirnov test for Gaussian distribution, this is probably caused by only having two data points here.

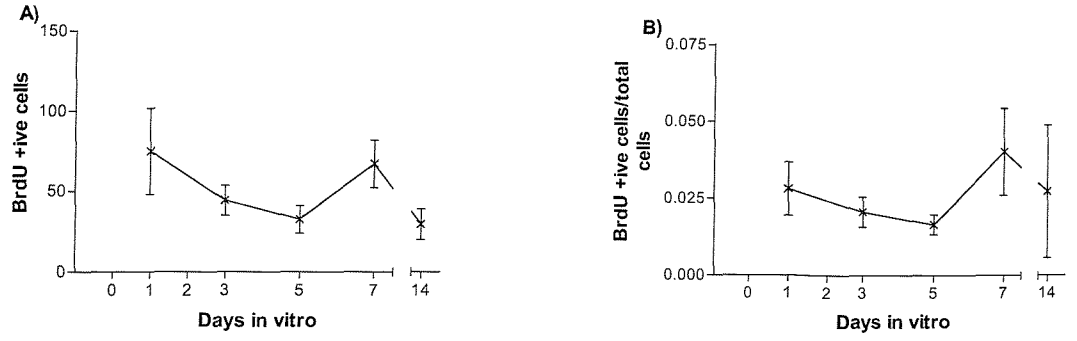

Fig 4.9: Proliferation profile of cultures grown in Neurobasal medium, using measurements from 10μm thick sections. Showing absolute numbers of BrdU positive cells **(A)**, and the proportion of granule cells detected as also incorporating BrdU **(B)**. Values are expressed as mean ± SEM, from 2 (days 5 and 14) or 4 (days 1, 3 and 7) cultures.

iii) Caspase-3 activation was unchanged over time in cultures grown in Neurobasal medium for up to 14 days.

In the cultures grown in NB medium both the actual numbers of cells expressing activated caspase-3 and the proportion of cells showing caspase-3 activation were unchanged at all the times examined in this experiment (**Fig 4.10**).

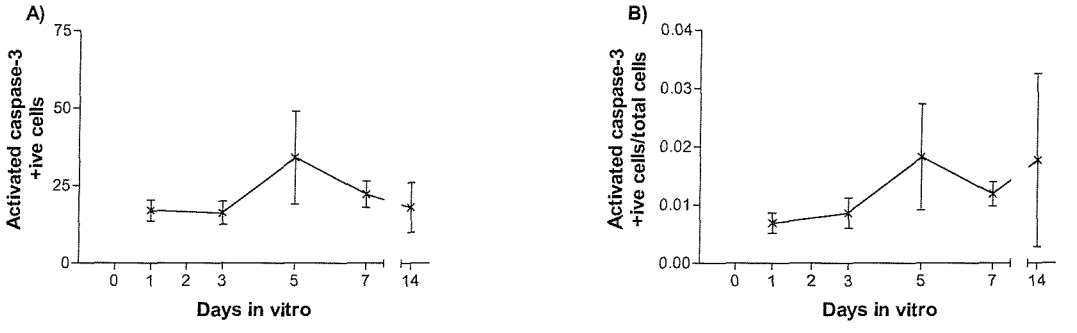

Fig 4.10: Activated caspase-3 profile of cultures grown in Neurobasal medium for up to 14 days, using measurements from 10μm thick sections. Showing absolute numbers of activated caspase-3 positive cells **(A)**, and the proportion of granule cells that expressed activated caspase-3 **(B)**. Values are expressed as mean ± SEM, from 2 (days 5 and 14) or 4 (days 1, 3 and 7) cultures.

4.3.4 Comparing cultures grown in different types of media for up to 14 days

i) Area and cell counts are generally greater when cultures are grown in Neurobasal medium but density is unchanged by media type.

When cultures are grown in either NB or HS medium for up to 14 days the media the cultures are grown in significantly affects the expected mean area and cell count of the GCL in the cultures (both $p<0.05$; two-way ANOVA). This difference in the expected means does not manifest itself as a significant difference between the two

media types at any particular time point in the experiment, but rather it reflects a trend for the measured area and estimated cell counts to be larger in those cultures grown in NB medium. Although the results show a very substantial change on both area and cell counts between media types on day 1, these differences are not significant, possibly due to the post test used as the Bonferroni test is considered conservative when large numbers of groups are compared. The increases in area and cell counts observed in NB cultures are both of a similar magnitude as the density of cells in the cultures grown in either medium is similar (p=0.102 for media and p=0.684 for interaction; **Fig 4.11**).

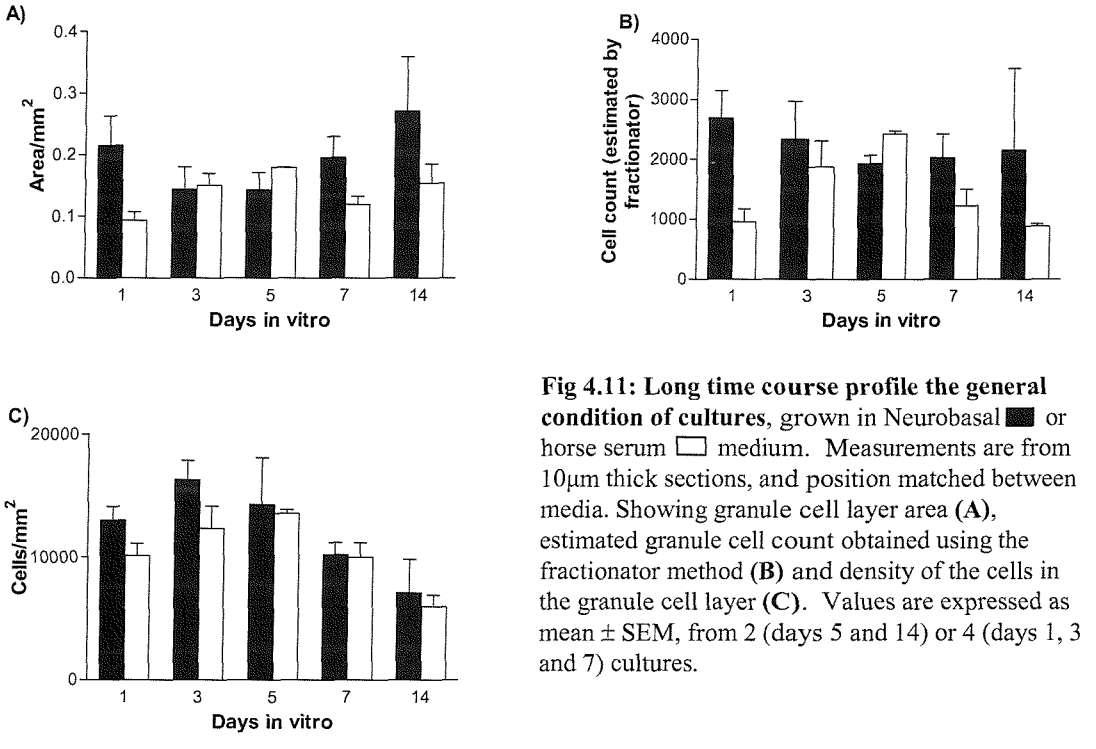

Fig 4.11: Long time course profile the general condition of cultures, grown in Neurobasal ■ or horse serum □ medium. Measurements are from 10μm thick sections, and position matched between media. Showing granule cell layer area **(A)**, estimated granule cell count obtained using the fractionator method **(B)** and density of the cells in the granule cell layer **(C)**. Values are expressed as mean ± SEM, from 2 (days 5 and 14) or 4 (days 1, 3 and 7) cultures.

ii) BrdU incorporation was unchanged by media type at any of the points examined over14 days.

Overall, both media types incorporated BrdU into a similar number of cells during the two hour application prior to fixation (p=0.427; two-way ANOVA; **Fig 4.12A**), and no differences were detected at any of the individual time points within the experiment. These observations also held true when proportion granule cells that had incorporated BrdU were considered (p=0.312; two-way ANOVA; **Fig 4.12B**).

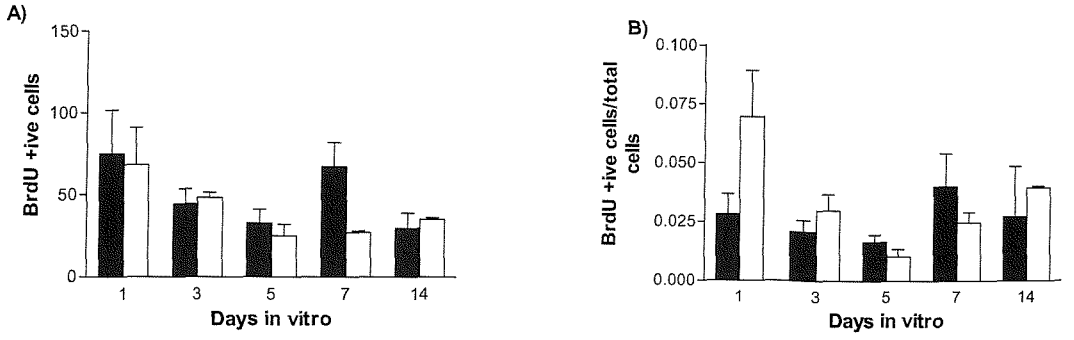

Fig 4.12: Long time course profile of BrdU incorporation in cultures, grown in Neurobasal ■ or horse serum □ medium. Measurements are from 10μm thick sections, and position matched between media. Showing absolute numbers of BrdU positive cells **(A)**, and the proportion of granule cells that incorporated BrdU in the 2 hours prior to fixation **(B)**. Values are expressed as mean ± SEM, from 2 (days 5 and 14) or 4 (days 1, 3 and 7) cultures.

iii) Caspase-3 activation is higher in cultures grown in horse serum medium.

Mean numbers of cells demonstrating caspase-3 activation differed significantly between media types ($p<0.001$; two-way ANOVA). Significantly more activated caspase-3 positive cells were detected in cultures grown in HS medium on day 1 (NB, 17.0±6.7 cells vs. HS, 78.5±40.4 cells; $p<0.05$) and day 7 (NB, 22.3±8.4 cells vs. HS, 89.3±59.0 cells; $p<0.05$) than in those grown in NB medium. This trend was evident but not statistically significant at the other time points (**Fig 4.13A**).

The proportion of activated caspase-3 positive cells, demonstrated significant interaction between the medium cultures were grown in and the time at which the cultures were fixed ($p<0.05$; two-way ANOVA), thus the differences between media types were not the same at every time point examined. However, cultures grown in horse serum medium had a greater proportion of activated caspase-3 positive cells than cultures grown in Neurobasal medium on day 1 (NB, 0.7±0.3 % of cells vs. HS, 8.4±4.2 % of cells; $p<0.001$) and on day 7 (NB, 1.2±0.4 % of cells vs. HS, 6.8±2.1 % of cells; $p<0.01$) and this trend holds on days 3 and 14, but on day 5 levels of caspase-3 activation appear very similar (**Fig 4.13B**).

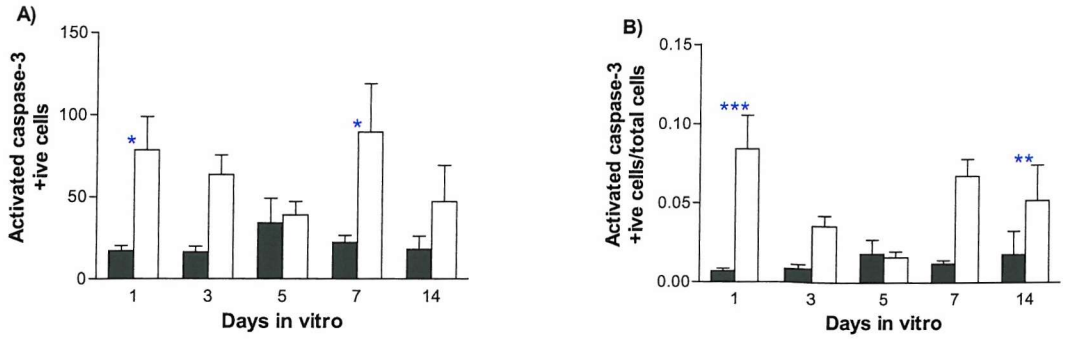

Fig 4.13: Long time course profile of caspase-3 activation in cultures, grown in Neurobasal ■ or horse serum □ medium. Measurements are from 10μm thick sections, and position matched between media. Showing absolute numbers of activated caspase-3 positive cells **(A)**, and the proportion of granule cells that expressed activated caspase-3 **(B)**. Values are expressed as mean ± SEM, from 2 (days 5 and 14) or 4 (days 1, 3 and 7) cultures. **Blue** *asterisks* denote significant differences between media types determined by two-way ANOVA with bonferroni's post hoc test, (* $p<0.05$, ** $p<0.01$, *** $p<0.001$).

4.3.5 Short time course experiment considering up to 5 days *in vitro* in cultures grown in horse serum medium

i) In horse serum cultures area, cell count and density all increased with age, the change in density was immediate but was delayed in both area and cell count measurements.

In the short time course experiment the number of cells in the GCL increased steadily from day 1 through to day 5, with cultures from day 5 having significantly more cells (1757±501 cells) than those on day 1 (948±197 cells; $p<0.001$) and day 2 (1315±86 cells; $p<0.05$; **Fig 4.14B**).

In contrast to the cell count, the area of the GCL remained constant for the first three days in culture before increasing significantly between day 3 (0.083±0.009mm^2) and day 5 (0.110±0.028mm^2; $p<0.05$; **Fig 4.14A**).

These two effects combine with the result that cell density increases significantly between day 1 (10987±1553 cells/mm^2) and day 2 (14963±1265 cells/mm^2; $p<0.01$) and remains constant and significantly elevated thereafter (day 3, 16016±2753 cells/mm^2; and day 5, 15953±1366 cells/mm^2; both $p<0.001$ vs. day 1; **Fig 4.14C**).

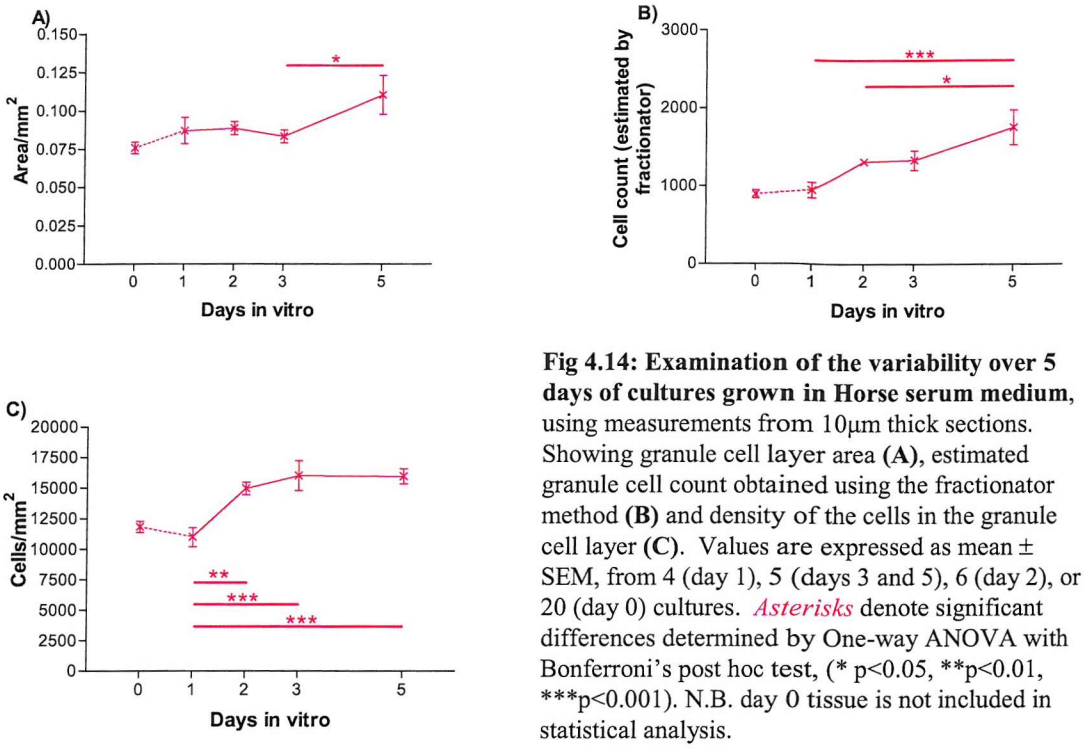

Fig 4.14: Examination of the variability over 5 days of cultures grown in Horse serum medium, using measurements from 10μm thick sections. Showing granule cell layer area **(A)**, estimated granule cell count obtained using the fractionator method **(B)** and density of the cells in the granule cell layer **(C)**. Values are expressed as mean ± SEM, from 4 (day 1), 5 (days 3 and 5), 6 (day 2), or 20 (day 0) cultures. *Asterisks* denote significant differences determined by One-way ANOVA with Bonferroni's post hoc test, (* $p<0.05$, ** $p<0.01$, *** $p<0.001$). N.B. day 0 tissue is not included in statistical analysis.

ii) BrdU incorporation was unchanged by growth for up to 5 days in horse serum medium.

In the cultures grown in HS medium, neither the actual number of cells incorporating BrdU nor the proportion of the total number of cells that these cells represent was significantly altered by the age of the cultures ($p=0.051$ and $p=0.070$ respectively; one-way ANOVA). In both cases, BrdU detection was highest on day 2 and then fell, but none of the changes are significant (**Fig 4.15**).

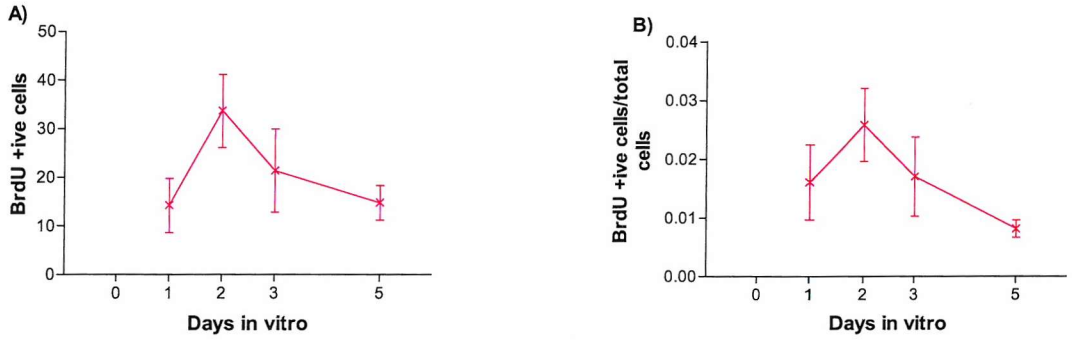

Fig 4.15: 5 day proliferation profile of cultures grown in horse serum medium, using measurements from 10μm thick sections. Showing absolute numbers of BrdU positive cells **(A)**, and the proportion of granule cells detected as also incorporating BrdU **(B)**. Values are expressed as mean ± SEM, from 4 (day 1), 5 (days 3 and 5), 6 (day 2), or 20 (day 0) cultures.

iii) Caspase-3 activation is unchanged by growth for up to 5 days in horse serum medium.

The number of activated caspase-3 positive cells was not significantly different over time in this experiment (p=0.249, one-way ANOVA) and nor was the proportion of cells in which caspase-3 was activated (p=0.380, one-way ANOVA; **Fig 4.16**).

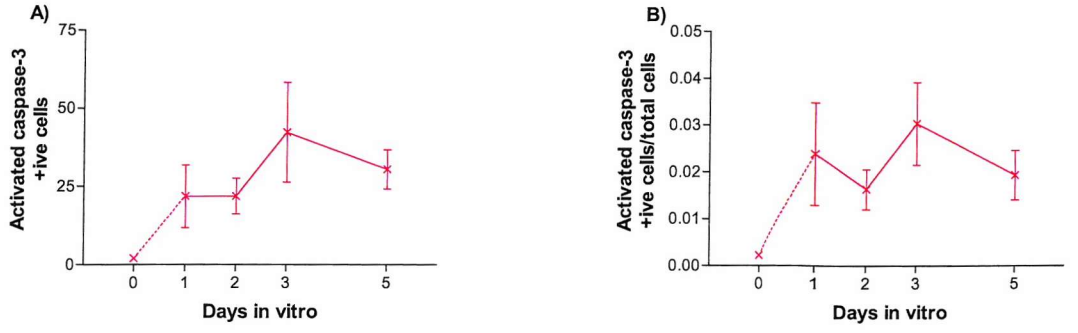

Fig 4.16: 5 day activated caspase-3 profile of cultures grown in horse serum medium, using measurements from 10μm thick sections. Showing absolute numbers of activated caspase-3 positive cells **(A)**, and the proportion of granule cells that expressed activated caspase-3 **(B)**. Values are expressed as mean ± SEM , from 4 (day 1), 5 (days 3 and 5), 6 (day 2), or 20 (day 0) cultures. N.B. day 0 tissue is not included in statistical analysis.

4.3.6 Short time course experiment considering up to 5 days *in vitro* in cultures grown in Neurobasal medium

i) The density of cells in cultures grown in Neurobasal medium decreased over time, but area and cell count were unchanged.

Cultures grown in NB medium were not significantly affected by age when both area and cell count were considered (p=0.476 and p=0.916 respectively; one-way ANOVA). However a significant decrease in the density between day 1 (15367±1196 cells/mm^2) and days 2 (12728±1310 cells/mm^2; $p<0.05$) and 5 (12714±1076 cells/mm^2; $p<0.05$), would indicate that the slightly, but not significantly, smaller area measured on day 1, combined with a slightly larger estimated cell count on the same day produces a significant change in the packing of the cells (**Fig 4.17**).

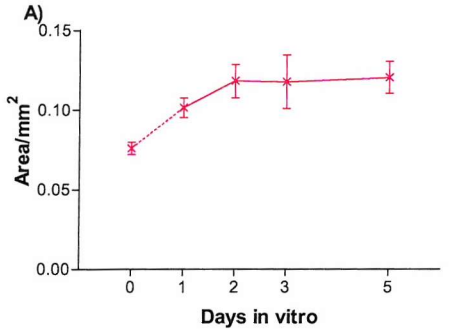

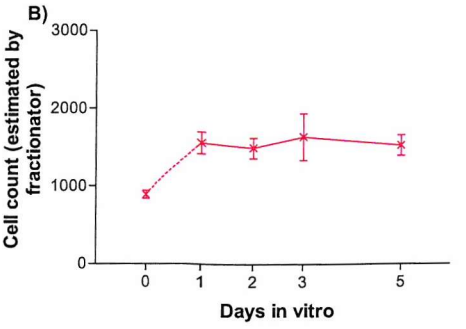

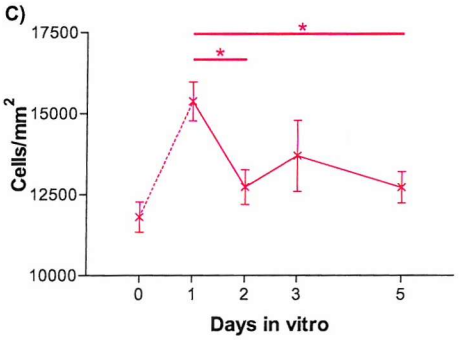

Fig 4.17: Variability of cultures grown in Neurobasal medium for up to 5 days, using measurements from 10μm thick sections. Showing granule cell layer area **(A)**, estimated granule cell count obtained using the fractionator method **(B)** and density of the cells in the granule cell layer **(C)**. Values are expressed as mean ± SEM , from 4 (day 1), 5 (days 3 and 5), 6 (day 2), or 20 (day 0) cultures. *Asterisks* denote significant differences determined by One-way ANOVA with Bonferroni's post hoc test, (* $p<0.05$, ** $p<0.01$, *** $p<0.001$). N.B. day 0 tissue is not included in statistical analysis.

ii) BrdU incorporation is maximal early in cultures grown in Neurobasal and then declines.

BrdU incorporation declined significantly between day 1 (45.0±28.9 cells) and day 3 (19.8±6.5 cells), with BrdU positive cell counts on days 2 and 5 similar to, but slightly higher, those on day 3 (Fig **4.18A**). This trend was exactly mirrored by the proportion of cells incorporating BrdU, which fell significantly between day 1 (2.9±1.7 % of cells) and day 3 (1.4±0.9 % of cells; $p<0.05$; **Fig 4.18B**), this is to be expected as the cell count between day 1 and day 5 is unchanged.

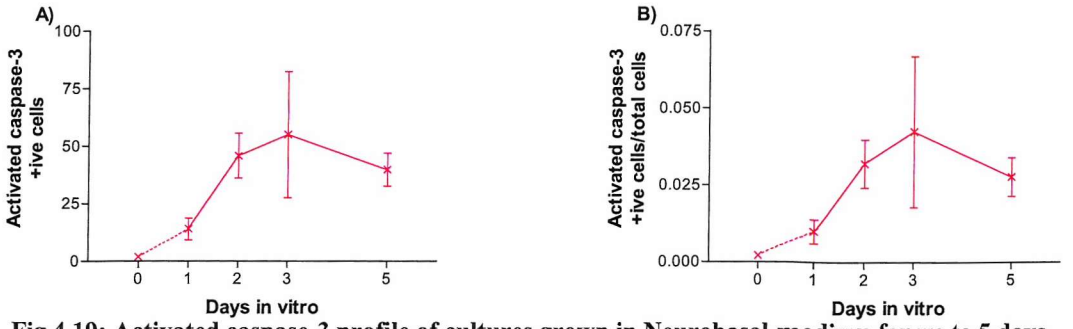

Fig 4.19: Activated caspase-3 profile of cultures grown in Neurobasal medium for up to 5 days, using measurements from 10μm thick sections. Showing absolute numbers of activated caspase-3 positive cells **(A)**, and the proportion of granule cells that expressed activated caspase-3 **(B)**. Values are expressed as mean ± SEM , from 4 (day 1), 5 (days 3 and 5), 6 (day 2), or 20 (day 0) cultures. N.B. day 0 tissue is not included in statistical analysis.

iii) Caspase-3 activation is unchanged over 5 days when grown in Neurobasal medium.

The number of activated caspase-3 positive cells was not significantly different over time in this experiment (p=0.121, one-way ANOVA) and nor was the proportion of cells in which caspase-3 was activated (p=0.208, one-way ANOVA). In both cases the trend is for an increase from day 1 to day 2, with the means then remaining relatively constant on days 3 and 5. The lack of a significant change is probably caused by the high variability in each group, especially noticeable on day 3 where the standard deviation is larger than the mean (activated caspase-3 cell count, 55.0±61.4 cells, and proportion 4.3±5.5 % of cells; **Fig 4.19**).

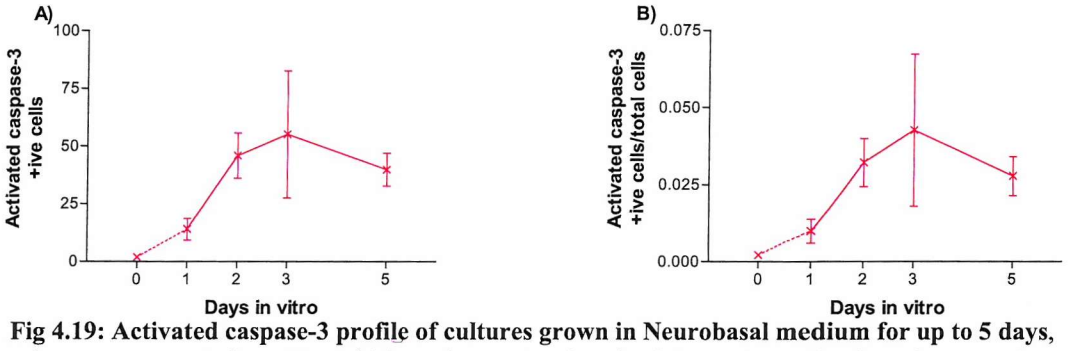

Fig 4.19: Activated caspase-3 profile of cultures grown in Neurobasal medium for up to 5 days, using measurements from 10μm thick sections. Showing absolute numbers of activated caspase-3 positive cells **(A)**, and the proportion of granule cells that expressed activated caspase-3 **(B)**. Values are expressed as mean ± SEM , from 4 (day 1), 5 (days 3 and 5), 6 (day 2), or 20 (day 0) cultures. N.B. day 0 tissue is not included in statistical analysis.

4.3.7 Comparing cultures grown in different types of media for up to 5 days

i) Media type had variable effects on area, cell count and density; area is larger in Neurobasal cultures, cell count is unchanged and density changes over time.

The number of cells in the GCL was not significantly altered by the medium the cultures were grown in ($p=0.078$; two-way ANOVA; **Fig 4.20B**), in this experiment. Cultures grown in Neurobasal medium tended to have significantly larger GCL areas ($p<0.01$; two-way ANOVA), this is a general trend and did not result in a significant difference at any particular time point (**Fig 4.20A**). The density of cells in this experiment showed significant interaction between day and media type ($p<0.001$; two-way ANOVA), and this resulted in significant differences between the cell densities of cultures grown in the different media types. On day 1 cultures grown in Neurobasal medium had a significantly higher cell density than those grown in horse serum medium (NB, 15367±1196 cells/mm^2 vs. HS, 10987±1553 cells/mm^2; $p<0.01$). Conversely, on day 5 cultures grown in horse serum medium had a significantly higher cell density than those grown in Neurobasal medium (NB, 12714±1076 cells/mm^2 vs. HS, 15953±1366 cells/mm^2; $p<0.05$; **Fig 4.20C**).

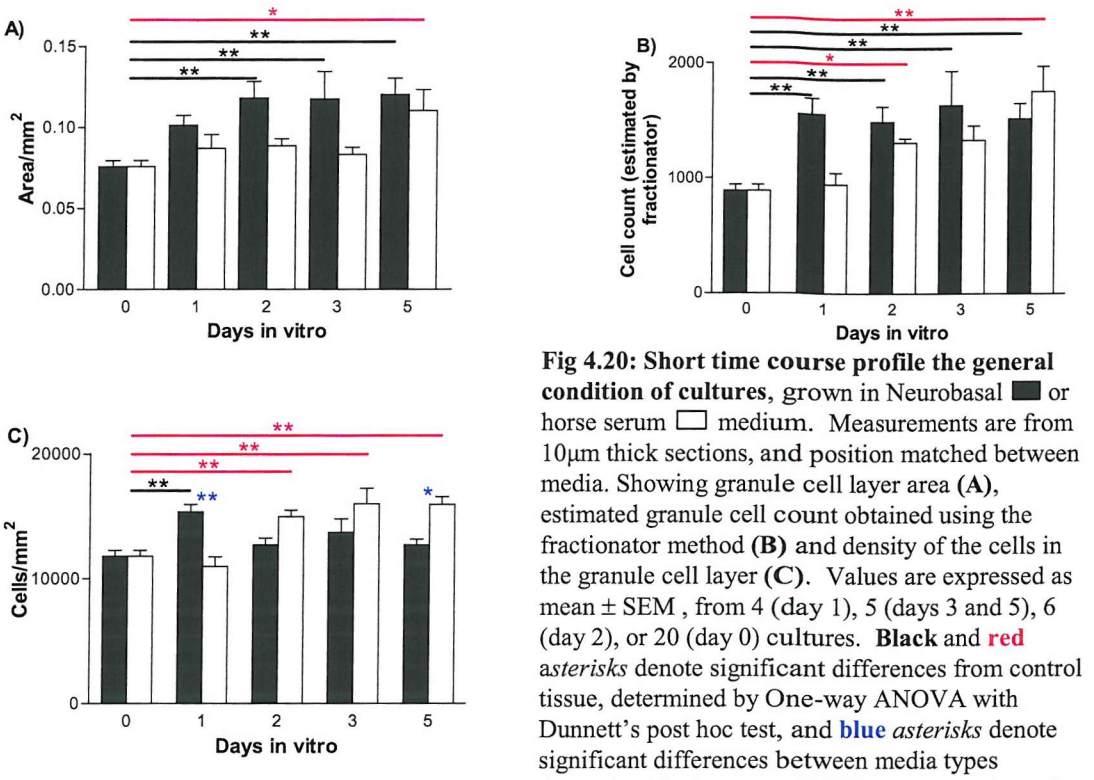

Fig 4.20: Short time course profile the general condition of cultures, grown in Neurobasal ■ or horse serum □ medium. Measurements are from 10μm thick sections, and position matched between media. Showing granule cell layer area **(A)**, estimated granule cell count obtained using the fractionator method **(B)** and density of the cells in the granule cell layer **(C)**. Values are expressed as mean ± SEM , from 4 (day 1), 5 (days 3 and 5), 6 (day 2), or 20 (day 0) cultures. **Black** and **red** *asterisks* denote significant differences from control tissue, determined by One-way ANOVA with Dunnett's post hoc test, and **blue** *asterisks* denote significant differences between media types determined by two-way ANOVA with bonferroni's post hoc test, (* $p<0.05$, ** $p<0.01$, *** $p<0.001$).

ii) Overall BrdU incorporation was not different between media types, but more positive cells were detected in cultures grown in Neurobasal medium initially.

On day 1 there were significantly more cells incorporating BrdU in cultures grown in NB medium than in those grown in HS medium (NB, 45.0±28.8 cells vs. HS, 14.3±11.1 cells; $p<0.05$). However overall the mean number of BrdU positive cells detected in the cultures did not differ between media types ($p=0.129$; two-way ANOVA; **Fig 4.21A**). When differences between the total number of cells present in the cultures was taken into consideration the difference between media types on day 1 was not significant (proportion of BrdU +ive cells; NB, 2.9±1.7% of cells, vs. HS, 1.6±1.3% of cells) and no overall difference was present ($p=0.558$; two-way ANOVA; **Fig 4.21B**).

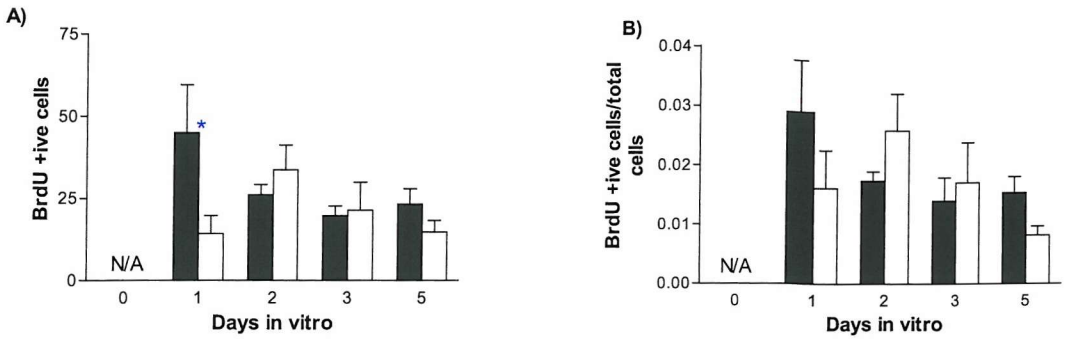

Fig 4.21: Short time course profile of BrdU incorporation in cultures, grown in Neurobasal ■ or horse serum □ medium. Measurements are from 10μm thick sections, and position matched between media. Showing absolute numbers of BrdU positive cells **(A)**, and the proportion of granule cells that incorporated BrdU in the 2 hours prior to fixation **(B)**. Values are expressed as mean ± SEM, from 4 (day 1), 5 (days 3 and 5), 6 (day 2), or 20 (day 0) cultures. **Blue** *asterisks* denote significant differences between media types determined by two-way ANOVA with bonferroni's post hoc test, (* $p<0.05$, ** $p<0.01$, *** $p<0.001$).

iii) Media type did not affect activated caspase-3 detection over 5 days in culture.

Overall, the mean number of activated caspase-3 positive cells detected in the cultures did not differ between media types ($p=0.311$; two-way ANOVA), and neither did the proportion of cells in which caspase-3 activation was detected ($p=0.481$; two-way ANOVA; **Fig 4.22**).

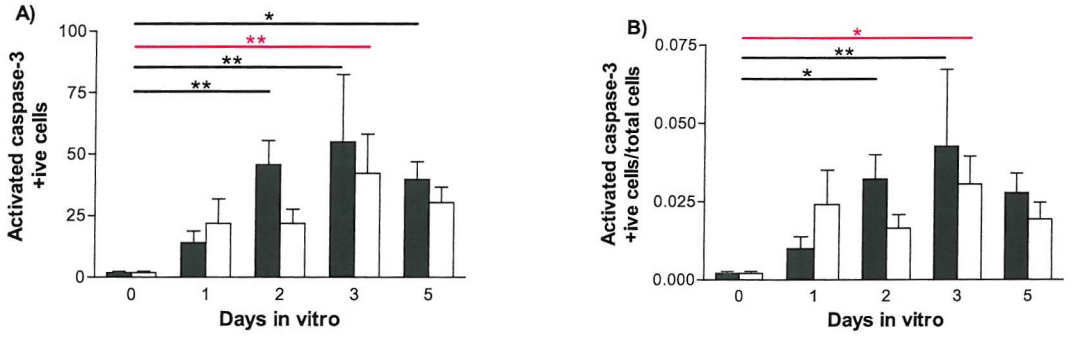

Fig 4.22: Short time course profile of caspase-3 activation in cultures, grown in Neurobasal ■ or horse serum □ medium. Measurements are from 10μm thick sections, and position matched between media. Showing absolute numbers of activated caspase-3 positive cells **(A)**, and the proportion of granule cells that expressed activated caspase-3 **(B)**. Values are expressed as mean ± SEM, from 4 (day 1), 5 (days 3 and 5), 6 (day 2), or 20 (day 0) cultures. **Black** and **red** a*sterisks* denote significant differences from control tissue, determined by One-way ANOVA with Dunnett's post hoc test, (* $p<0.05$, ** $p<0.01$, *** $p<0.001$).

iv) The time zero tissue differs greatly in GCL area, cell count, density and especially caspase-3 activation from cultures grown in either media type.

In addition to the groups of cultures grown in each media type for 1, 2, 3, or 5 days, in this experiment a further set of cultures were not grown in any culture medium but fixed immediately after preparation. These cultures were not analysed with all the other tissue as they don't necessarily belong to either media type, however subsequent to the main comparisons between media types all cultures were compared with this control group with a one-way ANOVA and Dunnett's post hoc test.

All cultures grown in Neurobasal medium had significantly more granule cells than the day 0 tissue (day 0, 889±229 cells, vs. day 1, 1560±278 cells, day 2, 1496±326 cells, day 3, 1638±672 cells, and day 5, 1523±297 cells; all $p<0.01$; **Fig 4.20B**), but only cultures from day 1 had a significantly higher cell density (day 0, 11802±2084 cells/mm^2 vs. day1, 15367±1196 cells/mm^2; $p<0.01$; **Fig 4.20C**). This is reflected in the fact that the GCL area increased significantly in the cultures from day 2 (0.118±0.026mm^2), day 3 (0.117±0.038mm^2) and day 5 (0.120±0.023mm^2) but not on day 1, compared with day 0 (0.076±0.017mm^2; all $p<0.01$; **Fig 4.20A**). Possibly suggesting that initial settling of these cultures results in a compression of the GCL in the *z*-direction, and then expansion in the *xy*-plane, or proliferation is having a significant influence on tissue structure. Cultures grown in horse serum medium had significantly increased density on day 2 (14963±1265 cells/mm^2), day 3 (16016±2753 cells/mm^2) and day 5 (15953±1366 cells/mm^2) compared with the day 0 (11802±2084 cells/mm^2; all $p<0.01$; **Fig 4.20C**) tissue, and this was mirrored by a large cell count on day 3 (day 0, 889±229 cells vs. day 3, 1334±284 cells) and significantly increased cell counts on days 2 and 5 (day 2, 1315±86 cells; $p<0.05$ vs. day 0; and day 5, 1757±501 cells; $p<0.01$ vs. day 0; **Fig 4.20B**). Unlike with the Neurobasal cultures the change in cell counts was not accompanied by a significant change in GCL area until day 5 (day 0, 0.08±0.02mm^2 vs. 0.11±0.03mm^2; $p<0.05$; **Fig 4.20A**), possibly indicating that the process of compression and expansion takes longer in the cultures grown in horse serum, a hypothesis that is further supported by the lack of a change in granule cell number between day 0 and day 1 in these cultures. The number of activated caspase-3 positive cells detected in the freshly prepared day 0 tissue was very low (1.9±2.3 cells), this represents the minimal levels of apoptosis *in vivo* in the postnatal rat . Increases over this initial level of activated caspase-3 expression were

observed in both media types and at all time points, with the increase reaching statistical significance on day 2 (45.8±24.0 cells; $p<0.01$) and day 5 (39.8±16.0 cells; $p<0.05$) in Neurobasal medium and on day 3 in both media (NB, 55.0±61.4 cells; and HS, 42.2±35.6 cells; both $p<0.01$; **Fig 4.22A**).

The proportion of cells showing caspase-3 activation was also very low in the day 0 tissue (0.21±0.25 % of cells) and the increases over this initial level of activated caspase-3 expression were observed in both media types and at all time points, with the increase reaching statistical significance on day 2 in Neurobasal medium (3.2±1.9 % of cells; $p<0.05$) and on day 3 in both media (NB, 4.3±5.5 % of cells; $p<0.01$; and HS, 3.0±2.0 % of cells; $p<0.05$; **Fig 4.22B**).

4.3.8 Reproducibility across time course experiments

The inter experiment variability in the cultures was examined by comparing the time points that overlapped in both time course experiments, days 1, 3, and 5. All cultures grown in HS medium were considered with two-way ANOVA, and Bonferroni post hoc tests permitted comparisons between experiments on individual days. The same analysis was also applied to all cultures grown in NB medium.

4.3.9 Reproducibility between experiments in horse serum based medium

i) Reproducibility of area between experiments was poor in cultures grown in horse serum medium, but cell counts and density did not differ significantly.

The area of the GCL showed significant interaction between the experiment the cultures were taken from and the time at which the cultures were fixed ($p<0.05$; two-way ANOVA), and thus the differences between the experiments were not the same at every time point compared. Areas were similar on day 1 but significantly larger in the long time course experiment on day 3 (long time course, 0.120±0.026mm^2, and short time course, 0.083±0.009mm^2; $p<0.01$) and day 5 (long time course, 0.154±0.044mm^2, and short time course, 0.110±0.028mm^2; $p<0.01$; **Fig 4.23A**). Mean granule cell counts were not significantly different at any individual time point between the two-experiments and although there appeared to be a tendency for the cell counts to be larger in the long time course experiment this was not statistically significant overall ($p=0.064$; two-way ANOVA; **Fig 4.23B**). These two factors had a

combined effect on density, with the overall means different between experiments ($p<0.05$; two-way ANOVA), but the trend for higher cell density in the short time course experiment was not significant at any individual point (**Fig 4.23C**).

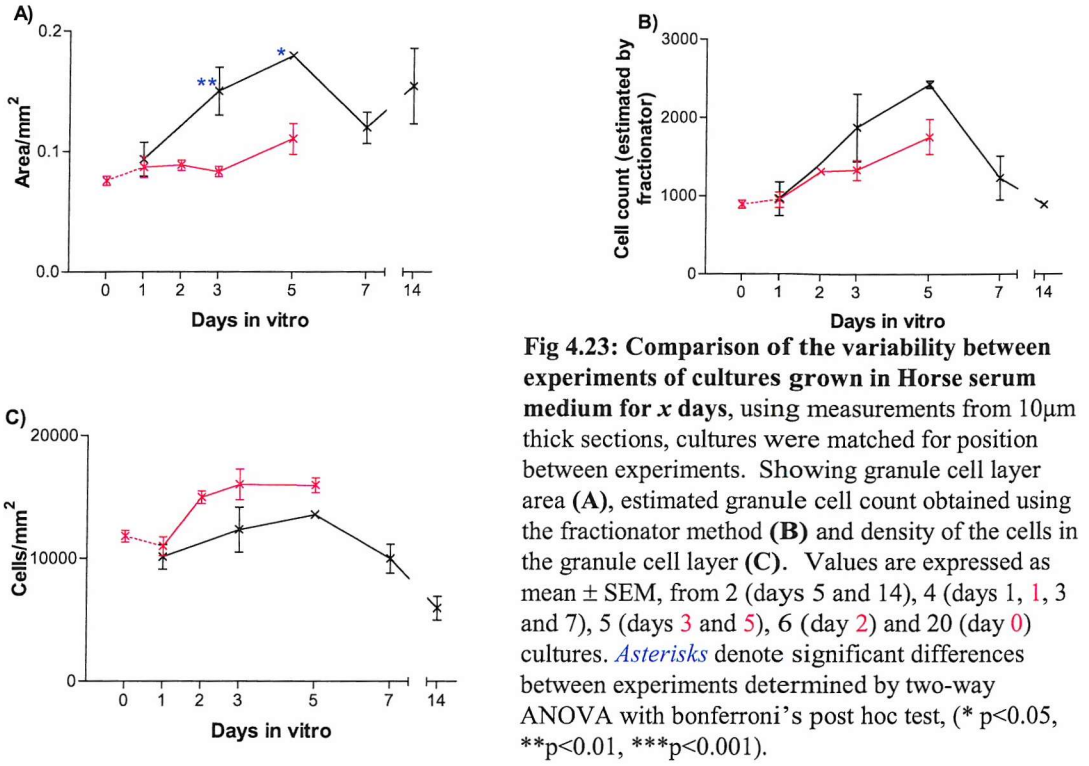

Fig 4.23: Comparison of the variability between experiments of cultures grown in Horse serum medium for *x* days, using measurements from 10μm thick sections, cultures were matched for position between experiments. Showing granule cell layer area **(A)**, estimated granule cell count obtained using the fractionator method **(B)** and density of the cells in the granule cell layer **(C)**. Values are expressed as mean ± SEM, from 2 (days 5 and 14), 4 (days 1, 1, 3 and 7), 5 (days 3 and 5), 6 (day 2) and 20 (day 0) cultures. *Asterisks* denote significant differences between experiments determined by two-way ANOVA with bonferroni's post hoc test, (* $p<0.05$, ** $p<0.01$, *** $p<0.001$).

ii) Reproducibility of BrdU incorporation in cultures grown in horse serum medium is poor.

The number of BrdU positive cells observed was significantly greater in the long time course experiment ($p<0.01$; two-way ANOVA). This is due to a significant difference on day 1 (long time course, 68.3±45.4 cells, and short time course, 14.3±11.1 cells; $p<0.01$), a trend that is continued on day 3 but is not statistically significant (**Fig 4.24A**). When the effect of the total number of cells present is also considered, the overall proportion of cells incorporating BrdU show significant interaction between day and experiment type ($p<0.05$; two-way ANOVA). The interaction occurs because the proportion of BrdU positive cells differs significantly between experiments on day 1 (long time course, 3.0±1.4% of cells, and short time course, 1.6±1.3% of cells; $p<0.01$) but is similar on days 3 and 5 (**Fig 4.24B**).

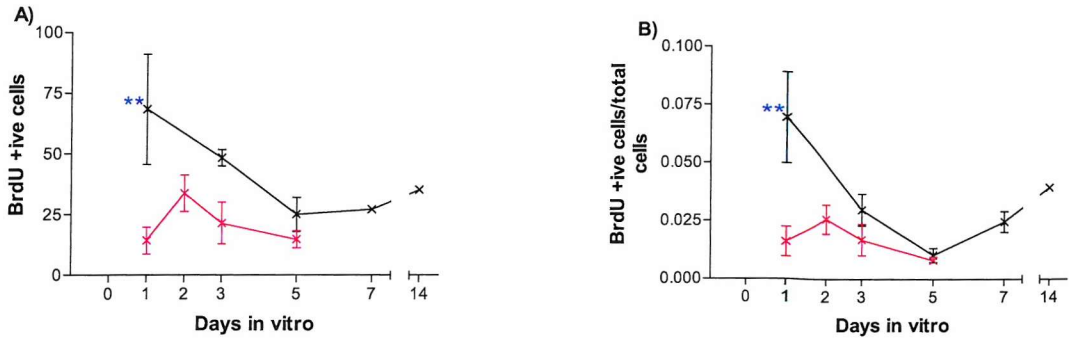

Fig 4.24: Comparison of proliferation profile of cultures grown in horse serum medium, using measurements from 10μm thick sections, cultures were matched for position between experiments. Showing absolute numbers of BrdU positive cells **(A)**, and the proportion of granule cells detected as also incorporating BrdU **(B)**. Values are expressed as mean ± SEM, from 2 (days 5 and 14), 4 (days 1, 1, 3 and 7), 5 (days 3 and 5), and 6 (day 2) cultures. *Asterisks* denote significant differences between experiments determined by two-way ANOVA with bonferroni's post hoc test, (* $p<0.05$, ** $p<0.01$, *** $p<0.001$).

iii) Detection of caspase-3 activation is not reproducible between experiments in cultures grown in horse serum medium.

The number of activated caspase-3 positive cells observed was significantly greater in the long time course experiment ($p<0.05$; two-way ANOVA). As with the BrdU count, this is due to a significant difference on day 1 (long time course, 78.5±40.4 cells, and short time course, 21.8±20.0 cells; $p<0.05$), a trend that is continued on day 3 but is not statistically significant (**Fig 4.25A**). When the effect of the total number of cells present is also considered, the overall proportion of cells incorporating BrdU show significant interaction between day and experiment type ($p<0.05$; two-way ANOVA). The interaction occurs because the proportion of BrdU positive cells differs significantly between experiments on day 1 (long time course, 8.4±4.2% of cells, and short time course, 2.4±2.2% of cells; $p<0.01$) but is similar on days 3 and 5 (**Fig 4.25B**).

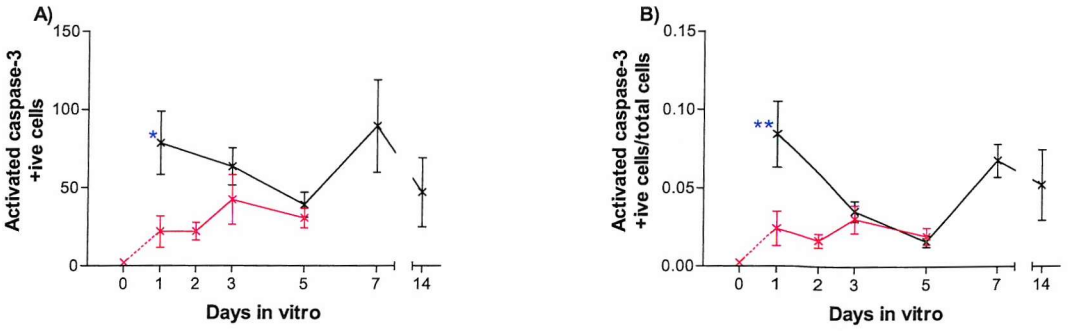

Fig 4.25: Comparison of activated caspase-3 profiles of cultures grown in horse serum medium, using measurements from 10μm thick sections, cultures were matched for position between experiments. Showing absolute numbers of activated caspase-3 positive cells **(A)**, and the proportion of granule cells that expressed activated caspase-3 **(B)**. Values are expressed as mean ± SEM, from 2 (days 5 and 14), 4 (days 1, 1, 3 and 7), 5 (days 3 and 5), 6 (day 2) and 20 (day 0) cultures. *Asterisks* denote significant differences between experiments determined by two-way ANOVA with bonferroni's post hoc test, (* $p<0.05$, ** $p<0.01$, *** $p<0.001$).

4.3.10 Reproducibility between experiments in Neurobasal medium

i) Cultures grown in Neurobasal medium had different areas and cell counts in the two experiments but density was unchanged.

In these cultures the area of the GCL and the number of cells it contained differed significantly between the two experiments (both $p<0.05$; two-way ANOVA), in both cases the cultures from the long time course had a tendency to be larger. However, none of the individual cell counts compared between experiments differed significantly (**Fig 4.26B**), whereas the areas were significantly different in the two experiments on day 1 (long time course, 0.22±0.10 cells/mm^2, and short time course, 0.10±0.01 cells/mm^2; $p<0.05$; **Fig 4.26A**).

The combination of these two effects was a density of cells in the two experiments that did not differ significantly, either overall ($p=0.582$; two-way ANOVA) or at any of the individual time points compared (**Fig 4.26C**).

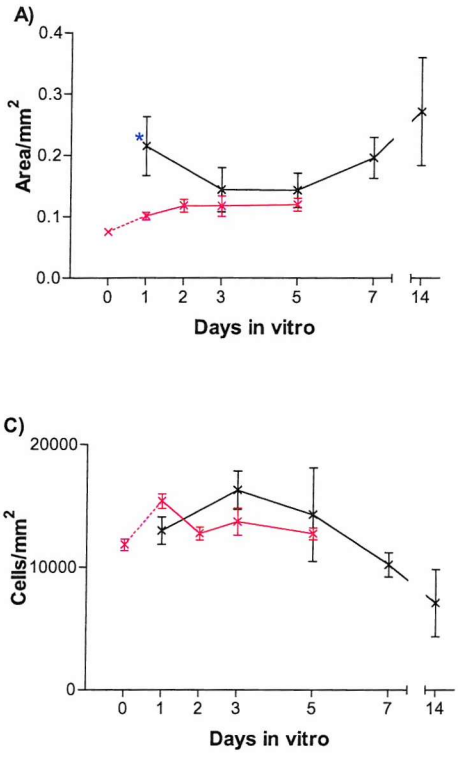

Fig 4.26: Comparison of the variability between experiments of cultures grown in Neurobasal medium for *x* days, using measurements from 10μm thick sections, cultures were matched for position between experiments. Showing granule cell layer area **(A)**, estimated granule cell count obtained using the fractionator method **(B)** and density of the cells in the granule cell layer **(C)**. Values are expressed as mean ± SEM, from 2 (days 5 and 14), 4 (days 1, 1, 3 and 7), 5 (days 3 and 5), 6 (day 2) and 20 (day 0) cultures. *Asterisks* denote significant differences between experiments determined by two-way ANOVA with bonferroni's post hoc test, (* $p<0.05$).

ii) BrdU incorporation is reproducible between experiments in cultures grown in Neurobasal medium.

The number of cells incorporating BrdU did not differ significantly between the two experiments ($p=0.081$; two-way ANOVA), however at each time point the cultures from the long time course experiment had larger (but not significantly larger) positive counts (**Fig 4.27A**). When the total number of cells present in the GCL was taken into account, the proportions of cells incorporating BrdU were virtually identical at each time point and were also not significantly different overall ($p=0.651$; two-way ANOVA; **Fig 4.27B**).

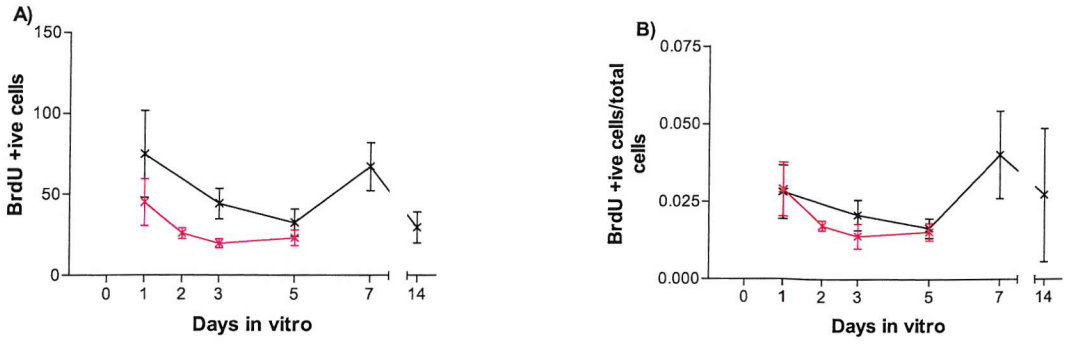

Fig 4.27: Comparing proliferation profiles of cultures grown in Neurobasal medium, using measurements from 10μm thick sections, cultures were matched for position between experiments. Showing absolute numbers of BrdU positive cells **(A)**, and the proportion of granule cells detected as also incorporating BrdU **(B)**. Values are expressed as mean ± SEM, from 2 (days 5 and 14), 4 (days 1, 1, 3 and 7), 5 (days 3 and 5), and 6 (day 2) cultures.

iii) Caspase-3 activation is variable but not statistically different between experiments in cultures grown in Neurobasal medium.

Activated caspase-3 positive cell profiles look very different between the two experiments the means appear very similar on days 1 and 5, but quite different on day 3. However this apparent difference is not statistically significant due to the very high variability observed in the short time course experiment at this time or indeed overall ($p=0.308$; two-way ANOVA; **Fig 4.28A**). The proportion of cells in which caspase-3 activation is detected follows a similar temporal profile to the number of activated caspase-3 positive cells and does not differ significantly between experiments ($p=0.200$; two-way ANOVA; **Fig 4.28B**).

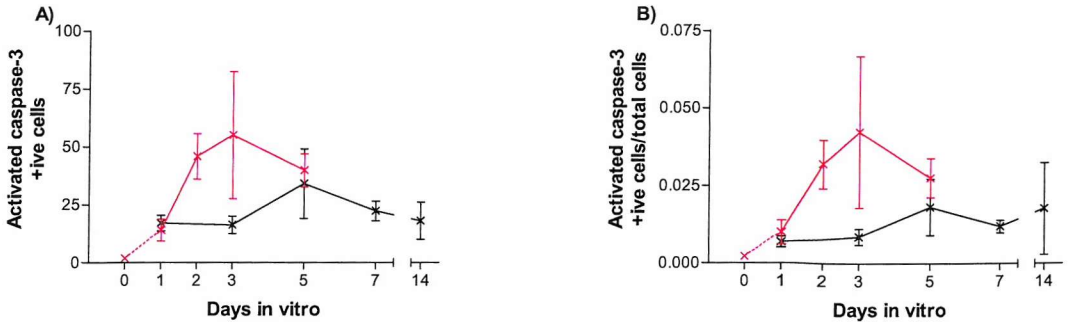

Fig 4.28: Comparing activated caspase-3 profiles of cultures grown in Neurobasal medium, using measurements from 10μm thick sections, cultures were matched for position between experiments. Showing absolute numbers of activated caspase-3 positive cells **(A)**, and the proportion of granule cells that expressed activated caspase-3 **(B)**. Values are expressed as mean ± SEM, from 2 (days 5 and 14), 4 (days 1, 1, 3 and 7), 5 (days 3 and 5), 6 (day 2) and 20 (day 0) cultures.

4.3.11 Summary

The larger granule cell counts and GCL areas are both in the long time course experiment, the fact that the density of cells is unchanged between experiments indicates that the differences in granule cell number could be due to inter litter variations.

An examination of reproducibility of results at 1, 3 and 5 DIV in both media showed that Neurobasal produced highly conserved results, with no significant changes in any of the first order derivatives used, although the activated caspase-3 data showed some variability on day 3 (Fig 4.28).

4.4 Discussion

The principle problem associated with the experiments described in the previous chapter related to variability between cultures. In these experiments we have demonstrated that the culture selection method, adopted as a result of that work, produces cultures that, when grown in Neurobasal medium, are uniform from day 2 for a further 3-5 days. These experiments have also shown that these results can be reproduced between different culture batches. The results obtained also indicated that differences, which were apparent between the media types in the previous chapter, are preserved in these experiments.

4.4.1 Slow changes in culture structure

The dentate granule cell density at later points is well matched between the different media types, and this would suggest that the changes occurring over time are similar. However closer examination of the temporal changes occurring in cultures grown in the different media types reveals that what is happening is actually quite different. In HS medium, the fall in cell numbers from day 7 suggests that more cells are dying in these cultures, as cell death is the only way to decrease the number of cells present. This is not born out by the activated caspase-3 staining, and implies other forms of cell death that we are not detecting must be responsible, a reasonable conclusion since activated caspase-3 does not identify all types of cell death.

By contrast, the cultures grown in NB medium appear to disperse from day 7, as the area of the GCL increases but the cell count does not. Unfortunately, neither of these changes is desirable in any model examining changes in cultures arising because of a treatment; where a stable control population is required. The dispersion is less of a problem, making longer-term studies in cultures grown in Neurobasal medium more acceptable than using horse serum medium, but ideally future experiments should last no longer than 7 days.

4.4.2 Rapid changes in culture structure.

The changes in cell number observed in the short time course experiment can all be accounted for with the exponential model of cell division, described earlier (Chapter 4.1.2), with the exception of the increase in cell number from day 1 to day 2 ($p<0.01$, one tailed t-test) in cultures grown in horse serum medium. In fact, the observed

changes in cell number are small enough that they could arise from a steady state pattern of cell division (again with the exception of day 1 to day 2 in HS medium; $p<0.01$), or any model lying between these two extremes. The assumption of no cell death is also unnecessary, as either of the models described can generate considerably more new cells than were required to generate the observed changes. However, the fact that between day 1 and day 2 in horse serum cultures proliferation alone is not sufficient to generate the observed change indicates that culture restructuring may be having an effect here. In the horse serum cultures, the area is unchanged, the number of cells is larger, but is not a significant increase, and the density of cells increases significantly. This suggests that between day 1 and day 2 the cells in these cultures are becoming compressed into a more densely packed granule cell layer. This could be either through reduced extracellular space or decreased cell volume, but cannot be due to increased proliferation since this would have been detected with high BrdU labelling. The fact that between day 3 and day 5 the area of these cultures increases significantly would tend to support this model, with a compression in the *z* axis being followed by a delayed expansion in the *xy* plane. This raises the obvious question, why should cultures grown in horse serum medium restructure over time, when those grown in Neurobasal medium do not?

To which the answer is cultures grown in Neurobasal medium do restructure, but it occurs earlier and in a more synergistic fashion with respect to thinning in the *z* axis and spreading in the *xy* plane. The significant change in cell count occurs between day 0 and day 1 in cultures grown in Neurobasal medium, with the change in area being complete by day 2 (Fig 4.20), whereas the same changes take until days 2 and 5 respectively in cultures grown in horse serum medium. Unfortunately detecting BrdU in the day 0 tissue was not possible, however the BrdU data from day 1 to day 3, in the short time course experiment, appears to follow an inverse log curve (Fig 4.18). And indeed a log transformation of the BrdU data for these days produces a linear regression line that suggests 65 cells could be labelled on day 0 (y intercept = 1.811, $r^2=0.9637$). The average day 0 cell count was 888.8 cells, using the exponential model BrdU labelling of 65 cells could add almost 360 new cells to this total, slightly over half the required change to reach an average of 1560 cells by day 1. This would suggest that this particular increase in total cell number is due to a rapid restructuring in these cultures. Therefore, it is unwise to use cultures until they are at least 2 days old if grown in Neurobasal medium and perhaps even older if grown in horse serum

medium. The day 0 values are compared with the short time course BrdU data, and not the long time course BrdU data, because they are drawn from the same animals, and high inter-litter variability was observed which is discussed below.

4.4.3 Reproducibility

In the newly plated cultures, reproducibility was poor in both media types between the two experiments, although it was better in the cultures grown in Neurobasal medium, possibly because of the more rapid rearrangement of the tissue in these cultures, discussed above. Many of the differences observed in the raw data obtained from the cultures could arise from inter-litter variability, as the changes in BrdU and activated caspase-3 are dependent on the number of cells present. The proportions of the total population identified as either BrdU or activated caspase-3 positive are unchanged between the two experiments in the cultures grown in Neurobasal medium. The density is also unchanged, indicating that although there are changes between experiments in the area and cell counts these changes are of a similar magnitude and the basic structure of the cultures does not vary. Therefore, the raw data obtained is useful for comparing cultures within an experiment and the 1st order derivatives are useful for comparing the results of multiple experiments.

4.4.4 Problems associated with variable culture thickness

The fact that the cultures thin and spread over time reduces the value of comparisons over time. Changes may not be due to an applied treatment but to different rates of thinning/spreading over time. Ideally, this problem could be eradicated if the entire culture could be described. Counting all the cells in all the sections to do this is clearly not feasible, as it would prevent adjacent sections from being used to identify BrdU and activated caspase-3 positive cells. Measuring the thickness of the cultures and then applying a scalar factor to the measurements obtained from a 10μm section might help correct for this. However, this approach would introduce significant inaccuracies by over estimating the number of cells present in a culture. This problem was described previously (Chapter 3.1.1), and the current model was developed to try to avoid it. Until a way of overcoming this problem can be found results demonstrating changes between time points should be treated with caution, but results demonstrating changes between treatments at the same time point can be considered reliable.

4.4.5 A defined model for examining changes in culture structure, cell proliferation and cell death in response to applied treatments over time.

The high reproducibility of results from cultures grown in Neurobasal medium, combined with the better stability of these cultures over time, the more consistent results from the mid-septal part of the hippocampus and the chemically defined nature of the medium makes Neurobasal medium the preferred growth medium for this new *in vitro* model of cell proliferation and death. Therefore, the model we have established will use cultures taken from the mid-septal hippocampus, matched for position between control and treatment groups with cultures for the treatment group coming from one hippocampus and the control cultures coming from the same septo-temporal position in the second hippocampus in each animal. Cultures will be grown in Neurobasal medium for at least two days before use and experiments will last no longer than 5 days.

This model will be used in the next chapter to investigate the effect of the chemoconvulsant kainate on proliferation and death.

Chapter 5

Effect of kainate on cell proliferation and death in the granule cell layer of OHSCs

5.1 Introduction

Chapters 3 and 4 identified a population of cultures, taken from the mid-septal part of the hippocampus and grown in a Neurobasal based medium, which produced a stable baseline for about 5 days from the second day *in vitro*. These cultures exhibited consistent absolute numbers of granule cells, numbers of proliferating (BrdU positive) cells and dying (activated caspase-3) cells. These stable control conditions permit the investigation of the effects of seizure on proliferation and death in OHSCs, which is the focus the work in this chapter.

5.1.1 Seizure induced neurogenesis

The induction of proliferation after seizures is well documented *in vivo* (Parent, et al., 1997; Bengzon, et al., 1997; Gray and Sundstrom, 1998; Nakagawa, et al., 2000), and to a lesser extent *in vitro* (Routbort, et al., 1999). However, the biological mechanisms responsible are not clear, and indeed there is still considerable debate as to the role of the neurogenesis. Is seizure-induced neurogenesis a repair phenomenon, replacing for example cells that die during the seizure, or is the neurogenesis part of the pathogenesis of epilepsy? Cell death in the granule cell layer after seizures is well documented (Bengzon, et al., 1997; Fujikawa, et al., 2000), which adds credence to the repair hypothesis for the role of increased neurogenesis. However, the increased neurogenesis appears to only be transient and long term survival of a cohort of these cells is no different to seizure free control animals at 28 days after seizure (Parent, et al., 1997). The case for a pathogenic role is strengthened by the observation of new granule cells in ectopic locations after seizures (Scharfman, et al., 2000). These cells are also hyper-excitable and form aberrant connections back onto the dentate granule cells, and thus could be part of the structural reorganisation that is thought to occur during epileptogenesis.

5.1.2 Seizure models

There are three general types of method used to generate seizures *in vivo*. Some groups use animals that are genetically prone to seizures which can then be induced for example, with sound (audiogenic kindling; Romcy-Pereira and Garcia-Cairasco, 2003) or in EL mice through swinging by the tail or tossing in the air (Nagatomo, et al., 2000). These methods of seizure induction are of little use in organotypic

cultures, as they don't have ears or tails. The other commonly used models are electrical kindling, in which pulses of current are applied to induce seizures (McIntyre, et al., 2002), and administration of chemoconvulsants, where chemicals such as kainate and pilocarpine are used to hyper-excite the tissue (Nadler, 1981; Leite, et al., 2002). Induction of electrical kindling requires the use of electrodes and would add further technical complications to the organotypic model, as the cultures need to be maintained in a sterile environment. By contrast, a chemoconvulsant can easily be added to the growth media at a known concentration and for a specific time. Additionally, our lab already has considerable experience in using kainate (or kainic acid), a chemoconvulsant found in a red algae (*Digenea*). It produces many changes in the hippocampus which are observed in epileptic tissue, including tonic-clonic electrical bursting (Vezzani, et al., 1994), mossy fiber sprouting (McAdory, et al., 1998; Routbort, et al., 1999; Wenzel, et al., 2000), cell death (Covolan, et al., 2000) and neurogenesis (Gray and Sundstrom, 1998). Kainate is widely used as a model for generating seizures, *in vivo* and *in vitro*, and thus we considered it an acceptable model to use on OHSCs. Previous studies in our laboratory have shown that 5μM kainate added to the growth media produces seizure activity in OHSCs (Best, et al., 1996) and a pattern of damage which mirrors that detected *in vivo* (Rimvall, et al., 1987).

5.1.2 Improving the detection of cell death

The method for detecting cell death in the cultures thus far has been to use immunostaining for activated caspase-3, which has been described as a marker of cells fated to undergo apoptotic death (Nijhawan, et al., 2000). However it has disadvantages, a recent publication has cast doubt on this (D'Sa-Eipper, et al., 2001) showed that in caspase-3 knockout embryonic mice apoptotic cell death could be induced. Other research has suggested that an apparently opposite effect can be observed with activated caspase-3 inducing cell proliferation (Yan, et al., 2001), which would, in some cell types, make it a marker of cell proliferation. In addition to this potential problem with using activated caspase-3 to identify cell death, the results obtained from the previous chapters suggested that the staining obtained is highly variable between cultures within each group, making detection of changes between groups difficult. Therefore, an additional method of detecting cell death is required, as currently this is the model's weakest area. As was previously discussed, the most

commonly used technique for quantifying cell death is by the application of propidium iodide (PI), however this method is inappropriate for these experiments because when this method is used a value for the whole thickness of the culture is obtained but in our model only a small part of each culture is analysed for cell counts and cell proliferation. If all cultures were of the same thickness the PI method may be appropriate but unfortunately, the thickness of the cultures varies with age. The other potential markers of cell death already discussed are terminal dUTP nick end-labelling (TUNEL) staining to mark apoptotic cells (Bengzon, et al., 1997), a method also used in a similar study to this only involving neo-cortical organotypic cultures (Haydar, et al., 1999), or counting condensed nuclei in the granule cell layer of sections stained with DAPI or Hoescht 33258 (Rivera, et al., 1998). These markers of cell death all have their own problems however, TUNEL stain identifies strand breaks in DNA and BrdU incorporation leads to a weakening of the DNA, possibly leading to fragmentation and thus false positive staining, which is why they were initially rejected. However another technique has recently been described, staining with Fluoro-Jade B (FJB), this is a fluorescent dye that exclusively stains degenerating neurons in their entirety including cell bodies, dendrites, axons and terminals. The authors report that it selectively stains dying neurons in many different *in vivo* models of neuro-degeneration, including the use of kainate, where staining is observed in parts of the hippocampal formation from about 4 hours after an intra-peritoneal kainate injection (Schmued, et al., 1997; Hopkins, et al., 2000).

5.1.3 Questions to be addressed

The aim is to establish a model in OHSCs, where responses to brain injury, specifically seizures, can be studied by quantification of changes in granule cell number, cell proliferation, and cell death in the dentate gyrus. To achieve this kainate is going to be used as a 'seizure' inducing chemoconvulsant. A pulse of BrdU labelling is will be used as a proliferative marker, activated caspase-3 will be used to identify apoptotic cells, FJB staining will be used to identify all dying cells and a stereological technique, the fractionator, will estimate granule cell number in thionine stained tissue. These techniques can then be used to assess changes induced in the cultures relative to matched cultures that remain untreated. These findings this can

then be compared to existing *in vivo* research to determine the value of the protocol as an *in vitro* model of seizures.

5.2 Methods

The experiments in this chapter cultures were prepared as described in chapter 2, with the method of selecting cultures for each well and the treatment the cultures subsequently received until fixation detailed in sections 5.2.1. The processing of the cultures after fixation was carried out as described in sections 3.2.3 – 3.2.5, covering cryo-sectioning, immunostaining and quantification of thionine, BrdU and activated caspase-3. The final section obtained was processed for Fluoro-Jade B and is described below in sections 5.2.2 and 5.2.3.

5.2.1 Quantification of cell proliferation and death in an *in vitro* model of seizure

Cultures from the mid-septal hippocampus were prepared as described in chapter 2, and systematically placed into inserts containing NB medium. At this time the cultures were divided into 2 paired groups with one hippocampus per animal contributing cultures to each group, for 3 days the cultures in both groups were treated identically. After 3 days *in vitro*, one of the groups was exposed to kainate (5μM) for up to 24 hours when the medium was changed to normal Neurobasal medium. The other group formed untreated time matched controls, which received medium changes at the same times as the kainate treated group. BrdU (10μM) was added to all the cultures 2 hours before fixing in 4% PFA. Kainate treated cultures and paired time matched controls were fixed 2,24 and 72 hours after kainate was added (Fig 5.1).

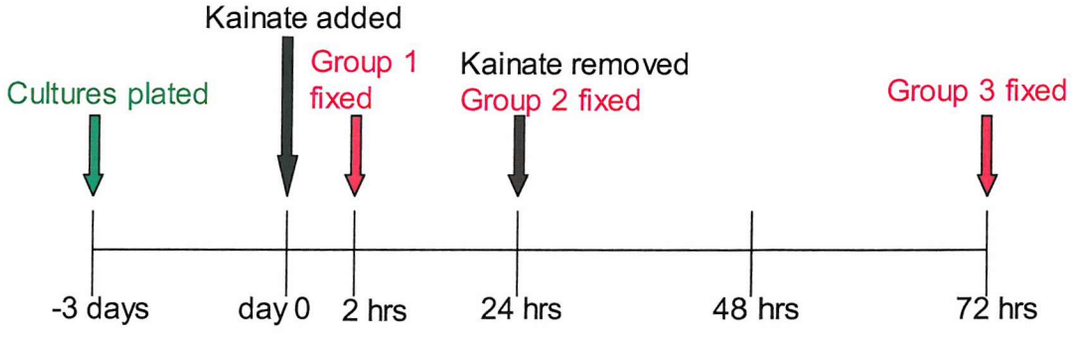

Fig 5.1: Time course for 5μM kainate experiment, cultures were grown for 3 days *in vitro* before the experiment began. BrdU (10μM) was added to all cultures 2 hours before fixation in 4% PFA. Cultures not treated with kainate and paired both for position and animal, fixed at the same time as the kainate treated cultures form a control.

5.2.2 Fluoro-Jade B/DAPI staining

Fluoro-Jade B staining was carried out according to the method described by Schmued with minor modifications (Schmued, et al., 1997). Sections were first immersed in a solution containing 1% sodium hydroxide in 80% alcohol for 2 minutes followed by 2 minute rinses in 70% ethanol and distilled water. Slides were then placed in a 0.06% potassium permanganate solution, on a shaker table, for 10 minutes. After a further 2 minute rinse in distilled water, slides were transferred to the Fluoro-Jade B/DAPI staining solution. The Fluoro-Jade B/DAPI solution was made immediately prior to use from stock solutions of Fluoro-Jade B and DAPI (both 10mg/100ml) in 0.1% acetic acid, in the proportions 4% Fluoro-Jade B, 2% DAPI and 92% acetic acid solution. Producing final dye concentrations of 0.0004% and 0.0002% for Fluoro-Jade B and DAPI respectively. After 30 minutes in the staining solution the slides were washed in distilled water (3x 1 min) and dried in a slide dryer (37°C, 2 hours). Once dry slides were placed in xylene for 1 minute and then cover-slipped with DPX.

5.2.3 Fluoro-Jade B quantification

Images of DAPI and Fluoro-Jade B staining were captured on an inverted Leica DM-IRBE epifluorescence microscope (Milton Keynes, U.K.) using a cooled Hamamatsu digital camera at 5x magnification. The area of DAPI or Fluoro-Jade B fluorescence was determined in Scion image (ver. 4.0.2; a PC based version of the program NIH image, which was developed at the U.S. National Institutes of Health and is available free on the Internet at http://rsb.info.nih.gov/nih-image/), using the density slice function, applied to the granule cell layer as a region of interest (Fig 5.2). Cell death was expressed as a percentage of the area in which Fluoro-Jade B fluorescence was detected above threshold within the cell layer divided by the area in which DAPI fluorescence was detected above a threshold in the same cell layer.

5.2.4 Statistical Analysis

For all quantification and analysis, slides were coded and counts carried out with the examiner blind to the age and treatment of each section. Cultures not matched for treatment across cell count, BrdU positive cell count and Fluoro-Jade B fluorescence quantification experiments were excluded from the analysis. (Activated caspase-3 matched cultures form a smaller sub set of this group). Statistical analysis between

different times in the same treatment group was by one way ANOVA with Bonferroni post hoc test, and statistical analysis between different treatments at the same time point was by two way ANOVA with Bonferroni post hoc test, with significance expressed at the 0.05, 0.01 and 0.001 levels.

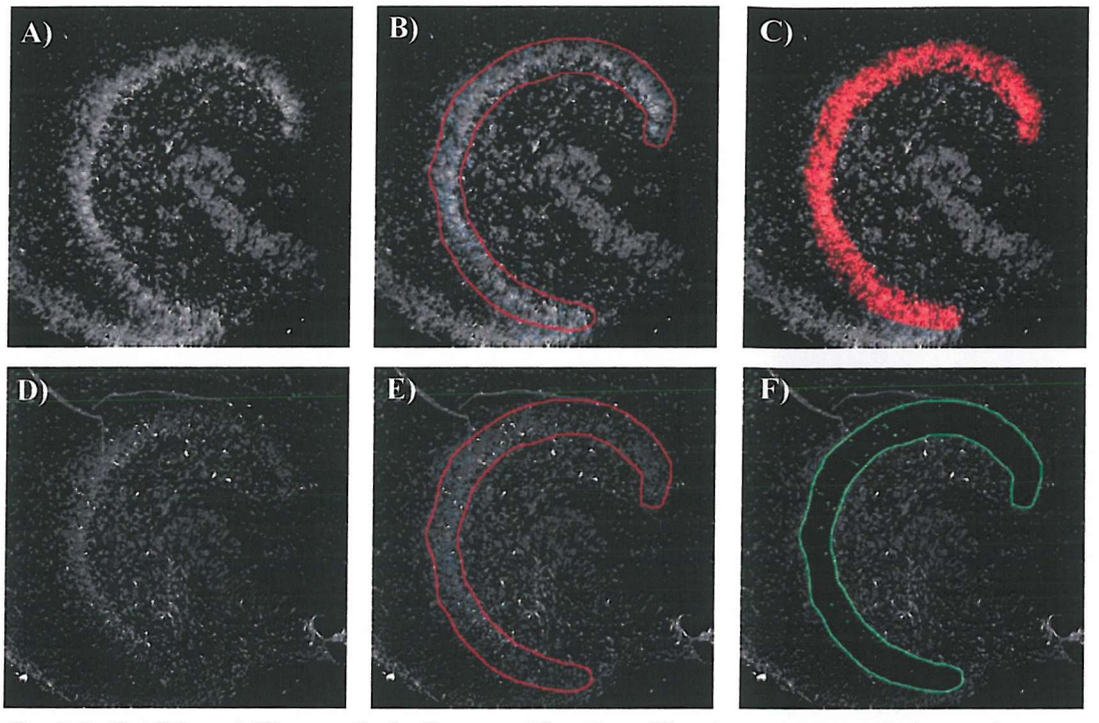

Fig 5.2: DAPI and Fluoro-Jade B quantification. The dentate gyrus is imaged at 10x for DAPI fluorescence (ex 330nm; em 450nm; **A**), and Fluoro-Jade B fluorescence (ex 475nm; em 535nm; **D**). Using functions within the Scion image software package, the granule cell layer is traced in the DAPI image, establishing a region of interest (**B**), which is copied across to the Fluoro-Jade B image (**E**). Pixels above a threshold value, within the region of interest are quantified (**C+F**).

5.3 RESULTS

All the cultures used were grown in Neurobasal medium, so unlike in the previous two chapters where comparisons between groups considered differences in types of growth medium, in this experiment the comparison is between kainate treated (seizure) medium and untreated (control) medium.

5.3.1 Area, cell count, and density in control cultures

Comparisons between the different times revealed no significant changes in the dentate granule cell layer area (Fig 5.3A) or cell density (Fig 5.3B) during the experiment, in control cultures. However, granule cell count altered significantly, with more cells present after 24 hours than in cultures fixed at 2 hours (24 hours, 2044 ± 108 cells, $n = 9$ vs. 2 hours, 1576 ± 190 cells, $n = 8$, $P < 0.05$), cultures fixed at 72 hours were not significantly different from those fixed at 2 or 24 (72 hours, 1770 ± 105 cells, $n = 5$; Fig. 5.3B).

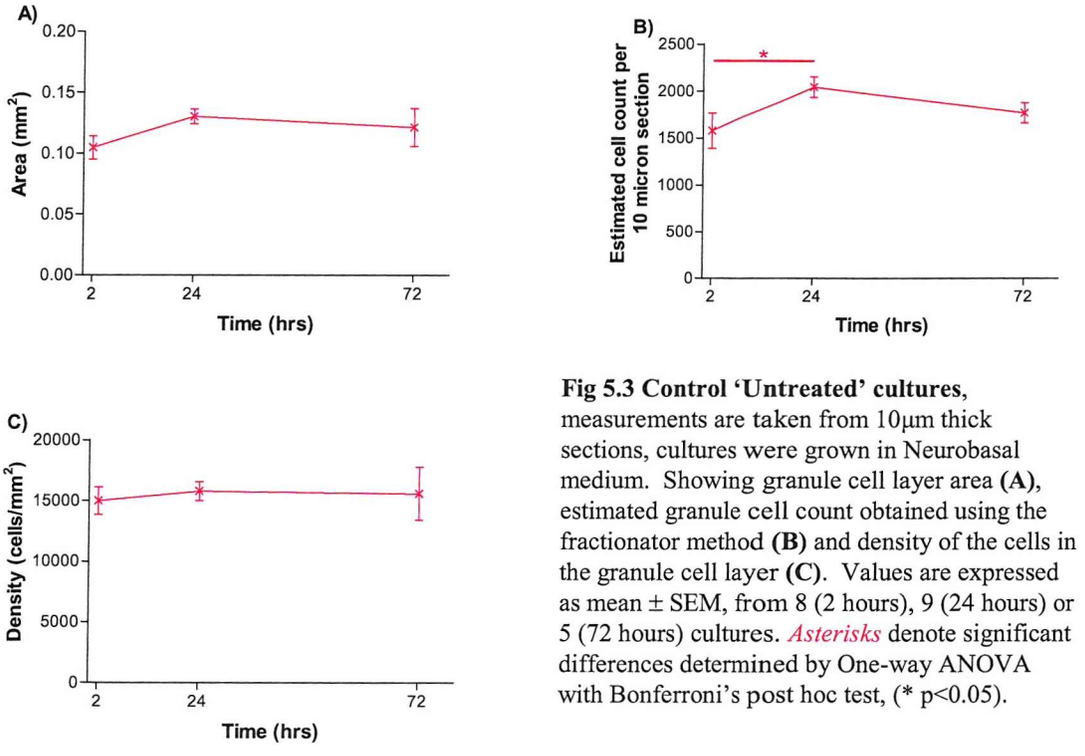

Fig 5.3 Control 'Untreated' cultures, measurements are taken from 10μm thick sections, cultures were grown in Neurobasal medium. Showing granule cell layer area **(A)**, estimated granule cell count obtained using the fractionator method **(B)** and density of the cells in the granule cell layer **(C)**. Values are expressed as mean ± SEM, from 8 (2 hours), 9 (24 hours) or 5 (72 hours) cultures. *Asterisks* denote significant differences determined by One-way ANOVA with Bonferroni's post hoc test, (* $p<0.05$).

5.3.2 Cell proliferation in control cultures

BrdU labelling in control cultures declined significantly over time with cell counts at 72 hours (25.4 ± 4.41 cells, $n = 5$) lower than at both 2 hours (48.25 ± 4.85 cells, $n = 8$; $P < 0.001$) and 24 hours (42.11 ± 4.23 cells, $n = 9$; $P < 0.01$), and although BrdU cell counts at 2 hours and 24 hours are not significantly different they do fit with a linear trend for a decline in BrdU positive cells over time. Proportions of BrdU labelled cells at both 24 hours (2.08 ± 0.22 % of cells, $n = 9$) and 72 hours (1.42 ± 0.20 % of cells, $n = 5$) are significantly lower than at 2 hours (3.25 ± 0.37 % of cells, $n = 8$; $p < 0.01$ vs. 24 hours and $p < 0.001$ vs. 72 hours) in control cultures, further supporting the evidence of the raw data for a steady decline in BrdU incorporation in the control cultures.

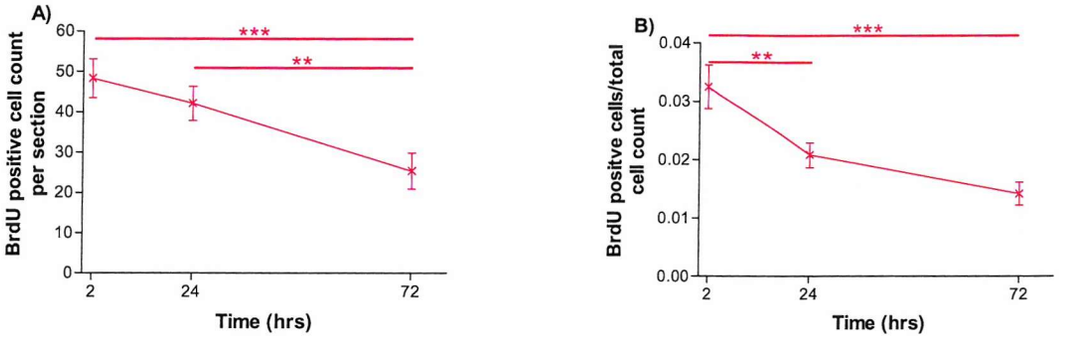

Fig 5.4: Profile of BrdU incorporation in control 'untreated' cultures, measurements are from 10μm thick sections. Showing absolute numbers of BrdU positive cells **(A)**, and the proportion of granule cells that incorporated BrdU in the 2 hours prior to fixation **(B)**. Values are expressed as mean ± SEM, from 8 (2 hours), 9 (24 hours) or 5 (72 hours) cultures. *Asterisks* denote significant differences determined by one-way ANOVA with bonferroni's post hoc test, (* $p<0.05$, ** $p<0.01$, *** $p<0.001$).

5.3.3 Cell death in control cultures

In control cultures the levels of Fluoro-Jade B detected did not vary significantly over time (Fig 5.5C), and neither did the total number of activated caspse-3 positive cells (Fig5.5A) or the proportion cells in which caspase-3 activation was detected (Fig5.5B).

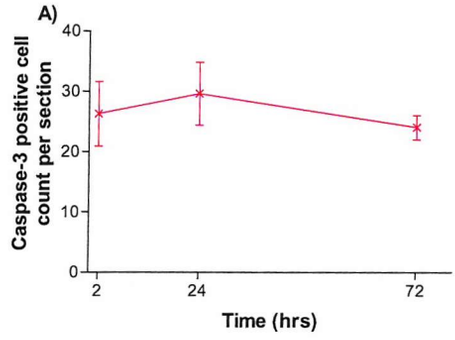

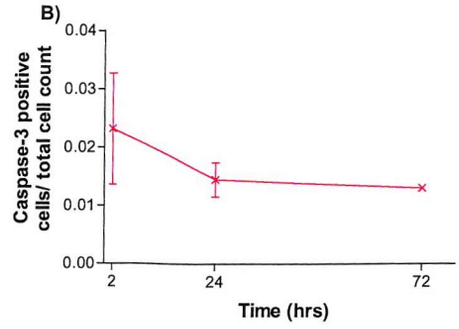

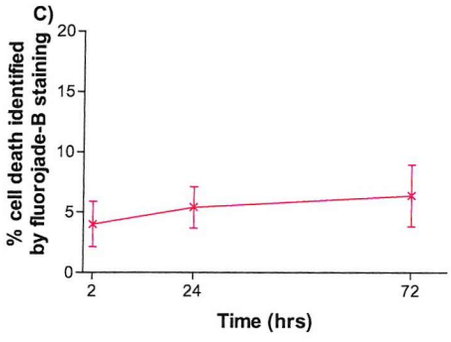

Fig 5.5: Profiles of cell death in control 'untreated' cultures, measurements are from 10μm thick sections. Showing absolute numbers of activated caspase-3 positive cells **(A)**, the proportion of granule cells in which caspase-3 activation was detected **(B)** and total cell death identified by fluorescence intensity mapping of Fluoro-Jade B over DAPI **(C)**. Values are expressed as mean ± SEM, in **A** + **B** from 8 (2 hours), 9 (24 hours) or 4 (72 hours) cultures, and in **C** from 4 (2 hours), 7 (24 hours) or 2 (72 hours) cultures.

5.3.4 Area, cell count, and density in cultures after kainate

Comparisons between the different times revealed no significant differences in the dentate granule cell layer area (Fig 5.6A) or cell count (Fig 5.6B) in cultures that had been exposed to 5μM kainate. The density of these cultures however decreased over time ($P < 0.01$) and is significantly lower at 72 hours than at 2 hours (72 hours, 11896 ± 935 cells/mm^2, $n = 5$ vs. 2 hours, 14819 ± 1099 cells/mm^2, $n = 8$, $P < 0.01$; Fig 5.6C). This decreased density is probably mainly due to a trend for increased area over time, however this did not reach statistical significance ($p=0.0582$).

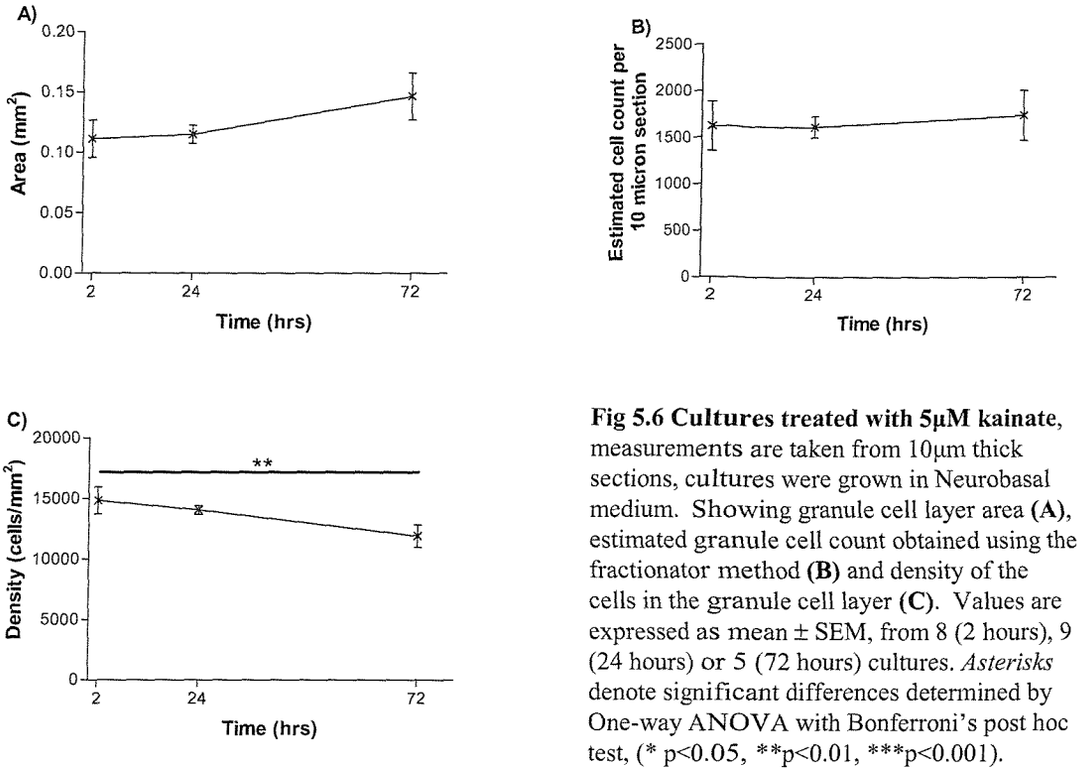

Fig 5.6 Cultures treated with 5μM kainate, measurements are taken from 10μm thick sections, cultures were grown in Neurobasal medium. Showing granule cell layer area **(A)**, estimated granule cell count obtained using the fractionator method **(B)** and density of the cells in the granule cell layer **(C)**. Values are expressed as mean ± SEM, from 8 (2 hours), 9 (24 hours) or 5 (72 hours) cultures. *Asterisks* denote significant differences determined by One-way ANOVA with Bonferroni's post hoc test, (* $p<0.05$, ** $p<0.01$, *** $p<0.001$).

5.3.5 Cell proliferation in cultures after kainate

After kainate treatment BrdU cell counts decrease significantly between 2 hours (39.25 ± 3.46 cells, $n = 8$) and 24 hours (16.67 ± 2.84 cells, $n = 9$, $P < 0.001$) and then increase significantly between 24 hours (16.67 ± 2.84 cells, $n = 9$) and 72 hours (37 ± 4.68 cells, $n = 5$, $P < 0.001$), finishing at a similar level to initial cell counts (Fig 5.7A). The same biphasic response was also observed when the proportion of cells incorporating BrdU is considered, a significantly lower proportion at 24 hours (1.60 ± 0.13 % of cells, $n = 9$) than at 2 hours (2.69 ± 0.36 % of cells, $n = 8$, $P < 0.01$) and 72 hours (2.42 ± 0.58 % of cells, $n = 5$, $P < 0.01$; Fig 5.7B).

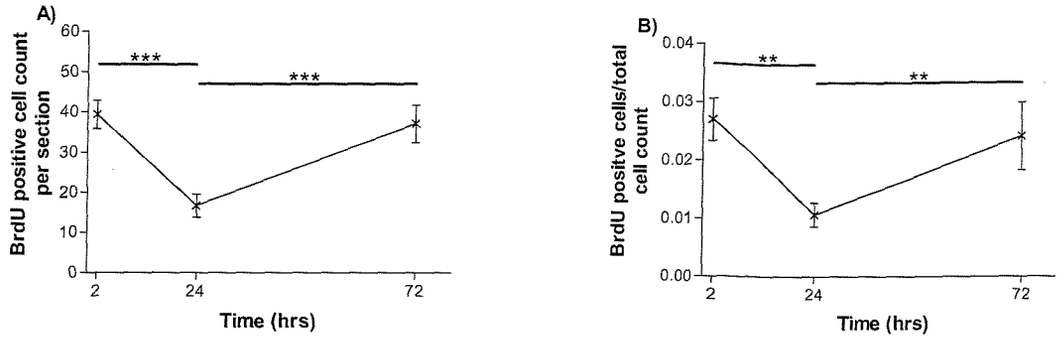

Fig 5.7: Profile of BrdU incorporation in cultures treated with 5μM kainate, measurements are from 10μm thick sections. Showing absolute numbers of BrdU positive cells **(A)**, and the proportion of granule cells that incorporated BrdU in the 2 hours prior to fixation **(B)**. Values are expressed as mean ± SEM, from 8 (2 hours), 9 (24 hours) or 5 (72 hours) cultures. *Asterisks* denote significant differences determined by one-way ANOVA with bonferroni's post hoc test, (* $p<0.05$, ** $p<0.01$, *** $p<0.001$).

5.3.6 Cell death in cultures after kainate

Fluoro-Jade B staining area was a significantly higher fraction of the dentate gyrus at 2 hours (15.3 ± 3.0 %, $n = 8$) than at 24 hours (4.9 ± 1.1 %, $n = 9$, $P < 0.001$) and 72 hours (3.8 ± 1.5 %, $n = 5$, $P < 0.001$) in cultures exposed to 5μM kainate (Fig 5.8C). Significantly more activated caspase-3 positive cells were observed in kainate treated cultures at 2 hours (34.0 ± 3.19 cells, $n = 4$) than at 24 hours (24.43 ± 2.14 cells, $n = 7$, $P < 0.001$) and 72 hours (22 ± 2.0 cells, $n = 2$, $P < 0.001$; Fig 5.8A). Additionally, the proportion of cells expressing activated caspase-3 labelled cells at both 24 hours (1.60 ± 0.13 % of cells, $n = 7$) and 72 hours (1.55 ± 0.76 % of cells, $n = 2$) are significantly lower than at 2 hours (2.63 ± 0.20 % of cells, $n = 4$, both $P < 0.01$) in kainate treated cultures (Fig 5.8B).

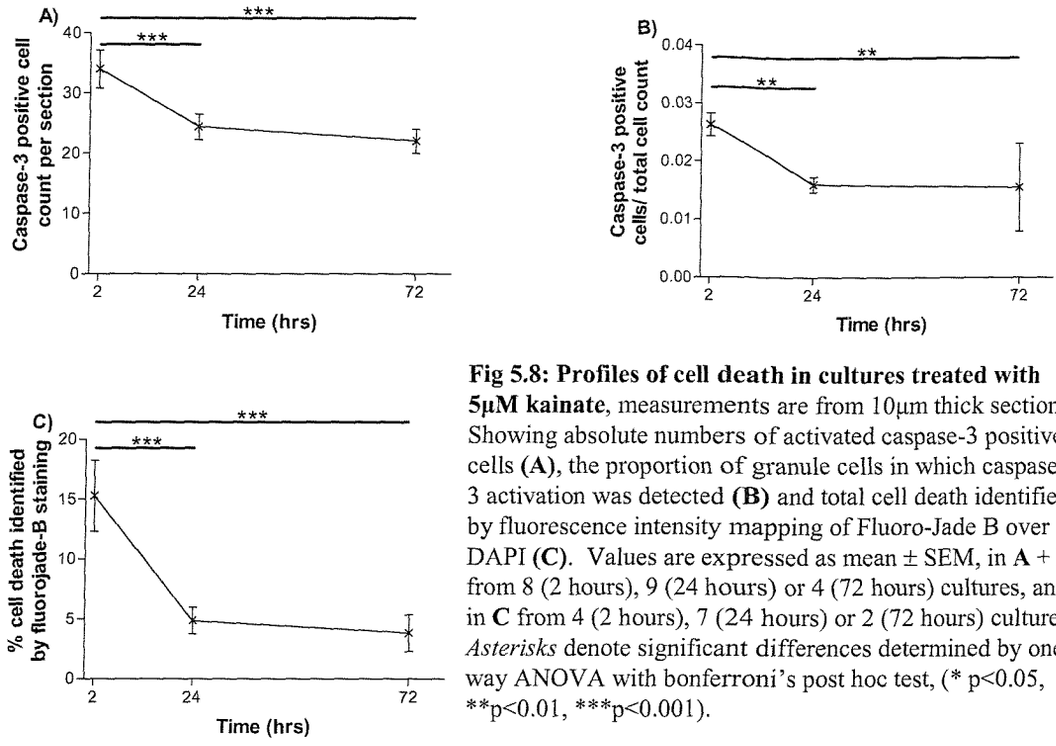

Fig 5.8: Profiles of cell death in cultures treated with 5μM kainate, measurements are from 10μm thick sections. Showing absolute numbers of activated caspase-3 positive cells **(A)**, the proportion of granule cells in which caspase-3 activation was detected **(B)** and total cell death identified by fluorescence intensity mapping of Fluoro-Jade B over DAPI **(C)**. Values are expressed as mean ± SEM, in **A** + **B** from 8 (2 hours), 9 (24 hours) or 4 (72 hours) cultures, and in **C** from 4 (2 hours), 7 (24 hours) or 2 (72 hours) cultures. *Asterisks* denote significant differences determined by one-way ANOVA with bonferroni's post hoc test, (* $p<0.05$, ** $p<0.01$, *** $p<0.001$).

5.3.7 Comparison of area, cell count, and density between kainate treated and control cultures

Sections from kainate treated cultures did not differ significantly from position and time matched controls in dentate granule cell layer area, at 2 hours (kainate, 0.111 ± 0.015 mm^2 vs. control, 0.105 ± 0.010 mm^2, both $n = 8$), 24 hours (kainate, 0.115 ± 0.008 mm^2 vs. control, 0.130 ± 0.006 mm^2, both $n = 9$) or 72 hours after the start of the experiment (kainate, 0.146 ± 0.019 mm^2 vs. control, 0.121 ± 0.015 mm^2, both $n = 5$; Fig. 5.9A). The estimated number of cells in the granule cell layer of sectioned cultures, was also not significantly different from position and time matched controls at 2 hours (kainate, 1624 ± 266 cells vs. control, 1576 ± 190 cells, $n = 8$), 24 hours (kainate, 1618 ± 115 cells vs. control, 2044 ± 108 cells, $n = 9$), or 72 hours (kainate, 1744 ± 269 cells vs. control, 1770 ± 105 cells, $n = 5$; Fig. 5.9B). However, over the whole experiment the treatment applied to the cultures resulted in a significant change in density ($p<0.05$; two-way ANOVA) but this trend for decreased cell density after kainate treatment was not significant at any of the individual time points examined; 2

hours (kainate, 14819 ± 1099 cells/mm^2 vs. control, 15010 ± 1139 cells/mm^2, n = 8), 24 hours (kainate, 14057 ± 357 cells/mm^2 vs. control, 15801 ± 774 cells/mm^2, n = 9), or 72 hours (kainate, 11896 ± 935 cells/mm^2 vs. control, 15598 ± 2190 cells/mm^2, n = 5; Fig. 5.9C).

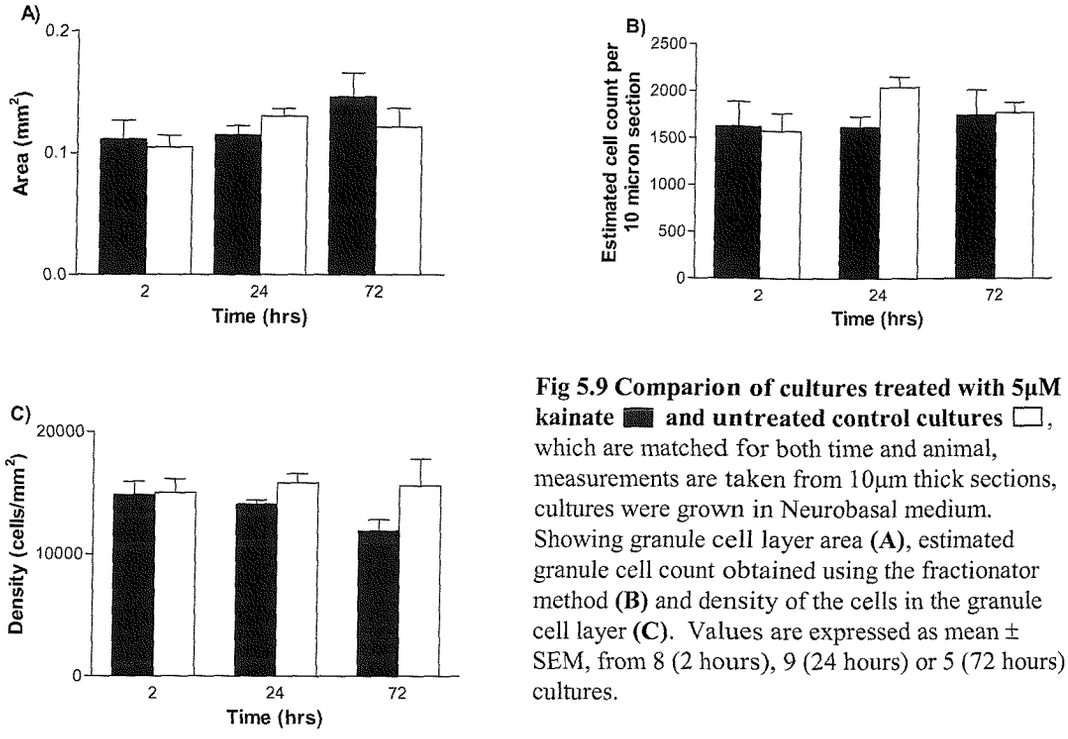

Fig 5.9 Comparion of cultures treated with 5μM kainate ■ and untreated control cultures □, which are matched for both time and animal, measurements are taken from 10μm thick sections, cultures were grown in Neurobasal medium. Showing granule cell layer area **(A)**, estimated granule cell count obtained using the fractionator method **(B)** and density of the cells in the granule cell layer **(C)**. Values are expressed as mean ± SEM, from 8 (2 hours), 9 (24 hours) or 5 (72 hours) cultures.

5.3.8 Comparison of BrdU incorporation between kainate treated and control cultures

The number of BrdU positive cells observed was significantly decreased by treatment with 5μM kainate at 24 hours after application (kainate, 16.67 ± 2.84 cells vs. control, 42.11 ± 4.23 cells, n = 9, $P < 0.01$) but were not significantly different at 2 hours (kainate, 39.25 ± 3.46 cells vs. control, 48.25 ± 4.85 cells, n = 8) or at 72 hours (kainate, 37.0 ± 4.68 cells vs. control, 25.4 ± 4.41 cells, n = 5; Table 1). Kainate treatment caused a similar trend for a decrease in the proportion of cells labelled with BrdU 24 hours after application, however this did not reach statistical significance (kainate, 1.60 ± 0.13 % of cells vs. control, 2.08 ± 0.22 % of cells, n = 9). As with the raw BrdU positive cell counts, the proportions of BrdU positive cells in control and kainate cultures were not significantly different at 2 hours (kainate, 2.69 ± 0.36 % of

cells vs. control, 3.25 ± 0.37 % of cells, n = 8) or at 72 hours (kainate, 2.42 ± 0.58 % of cells vs. control, 1.42 ± 0.20 % of cells, n = 5; Fig. 2A)

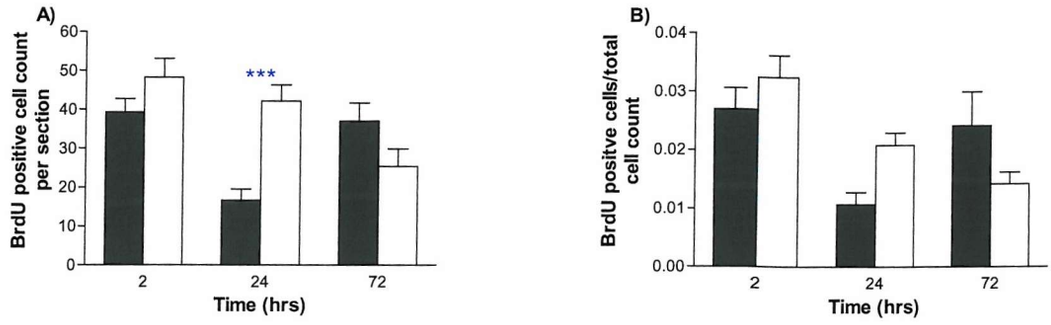

Fig 5.10: Profile of BrdU incorporation in cultures treated with 5μM kainate ■ and untreated control cultures □ , which are time and animal matched, measurements are from 10μm thick sections. Showing absolute numbers of BrdU positive cells **(A)**, and the proportion of granule cells that incorporated BrdU in the 2 hours prior to fixation **(B)**. Values are expressed as mean ± SEM, from 8 (2 hours), 9 (24 hours) or 5 (72 hours) cultures. *Asterisks* denote significant differences between treatments determined by two-way ANOVA with bonferroni's post hoc test, (* $p<0.05$, ** $p<0.01$, *** $p<0.001$).

5.3.9 Comparison of cell death between kainate treated and control cultures

Kainate induced a significant increase in the amount of Fluoro-Jade B staining detected 2 hours after kainate addition (kainate, 15.3 ± 3.0 %, vs. control, 4.0 ± 1.9 %, n = 8, $P < 0.05$) but not at 24 hours (kainate, 4.9 ± 1.1 %, vs. control, 5.4 ± 1.7 %, n = 9) or 72 hours (kainate, 3.8 ± 1.5 %, vs. control, 6.4 ± 2.6 %, n = 5) compared with matched controls, from this a transient increase in some types of cell death occur shortly after kainate application.

Sections from kainate treated cultures did not differ significantly from position and time matched controls in the number of cells expressing activated caspase-3, at 2 hours (kainate, 34.0 ± 3.19 cells vs. control, 26.25 ± 5.36 cells, n = 4), 24 hours (kainate, 24.43 ± 2.14 cells vs. control, 29.57 ± 5.20 cells, n = 7) or 72 hours after the start of the experiment (kainate, 22.0 ± 2.0 cells vs. control, 24.0 ± 2.0 cells, n = 2). Kainate treatment did not significantly alter the proportion of cells labelled with activated caspase-3 in the dentate gyrus at 2 hours (kainate, 2.63 ± 0.20 % of cells vs. control, 2.31 ± 0.95 % of cells, n = 4) 24 hours (kainate, 1.60 ± 0.13 % of cells vs. control, 1.45 ± 0.29 % of cells, n = 7), or at 72 hours (kainate, 1.55 ± 0.76 % of cells vs. control, 1.30 ± 0.03 % of cells, n = 2; Fig. 3A) after administration compared with position and time matched controls.

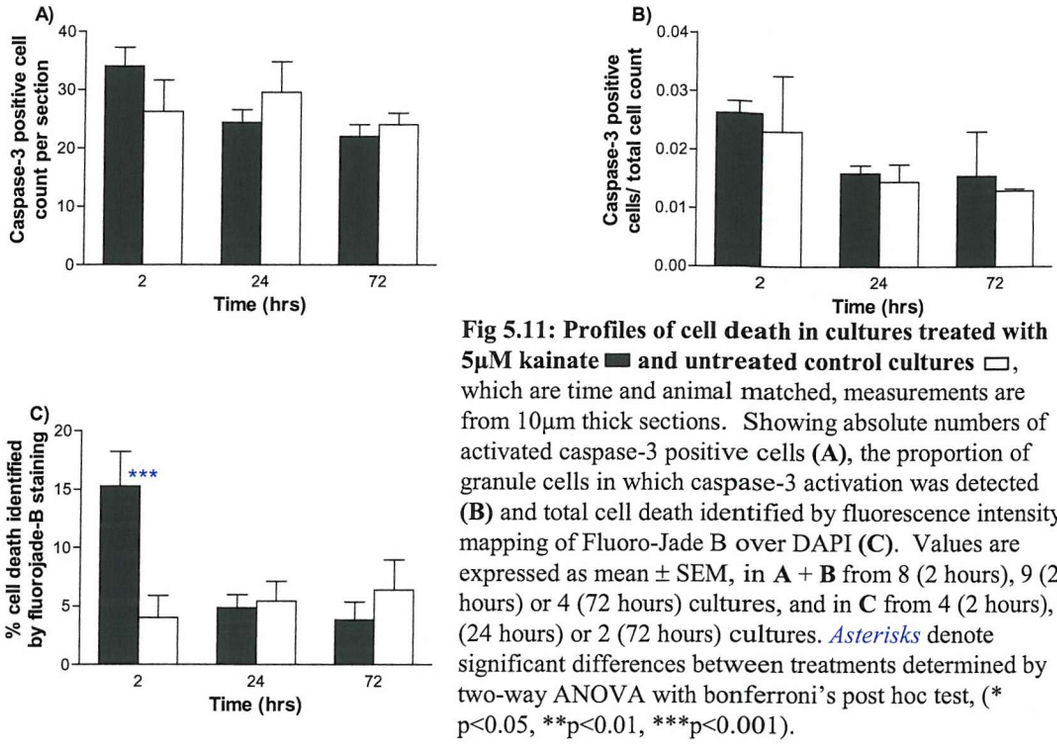

Fig 5.11: Profiles of cell death in cultures treated with 5μM kainate ■ and untreated control cultures □, which are time and animal matched, measurements are from 10μm thick sections. Showing absolute numbers of activated caspase-3 positive cells **(A)**, the proportion of granule cells in which caspase-3 activation was detected **(B)** and total cell death identified by fluorescence intensity mapping of Fluoro-Jade B over DAPI **(C)**. Values are expressed as mean ± SEM, in **A** + **B** from 8 (2 hours), 9 (24 hours) or 4 (72 hours) cultures, and in **C** from 4 (2 hours), 7 (24 hours) or 2 (72 hours) cultures. *Asterisks* denote significant differences between treatments determined by two-way ANOVA with bonferroni's post hoc test, (* $p<0.05$, ** $p<0.01$, *** $p<0.001$).

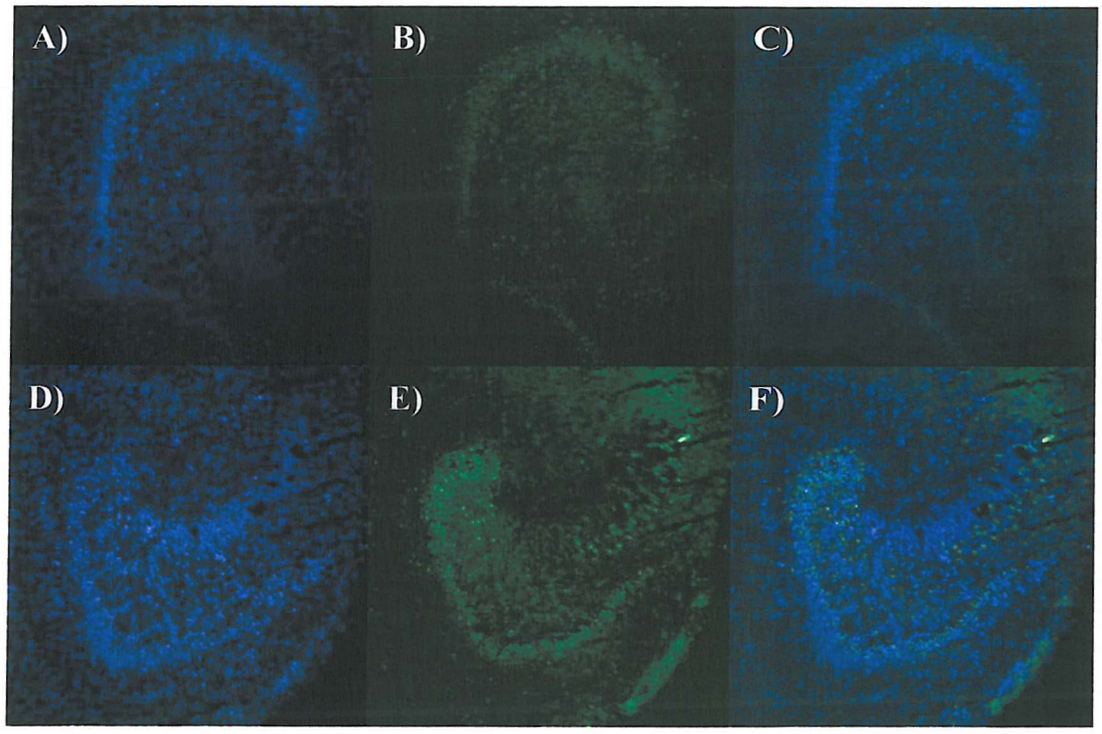

Fig 5.12: DAPI and Fluro-Jade B (FJB) staining in OHSC's. Showing a control culture **(A-C)** and a culture 2 hours after application of 5μM kainate **(D-F)**. The granule cell layer is identified with DAPI staining **(A+D)**, cell death is identified with FJB staining **(B+E)**, and composite images **(C+F)** identify the cell death as being principally located around the subgranular zone in response to kainate treatment.

5.4 Discussion

The experiments described above are performed on cultures that have been maintained *in vitro*, under identical control conditions for 3 days before use to allow the tissue to recover from the trauma involved in preparation. The time points discussed hereafter are therefore in addition to these three days in culture. This is an important consideration as in immature dentates considerable changes occur in a short space of time (chapter 4).

5.4.1 Basal responses of cultures grown in Neurobasal medium

A significant increase in cell counts between 2 hours and 24 hours in untreated control cultures, with no accompanying change in cell density is likely to be due to the settling or restructuring process (chapter 4.4.2), especially as the increase in cell counts is accompanied by a trend for larger GCL area, although this is not statistically significant.

It is possible that part of the rise in the number of granule cells detected is due to the proliferation, however application of equation 4 (chapter 4.1.2) to the number of BrdU labelled cells detected predicts a maximal contribution to cell count from proliferation of about 265 cells, or less than 60% of the observed increase. This expansive estimate of the possible increase in granule cell numbers arising from the observed proliferation does not consider depletion of cell numbers due to cell death. This coupled with the fact that proliferation continues to decline in control cultures throughout the experiment, suggest the increase is predominantly due to restructuring. Although this is unfortunate, as the same restructuring will affect the results obtained after exposure to kainate, making temporal comparisons difficult, it does not affect comparisons between treatments at each time point. Importantly, cell death is unchanged in the control cultures over the duration of the experiment, the constant level of cell death was apparent in both the 'necrotic' quantification by FJB staining, and the 'apoptotic' quantification of activated caspase-3 positive cells. This demonstrates that death is not part of the restructuring processes discussed above, and changes in cell death after exposure to kainate can confidently be interpreted as effects due to the kainate, free from temporal variations. Cell proliferation decreased in the control cultures over time. This effect is also seen *in vivo*, where the level of proliferation is highest very soon after birth, during the dentate gyrus's formation

(Altman and Bayer, 1990). There then follows a steady decline in proliferation, which continues out into adulthood (Lewis, 1978; Cameron and McKay, 2001). The trend for this decrease is present, but was not detected, in the long time course experiment in chapter 4. This is probably due to the large BrdU cell counts observed at very early times which result in high experimental variability, and the low number of animals considered at each point, combining to obscure the trend in that experiment. The larger number of cultures and the more temporally stable data obtained in this experiment permit statistical confirmation of an agreement between our *in vitro* model and the *in vivo* record.

5.4.2 Effect of kainate on cell proliferation

There are two clear phases to the proliferation in our culture model in the 72 hours after kainate administration. A dramatic and significant fall in the number of cells incorporating BrdU, and by inference proliferating cell numbers, between 2 hours and 24 hours was observed. This has not been reported for adult animals, however, a similar but more prolonged decrease in cell proliferation in immature rats has been described (McCabe, et al., 2001). McCabe et al. found decreased proliferation for 4 days after a series of 25 seizures induced in P0-P4 rats, while the same seizure induction in adult (P60-P69) rats resulted in significantly increased proliferation.
Why is this decrease in cell proliferation occurring?
One possibility is that the precursor cell population is selectively vulnerable to the kainate and are killed. It is possible to selectively eliminate some of the dividing cells in the subventricular zone, significantly reducing proliferation, which then recovers over the next 10 days (Doetsch, et al., 1999). We also observed a recovery phase in our proliferation between 24 hours and 72 hours and an early phase of cell death (present at 2 hours), which combined with the observations of Doetsch el al, appear to support a hypothesis of progenitor cell death and then recovery. However, while the data appear to fit with a hypothesis that progenitor cells are dying, the timing of the recovery is considerably faster in our cultures. Additionally, an experiment severely ablating the number of proliferating cells in the GCL, using irradiation, found that recover of BrdU labelling to control levels had not occurred by 120 days after irradiation (Tada, et al., 2000), suggesting a very slower recovery of proliferating cells in the dentate than we observed. Thus, an alternative hypothesis could involve a temporary inactivation of the progenitor cells by kainate, rather than the death of these

cells, with a resumption of division once the kainate's activity has subsided, seen at 72 hours in this experiment. Since we used tissue from neonatal animals, which may have a greater proliferative capacity than the young adult animals Tada used, and the kainate injury did not produce as severe an ablation of cell proliferation as the irradiation injury, either of the above mechanisms are possible.

5.4.3 Kainate and cell death

We observed a rapid phase of cell death after kainate administration, with significant death present at 2 hours and both FJB and activated caspase-3 labelling falling to control levels by 24 hours. Historically, there has been considerable debate as to whether cell death occurs after seizures in immature animals, however many models are now accepted as producing cell death *in vivo* (reviewed in (Wasterlain, et al., 2002)), and this death can occur in the first 24 hours (Sankar, et al., 1998). In experiments using kainate as the chemoconvulsant it has been noted that the cell death observed in immature animals is less than in mature animals, and this could be due to a desensitisation of immature animals to repeated kainate injections, which is mediated through a down regulation of kainate receptor expression (Tandon, et al., 2002). In our experiments the kainate is applied for 24 hours, after which time the cultures could be desensitised, and thus not prone to cell death, electrophysiological recordings could assess the presence, and intensity of any evoked seizure activity. While, the very early phase of cell death we observed indicates that some cells are dying, currently we can only speculate as to their phenotype. These dying cells are principally located on the hilar side of the GCL, where the SGZ is located, rather than the molecular side (Fig 5.12). As was discussed above, it is possible that during the seizure some of the progenitor cells are dying, and with the desensitisation the remaining population of precursor cells may become activated and begin dividing to replace the cell loss, potentially explaining the increases in cell proliferation observed after seizures *in vivo* (Gray and Sundstrom, 1998).

5.4.4 Kainate and dispersion

Dispersion, or spreading out, of the dentate granule cell layer has been reported as a consequence of some types of temporal lobe epilepsy (Houser, 1990; Lurton, et al., 1998). Dispersion correlates well with mossy fibre sprouting and gliosis, and is dependent on granule cell death (Lurton, et al., 1997). A similar phenomenon has also been observed in an *in vivo* murine model using kainate to induce seizures (Bouilleret, et al., 1999)(Gray, unpublished observations). We found a trend for decreased density over time in kainate treated cultures whereas density in control cultures did not change, the largest apparent difference is at 72 hours, and at this time the area of these cultures appears to be larger (although neither of these observations reach statistical significance). Since the number of granule cells present in the kainate cultures does not change over time this indicates that the apparent change in density is not due to cell death within the GCL, but is due to dispersion. The reasons for, and the mechanisms of granule cell dispersion are poorly understood. Lurton et al. speculate that the dispersion observed in adults is a reversion to a developmental migration program, perhaps mediated by Brain derived neurotrophic factor (BDNF), as this is over-expressed with the same periodicity as the dispersal effects of kainate (Lurton, et al., 1997). The observations of Elliott et al. support this hypothesis, they have demonstrated that many of the genes involved in cell migration during development are reactivated after pilocarpine induced seizures (Elliott, et al., 2003). Our ability to detect dispersion in this culture model could prove useful in identifying the mechanisms underlying the phenomenon.

5.4.5 Potential modifications to cell labels visualised in the model

The *in vitro* model for analysing cell proliferation and cell death after seizures demonstrated in this chapter although considerably evolved from the initial model could still be improved by modification. As yet the initial goal of identifying changes in neurogenesis has not been achieved, the feasibility of quantifying double-labelled tissue has not been explored in these experiments. The recent identification of additional markers for immature neurons and stem cells such as doublecortin (Nacher, et al., 2001) and Lewis-X (CD15) (Capela and Temple, 2002), suggest that in one section BrdU and doublecortin labelling could identify neurogenesis and in the adjacent section BrdU and Lewis-X labelling could be used to mark active stem cells.

The use of Fluoro-Jade B to identify cell death is a successful modification of the protocol described in the previous chapter, however the information gained from the tissue stained with FJB could be greatly increased. The FJB stain can be applied after a DAB visualized immunostain, and thus could be applied to the section stained for activated caspase-3, combining the measure for total cell death with the measure of apoptotic death. Additionally while it was initially thought that caspase-3 activation was a terminal step for a cell, and guaranteed its apoptotic fate, recent publications have cast doubt on this (D'Sa-Eipper, et al., 2001). Furthermore, other research has suggested that an apparently opposite effect can be observed with activated caspase-3 inducing cell proliferation (Yan, et al., 2001). A potential replacement apoptotic marker is cleaved-PARP (poly ADP-ribose polymerase). PARP, a protein that is essential for cell viability and is involved in DNA repair, is cleaved by activated caspase-3 and is thus a step further down the apoptotic pathway (Wang, 2000). Currently PARP cleavage is considered fatal to the cell however it is possible that as with activated caspase-3 an exception to this rule could be found but until that time cleaved PARP might be a better marker to use in conjunction with the FJB staining. Unfortunately, studies have also cast doubt on both caspase-3 and PARP as purely apoptotic markers (Wang, 2000).

5.4.6 Possible improvements to stereological quantification in the model

The accuracy and efficiency of the stereological quantification of granule cell number could also be improved. Firstly, the accuracy of the estimate is limited by the size of the objects (granule cells) being counted. Ideally cell counting would use as small an object as possible for counting, nucleoli (with a diameter of approximately 2μm) are recommended, as a change in the size of the object being counted can radically alter the number of objects that can be counted in each counting frame (Guillery and Herrup, 1997). Unfortunately dentate granule cells contain multiple nucleoli in random positions within the cell and so cannot be counted, as if they were cells could be counted multiple times if more than one nucleolus fell in the counting frames and worse its not possible to include and exclude a cell which has a nucleolus inside the counting frame and one outside. This meant that whole cells had to be counted, a dentate granule cell is approximately 10μm in diameter and could easily swell to 12μm, under different experimental conditions, which would introduce an error of up to 20%, it is for this reason that comparisons made in these experiments are between

10μm sections and no attempt to scale the numbers up to whole animals has been made. One method to assess this potential problem is to use an additional stereological probe the nucleator when performing each fractionator probe. The nucleator estimates the cross-sectional area of measured cells and so can be used to detect changes in cell diameter, adding information to the cell density calculation. Secondly, the counting frame used for sampling could be smaller; this would result in fewer cells counted and a reduction in sampling time. This change would not greatly alter the accuracy of the estimate, as currently the large counting frame tends to produce highly variable values each time it is thrown based on whether it falls entirely in the centre of the granule cell layer or on the edge. Unfortunately the shape of the granule cell layer means its ratio of perimeter to area is quite high producing more counting frames partly out of the ROI than would be obtained if a more regularly shaped structure was being examined. A smaller counting frame would reduce the range and thus the standard deviation of cells observed per counting frame, the major contributor to the Schaeffer coefficient of error. A third improvement would be to take thicker sections (for example 20μm thick), and perform the full optical fractionator on the middle part of the sections. The final improvement associated with the stereology relates to the identification of cells. Counting whole cells using the thionine stain is difficult because the edges of cells are not always easily defined (Fig 2.6) and some cells appear to be rounder than others, this makes including or excluding these cells from counting frames subjective. In order to reduce this subjectivity counting the nucleus of cells could be used, the nucleus of a granule cell is large (typically approximately 8μm) and roughly spherical, but importantly the edges when visualized using DAPI stain are sharp. Two further advantages to switching from thionine to DAPI stains for granule cell counting are: i) pyknotic cells can be counted using DAPI with this being carried out simultaneously to the stereological estimate of granule cell number. And ii) the FJB method already involves staining a section with DAPI, and this frees the section stained with thionine to receive a different stain potentially increasing the information obtained from each culture.

5.4.7 The future of neurogenesis and cell death quantification in the OHSC model

These modifications could potentially produce significant improvements in the model described here, providing an excellent model for studying neurogenesis and cell death *in vitro* not only after seizure, but also in ischaemia, traumatic brain injury, and potentially in assessing the efficacy of treatments for neuro-degenerative diseases such as Alzheimer's.

Chapter 6

In vivo 'clonal' proliferation after seizures

6.1 Introduction

The work described in chapters 2-5 focuses on the development of a novel *in vitro* model for investigating the effects of seizures on neurogenesis in immature animals. However, this is not the only possible approach to the investigation of seizure-induced neurogenesis. There are already several models of seizures described *in vivo*, in which neurogenesis can be studied. The principle seizure models currently in use have already been described (Chapter 5.1.2), the model that our lab uses relies on the chemo-convulsant kainate (Sundstrom, Mitchell et al., 1993; Gray and Sundstrom, 1998; Gray, May et al., 2002). In the culture experiments a known concentration of kainate is easily added to the growth media, however, methods of application are more complicated *in vivo*. Some studies use an intraperitoneal injection to induce seizures; effects induced with this technique produce bilateral changes. Other studies use unilateral intracerebroventicular (ICV) or intrahippocampal (IH) to generate seizures activity and an excitotoxic lesion in one hemisphere, while the contralateral hemisphere suffers seizure activity without the excitotoxic pathology (Nadler, Shelton et al., 1980).

6.1.1 *In vivo* identification of changes in cell proliferation after seizures

Many experiments examining cell proliferation after seizures use point/pulse labelling to identify proliferating cells (Parent, Yu et al., 1997; Nakagawa, Aimi et al., 2000). These protocols are all similar to the method used in chapters 3-5 to identify a fraction of cells dividing at the time of sacrifice. A seizure or series of seizures is induced, and then a 'pulse' of a proliferation tag such as BrdU or ^{3}H-thymidine is administered. The animal is sacrificed shortly after the proliferation tag has been introduced; the number of labelled cells detected represents a proportion of the total proliferating population at the time of sacrifice. Using this method different groups have established that proliferation increases between day 1 and day 3, remains elevated until about day 7 and then falls to normal or slightly below normal levels (Parent, Yu et al., 1997; Nakagawa, Aimi et al., 2000). The point labelling protocol cannot identify the populations of cells responsible for these increases, and thus considerable speculation as to the mechanisms involved has arisen. The two principle theories proposed to describe these changes are, increased rates of division of existing active progenitor cells through decreased cell cycle times, and activation of a second

quiescent or slowly dividing population of cells. Recent experiments in our laboratory indicate that a combination of these two theories is the most probable scenario (Gray, May et al., 2002).

6.1.2 Current evidence for the proposed mechanisms of increased cell proliferation observed after seizure.

Seaberg and van Der Kooy used primary dissociate culture methods to identify types of dividing cells present in different parts of the rodent brain in both in immature and mature animals. They concluded that in adult animals only restricted progenitor cells and not stem cells reside in the dentate gyrus and suggested that the previously reported decrease in proliferation with aging (Kuhn, Dickinson-Anson et al., 1996) was due to a steady decline in the number of restricted progenitors that persist in aged animals (Seaberg and van Der, 2002). A more rapid division of the remaining progenitor cells in this model could produce an increase in the number of proliferating cells detected after seizure.

The evidence in favour of a quiescent or slowly dividing is reviewed in considerable detail by Seri et al. who conclude that neurogenesis in the SGZ is dependent on two populations of dividing cells, a stem cell population probably derived from astrocytes, which generate a second restricted progenitor cell population (Seri and Alvarez-Buylla, 2002). The fact that an actively proliferating astrocytic population was not obtained by Seaberg and van Der Kooy in primary culture could be due to the specific culture conditions used. A recent study by Gray et al. implies both mechanisms are involved (Gray, May et al., 2002). Immature (1 month) and adult (3 month) rats produce the same number of BrdU labelled cells in response to ICV kainate induced seizures despite a 30% decrease in proliferation in the ICV saline injected control animals between the two age groups. The significant increase at one month is unlikely to be due to significantly decreased cell cycle time as at this age the cell cycle is close to the minimum cycle time of P1-P12 (Lewis, 1978), suggesting activation of quiescent cells. By 3 months the cell cycle is longer (Cameron and McKay, 2001) and hence the basal proliferation is lower, however the proliferation after seizure is the same. The similarity between BrdU cell counts in the two ages could be due to two profiles of proliferation that are coincidently the same on day 7 after seizure when Gray et al. examined them, and differ at other (not examined) times. However equally it could arise from a combination of the same activation of

quiescent cells and a temporary decrease in cell cycle time to that of the immature animals.

6.1.3 Markers of proliferation

Although BrdU is currently the preferred marker for identifying proliferating cells, especially if the phenotype of newly born cells is also being identified (Eriksson, Perfilieva et al., 1998; Aberg, Aberg et al., 2000; Arvidsson, Kokaia et al., 2001; Kempermann, Gast et al., 2003), other markers exist. In early studies ^{3}H-thymidine was commonly used as a tag of dividing cells (Altman and Das, 1965; Bayer, 1980; Cameron, McEwen et al., 1995), however the technical difficulties associated detection limit its value as a marker (discussed in chapter 2.1.2), and specific proteins are expressed during the cell cycle. The principle reason for BrdU's utility in identifying cell phenotype is its persistence in the post-mitotic cell, permitting multiple labelling with phenotypic markers at longer survival times after administration (Kempermann, Gast et al., 2003). While the cell cycle proteins are tightly regulated and only expressed at certain points during the cell cycle and thus make poor markers for identifying cell phenotype in survival experiments they are useful markers as point proliferation markers. Many proteins that are linked with aspects of the cell cycle and there is considerable debate as to the expression profiles of most of these proteins. Two of the most commonly described cell cycle markers are proliferating cell nuclear antigen (PCNA), and Ki-67. These are both expressed throughout the entire cell cycle. Ki-67 is used diagnostically to identify the proliferative activity of tumours, and is not reported as labelling cells undergoing repair (Scholzen and Gerdes, 2000). PCNA, like BrdU, is the subject of some debate as to whether it is expressed in cells undergoing DNA repair, some studies infer a role, (Scholzen and Gerdes, 2000; Uberti, Piccioni et al., 2001). Palmer et al. used a dose of irradiation to induce DNA damage in density-arrested normal diploid fibroblasts, using fibroblasts with log phase growth as positive controls. Although BrdU was available for incorporation throughout the period of DNA repair they observed BrdU positive cells only in the dividing population, indicating that if BrdU is incorporated during DNA repair it is at a density that is below levels requires for detection (Palmer, Willhoite et al., 2000). Gould et al. used two different types of lesion to induce cell death, and found similar changes in BrdU, ^{3}H-thymidine and PCNA labelling, suggesting PCNA detection is also not significantly increased in

cells undergoing DNA repair (Gould and Tanapat, 1997). However, the possibility of PCNA detection in non-proliferative cells should still be taken into consideration when using PCNA labelling. Other markers such as the cyclin dependent kinase $p34^{cdc2}$ are expressed only at specific points in the cell cycle. $p34^{cdc2}$ is required for progression from G2 to M phase of the cell cycle and thus its expression is highest at this point, however it is thought to be present throughout the cell cycle except in the M-phase (Brott, Alvey et al., 1993; Uberti, Piccioni et al., 2001), and the exact duration that it is detectable for is uncertain, this limits the value of these cell cycle markers, since determining the fraction of the total dividing cell population is difficult.

6.1.4 Combining clonal and point proliferation measurements

Several proteins involved in cell cycle regulation have been favourably compared to BrdU labelling as a point proliferation marker, and studies have used evaluation of more than one marker of proliferation to corroborate their findings (Gould and Tanapat, 1997; Uberti, Piccioni et al., 2001; Jin, Minami et al., 2001; Kee, Sivalingam et al., 2002). However, a thorough study of the literature produced only one published example of the use of a cell cycle protein as a point proliferation marker and BrdU as a clonal marker (Dayer, Ford et al., 2003). This approach can potentially significantly increase the information gained about the dividing population under normal conditions and after seizure. BrdU labelling alone could identify the total number of clonal cells produced between administration and sacrifice, and PCNA labelling alone could identify the total number of cells in the cell cycle at the time of sacrifice. However, double labelling with both BrdU and PCNA should identify 3 different populations of cells, those positive for BrdU only, those positive for PCNA and BrdU and those positive for PCNA only. BrdU only cells are post-mitotic cells derived from a cell that was dividing when the BrdU was added and which have exited the cell cycle between BrdU addition and sacrifice. PCNA and BrdU positive cells are actively dividing clonal cells, derived from cells that were dividing at the time of BrdU addition and which are dividing at sacrifice. Finally, cells that only express PCNA are cells that are dividing at sacrifice but are not derived from a cell in the S-phase when BrdU was added.

6.1.5 Problems associated with BrdU labelling *in vivo*

Following the fate of a group of dividing cells using BrdU is fine under control conditions, however introducing a seizure into the model complicates things. One of the problems associated with BrdU labelling in adult animals is the presence of the blood brain barrier, the permeability of which may be altered by the seizure activity. If the BrdU is available for incorporation at the time of seizure, changes in the blood brain barrier could alter the incorporation of BrdU into dividing cells. This means that the cells in S-phase at the time of the seizure cannot all be labelled with a pulse of BrdU, as this could introduce a difference between BrdU incorporation in control and treatment groups. However, if the pulse is applied approximately 1 cell cycle before the seizure then many of the cells dividing at the time of the seizure will be BrdU labelled, and unincorporated BrdU will have been cleared from the body eliminating the possibility of confounding effects from blood brain barrier disruption. A second problem associated with use of a pulse of BrdU as a label is dilution. Since BrdU is not endogenous to the cell cycle, but applied, when a pulse of BrdU is incorporated into dividing cells, only a limited quantity is present in each cell. Every cell division therefore produces a dilution in the BrdU density within the dividing cells, after a number of divisions the density of BrdU labelling will have dropped below the threshold required for detection and cells that contain BrdU are missed in analysis. Result obtained in two studies indicate that BrdU dilution probably occurs after about 4 cell cycles (Hayes and Nowakowski, 2002; Dayer, Ford et al., 2003). These two problems have a cumulative effect, in order to overcome the potential confounding effects of blood brain barrier disruption by seizures, earlier BrdU application can be used, however this decreases the number of cell cycles that can be followed after seizures without having to consider BrdU dilution. If the BrdU is applied 24 hours prior to seizure, dilution, based on the studies of Hayes, and Dayer, is predicted to be a factor after about 3 cell cycles after kainate administration.

6.1.6 Possible role for cell death in promoting neurogenesis *in vivo*

The experiments described in the previous chapter demonstrated a significant increase in cell death shortly after kainate application, which preceded a biphasic proliferative response. Cell death has also been detected in post injury responses in several *in vivo* models, including excitotoxic and mechanical lesions of the granule cell layer (Gould and Tanapat, 1997), and seizures (Sloviter, Dean et al., 1996; Bengzon, Kokaia et al.,

1997). However, there is considerable debate as to a possible causative role in the neurogenesis observed post injury, with electroconvusive therapy and other seizure models reporting no dentate granule cell death (Nakagawa, Aimi et al., 2000; Madsen, Treschow et al., 2000), and another group reporting that inhibition of the death produces increased neurogenesis (Ekdahl, Mohapel et al., 2001). Therefore, the examination of granule cell viability after seizures is also of considerable interest.

6.1.7 Questions to be addressed

The principle aim of these experiments is to examine the general profile of cell proliferation through time after seizures, while simultaneously following the survival and proliferation of a cohort of the cells dividing at the time of seizure as observations in our culture model suggest that these cells may be dying. Unilateral ICV kainate injection will be used to generate seizures, point proliferation will be quantified by PCNA immunostaining and immature neurons will be quantified by Doublecortin immunostaining. These observations should permit comparisons with existing control and kainate experiments. The labelling of a cohort of cells will be achieved with a series of three closely spaced BrdU pulses, the size of this cohort can then be compared at different times after kainate and saline injections, and the proliferative activity of the cohort can be investigated with PCNA double-labelling. We refer to changes in this cohort of cells and their progeny as 'clonal' proliferation. Additionally, Fluoro-Jade B (FJB) staining will be used to investigate the varying reports of cell death in the dentate gyrus as a consequence of seizures.

6.2 Methods

The general methods for this chapter are outlined below, with details of the exact tissue sampling outlined immediately before each accompanying results section.

6.2.1 Injections and Surgery

Sixty seven male Wistar rats (200 – 260g) received a course of three intraperitoneal injections of 5-bromodeoxyuridine (50mg/kg dissolved in sterile distilled water) at two hour intervals after weighing. 24 hours after the first BrdU injection 6 animals were sacrificed (see below) forming an un-operated control group (UOP).
In the remaining sixty one animals deep anaesthesia was induced using a combination of 25% Hypnorm (0.315 mg/ml fentanyl citrate and 10 mg/ml fluanisone; Jannsen) and 25% Hypnovel (5mg/ml midazolam; Roche) in sterile distilled water (50%). Under this anaesthesia rats were placed in a stereotactic frame, and kainic acid (0.5μg in 0.5μl of Sorensen's buffer) was administered into the left lateral ventricle over a 15-minute period into 33 rats using a 10μl Hamilton syringe at the following stereotactic co-ordinates (AP: +4.3mm interaural; ML +4.3mm from the midline and DV –3.3mm from the dura), a further 28 rats received a similar injection of 0.9% saline forming a operated controls. Groups of rats were then sacrificed 6 hours, 2, 5, 7, and 9 days later.

6.2.2 Sacrifice, perfusion and sectioning.

For all rats, sacrifice was by administration of a terminal dose of phentobarbitone, and was followed by transcardiac perfusion initially with 50mls 0.9% saline, followed by 50mls 4% paraformaldehyde pH 7.4,whole brains were then removed and post fixed in 4% paraformaldehyde and stored at 4˚C. Sections containing hippocampal formation were produced for immunochemistry on a vibrotome (Leica) cutting in the coronal plane at a thickness of 40μm; approximately 100 sections, comprising the entire hippocampal formation from each brain, were collected and stored in a sequential manner – such that the position within the hippocampus of any individual section could be identified.

6.2.3 Immunohistochemistry

Single label immunohistochemistry was performed on free-floating sections for BrdU or Doublecortin (Dcx). Double labelling of BrdU and proliferating cell nuclear antigen (PCNA) was performed on sections dried on to gelatinised slides. All immunohistochemistry was performed on systematically sampled tissue, with the initial section selected at random and subsequent sections being taken at constant intervals thereafter, ensuring that the entire dentate is sampled. BrdU single labelling and Fluoro-Jade B staining were performed on 6 sections per animal, BrdU and PCNA double labelling was performed on 3 sections per animal and Dcx staining was performed on 2 sections per animal.

For single stain immunohistochemistry tissue processed for BrdU was exposed to 2N HCl at 37˚C for 20 minutes. All tissue processed for single immunohistochemistry received multiple washes in Tris-Buffered Saline (TBS; 0.1M, pH7.4), followed by incubation with 3% H_2O_2 in distilled water for 10 minutes to eliminate non-specific peroxidase activity. Further TBS washes were followed by overnight incubation with primary antibody to either BrdU (rat monoclonal, 1:1000; Oxford Biotech) or Doublecortin (Guinea pig polyclonal, 1:5000; Chemicon) in TBS containing 0.1% triton and 0.05% Bovine Serum Albumin (TBS-TS) at 4˚C, tissue processed for BrdU also had 1% Normal Goat Serum (Sigma) present with the primary antibody. Following multiple washes in TBS, tissue was incubated in TBS-TS with the appropriate biotinylated secondary antibody, raised against either rat (goat, 1:200; Vector) or guinea pig (donkey, 1:200; Chemicon) for 1 hour. TBS washes were repeated and a Horseradish peroxidase conjugated Streptavidin-biotin complex (HRP-ABC, 1:200; DAKO) in TBS-TS was applied for 1 hour, further washing in TBS was followed by visualization with 3,3-Diaminobenzene (DAB, brown; Vector) and a final set of washes. Sections were mounted on gelatinised slides and received a light Thionine counter-stain to identify the granule cell layer. Thionine staining was obtained by placing slides in distilled water containing 1% Thionine followed by differentiation in 90% Ethanol with 0.5% Acetic acid until a consistent staining intensity was observed. All sections were dehydrated through 1 minute washes in alcohol (70%, 90% and 2x 100%) and then xylene before cover-slipping with DPX (Sigma).

For double stain immunochemistry of BrdU and PCNA sections mounted onto slides, which were placed in citrate buffer at room temperature (pH 6.0; 300ml) and heated in a microwave oven at full power for 3 minutes 30 seconds and then simmered for a further 5 minutes at low power. Slides were removed from the microwave oven and left stand on the bench in the hot citrate buffer for 20 minutes while it cooled. Slides were then transferred to 2N HCl and heated in a water bath (37°C; 30 minutes), followed by repeated TBS washes, and incubation with 3% H_2O_2 in distilled water (10 minutes). Further TBS washes were followed by overnight incubation with a cocktail of primary antibodies to BrdU (rat monoclonal, 1:1000; Oxford Biotech) and PCNA (mouse monoclonal, 1:250; Chemicon) in TBS-TS at 4°C. Following multiple washes in TBS, tissue was incubated in TBS-TS with a biotinylated secondary antibody, raised against rat (goat, 1:200; Vector) for 1 hour. TBS washes were repeated and HRP-ABC (1:200; DAKO) in TBS-TS was applied for 1 hour, further washing in TBS was followed by visualization with DAB (Vector). More TBS washes were followed by incubation with a biotinylated secondary antibody, raised against mouse (sheep, 1:500; Amersham Life sciences) for 1 hour. TBS washes were repeated and an Alkaline Phosphatase conjugated Streptavidin-biotin complex (AP-ABC, 1:200; DAKO) in TBS-TS was applied for 1 hour, further washing in TBS was followed by visualization with Fast Red (Boerhinger Mannheim) in TBS (pH 8.2). Sections were then wet mounted in moviol.

6.2.4 Fluoro-Jade B (FJB) and DAPI staining

Fluoro-Jade B staining was carried out according to the method described by Schmued with slight modification (Schmued, Albertson et al., 1997). Sections were mounted on to gelatinised slides and air dried overnight. Slides were immersed in a solution containing 1% sodium hydroxide in 80% alcohol for 2 minutes followed by 2 minute rinses in 70% ethanol and distilled water. Slides were then placed in a 0.06% potassium permanganate solution, on a shaker table, for 10 minutes. After a further 2 minute rinse in distilled water, slides were transferred to the Fluoro-Jade B/DAPI staining solution. The Fluoro-Jade B/DAPI solution was made immediately prior to use from stock solutions of Fluoro-Jade B and DAPI (both 10mg/100ml) in 0.1% acetic acid, in the proportions 4% Fluoro-Jade B, 2% DAPI and 92% acetic acid solution, producing final dye concentrations of 0.0004% and 0.0002% for Fluoro-Jade B and DAPI respectively. After 30 minutes in the staining solution, the slides were

washed in distilled water (3x 1 min) and dried in a slide dryer (37°C, 2 hours). Once dry slides were placed in xylene for 1 minute and then cover-slipped with DPX.

6.2.5 Cell Quantification and statistical analysis

A blind counting methodology was employed for all quantification, with slides coded such that the examiner was blind to the treatment of the tissue; the code was not broken until all cell counting was complete.

Cell counting: In all treatment groups, separate cell counts were obtained for the hippocampi ipsilateral to the ICV injection and from the hippocampi in the opposite hemisphere (contralateral) to the injection. In un-operated animals, the left hippocampus is defined as ipsilateral, as this is the hemisphere into which ICV injections were administered in animals that received surgery. Additionally, BrdU single labelled sections were also analysed for cluster distribution; a cluster was defined as contiguous BrdU positive labelling. Estimated cell/cluster counts are expressed per dentate rather than per section (producing a more robust analysis as the sample number becomes the number of animals used rather than the number of sections sampled). Counts from all sections in each animal were added, this total was then multiplied by the intersection interval to calculate a count per dentate, from which a mean and standard deviation were obtained. Although this method will overestimate any counts, the proportion by which the cell counts are overestimated remains the same between groups because the sampling method for all sections is identical, and thus different groups can be compared. (Note: overestimation arises because all cells in a 40μm section are counted. Cells that are near to the cut surface of the section can be cut in two by the sectioning process, these cells would then be counted twice if all sections were counted, when only one cell existed. This over estimation would also apply if the cell counts expressed per 40μm section; see also chapter 3.1.1).

Statistical Analysis: Three variables are considered in all analysis, treatment type (kainate or saline injection), hippocampal side (ipsilateral or contralateral)(all considered as column factors), and time after treatment (row factor). Some of the variables within treatment type and hippocampal side are related and others are not. Therefore, comparisons are made between ipsilateral and contralateral dentates in saline injected groups and in kainate injected groups. Additionally, comparison is

made between ipsilateral dentates of groups that received saline or kainate injections, and a similar comparison is made between treatment types in contralateral dentates. However, ipsilateral dentates taken from kainate injected animals are not related to contralateral dentates from saline injected animals and vice versa, so these comparisons were not made.

Multiple two-way ANOVA's were used to investigate responses to the factors detailed above, with Bonferroni post hoc comparison testing for specific differences between means of the column factors at each time (row factor). Subsequent one-way ANOVA with Bonferroni post hoc comparisons were used to investigate changes over time in each of the four dentate conditions (kainate ipsilateral, kainate contralateral, saline ipsilateral and saline contralateral). All data are expressed as mean ± standard deviation. These values are expressed per dentate, and all statistical differences reported are Bonferroni post hoc comparisons unless otherwise stated.

6.2.6 Fluoro-Jade B quantification and analysis

Images of DAPI and Fluoro-Jade B staining in the apex of the granule cell layer in ipsilateral dentates were captured on an inverted Leica DM-IRBE epifluorescence microscope (Milton Keynes, U.K.) using a cooled Hamamatsu digital camera at 10x magnification. The area of DAPI or Fluoro-Jade B fluorescence was determined in Scion image (ver 4.0.2; a PC based version of the program NIH image, which was developed at the U.S. National Institutes of Health and is available free on the Internet at http://rsb.info.nih.gov/nih-image/), using the density slice function, applied to the granule cell layer as a region of interest. For each animal the number of DAPI positive and FJB positive pixels in all 6 sections was summed, and cell death expressed as a percentage of the area in which Fluoro-Jade B fluorescence was detected above threshold within the cell layer divided by the area in which DAPI fluorescence was detected above a threshold in the same animal. Ipsilateral dentates from saline and kainate treatment groups were compared by Kruskal-Wallis test with Dunn's post test, as the data is not normally distributed.

6.3 Results

Five rats did not recover from surgery, the hippocampus of one rat was damaged on removal from the skull and subsequent experiments showed the stereotactic injection track was incorrectly positioned in 5 rats, and one rat did not exhibit BrdU immunostaining. These animals were therefore excluded from subsequent analysis. The remaining animals were distributed across the time points as follows: 6 hours (5 control and 5 kainate), 2 days (5 control and 5 kainate), 5 days (5 control and 5 kainate), 7 days (4 control and 4 kainate) and 9 days (5 control and 6 kainate), in addition to the 6 time 0 un-operated controls.

6.3.1 BrdU labelling of proliferating cells

Quantification of the number of BrdU positive cells within each dentate gyrus was performed on every 18th section, resulting in sampling of six 40μm sections per animal, the sum of BrdU positive cell counts from each group of six dentates was then multiplied by the intersection interval. The resultant value is a slight over estimation the actual number of BrdU positive cells in each dentate as cells that are on the edge of each section could be cut in half and so are effectively counted twice (Discussed more fully in chapter 3.1.1), however all groups experience the same quantification method and their relationships should be unaffected. Sections were taken from un-operated day 0 controls and from both kainate and saline injected rats at all time points (6 hours (day 0.25), and days 2, 5, 7 and 9).

i) Un-operated control rats from day 0 have the same number of BrdU labelled cells in each dentate.

The number of BrdU positive cells detected in the dentates taken from each hemisphere of un-operated rats sacrificed at the time of surgery was not significantly different ($p=0.29$, paired two-tailed students t-test). In these animals the left hemisphere was designated 'ipsilateral' for subsequent analysis as this is the hemisphere that the unilateral ICV injections were administered to.

ii) BrdU cell counts do not differ between ipsilateral and contralateral dentates in control animals that received a unilateral ICV saline injection.

There were no significant differences in the number of BrdU positive cells detected between ipsilateral (ipsi) and contralateral (contra) dentates in animals receiving ICV saline injections ($p = 0.95$; two way ANOVA). Numbers of BrdU cells labelled changed significantly over the entire experiment ($p<0.01$; two-way ANOVA), however none of the individual changes between days demonstrated statistical differences (determined by Bonferroni post test). The trend is for increased BrdU cell counts to day 2 (ipsi, 6732±1510 cells, and contra, 6566±932 cells), with BrdU positive cell numbers then remaining constant on days 5 and 7, falling slightly on day 9 (ipsi, 4860±2771 cells, and contra, 4842±1469 cells; **Fig 6.1A**).

iii) BrdU cell counts vary over time after ICV kainate and there is no difference between counts ipsilateral and contralateral to the kainate injection.

The ipsilateral profile demonstrates a sharp, and significant, threefold rise in BrdU positive cells from 6 hours (3236±1372 cells) to a peak on day 2 (9810±1840 cells; $p<0.001$) and then falls, remaining significantly elevated on day 5 (6934±1858 cells; $p<0.05$ vs. 6 hours). The decrease in BrdU positive cells from a peak on day 2 becomes significant on day 7 (6102±1710 cells; $p<0.05$) and day 9 (4803±1433 cells; $p<0.001$; **Fig 6.1B**). Considering changes over time within groups using one-way ANOVA, the contralateral BrdU profile does not vary significantly; although the trend is for a slight increase from 6 hours to day 2, and a slight decrease from day 5 to day 9.

The number of BrdU cells detected varied over time both ipsilateral and contralateral to the kainate injection in a broadly similar pattern (**Fig 6.1B**) resulting in no overall differences between the two hemispheres ($p = 0.80$; two-way ANOVA). Although there are no individual significant differences, at 6 hours there are fewer cells ipsilaterally (3236±1372 cells) than contralaterally (4518±1418 cells), and this is reversed by day 2 (ipsi, 9810±1840 cells, and contra, 7484±1297 cells), at all later time points cell numbers are closely matched.

iv) Kainate injection increases the number of BrdU positive cells detected at day 2 post kainate in the ipsilateral dentate, compared with saline injected controls.
On day 2, injection of kainate caused a significant increase in the number of BrdU positive cells compared with ICV saline injection (kainate, 9810±1840 cells, vs. saline, 6732±1510 cells; $p<0.05$), at all other times BrdU numbers were similar between treatments (**Fig 6.1C**), and if the entire course of the experiment is considered then no significant change in the overall number of BrdU positive cells resulted from injection of kainate or saline ($p=0.40$; two-way ANOVA).

v) Kainate injection does not alter the number of BrdU positive cells detected in the contralateral dentate, compared with saline injected controls.
There was no significant difference between BrdU counts contralateral to the kainate and saline injections ($p=0.27$; two-way ANOVA; **Fig 6.1D**).

vi) Over time kainate injection induces a significant increase in BrdU positive cells, both ipsilaterally and contralaterally, when compared with day 0 un-operated controls; whereas saline injection does not.
ICV kainate injection produces a significant increase in the number of BrdU labelled cells detected on the side of the injection two days after surgery compared with the number detected in dentates taken from the same hemisphere of rats sacrificed at the time of surgery, day 0 (ipsi kainate day 2, 9810±1840 cells, vs. ipsi un-operated day 0, 4521±1236 cells; $p<0.01$, one way ANOVA with Dunnett's post test; **Fig 6.1C**). In the contralateral dentate, numbers of BrdU positive cells are significantly lower in un-operated animals sacrificed on the day of surgery (day 0, 4146±942 cells) than in animals that received ICV kainate and were sacrificed 2 or 5 days later (day 2, 6566±932 cells, and day 5, 6800±1484 cells; both $p<0.05$, one-way ANOVA with Dunnett's post test; **Fig 6.1D**). BrdU cell numbers did not differ significantly between un-operated animals and animals that received ICV saline (**Figs 6.1C and 6.1D**).

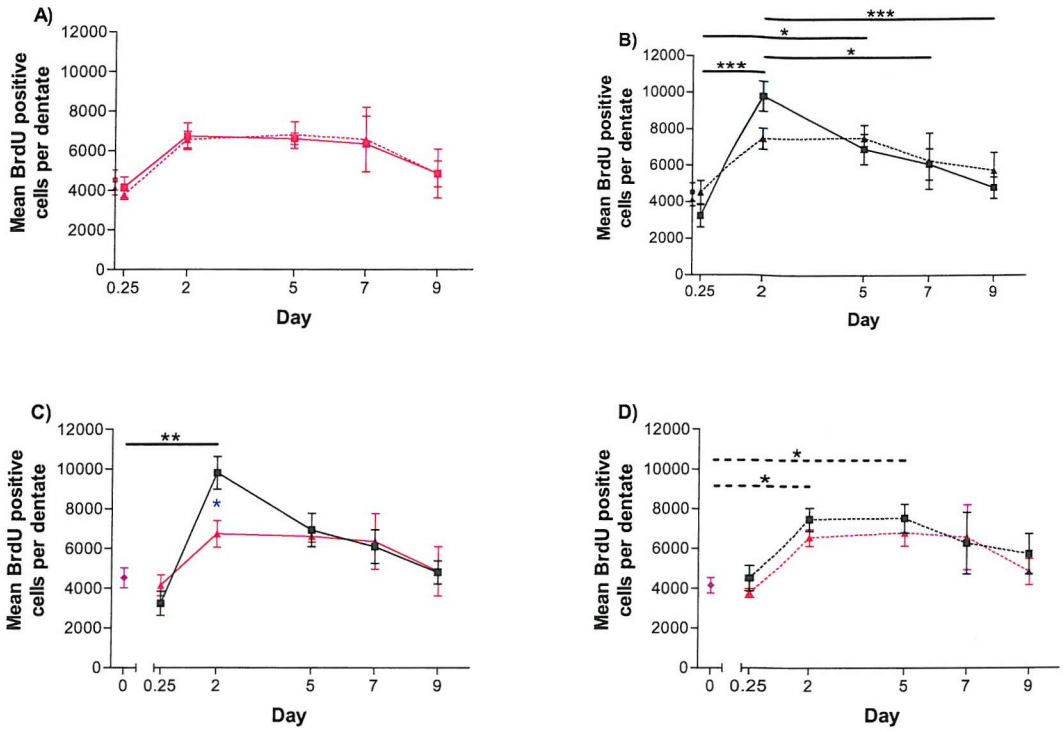

Fig 6.1: Profiles of BrdU labelling in dentates of animals receiving unilateral i.c.v. injections of either saline or kainate, and BrdU labelling of day 0 un-operated control data. Showing the profile of BrdU labelling in ipsilateral (solid lines) and contralateral (dotted lines) dentates after saline injection **(A)** and after kainate injection **(B)**. The profile of BrdU labelling is also considered in ipsilateral dentates after kainate or saline injection and in un-operated controls **(C)** and similarly in contralateral dentates **(D)**. All values are expressed as mean ± SEM, taken from 4-6 animals per treatment with 6 sections systematically sampled from each animal and scaled by the inter section interval.
Statistical analysis between treatments in all graphs is by two-way ANOVA with Bonferroni post hoc test, blue *asterisks* denote significant differences.
In **(A)** and **(B)**, analysis over time within groups is by one-way ANOVA with Bonferroni post hoc test (* $p<0.05$, ** $p<0.01$, *** $p<0.001$), un-operated controls were excluded from this analysis.
In **(C)** and **(D)** all data are compared to un-operated controls using one-way ANOVA with Dunnett's post hoc test, *asterisks* denote significant differences from controls (* $p<0.05$, ** $p<0.01$).

vii) BrdU cluster size profiles do not differ between animals that received unilateral ICV saline or kainate injection, either ipsilateral or contralateral to the injection.

While BrdU cluster sizes vary significantly over the course of these experiments, these changes are similar in all treatment groups. There was no significant difference between ipsilateral and contralateral dentates in saline ($p=0.76$; two-way ANOVA;

Fig 6.2C inset) or kainate (p=0.37; two-way ANOVA; **Fig 6.2C inset**) injected animals. Additionally, there was no significant difference between dentates ipsilateral to either saline or kainate injection (p=0.19; two-way ANOVA; **Fig 6.2C inset**), and there was no significant difference between dentates contralateral to the injection (p=0.89; two-way ANOVA; **Fig 6.2C inset**).

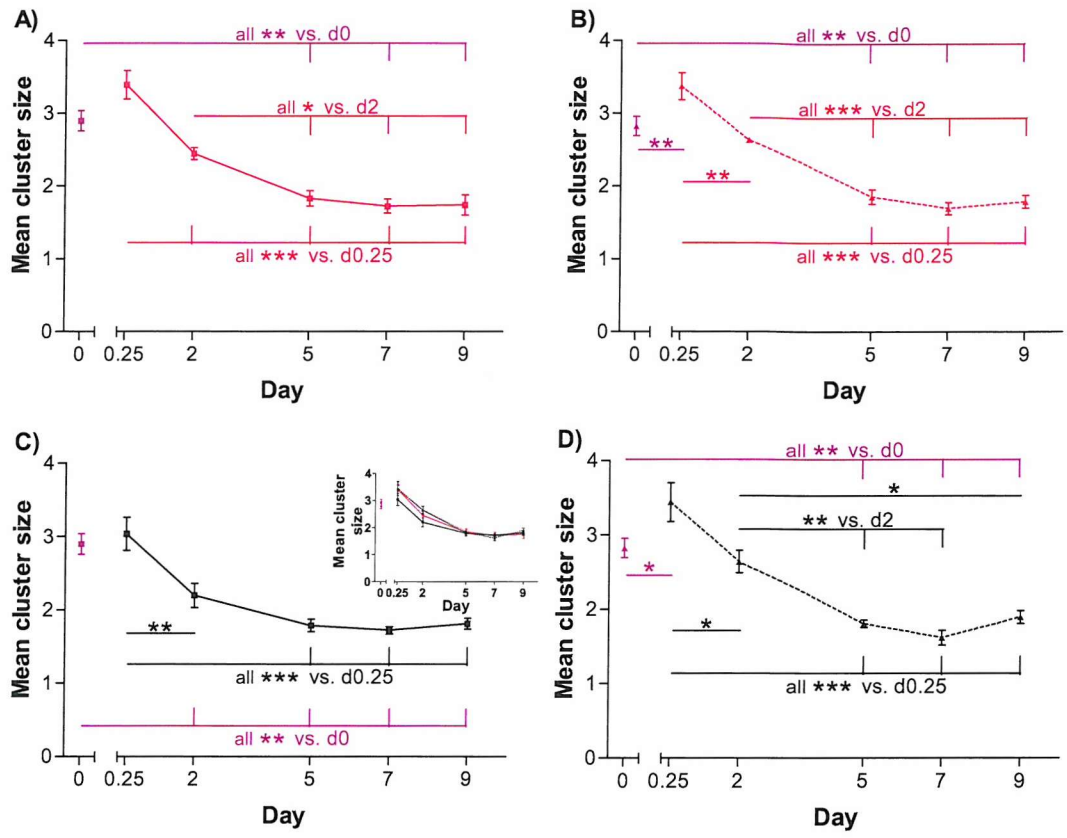

Fig 6.2: Profiles of average BrdU cluster sizes in dentates of animals receiving unilateral i.c.v. injections of either saline or kainate, and BrdU labelling of day 0 un-operated control data. Showing the profile of BrdU cluster size in saline injected animals ipsilateral to the injection **(A)** and contralateral to the injection **(B)** The profile of BrdU cluster size is also considered after i.c.v. kainate injection in ipsilateral **(C)** and contralateral dentates **(D)**. Inset in **(C)** represents an overlay of all the groups. All values are expressed as mean ± SEM, taken from 4-6 animals per treatment with pooled BrdU cell and cluster counts from 6 systematically sampled sections per animal. Black and red *asterisks* denote significant differences within groups over time determined by one-way ANOVA with Bonferroni post hoc test (* $p<0.05$, ** $p<0.01$, *** $p<0.001$), un-operated controls were excluded from this analysis. Purple *asterisks* denote significant differences from un-operated controls, determined by one-way ANOVA with Dunnett's post hoc test, (* $p<0.05$, ** $p<0.01$, *** $p<0.001$).

viii) BrdU cluster size peaked at 6 hours and then decreased over time in groups examined.

A significant increase in the mean BrdU cluster size was observed between 'contralateral' dentates from un-operated day 0 control animals (2.83±0.32 cells per cluster) and contralateral dentates from saline (3.37±0.416 cells per cluster; $p<0.01$ Dunnett's) or kainate (3.44±0.59; $p<0.05$ Dunnett's) injected animals sacrificed 6 hours later. This trend was present in the ipsilateral dentates, but did not reach statistical significance (un-operated, 2.90±0.34 cells per cluster; saline, 3.39±0.44 cells per cluster; and kainate, 3.04±0.51 cells per cluster).

BrdU cluster sizes then fell with time, approximately following a decay curve, such that at all subsequent times examined mean BrdU cluster sizes were significantly lower than the corresponding 6 hour cluster size (Tables 6.1 and 6.2).

Kainate	Ipsilateral					Contralateral				
	Mean	S.D.	p vs. day 0 (Dunnett's)	p vs. 6 hrs (Bonferroni)	p vs.day 2 (Bonferroni)	Mean	S.D.	p vs. day 0 (Dunnett's)	p vs. 6 hrs (Bonferroni)	p vs. day 2 (Bonferroni)
Day 0	2.90	0.34	-	-	-	2.83	0.32	-	-	-
6 hours	3.04	0.51	ns	-	-	3.44	0.59	<0.05	-	-
Day 2	2.20	0.37	<0.01	<0.01	-	2.65	0.34	ns	<0.05	-
Day 5	1.79	0.19	<0.01	<0.001	ns	1.81	0.11	<0.01	<0.001	<0.01
Day 7	1.72	0.09	<0.01	<0.001	ns	1.62	0.20	<0.01	<0.001	<0.01
Day 9	1.81	0.18	<0.01	<0.001	ns	1.90	0.21	<0.01	<0.001	<0.05

Table 6.1: Differences in mean BrdU cluster sizes over time in unilateral ICV kainate injected animals.

Saline	Ipsilateral					Contralateral				
	Mean	S.D.	p vs. day 0 (Dunnett's)	p vs. 6 hrs (Bonferroni)	p vs.day 2 (Bonferroni)	Mean	S.D.	p vs. day 0 (Dunnett's)	p vs. 6 hrs (Bonferroni)	p vs. day 2 (Bonferroni)
Day 0	2.90	0.34	-	-	-	2.83	0.32	-	-	-
6 hours	3.39	0.44	ns	-	-	3.37	0.42	<0.01	-	-
Day 2	2.44	0.19	ns	<0.001	-	2.64	0.07	ns	<0.01	-
Day 5	1.83	0.24	<0.01	<0.001	<0.05	1.86	0.22	<0.01	<0.001	<0.001
Day 7	1.72	0.19	<0.01	<0.001	<0.05	1.70	0.16	<0.01	<0.001	<0.001
Day 9	1.74	0.31	<0.01	<0.001	<0.05	1.79	0.20	<0.01	<0.001	<0.001

Table 6.2: Differences in mean BrdU cluster sizes over time in unilateral ICV saline injected animals.

ix) Summary of BrdU time course findings

Unilateral injection of an isotonic fluid (saline) does not induce changes in BrdU labelling compared with labelling observed contralateral to the injection.

Injection of kainate into the left cerebroventrical produces an increase in the number of BrdU positive cells detected in both the adjacent and opposite dentates after 2 days,

whereas saline injection does not. This increase in BrdU cell counts in kainate injected animals is larger ipsilateral to the injection than in the contralateral dentate. This is because in ipsilateral dentates significantly more BrdU cells are detected on day 2 after kainate injection than after saline injection, whereas contralaterally BrdU cell counts do not differ between kainate and saline animals.

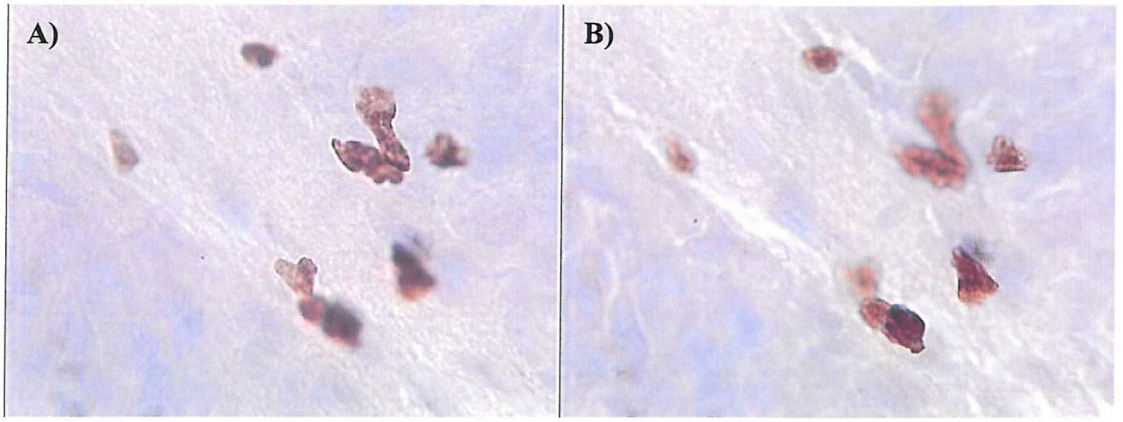

Fig 6.3: High magnification images of BrdU clusters. Transmission images (100x) in two different focal planes (**A+B**) show BrdU positive cells, forming clusters of various sizes, that extend in 3 dimensions.

6.3.2 Effects on Neurogenesis determined by doublecortin labelling

Increases in both cell proliferation and neurogenesis have been reported as consequences of seizures. The BrdU pre-labelling protocol we used in these experiments did not detect an increase in cell proliferation of the same magnitude as is observed in post-labelling protocols. Therefore, it is important to establish that the predicted increase neurogenesis is observed. Doublecortin (Dcx) immunostaining was used to assess the number of immature neurons, and hence the level of neurogenesis, present in the dentate gyrus at various times after either an ICV kainate or saline injection.

Quantification of the number of Dcx positive cells within each dentate gyrus was performed on every 48th section, resulting in sampling of two 40μm sections per animal, the sum of BrdU positive these cell counts was then multiplied by the intersection interval. Sections were taken from both kainate and saline injected rats at day 2, day 5, and day 7).

i) Doublecortin cell counts are not affected by ICV saline injection in control animals.

There were no significant differences in the number of Dcx positive cells between ipsilateral and contralateral dentates in animals receiving ICV saline injections ($p = 0.54$; two way ANOVA). Analysis showed that overall the day of sacrifice had a significant effect on the number of Dcx positive cells present ($p<0.05$; two-way ANOVA), however when each side was considered there are no significant changes over time (ipsi, $p=0.11$, and contra $p=0.12$; both one way ANOVA), and there are no specific significant differences between individual time points as assessed by Bonferroni's post test (**Fig 6.4A**).

ii) Doublecortin expression is dependent on both time of sacrifice and perhaps side of the brain in animals receiving a unilateral ICV kainate injection.

The number of Dcx cells is significantly greater in the ipsilateral dentate than the contralateral dentate in kainate injected rats on day 5 (ipsi, 34877±6369 cells, and contra, 21216±1628 cells; $p<0.001$) and day 7 (ipsi, 35052±2247 cells, and contra, 18312±4543 cells; $p<0.001$; **Fig 6.4B**). Additionally, the overall comparison

indicates a significant change between ipsilateral and contralateral dentates ($p<0.001$; two-way ANOVA) and a significant change in Dcx cells over time ($p<0.001$; two-way ANOVA), this analysis also indicated significant interaction between the two factors ($p<0.05$). This is because Dcx does not change significantly over time in contralateral dentates ($p=0.09$; one-way ANOVA), but increases significantly in the ipsilateral dentates ($p<0.01$; one-way ANOVA). Dentates from the ipsilateral hemisphere of animals sacrificed on day 2 (19939±5284 cells) have significantly fewer Dcx positive cells than those sacrificed on day 5 (34877±6369 cells; $p<0.001$) and day 7 (35052±2247 cells; $p<0.001$; **Fig 6.4B**).

iii) Kainate injection increases the number of doublecortin positive cells in the ipsilateral dentate, compared with saline injected controls.

The number of Dcx cells is significantly greater in the ipsilateral dentate of kainate injected rats than in saline injected rats on day 5 (kainate, 34877±6369 cells, and saline, 18595±2924 cells; $p<0.001$) and day 7 (kainate, 35052±2247 cells, and saline, 13704±5919 cells; $p<0.001$; **Fig 6.4C**). Overall comparison between ipsilateral dentates taken from animals injected with either kainate or saline indicates both a significant change in Dcx positive cells dependent on treatment ($p<0.001$; two-way ANOVA) and a significant change dependent on age ($p<0.05$; two-way ANOVA), this analysis also indicated significant interaction between the two factors ($p<0.001$; **Fig 6.4C**).

iv) Kainate injection does not alter the number of doublecortin positive cells detected in the contralateral dentate, compared with saline injected controls.

In the contralateral dentates examined during the course of the entire experiment, the fluid injected did not cause significant change to the number of Dcx positive cells ($p=0.18$; two-way ANOVA; **Fig 6.4D**). This may be due to only sampling 2 sections per animal, with a greater sampling frequency the slight trend for increased Dcx in the kainate tissue at later times may reach statistical significance.

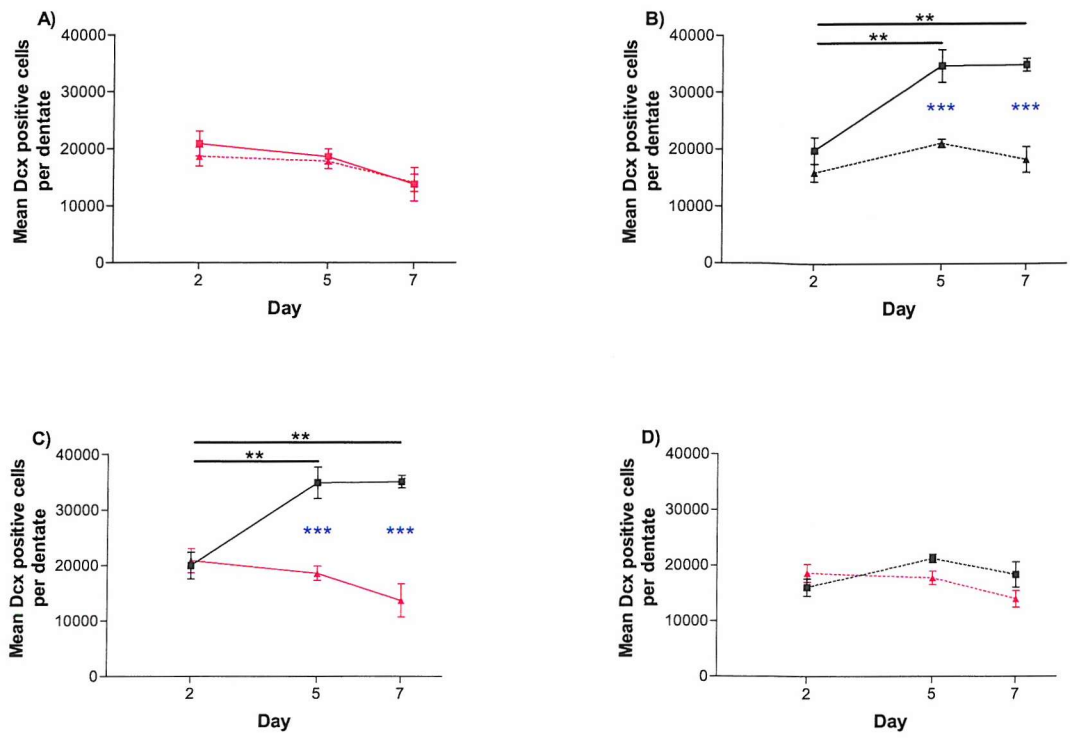

Fig 6.4: Profiles of Doublecortin (Dcx) expression in of animals receiving unilateral i.c.v. injections of either saline or kainate. Showing the profile of Dcx expression in saline injected animals ipsilateral to the injection **(A)** and contralateral to the injection **(B)** The profile of Dcx is also considered after i.c.v. kainate injection in ipsilateral **(C)** and contralateral dentates **(D)**. Inset in **(C)** represents an overlay of all the groups. All values are expressed as mean ± SEM, taken from 4-6 animals per treatment with 6 sections systematically sampled from each animal and scaled by the inter section interval. Black and red *asterisks* denote significant differences within groups over time determined by one-way ANOVA with Bonferroni post hoc test (* $p<0.05$, ** $p<0.01$, *** $p<0.001$), un-operated controls were excluded from this analysis. Purple *asterisks* denote significant differences from un-operated controls, determined by one-way ANOVA with Dunnett's post hoc test, (* $p<0.05$, ** $p<0.01$, *** $p<0.001$).

v) Summary of doublecortin time course findings

Unilateral injection of saline does not induce changes in Dcx labelling compared with labelling observed contralateral to the injection.

Injection of kainate into the left cerebroventrical produces an increase in the number of Dcx positive cells detected in the adjacent dentate after 5 and 7 days compared with saline injected controls. The ipsilateral increase in Dcx labelling after kainate

injection lags behind the increase in BrdU labelling. Contralaterally Dcx did not appear to change.

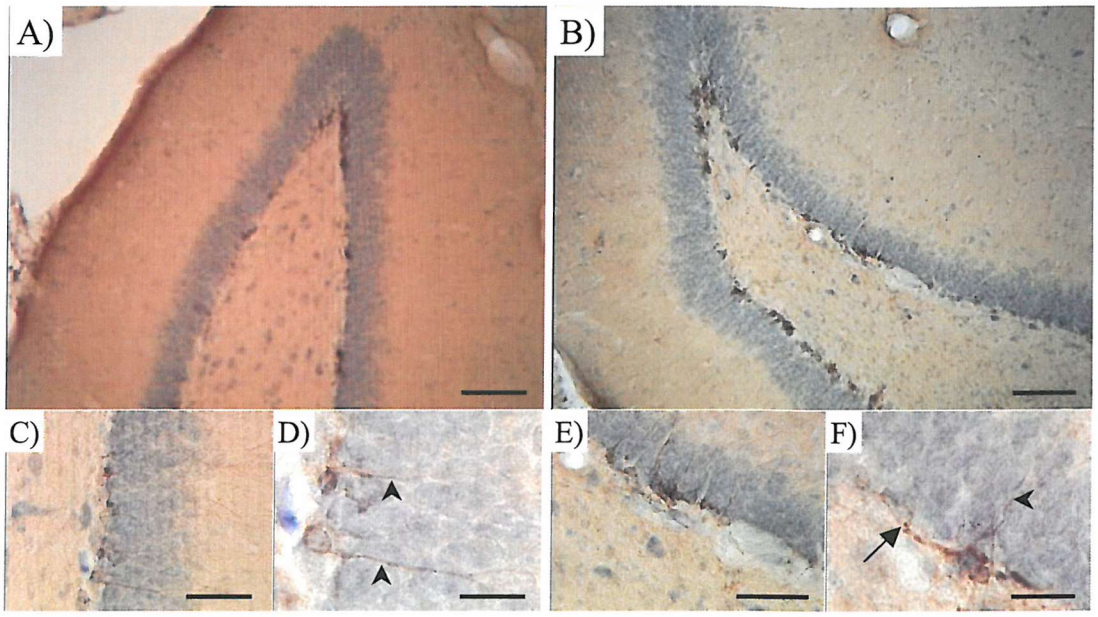

Fig 6.5: Doublecortin immunostaining on day 5 in control and kainate animals. Low magnification images (10x) of ipsilateral dentates from control **(A)** and kainate **(B)** injected aniamls, showing comparative staining densities. Higher magnification images (40x **C+E** and 100x **D+F**) show doublecortin positive processes extending radially across the granule cell layer and into the molecular layer (**C+E**, and arrowheads in **D+F**). Additionally, processes running parallel to the subgranular zone are present after kainate (arrow in **F**). Scale bars: A+B, 200μm; C+E, 50μm; D+F, 20μm.

6.3.3 'Clonal' and point proliferation determined by BrdU and PCNA labelling

PCNA and BrdU double labelling were used to assess the different types of proliferation occurring in the dentate gyrus. The total number of BrdU positive cells reflects all the surviving cells that are derived from cells dividing before the surgery (**Fig 6.6**; all red cells). The numbers of cells that have incorporated BrdU but do not express PCNA (BrdU only) are post mitotic cells that are not in the cell cycle at the time of sacrifice (**Fig 6.6**; red only cells). The total number of PCNA positive cells reflects all the cells that are in the cell cycle at the time of sacrifice (**Fig 6.6**; all blue cells). The cells that express PCNA but have not incorporated BrdU (PCNA only) are actively dividing cells (at the time of sacrifice) that are not derived from the population of cells we identified as dividing prior to surgery (**Fig 6.6**; only blue cells), up to the point that dilution of the BrdU label limits its detection (**Fig 6.6C** *far right*). The number of cells labelled for both PCNA and BrdU reflects the cells that are currently in the cell cycle and are derived from cells dividing before the surgery (**Fig 6.6**; blue and red checked cells), until BrdU is diluted below detection levels. Finally, the proportion of the total number of PCNA positive cells that are also positive for BrdU is a measure of the contribution to current division that the pre-labelled cells are making.

Quantification of these factors within each dentate gyrus was performed on every 36^{th} section, resulting in systematic sampling of three 40μm sections per animal, the sum these cell counts was then multiplied by the intersection interval. Sections were taken from both kainate and saline injected rats at day 0.25, day 2, and day 5).

Initially control conditions are analysed; to identify if injection of a bolus of saline induces an effect on cell proliferation compared with tissue from the same animal that has not received a mechanical trauma. Analysis will compare relevant anatomical dentates with respect to the different types of BrdU and PCNA labelling found.

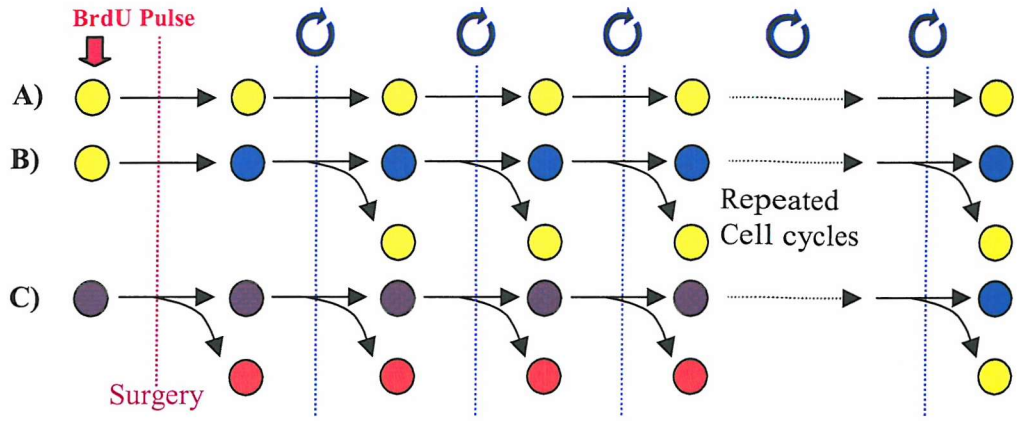

Fig 6.6: Distribution of proliferation markers. In the pre-labelling paradigm cells that are not dividing do not incorporate BrdU or express PCNA, these cells form the bulk of the granule cell layer and are not detected by this experiment **(A)**. All cells that begin to divide express PCNA while they are in the cell cycle, but cease to express it shortly after leaving the cell cycle **(B)**. In addition to expressing PCNA, cells in S-phase of division at the time of the BrdU pulse incorporate BrdU. If these BrdU labelled cells cease to divide then they will cease to express PCNA, but BrdU labelling will persist **(C)**. However, in BrdU labelled cells after each division the concentration of incorporated BrdU decreases, if it falls below the limit of detection these cells will not be counted for BrdU, but the dividing cells will still be PCNA positive **(C** *far right*).

6.3.3.1 Saline (ipsilateral vs. contralateral)

i) Total BrdU cell counts do not differ between ipsilateral and contralateral dentates in control animals that received a unilateral ICV saline injection, but do change over time.

There were no significant differences in the total number of BrdU positive cells between ipsilateral and contralateral dentates in animals receiving ICV saline injections ($p = 0.87$; two-way ANOVA). Analysis showed that the day of sacrifice is a significant factor in determining the total number of BrdU positive cells detected ($p<0.01$; two-way ANOVA). When each side was considered individually the total number of BrdU cells detected changed over time in the ipsilateral ($p<0.05$; one-way ANOVA) but not the contralateral dentate ($p=0.17$; one way ANOVA), this resulted in a significant increase in the total BrdU cells detected between 6 hours (3010±587 cells) and 5 days (4435±1021 cells; $p<0.05$) in the ipsilateral dentate (**Fig 6.7A**).

ii) BrdU only cell counts do not differ between ipsilateral and contralateral dentates in control animals that received a unilateral ICV saline injection, but do change over time.

There were no significant differences in the number of BrdU only cells between ipsilateral and contralateral dentates in animals receiving ICV saline injections ($p=0.73$; two way ANOVA). Analysis showed that overall the day of sacrifice did have a significant effect on the number of BrdU only cells detected ($p<0.01$; two-way ANOVA). When each side was considered individually the total number of BrdU cells detected changed over time in the contralateral ($p<0.05$; one-way ANOVA) but not the ipsilateral dentate ($p=0.13$; one way ANOVA), this resulted in a significant increase in the number of BrdU only cells detected between 6 hours (382±259 cells) and 5 days (1051±531 cells; $p<0.05$) in the contralateral dentate (**Fig 6.7B**).

iii) Total PCNA cell counts do not differ between ipsilateral and contralateral dentates in control animals that received a unilateral ICV saline injection, but do change over time.

There were no significant differences in the total number of PCNA positive cells between ipsilateral and contralateral dentates in animals receiving ICV saline injections ($p = 0.65$; two way ANOVA). Analysis showed that overall the day of sacrifice was a significant factor on the total number of PCNA positive cells detected ($p<0.001$; two-way ANOVA). When each side was considered individually the total number of PCNA cells detected changed over time in the ipsilateral ($p<0.01$; one-way ANOVA) but not the contralateral dentate ($p=0.059$; one way ANOVA), this resulted in animals sacrificed on day 5 (10915±3248 cells; $p<0.05$) having significantly increased total PCNA cell counts than at 6 hours (6516±1074 cells; $p<0.05$) and on day 2 (6379±1139 cells; $p<0.05$) in the ipsilateral dentate (**Fig 6.7C**).

iv) PCNA only cell counts do not differ between ipsilateral and contralateral dentates in control animals that received a unilateral ICV saline injection, but do change over time.

There were no significant differences in the number of PCNA only cells between ipsilateral and contralateral dentates in animals receiving ICV saline injections ($p=0.45$; two way ANOVA). Analysis showed that overall the day of sacrifice did have a significant effect on the number of PCNA only cells detected ($p<0.001$; two-way ANOVA), with animals sacrificed on day 5 (7430±2495 cells; $p<0.05$) having significantly increased PCNA only cell counts than at 6 hours (4090±1064 cells; $p<0.05$) and on day 2 (3845±1086 cells; $p<0.05$) in the ipsilateral dentate, and increased PCNA only cell counts between 6 hours (3607±1119 cells) and 5 days (6134±1393 cells; $p<0.05$) in the contralateral dentate (**Fig 6.7D**).

v) The number of cells positive for both PCNA and BrdU do not differ between ipsilateral and contralateral dentates, or over time in control animals that received a unilateral ICV saline injection.

There were no significant differences in the total number of BrdU positive cells between ipsilateral and contralateral dentates in animals receiving ICV saline injections ($p=0.73$; two way ANOVA). Analysis showed that overall the day of sacrifice did not have a significant effect on the total number of BrdU positive cells detected ($p=0.067$; two-way ANOVA; **Fig 6.7E**).

vi) The fractional contributions of BrdU pre-labelled cells to the total dividing cell population (BrdU+PCNA/ Total PCNA) in control animals that received a unilateral ICV saline injection do not change between ipsilateral and contralateral dentates, but are different over time.

There were no significant differences in the proportions of the total dividing population that are pre-labelled BrdU positive cells between ipsilateral and contralateral dentates in animals receiving unilateral ICV saline injections ($p=0.88$; two-way ANOVA), and Bonferroni post tests found no differences between ipsilateral and contralateral dentates at individual sacrifice points. A significant overall change in proportions over time was observed ($p<0.05$; two-way ANOVA), however when each hemisphere is considered separately these differences are not significant (ipsi, $p<0.15$ and contra, $p<0.16$; one-way ANOVA) and no individual changes reach statistical significance with Bonferroni post tests (**Fig 6.7F**).

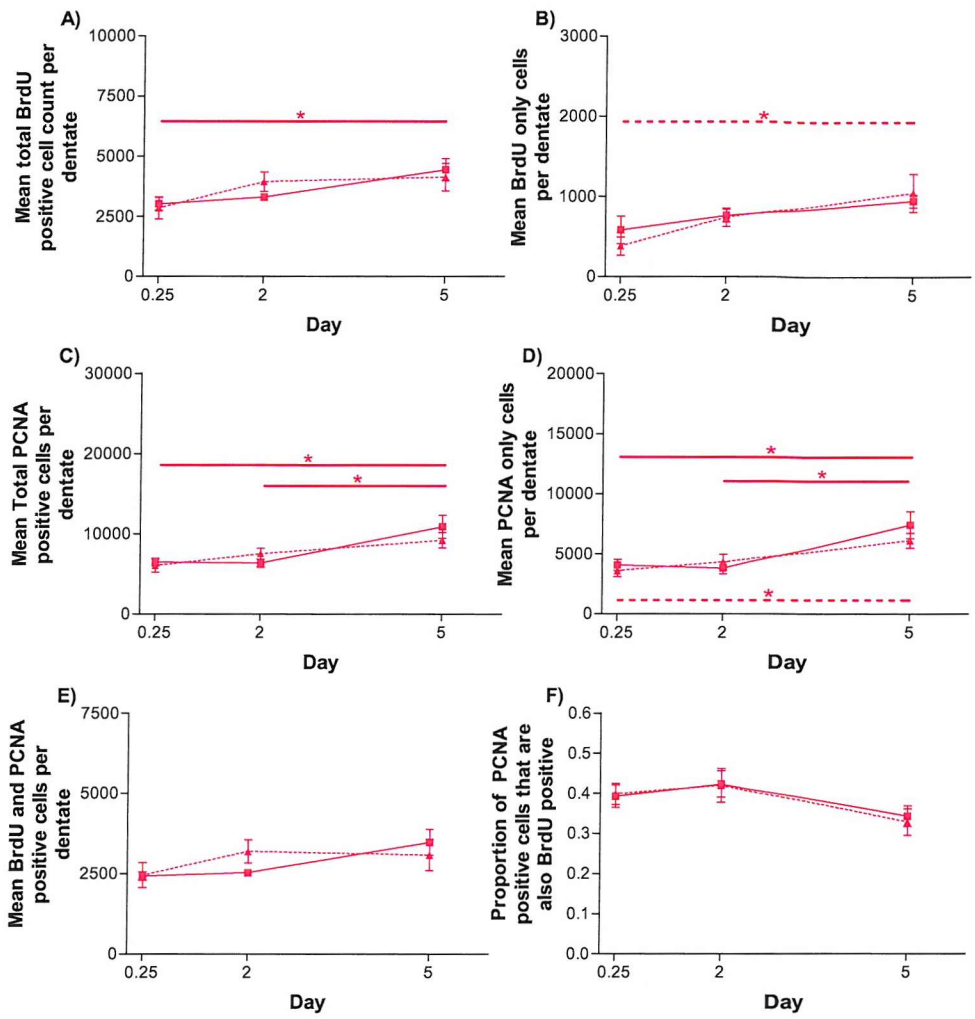

Fig 6.7: Profiles of proliferation in ipsilateral *(solid lines)* and contralateral *(dotted lines)* dentates of animals receiving unilateral i.c.v. saline injections. Cell proliferation is investigated using two markers; pre-injection tagging of cells in the cell cycle with BrdU and identification of cells in the cells cycle at the time of sacrifice using PCNA. Different marker labelling combinations represent different populations of cells, the total number of cells derived from pre-labelled cells **(A)** and the total number of cells dividing at sacrifice **(C)** can be sub divided into a population of pre-labelled cells that have ceased to divide **(B)**, a population of cells that were not dividing before the injection but are at sacrifice **(D)**, and a population of cells that were dividing before the injection and are dividing at sacrifice **(E)**. The fractional contribution of BrdU pre-labelled cells to the total population of cells in the cell cycle at sacrifice is also examined **(F)**. Values are expressed as mean ± SEM, and are taken from 5 animals with 3 sections systematically sampled from each animal and scaled by the inter section interval, except in **(F)**, where data is per section from 15 sections. *Asterisks* denote significant differences within ipsilateral *(solid lines)* and contralateral *(dotted lines)* dentates determined by One-way ANOVA with Bonferroni post hoc test (* $p<0.05$).

vii) Summary of proliferation in unilateral ICV saline injected rats.

Unilateral injection of saline does not induce significant changes in proliferation in the dentate ipsilateral to the injection compared with that in the contralateral dentate. Both dentates show a slight but steady and significant increase in Total BrdU labelling over time, and this corresponds with a similar steady increase in BrdU only labelling, indicating a constant production of post-mitotic cells in the saline injected animals over 5 days. Saline appears to produce a delayed bilateral increase in proliferation, which is principally derived from cells not labelled with BrdU. However, the fraction of BrdU positive cells that continue to divide is unchanged throughout.

6.3.3.2 Kainate (ipsilateral vs. contralateral)

Using the same six parameters as in the previous section the results of kainate injection are analysed; to identify if injection of a bolus of kainate induces similar effects on cell proliferation on both the side it is injected and the contralateral side.

i) Total BrdU cell counts do not differ between ipsilateral and contralateral dentates in animals that received a unilateral ICV kainate injection, but do change over time.

The total number of BrdU cells appears to be greater in ipsilateral dentates than contralateral dentates in kainate injected rats (**Fig 6.8A**). However, overall these differences are not significant ($p=0.064$; two-way ANOVA), and neither are Bonferroni post test comparisons between ipsilateral and contralateral dentates at each sacrifice time. Changes in total BrdU numbers were significant over time ($p<0.001$; two-way ANOVA), with ipsilateral increases from 6 hours (2722±265 cells) to day 2 (8186±740 cells; $p<0.01$) and day 5 (7423±3117 cells; $p<0.01$), and a contralateral increase from 6 hours (2974±872 cells) to day 5 (6228±2293 cells; $p<0.05$; **Fig 6.8A**).

ii) BrdU only cell counts do not differ between ipsilateral and contralateral dentates in animals that received a unilateral ICV kainate injection, but do change over time.

The number of BrdU only cells appears to be greater in ipsilateral dentates than contralateral dentates in kainate injected rats (**Fig 6.8B**). However, overall these

differences are not significant ($p=0.077$; two-way ANOVA), and neither are Bonferroni post test comparisons between ipsilateral and contralateral dentates at each sacrifice time. Changes in numbers of cells only labelled for BrdU were significant over time ($p<0.001$; two-way ANOVA), with ipsilateral increases from 6 hours (504±274 cells) to day 2 (1771±195 cells; $p<0.01$) and day 5 (2059±863 cells; $p<0.01$), and a contralateral increase from 6 hours (432±243 cells) to day 5 (1721±921 cells; $p<0.05$; **Fig 6.8B**).

iii) Total PCNA cell counts are different both between ipsilateral and contralateral dentates and between sacrifice times after a unilateral ICV kainate injection.
The total number of PCNA cells is significantly increased in ipsilateral dentates on day 2 (ipsi, 23062±6326 cells, and contra, 13982±1575 cells; $p<0.05$), and overall compared with contralateral dentates in animals receiving an ICV kainate injection ($p<0.05$; two-way ANOVA; **Fig 6.8C**). Total PCNA numbers also changed significantly over time ($p<0.001$; two-way ANOVA), with both ipsilateral and contralateral increases from 6 hours (ipsi, 5234±951 cells, and contra, 5573±1305 cells) to day 2 (ipsi, 23062±6326 cells; $p<0.01$, and contra, 13982±1575 cells; $p<0.001$) and day 5 (ipsi, 19102±10267 cells; $p<0.05$, and contra, 12917±3993; $p<0.01$; **Fig 6.8C**).

iv) PCNA only cell counts are different both between ipsilateral and contralateral dentates and between sacrifice times after a unilateral ICV kainate injection.
The number of PCNA only cells labelled is significantly greater overall in ipsilateral dentates than contralateral dentates in animals receiving an ICV kainate injection ($p<0.05$; two-way ANOVA; **Fig 6.8D**), although this change is not significantly different at any individual point (Bonferroni post tests). Changes in PCNA only numbers were also significant over time ($p<0.001$; two-way ANOVA), with both ipsilateral and contralateral increases from 6 hours (ipsi, 3017±655 cells, and contra, 3031±898 cells) to day 2 (ipsi, 16646±5745 cells; $p<0.05$, and contra, 9670±1431 cells; $p<0.001$) and in contralateral dentates from 6 hours to day 5 (contra, 8410±2695; $p<0.01$; **Fig 6.8D**).

v) Cells both expressing PCNA and incorporating BrdU do not differ between ipsilateral and contralateral dentates in animals that received a unilateral ICV kainate injection, but do change over time.

The number cells labelled with both PCNA and BrdU appears to be greater in ipsilateral dentates than contralateral dentates in kainate injected rats (**Fig 6.8E**). However, overall these differences are not significant ($p=0.10$; two-way ANOVA), and neither are Bonferroni post test comparisons between ipsilateral and contralateral dentates at each sacrifice time. Changes in the number of cells labelled for both PCNA and BrdU are significant over time ($p<0.001$; two-way ANOVA with repeated measures), with ipsilateral increases from 6 hours (2218±477 cells) to day 2 (6415±746 cells; $p<0.01$) and day 5 (5364±2361 cells; $p<0.05$; **Fig 6.8E**).

vi) The fractional contributions of BrdU pre-labelled cells to the total dividing cell population (BrdU+PCNA/ Total PCNA) in kainate-injected animals do not change between ipsilateral and contralateral dentates, but do differ over time.

There are no significant differences in the proportions of the total dividing population that are pre-labelled BrdU positive cells between ipsilateral and contralateral dentates in animals receiving unilateral ICV saline injections ($p=0.17$; two-way ANOVA), and Bonferroni post tests found no differences between ipsilateral and contralateral dentates at individual sacrifice points. A significant overall change in the proportions over time was observed ($p<0.001$; two-way ANOVA), this is due to a bilateral decrease in the proportion of BrdU labelled cells that continue to divide between 6 hours (ipsi, 0.429±0.129, and contra, 0.488±0.178) and 2 days (ipsi, 0.297±0.079, and contra, 0.333±0.156; both $p<0.05$). Additionally an ipsilateral decrease between 6 hours and day 5 (0.314±0.150; $p<0.05$; **Fig 6.8F**) was observed.

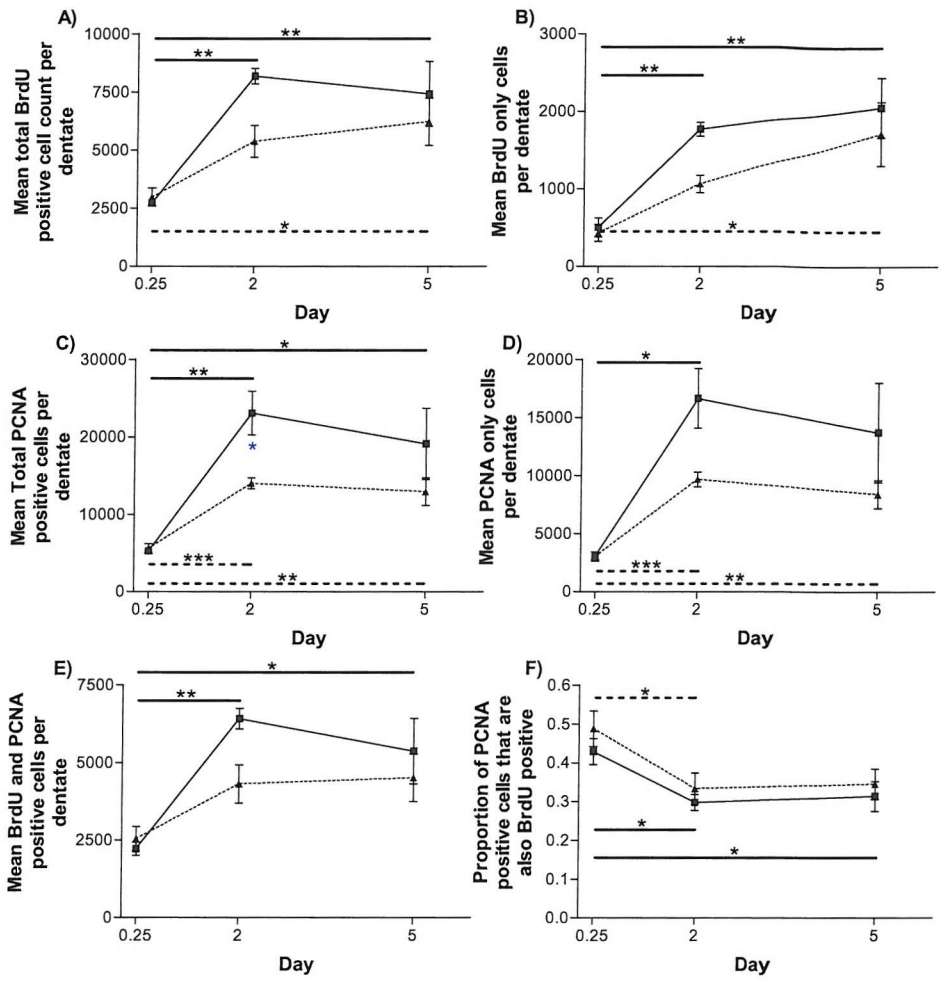

Fig 6.8: Profiles of proliferation in ipsilateral *(solid lines)* and contralateral *(dotted lines)* dentates of animals receiving unilateral i.c.v. kainate injections. Cell proliferation is investigated using two markers; pre-injection tagging of cells in the cell cycle with BrdU and identification of cells in the cells cycle at the time of sacrifice using PCNA. Different marker labelling combinations then represent different populations of cells, the total number of cells derived from pre-labelled cells **(A)** and the total number of cells dividing at sacrifice **(C)** can be sub divided into a population of pre-labelled cells that have ceased to divide **(B)**, a population of cells that were not dividing before the injection but are at sacrifice **(D)**, and a population of cells that were dividing before the injection and are dividing at sacrifice **(E)**. The fractional contribution of BrdU pre-labelled cells to the total population of cells in the cell cycle at sacrifice is also examined **(F)**. Values are expressed as mean ± SEM, and are taken from 5 animals with 3 sections systematically sampled from each animal and scaled by the inter section interval, except in **(F)**, where data is per section from 15 sections. Black *asterisks* denote significant differences within ipsilateral *(solid lines)* and contralateral *(dotted lines)* dentates determined by One-way ANOVA with Bonferroni post hoc test and **blue** *asterisks* denote significant differences between hemispheres determined by two-way ANOVA with Bonferroni post hoc test, (* $p<0.05$, ** $p<0.01$, *** $p<0.001$).

vii) Summary of proliferation in unilateral ICV kainate injected rats.

Unilateral injection of kainate induces significant changes in proliferation in the dentate ipsilateral to the injection compared with that in the contralateral dentate. While dentates from both hemispheres follow the same general trends, these are significantly more pronounced in the ipsilateral dentates. Kainate injection results in significant increases in both 'clonal' and point proliferation (total BrdU labelling, and total PCNA labelling respectively) over time, in both dentates, and the increases in BrdU only labelled cells also indicates an increase in post mitotic cells over time. Importantly, the actively dividing 'clonal' population (BrdU and PCNA labelled) is only significantly increased in the ipsilateral dentates.

6.3.3.3 Ipsilateral kainate vs. saline injection.

Using the same six parameters as in the previous sections, the direct results of kainate injection are compared to those of saline injection; to identify changes in cell proliferation that injection of a bolus of kainate induces but injection of a bolus of saline does not.

i) Total BrdU incorporation is greater in the ipsilateral dentates of animals receiving a unilateral ICV kainate injection than those receiving saline.

In the ipsilateral dentates the total number of BrdU positive cells overall was increased in animals receiving kainate injections ($p<0.001$; two-way ANOVA), with significant increases on day 2 (kainate, 8186±740 cells, vs. saline, 3298±143 cells; $p<0.001$), and day 5 (kainate, 7423±3117 cells, vs. saline, 4435±1021 cells; $p<0.01$) after ICV kainate compared with saline (**Fig 6.9A**).

ii) BrdU only cell counts are larger in the ipsilateral dentates of animals receiving a unilateral ICV kainate injection than in those receiving saline.

In the ipsilateral dentates the number of cells only positive for BrdU overall was increased in animals receiving kainate injections ($p<0.001$; two-way ANOVA), with significant increases on day 2 (kainate, 1771±195 cells, vs. saline, 763±175 cells;

$p<0.01$), and day 5 (kainate, 2059±863 cells, vs. saline, 950±176 cells; $p<0.01$) after ICV kainate compared with saline (**Fig 6.9B**).

iii) Total PCNA counts are greater in the ipsilateral dentates of animals receiving a unilateral ICV kainate injection than those receiving saline.

In the ipsilateral dentates the total number of PCNA positive cells overall was increased in animals receiving kainate injections ($p<0.001$; two-way ANOVA), with a significant increase on day 2 (kainate, 23062±6326 cells, vs. saline, 6379±1139 cells; $p<0.001$), after ICV kainate compared with saline (**Fig 6.9C**).

iv) PCNA only cell counts are larger in the ipsilateral dentates of animals receiving a unilateral ICV kainate injection than in those receiving saline.

In the ipsilateral dentates the number of cells only positive for PCNA overall was increased in animals receiving kainate injections ($p<0.01$; two-way ANOVA), with a significant increase on day 2 (kainate, 16646±5745 cells, vs. saline, 3845±1086 cells; $p<0.01$) after ICV kainate compared with saline (**Fig 6.9D**).

v) PCNA and BrdU co-labelling is greater in the ipsilateral dentates of animals receiving a unilateral ICV kainate injection than those receiving saline.

In the ipsilateral dentates the number of PCNA and BrdU double labelled cells overall was increased in animals receiving kainate injections ($p<0.001$; two-way ANOVA), with significant increases on day 2 (kainate, 6415±746 cells, vs. saline, 2534±195 cells; $p<0.001$), and day 5 (kainate, 5364±2361 cells, vs. saline, 3485±901 cells; $p<0.05$) after ICV kainate compared with saline (**Fig 6.9E**).

vi) The fractional contribution of BrdU pre-labelled cells to the total dividing cell population (BrdU+PCNA/ Total PCNA) is reduced on day 2 in ipsilateral dentates of animals receiving a unilateral ICV kainate injection compared with those receiving saline.

Overall, the proportions of the total dividing population that are pre-labelled BrdU positive cells are not different between ipsilateral dentates in animals receiving either

kainate or saline as a unilateral ICV injection ($p=0.11$; two-way ANOVA). However, on day 2 after surgery there is a significant decrease in the proportion in the dentates of kainate injected animals compared with animals that received saline injection (kainate, 0.297 ± 0.079, and saline, 0.424 ± 0.162; $p<0.05$; **Fig 6.9F**).

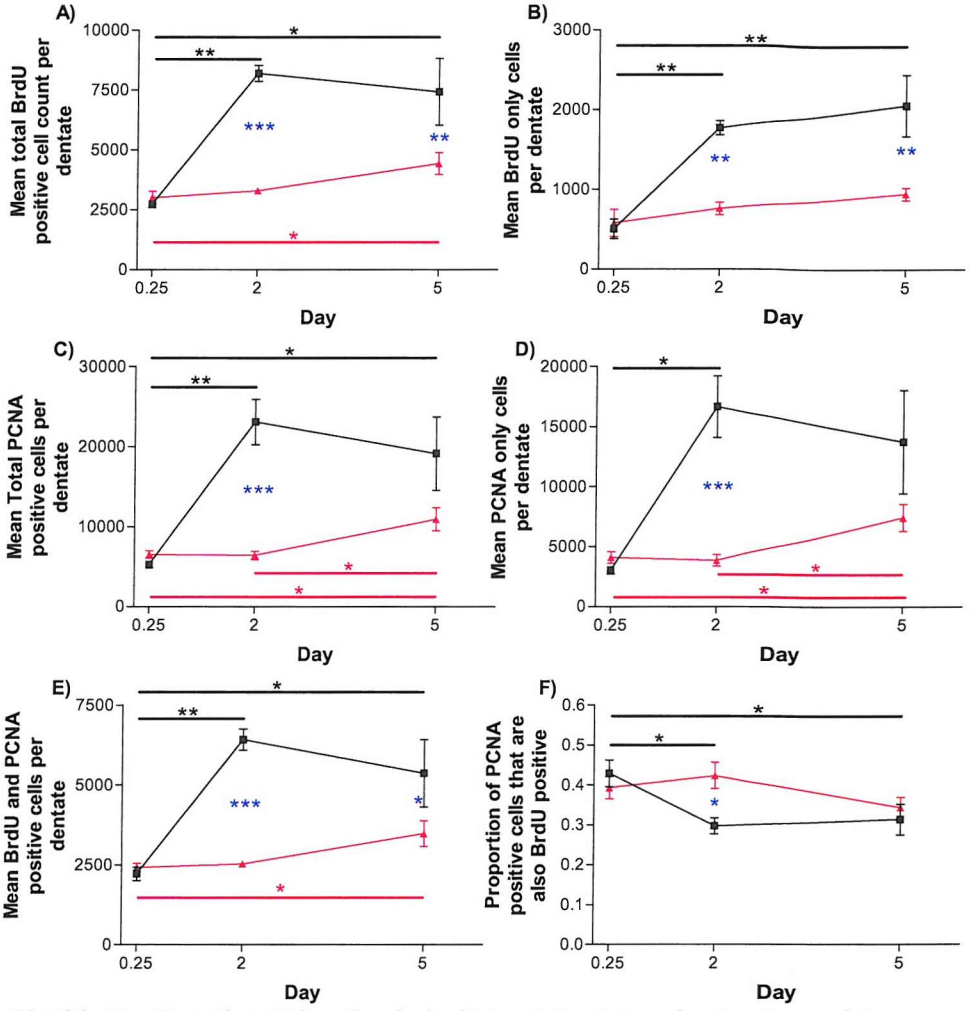

Fig 6.9: Profiles of proliferation in ipsilateral dentates of animals receiving unilateral i.c.v. kainate or saline injection. Cell proliferation is investigated using two markers; pre-injection tagging of cells in the cell cycle with BrdU and identification of cells in the cells cycle at the time of sacrifice using PCNA. Different marker labelling combinations then represent different populations of cells, the total number of cells derived from pre-labelled cells **(A)** and the total number of cells dividing at sacrifice **(C)** can be sub divided into a population of pre-labelled cells that have ceased to divide **(B)**, a population of cells that were not dividing before the injection but are at sacrifice **(D)**, and a population of cells that were dividing before the injection and are dividing at sacrifice **(E)**. The fractional contribution of BrdU pre-labelled cells to the total population of cells in the cell cycle at sacrifice is also examined **(F)**. Values are expressed as mean ± SEM, and are taken from 5 animals with 3 sections systematically sampled from each animal and scaled by the inter section interval, except in **(F)**, where data is per section from 15 sections. Black and red *asterisks* denote significant differences within kainate and saline dentates respectively determined by One-way ANOVA with Bonferroni post hoc test and **blue** *asterisks* denote significant differences between treatments determined by two-way ANOVA with Bonferroni post hoc test, (* $p<0.05$, ** $p<0.01$, *** $p<0.001$).

vii) Summary of proliferation in the ipsilateral dentates of unilateral ICV kainate and saline injected rats.

Kainate induces a significant increase in proliferation in the dentate ipsilateral to its injection, compared with saline injection, this increase occurs in both 'clonal' and point proliferation observations, and is time dependent. These increases all occur between 6 hours and 2 days after injection, and remain elevated until day 5 after injection, although this time is not statistically significant for the point proliferation data. The significant increase in BrdU only labelled cells indicates that kainate produces an increase in post-mitotic cells, which could correlate with increased neurogenesis. On day 2 after the injection the proportion of the point proliferation detected, which is due to proliferation of 'clonal' cells is significantly reduced in the animals that have received kainate.

6.3.3.4 Contralateral kainate vs. saline injection.

Using the same six parameters as in the previous sections, the contralateral results of kainate injection are compared to those of saline injection; to identify changes in cell proliferation that are induced contralaterally to a kainate injection but are not induced contralaterally to a saline injection.

i) Overall total BrdU incorporation is greater in the contralateral dentates of animals receiving a unilateral ICV kainate injection than those receiving saline.

In the contralateral dentates the total number BrdU positive cells detected overall was increased in animals receiving kainate injections ($p<0.001$; two-way ANOVA), however this is a general trend and was not reflected by significant increases at any of the individual times examined (**Fig 6.10A**).

ii) Overall BrdU only cell counts are greater in contralateral dentates of animals receiving a unilateral ICV kainate injection than those receiving saline.

In the contralateral dentates the number of cells only positive for BrdU overall was increased in animals receiving kainate injections ($p<0.001$; two-way ANOVA), however

this is a general trend and was not reflected by significant increases at any of the individual times examined (**Fig 6.10B**).

iii) Total PCNA incorporation is greater in the contralateral dentates of animals receiving a unilateral ICV kainate injection than those receiving saline.

In the contralateral dentates, the total number of PCNA positive cells detected overall was increased in animals receiving kainate injections ($p<0.001$; two-way ANOVA), with significant increases on day 2 (kainate, 13982±1575 cells, vs. saline, 7538±1540 cells; $p<0.001$), and day 5 (kainate, 12917±3993 cells, vs. saline, 9216±2115 cells; $p<0.05$) after ICV kainate compared with saline (**Fig 6.10C**).

iv) PCNA only cell counts are greater in contralateral dentates of animals receiving a unilateral ICV kainate injection than those receiving saline.

In the contralateral dentates the number of cells only positive for PCNA overall was increased in animals receiving kainate injections ($p<0.001$; two-way ANOVA), with a significant increase on day 2 (kainate, 9670±1431 cells, vs. saline, 4342±1412 cells; $p<0.001$) after ICV kainate compared with saline (**Fig 6.10D**).

v) PCNA and BrdU co-localization is unchanged in the contralateral dentates of animals receiving a unilateral ICV kainate and saline injections.

In the contralateral dentates the number PCNA and BrdU double-labelled cells detected was not significantly different between animals that received either saline or kainate as an ICV injection ($p=0.051$; two-way ANOVA), although there was a trend for increased PCNA and BrdU labelling in kainate injected animals (**Fig 6.10E**).

vi) The fractional contributions of BrdU pre-labelled cells to the total dividing cell population (BrdU+PCNA/ Total PCNA) are unchanged in the contralateral dentates of animals receiving a unilateral ICV injection of kainate or saline.

Overall, the proportions of the total dividing population that are pre-labelled BrdU positive cells are not different between contralateral dentates in animals receiving either kainate or saline as a unilateral ICV injection are not different($p=0.85$; two-way

ANOVA), and Bonferroni post tests reveal no differences at any of the sacrifice times (**Fig 6.10F**). However, the general profile appears to follow that of the ipsilateral dentates, with a fall in the fraction of the total dividing cell population that is derived from clonal proliferation decreasing on day 2 in the kainate treated animals (**Fig 6.9F**).

vii) Summary of proliferation in the contralateral dentates of unilateral ICV kainate and saline injected rats.

Kainate induces a significant increase in point proliferation in the contralateral dentate between 6 hours and 2 days after injection, compared with a saline injection, point proliferation then remains elevated until at least 5 days after the injection. By contrast, while there is a trend for increased 'clonal' proliferation in contralateral dentates of animals receiving kainate injection this trend is not statistically significant when compared with saline injected controls. Thus, existing proliferating cells may not be responsible for the increases in cell division observed in contralateral dentates after kainate.

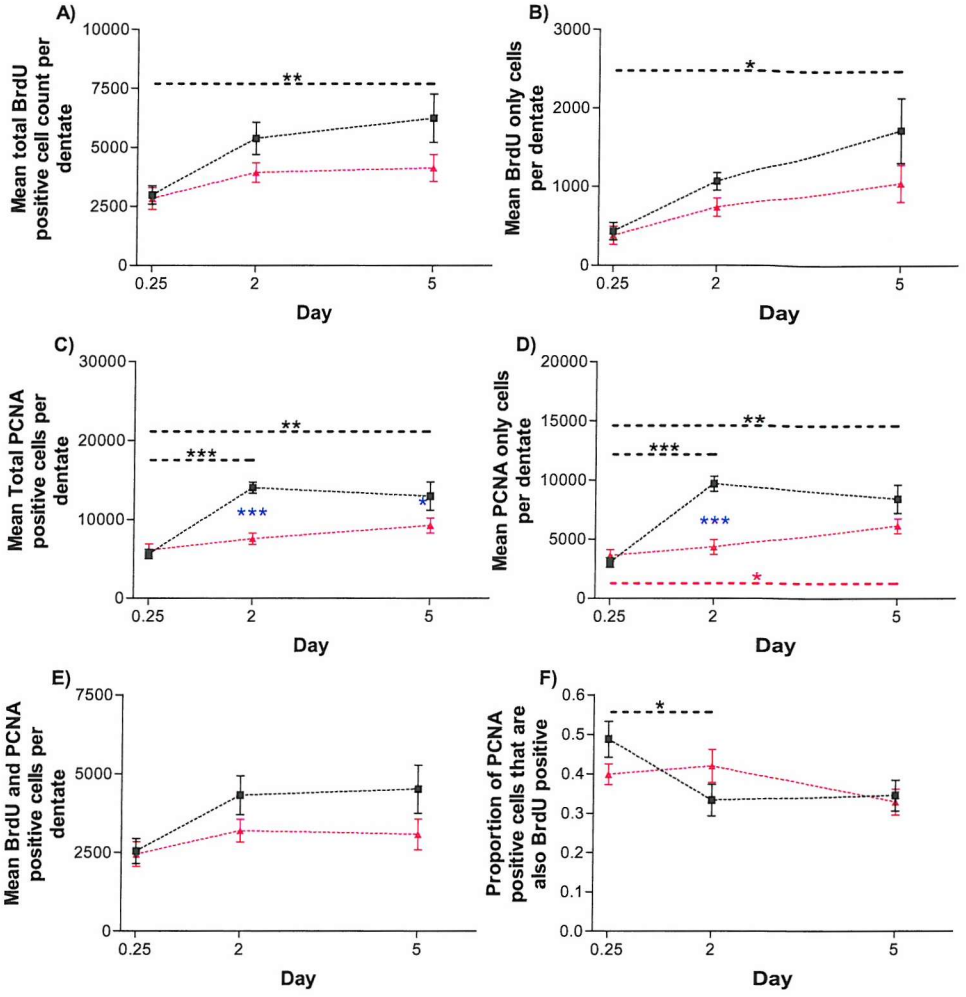

Fig 6.10: Profiles of proliferation in dentates contralateral to i.c.v. kainate or saline injection. Cell proliferation is investigated using two markers; pre-injection tagging of cells in the cell cycle with BrdU and identification of cells in the cells cycle at the time of sacrifice using PCNA. Different marker labelling combinations then represent different populations of cells, the total number of cells derived from pre-labelled cells **(A)** and the total number of cells dividing at sacrifice **(C)** can be sub divided into a population of pre-labelled cells that have ceased to divide **(B)**, a population of cells that were not dividing before the injection but are at sacrifice **(D)**, and a population of cells that were dividing before the injection and are dividing at sacrifice **(E)**. The fractional contribution of BrdU pre-labelled cells to the total population of cells in the cell cycle at sacrifice is also examined **(F)**. Values are expressed as mean ± SEM, and are taken from 5 animals with 3 sections systematically sampled from each animal and scaled by the inter section interval, except in **(F)**, where data is per section from 15 sections. Black and red *asterisks* denote significant differences within kainate and saline dentates respectively determined by One-way ANOVA with Bonferroni post hoc test and **blue** *asterisks* denote significant differences between treatments determined by two-way ANOVA with Bonferroni post hoc test, (* $p<0.05$, ** $p<0.01$, *** $p<0.001$).

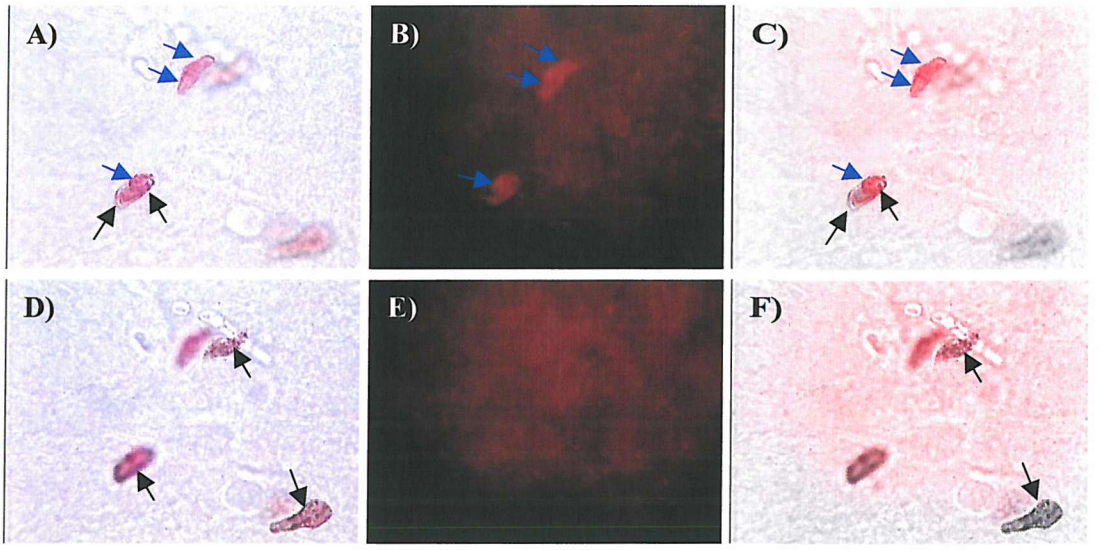

Fig 6.11: High magnification images of BrdU and PCNA labelling. Transmission images in two different focal planes (**A+D**) show BrdU positive cells (Black) and PCNA positive cells (Red). PCNA cells are visualised using fast red, which fluoresces and can be used to clearly identify PCNA positive cells (**B+E**). A composite of the transmission and fluorescence images illustrates cells co-localising both BrdU and PCNA (**C+F**). Arrows indicate cells in the focal plane of the image, stained for BrdU (Black) or PCNA (Blue).

6.3.4 Fluoro-Jade B measurement of cell death

Cell death is a well-documented consequence of kainate-induced seizures; within the hippocampal formation it is generally reported as being localised in the CA3 pryamidal neurons, however some reports identified cell death in the dentate, and the work in the previous chapter identified an early phase of cell death in the granule cell layer of organotypic cultures. Additionally, research has suggested that cell proliferation may be driven by cell death, possibly of progenitor cells, the clonal proliferation paradigm is ideally suited to further investigate a potential correlation between proliferation and cell death should be examined.

i) Cell death was not detected by Fluoro-Jade B staining in the contralateral dentates of either treatment group.

Fluoro-Jade B (FJB) staining above background was not detected ipsilateral to an ICV saline injection and was also absent in all contralateral dentates examined. Analysis of

ipsilateral denates after saline injection is included to permit comparison with dentates ipsilateral to a kainate injection, in which some FJB staining was present (**Fig 6.13**).

ii) Kainate induces significantly increased granule cell death in the dentate gyrus ipsilateral to its injection, compared to a saline injection.

In ipsilateral dentates, the measured percentage of the total granule cell layer staining for FJB is significantly greater in kainate injected animals on day 2 (4.24±6.97% staining) and day 9 (4.28±4.55% staining), than in saline injected animals (day 2, 0.06±0.04% staining, and day 9, 0.09±0.07% staining; both $p<0.05$, Kruskal-Wallis test with Dunn's post test). Cell death at 6 hours followed a similar pattern, but failed to reach statistical significance (kainate, 3.33±7.23% staining, and saline, 0.12±0.12% staining; **Fig 6.12A**). However, FJB staining is not a consistent feature in all animals exposed to kainate, with only 6 of the 16 kainate treated animals examined having FJB staining greater than 2.5% of the GCL (**Fig 6.12B**).

iii) No correlation between Fluoro-Jade B staining and BrdU positive cell counts was observed in the ipsilateral dentates of animals receiving a unilateral ICV injection of kainate or saline.

In dentates ipsilateral to a saline injection cell death determined by FJB does not correlate linearly with clonal cell proliferation at 6 hours ($r=0.2$, $p=0.92$; Spearman's rank correlation), 2 days ($r=-0.3$, $p=0.68$; Spearman's rank correlation) or 9 days ($r=0.1$, $p=0.95$; Spearman's rank correlation) after the injection (**Fig 6.12B**). Similarly, after kainate injection there is no correlation between FJB staining and BrdU labelling at 6 hours ($r=0.1$, $p=0.95$; Spearman's rank correlation), 2 days ($r=0.15$, $p=0.78$; Spearman's rank correlation) or 9 days ($r=0.26$, $p=0.69$; Spearman's rank correlation; **Fig 6.12B**).

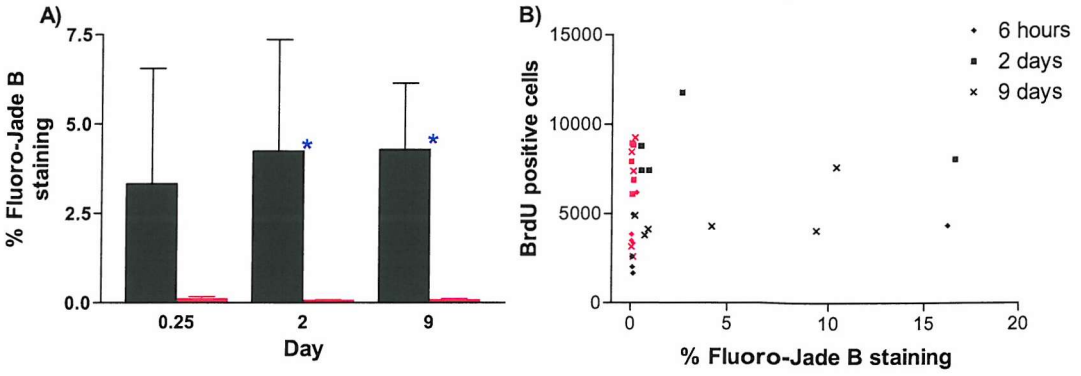

Fig 6.12: Fluoro-Jade B expression in ipsilateral dentates of animals receiving unilateral i.c.v. injections of either saline or kainate. Showing the area of Fluoro-Jade B staining as a percentage of the total granule cell layer area, measured by DAPI staining **(A).** Values are expressed as mean ± SEM, taken from 4-6 animals per treatment with 6 sections systematically sampled from each animal. *Asterisks* denote significant differences within groups over time determined by Kruskal-Wallis test with Dunn's post hoc test (* $p<0.05$). The distribution of Fluoro-Jade B cell death is compared with 'clonal' BrdU labelling **(B)**, in ipsilateral dentates from both saline and kainate injected animals.

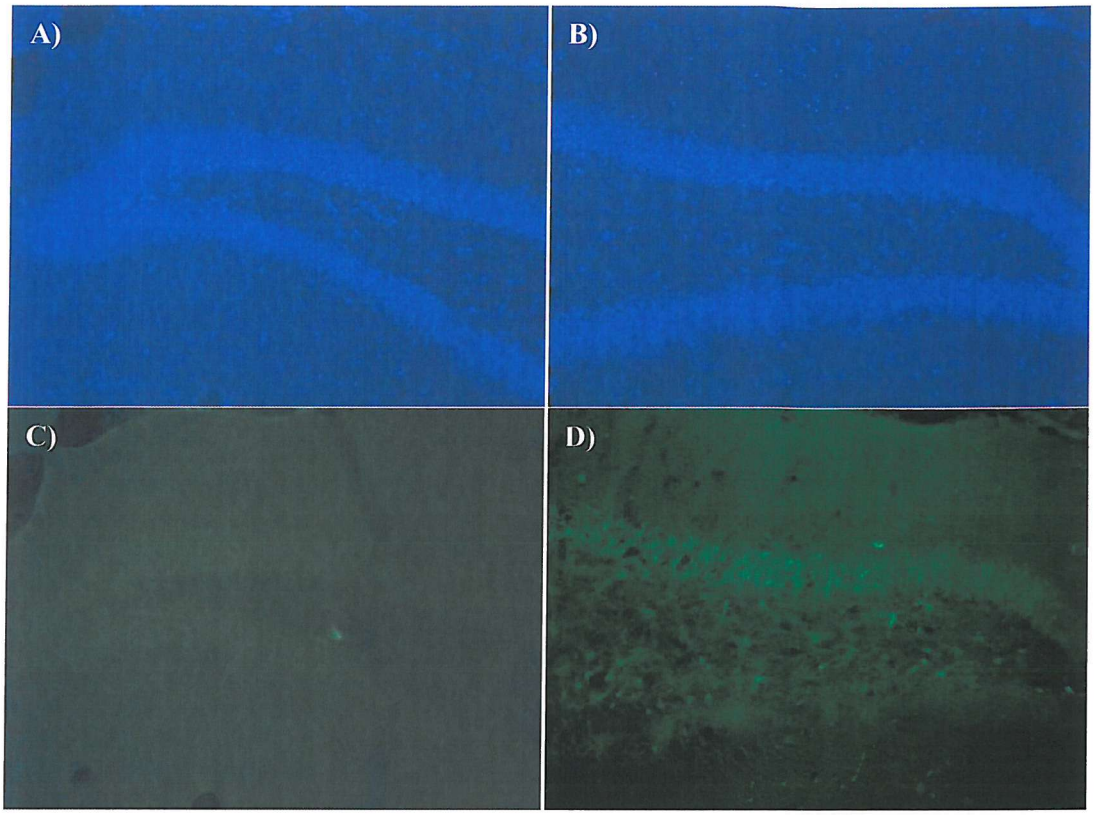

Fig 6.13: DAPI and Fluro-Jade B (FJB) staining ipsilateral to saline or kainate injection. Showing a dentate ipsilateral to an ICV saline injection **(A+C)** or ICV kainate injection **(B+D)**. The granule cell layer is identified with DAPI staining **(A+B)**, and cell death is identified with FJB staining **(C+D).** The distribution of cell death appears to be throughout the entire GCL and not restricted to the SGZ.

6.4 Discussion

6.4.1 Ipsilateral and contralateral dentates in the saline injected animals

No differences were observed in any of the parameters considered between ipsilateral and contralateral dentates in animals receiving an ICV saline injection. This indicates that injection of a bolus of liquid does not have an effect on overall proliferation (PCNA labelling), clonal proliferation (BrdU labelling), neurogenesis (Dcx labelling), or cell death (FJB staining), compared with the opposite hippocampus, which does not receive an injection. Alternatively, the surgery and injection may produce an effect, but this effect is bilateral, and independent of the injection side.

6.4.2 Basal cell proliferation and neurogenesis in saline injected 'control' animals

Significant increases in Total PCNA cell counts and PCNA only cell counts between 6 hours and day 5 were observed, and these results are surprising, because in a control population cell division is expected to be constant over time. The significant increase in total PCNA occurs only in the ipsilateral dentate and thus might be considered to be as a direct consequence of the injected saline, however the trend is followed in the contralateral dentate, and significant increases are seen in both dentates when proliferation of cells that were not dividing prior to the surgery (PCNA only) are considered (**Fig 6.7A**). This would suggest that the trauma related to the surgery might have an effect on basal levels of proliferation. Studies have shown that both chronic and, importantly, acute stress decrease neurogenesis (Gould, Tanapat et al., 1998; McEwen, 1999); the handling and injury related to surgery in all these experiments are likely to result in some acute stress and thus could cause a short term decrease in proliferation, which is beginning to recover by 24 hours. This conclusion is further supported by two-way ANOVA analysis of immature neuron numbers identified by Dcx staining, which identified a bilateral trend for decreased neurogenesis between day 2, and day 7 (**Fig 6.4A**), although no individual significant differences were detected. These two points might be considered contradictory, however it will take some time for a change in proliferation to be reflected as a change in neurogenesis. In mice, Dcx is expressed in immature neurons for 7-10 days (Kempermann, Gast et al., 2003), and so a small change

on one day to the number of cells added to this large population of immature neurons is unlikely to be detected. Thus, a decrease in basal proliferation at 6 hours will not correlate with an instant decrease in Dcx labelling. However, a sustained decrease in proliferation over a number of days will begin to be reflected by a reduction in the number of Dcx positive cells observed. Similarly, there will be a lag between recovery of basal levels of proliferation and recovery of basal levels of Dcx expression. Examination of PCNA and Dcx labelling in un-operated animals could identify basal levels of proliferation and neurogenesis before surgery and thus clarify this point. However, further evidence supporting this hypothesis comes from PCNA and Dcx counts in ipsilateral dentates of animals injected with kainate where Dcx increases lag behind PCNA increases (**Fig 6.4 and Fig 6.8**), which are discussed in more detail below.

6.4.3 Pre-labelled 'clonal' modelling of proliferation in saline injected animals

In early work investigating cell division using BrdU as a marker Nowakowski used an assumption that the cell division followed a steady-state model (Nowakowski, Lewin et al., 1989). In this steady-state model a series of asymmetric cell divisions by a stem cell occurs, each division generates a new 'post-mitotic cell' and regenerates the stem cell; the number of post mitotic cells increases at a rate of 1 per cell cycle while the number of dividing cells remains constant (**Fig 6.14A**). Subsequent experiments have lead to a partial redefining of this model, with the realisation that other paradigms of division can produce an increase in cell numbers that on average follows the original steady state model. For example: a combination of asymmetric divisions, regenerative symmetric divisions (producing 2 stem cells) and terminal symmetric divisions (producing 2 post-mitotic cells) if occurring in the ratio 2:1:1 generates an average of one new 'post mitotic' cell per cell division (Nowakowski and Hayes, 2001), and a regenerative cell division combined with a terminal cell division produces the same profile (**Fig 6.14B-G**).

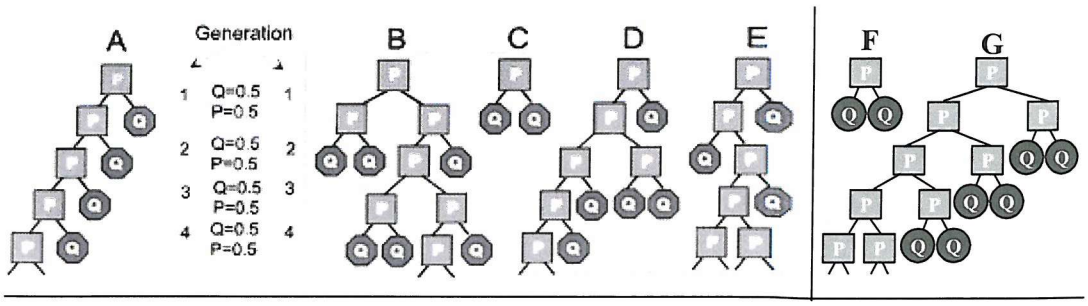

Fig 6.14: Three populations undergoing steady-state growth. At every cell cycle, all have a constant number of proliferative cells (P) and produce the same number of post-proliferative cells (Q), i.e. at each generation P = Q = 0.5. In the population on the left, all cells have the same lineage in which each proliferating cell divides asymmetrically. In the population in the middle, the lineages vary. Here an initial population of four cells (B–E) beget daughters and granddaughters that are assigned a P/Q fate randomly. If the overall population is a mixture (1:2:1) of all three possible types of cell division, then the number of proliferating cells and the output of this population are the same as that shown in A at every generation. In the population on the right an initial population of two cells (F and G) divide symmetrically with two possible types of fate (both P or both Q). If the chance of each division fate is equal then the number of proliferating cells and the output of this population are the same as that shown in A at every generation. Adapted from Nowakowski & Hayes (2001).

In our experiments, the number of pre-labelled cells that continue to divide after the saline injection are unchanged overtime, while pre-labelled cells that have exited the cell cycle (BrdU only) increase steadily (**Fig 6.7B+E**). This profile fits the steady-state model described above. However, it cannot be the only process occurring, as the rate of increase in labelled cell numbers is not equivalent to 1 new cell per cell cycle. Between 6 hours and day 5 the number of BrdU only cells undergoes at most a 2.75 fold increase (**Fig 6.7B**), however with a cell cycle time of about 25 hours (Cameron and McKay, 2001), after about 4 cell cycles a 4 fold increase would be anticipated. A more detailed study of proliferation in the dentates of two strains of mice, in which numbers of proliferating cells differed significantly, found that throughout the 10 days after BrdU labelling cells were lost at a rate of about 0.4% of cells per hour (Hayes and Nowakowski, 2002). In our experiment in the 114 hours between 6 hours and day 5, this is equivalent to a drop of approximately 45%, if these dying cells are added to the count at 5 days then a 4 fold increase occurs between 6 hours and 5 days (saline contra, 6 hours 382 cells and 5 days 1524 cells (1051 + 473)). Another study has examined the loss of BrdU labelled cells in rats, they found a 29% drop in labelled cells between day 6 and day 16 (equivalent to 0.12% of cells per hour), and a 28% drop between day 16 and day 28 (0.10% of cells per hour) (Dayer, Ford et al., 2003). Although the work of Dayer et al.

does not consider cell death in the early phase of BrdU labelling, between 24 hours and 6 days after BrdU injection, where our experiments reside, their work suggests the rate of cell death is lower in rats than in mice, and probably accounts for about a 15% drop in detected cells. The rest of the disparity between observed and expected numbers of BrdU labelled cells is probably due to dilution, which is discussed in detail below. The above results demonstrate that the assumption of some BrdU loss over time through cell death is reasonable; and therefore our data from saline injected animals present a good fit to a steady-state model of proliferation.

6.4.4 Effect of dilution on the persistence of BrdU in dividing cell populations

The study of Hayes et al. identified and quantified many of the factors influencing detection of proliferating cells using BrdU, including the cell loss through death discussed above. Their work also identified the average number of divisions that a cell could undergo before the BrdU contained within the nucleus became diluted beyond their ability to detect it. This is especially useful for our analysis as the methods used in the two experiments are very similar. Hayes applied a series of IP BrdU injections at intervals of 4 hours for either 12 or 24 hours and then sacrificed the animals at different times (ranging from 4.5 hours to 240 hours after first BrdU injection) and quantified BrdU labelling at each time (**Fig 6.15**). Their results demonstrated a linear increase in BrdU labelling for approximately 48 hours (3 cell cycles in the mouse), as labelled cells divided maintaining their numbers and producing BrdU labelled 'post mitotic' cells. Dilution of BrdU was determined to have occurred shortly after this point as the number of BrdU labelled cells fell slightly. This occurred because the proliferating cells divide and the BrdU in the daughter cells falls below detection levels producing two undetectable cells. The BrdU labelled 'post mitotic' cells are unaffected by dilution because they are not dividing and these cells continue to be detected.

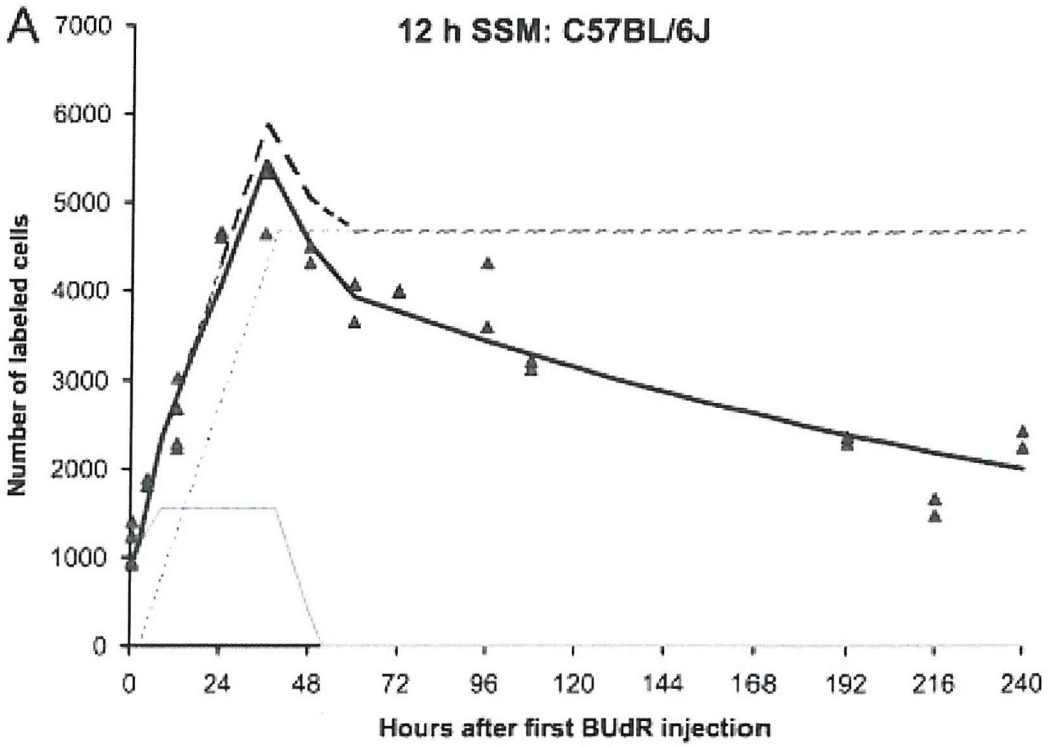

Fig 6.15: Interpretation of a saturation labelling BrdU curve. (A) A mathematical model of the behavior of the proliferating population in the adult dentate gyrus was based on the assumption of steady-state dynamics, a T_s value measured independently, and a least-squares fit to the data collected from a 12 h saturation paradigm in C57BL/6J. Labeling of the proliferating population (P; gray line) is complete in less than 12 h after the first BUdR injection; the number of labeled P cells remains constant until the dilution detection limit (DDL) is reached, after which it drops rapidly to 0. The number of labeled post-mitotic cells (Q) produced (dotted line) rises linearly to a peak approximately coincident with the DDL, after which, in the absence of cell death, that number would remain constant. Thus, in the absence of any cell death, the expected number of labeled cells at any point (dashed line) is equal to the sum of P and Q. Any deviation of the curve fit to the data (heavy black line) from the expected number of labeled cells (dashed line) is most likely attributable to cell death in the newly produced cells. Values for the total number of proliferating cells, T_c, T_s, and the incidence of cell death per unit time can be calculated from the curve. Adapted from Hayes And Nowakowski (2002).

The results we obtained from the dentates of saline injected animals appear to fit this model fairly well (**Fig 6.1A**), with a peak in BrdU labelling and subsequent dilution probably beginning between day 3 and day 6 (in the region of 3-4 cell cycles with a cell cycle time of 25 hours (Cameron and McKay, 2001)). The labelling then fits the slow

loss of BrdU labelled cells discussed above, from day 6 through to day 10 (all time points correspond to one day earlier in the results section as graph timescales start from day 0 being surgery and BrdU was administered from 24 hours prior to surgery). However, one result from our experiments would tend to disagree with this model, cells expressing both BrdU and PCNA at 6 days suggest that complete dilution of BrdU in dividing cells has not occurred by this point. In fact, the number of cells that are BrdU and PCNA positive is unchanged over the 5 days examined, suggesting no dilution is occurring at all. There are at least two possible reasons for this. PCNA could be expressed for a short time in cells that have exited the cell cycle this would lead to overestimation of the number of pre-labelled cells that continue to divide and an apparently delayed point of BrdU dilution. A threefold difference between PCNA and BrdU labelled cells is predicted from the ratio of PCNA expression time (the whole cell cycle ~25 hours) to BrdU labelling time (the S-phase ~8 hours) in a dividing cell. In the saline experiments the number of PCNA positive cells is only approximately 2-3 times greater than the number of BrdU labelled cells, indicating extended PCNA labelling after cells have entered G_0 is unlikely. Alternatively, the population of dividing cells could be more complicated than the steady-state model. Work from Alverz-Bullya's group have identified a mechanism for neurogenesis in the subventricular zone (SVZ) involving 3 different types of proliferating cells, where a slowly dividing stem cell population (B cells), are combined with a rapidly dividing progenitor population (C cells) and a migratory restricted neuroblast population (A cells) (Doetsch, Caille et al., 1999; Doetsch, Petreanu et al., 2002). They have also proposed a similar model in the sub-granular zone (SGZ) of the dentate gyrus, this model has only two different types of dividing cell, possibly reflecting the reduced length of migration following neurogenesis in the dentate, the slowly dividing B cells remain and a second rapidly dividing progenitor population (D cells). C and D cells in the two models are probably similar, however they differ in appearance and mitotic activity; C cells are large and can undergo many rapid divisions, D cells are small and divide less frequently (Seri, Garcia-Verdugo et al., 2001).

A model with two different proliferating cell populations, with different cell cycle times, could result in an extended period of BrdU and PCNA co-labelling, whilst retaining the steady-state proliferation and BrdU dilution features demonstrated by Nowakowski. The

slowly dividing (B cells) population will become diluted below detection levels more slowly than the rapidly dividing (D cells; **Fig 6.16**). For example, if the cell cycle time for B cells is twice (48 hrs) that of D cells (24 hours) then some dividing cells would continue to be labelled until for 144 hours (6 days), assuming 3 cell cycles before dilution. This compares with dilution of a purely D cell population at 72 hours, and if the B cell cycle is longer, the time before dilution could be further extended.

Using this hypothesis for cell division, the actual number of BrdU and PCNA positive cells detected from a single pulse of BrdU would change over time, which our data did not appear to do (**Fig 6.7A**). However, it does overcome the fundamental problem of BrdU and PCNA double labelling after BrdU dilution should have occurred.

Nowakowski et al. considered the possibility of two dividing populations in some of their early work and concluded that the "fit to the equations of a two population model was not significantly better" than a single population (Nowakowski, Lewin et al., 1989). Thus, their work does not exclude the possibility of more than one cell cycle length. Additionally, when comparing one and two population models Nowakowski et al. assumed both cell cycle time and S-phase duration were altered. However, there is no evidence to suggest that S-phase is changed when cell cycle length alters, in fact S-phase remains unchanged in the dentates of immature and adult rats, when cell cycle time increases (Lewis, 1978; Cameron and McKay, 2001). S-phase is where the genome is replicated and the length of the genome remains the same within a species, it is reasonable to assume that the time taken to complete replication is unlikely to change, unless enzyme activity is specifically hindered, for example by altering body temperature.

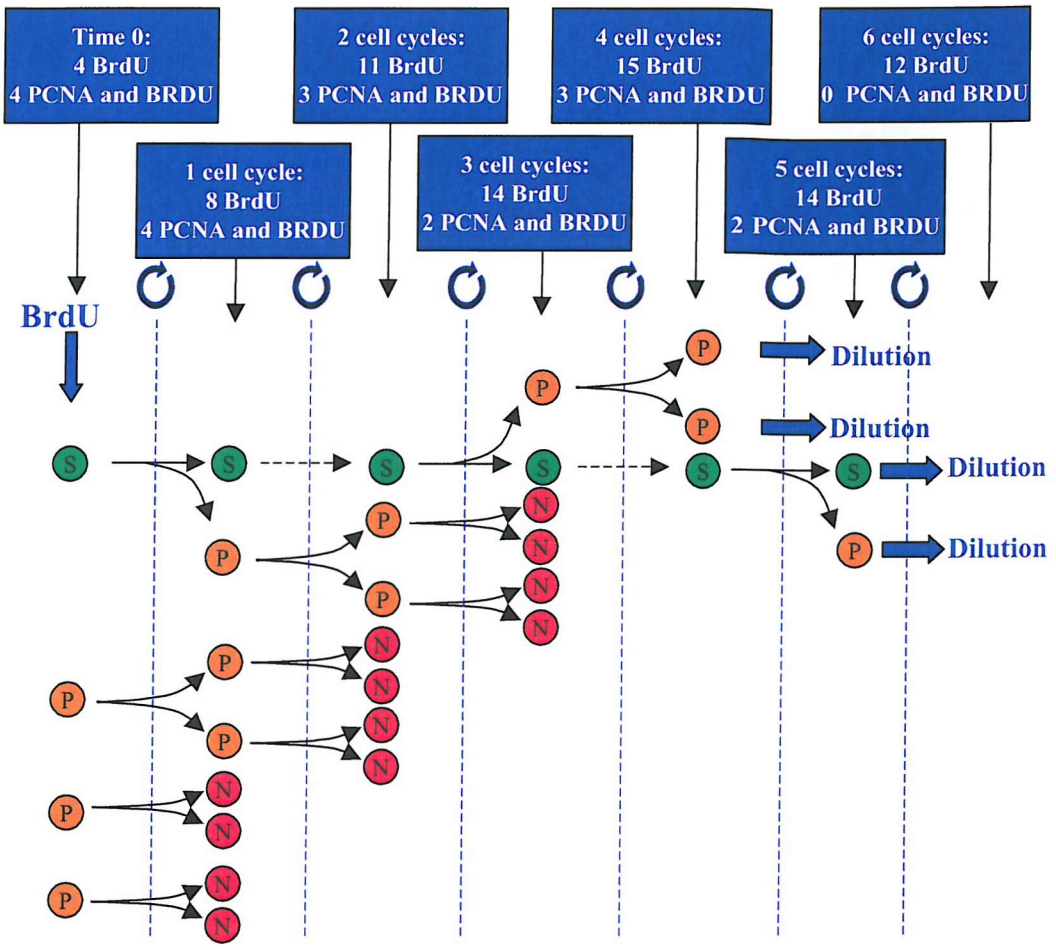

Fig 6.16: BrdU and PCNA expression in a model with two populations of dividing cell. Steady state model proliferation occurs over time however BrdU labelling follows an approximately steady-state profile for about 3 cell cycles. A more complex profile can produce steady state proliferation until after the first 3 cell cycles when dilution occurs. Stem cell (S) a symmetric division every other cell cycle, with the resultant progenitor cell (P) dividing symmetrically to form 2 progenitor cells, which both subsequently symmetrically divide to produce neurons (N). Cell cycle is based on progenitor cell cycle time, stem cell cycle time is twice as long as progenitor cell cycle time. If stem cells have the same cell cycle time as progenitor cells but rest in G_0 for one cell cycle between successive divisions then BrdU and PCNA co-labelling would be 3 after 1 cell cycle and 1 after 3 and 5 cell cycles.

6.4.5 Distribution of BrdU positive cells and proliferation models.

Long term (up to 11months) persistence of BrdU labelling has been described (Kempermann, Gast et al., 2003), at this time the labelling only detects single cells. This

is in stark contrast to shortly (24 hours) after BrdU administration where in addition to single BrdU labelled cells, groups of BrdU labelled cells are present (in clusters containing from 2 cells to ~12 cells; Fig 6.3). Many of the cells in the large clusters are dividing cells that disappear through dilution after a short time, however migration of the cells has also been documented (Kuhn, Dickinson-Anson et al., 1996), typically cells generated in the SGZ migrate a distance of 50-100μm, this migration takes place in less than 7 days (Kempermann, Gast et al., 2003). Seki considered the number of cells in a cluster 1, 3, and 7 days after a single BrdU injection. He found the proportion of single cells increased during the experiment, the proportion of pairs of cells did not change significantly (although the trend was for a decrease) and the proportion of cells in clusters of 3 or more fell significantly (Seki, 2002). However, importantly large clusters of cells still exist 7 days after the BrdU pulse, this can be interpreted as further evidence for a model of proliferation using two dividing cell populations with different cell cycle times. By 7 days, migration has separated post mitotic neurons and BrdU label dilution has rendered rapidly dividing cells undetectable, therefore large clusters are presumably derived from the slowly dividing cells.

Our experiments produced similar results, with average cluster sizes of approximately 3.5-4 cells per cluster at the early points, and then falling to an average size of almost 2 cells per cluster on days 6, 8, and 10 after BrdU addition (**Fig 6.2**, days 5, 7, and 9 after surgery). If the slowly dividing cells were not present, the average cluster size would be closer to 1 since post mitotic cells have migrated apart.

6.4.6 Disparity in BrdU labelling between immuno-labelling protocols

Immunostaining of saline injected control tissue for BrdU is different on day 2 after saline injection, when BrdU was single labelled (**Fig 6.1A**), and when BrdU and PCNA were double-labelled (**Fig 6.7A**). There are two possible explanations for this difference; the antigen retrieval process is different between the two staining processes, and the sampling of the sections is different. Although the double-labelling staining protocol was developed to maximise staining, by finding optimal microwave and acid treatment times and by using an amplification step (the avidin-biotin complex) in the secondary labelling rather than using direct application of a fluorescent secondary antibody, it is possible that

the additional microwave treatment step decreases detection of BrdU. A corresponding reduction in BrdU labelling was observed between the two immunohistochemical protocols in kainate injected animals, although this effect was smaller (**Fig 6.1B and Fig 6.8A**). The smaller decrease observed in kainate-injected animals may be related to the sampling techniques used. In the single labelling run 6 sections were sampled, throughout the entire extent of the hippocampus, the double labelling protocol used only 3 sections, again sampled evenly throughout the whole hippocampus, however these sections correspond to a slightly more ventral distribution of sections than was obtained for the single labelling immunostaining. Differential levels of lesion have been reported between dorsal and ventral parts of the hippocampus after unilateral ICV kainate injection (Nadler, Perry et al., 1978), and a similar phenomenon could be obtained with the increased proliferation. Further support for this explanation comes from the work described in chapter 3, which described variation in cell proliferation along the septo-temporal axis in postnatal day 5 cultures.

6.4.7 Kainate induces changes in the dentate gryus

The results discussed thus far, obtained from saline injected animals are broadly similar ipsilateral and contralateral to the injection site. Our results identified four major differences in the ipsilateral dentates of animals receiving kainate injections when compared to saline injected controls. These are, increased point cell proliferation, identified by PCNA labelling, increased 'clonal' proliferation identified from BrdU pre-labelling, increased neurogenesis, identified by Dcx immunostaining, and induction of cell death identified by FJB staining.

6.4.8 Increased point cell proliferation induced by kainate, ipsilateral to its injection.

Currently, the most comprehensive study of point cell proliferation after seizures is by Nakagawa et al., they used a single IP injection of BrdU, 3 hours before sacrifice 1, 3, 5, 7, 10 and 13 days after an IP kainate injection had induced seizures. They found elevated proliferation on days 3, 5, and 7 (Nakagawa, Aimi et al., 2000). An earlier study of Parent et al. found similar results, however this work is not truly a study of point proliferation. They used a series of 4 IP BrdU injections at 2 hour intervals, given either

1, 3, 6, 13 or 27 days after IP pilocarpine injection had induced seizures, animals were sacrificed 24 hours after BrdU administration (with the exception of 1 day animals, which were sacrificed 1-4 hours after final BrdU injection). This method identified that the area of BrdU immunostaining increased as a percentage of the total GCL and SGZ area after 3 days and remained significantly elevated until day 13, with increased numbers of cells proliferating implicit in these observations (Parent, Yu et al., 1997). We could not use a short pulse of BrdU, administered shortly before sacrifice, to identify point proliferation because our experiment had already used an early pulse of BrdU to label a population of dividing cells so that their survival and that of their clones could be followed. We therefore used PCNA, as a marker of point proliferation. PCNA is detected in all cells in the cell cycle and so will detect more cells than BrdU (which only labels S-phase cells) when used as a point proliferation marker. The increases in PCNA labelling on day 2 and day 5 after kainate injection observed in these experiments agree with the observations of others that after seizures point proliferation is significantly increased (Parent, Yu et al., 1997; Nakagawa, Aimi et al., 2000). Our results also narrow down the window for this increase, as neither of the above studies examined proliferation on day 2 after seizure induction.

6.4.9 'Clonal' cell proliferation increases are not the sole cause of the point cell proliferation increases induced by kainate, ipsilateral to its injection.

The point proliferation experiments have clearly demonstrated that cell proliferation in the SGZ is altered by seizures, and the temporal profile for these changes is now well documented. However, the mechanisms through which these changes occur have yet to be elucidated. In order to follow the fates of a limited number of dividing cells and their progeny as they progressed through the consequences of seizure induction we used a 'clonal' BrdU labelling protocol. This technique has recently been described in un-injured animals (Hayes and Nowakowski, 2002), and the results obtained correlated well with our saline injected control results (**Fig 6.1**). After kainate the same 'clonally' labelled cells divide, producing significantly increased cell counts 2 days after seizures compared with saline injected controls (**Fig 6.1 and Fig 6.9A**). The normally dividing cell population therefore, as might be expected, responds to the kainate, contributing

significantly to the observed point increases in proliferation. However, the increase in total proliferation (total PCNA) at 2 days after seizure is significantly greater than the increase in active 'clonal' proliferation at the same time (BrdU and PCNA; **Fig 6.7E**). Only about 30% of the proliferation on day 2 in dentates ipsilateral to a kainate injection is derived from the pre-labelled population, significantly less than the 42% of proliferation in saline injected controls at the same time. This suggests that another cell population is responding to kainate injection by dividing. To demonstrate this however the possibility of other confounding factors such as BrdU label dilution need to be ruled out.

6.4.10 Kainate alters the length of cell cycle in BrdU labelled 'clonal' cells, and alters the model of proliferation that best describes their proliferation profile.

Although exact changes in the cell cycle length cannot be measured directly in these experiments, it is possible infer differences from changes in the different BrdU positive populations. Since both the BrdU only cell count and the BrdU + PCNA cell count are significantly increased it is likely that the cell cycle time is shortened by the addition of kainate. The overall increase in the total BrdU positive population could probably be achieved if kainate caused a switch to exponential cell division, with all daughter cells remaining in the cell cycle. However, this would produce no new BrdU only 'post-mitotic' cells, and a significant increase in this cell population is observed. A decrease in the cell cycle time from the reported 25 hours in 10 week old rats (Cameron and McKay, 2001) to the shortest reported time (16 hours at 2-3 weeks) (Lewis, 1978) is sufficient to permit completion of an additional cell cycle between the 6 hour and 2 days points examined. This would permit the generation of additional BrdU only labelled cells. However a partial move away from the steady state profile of proliferation must also occur. If the steady state profile was retained and the cell cycle time decreased an increase in both total BrdU and BrdU only labelling would occur, but BrdU and PCNA counts would remain unchanged until dilution occurred (**Fig 6.16**). The significant increase in BrdU + PCNA double labelled cells can only arise as a consequence of the dividing 'clonal' cells switching to regenerate themselves more frequently after the kainate treatment.

6.4.11 Dilution of BrdU label from 'clonal' cells is unlikely occur earlier than 2 days after kainate injection in dentates ipsilateral to the injection.

Previous studies suggest that dilution of BrdU below detection levels occurs after 3-4 cell cycles (Hayes and Nowakowski, 2002), and results from saline injected controls in these experiments supported this conclusion, with dilution occurring between day 2 and day 5 after saline injection (3-6 days after BrdU labelling). However, the observation that kainate injection may shorten cell cycle time in the dentate ipsilateral to the injection should produce earlier dilution of BrdU, since cell cycles are complete more rapidly. Cluster analysis can be used to identify if dilution patterns are significantly different between experiments. A BrdU labelled cell on its own forms a cluster of size 1, with a single division the cluster grows to size 2 (2 BrdU labelled cells). The size of the cluster is affected by 3 variables; the number of divisions, the rate cells migrate from the cluster and the rate that dilution eliminates cells from clusters and breaks them up (**Fig 6.17**). Clusters will continue to grow, unless all the cells in the cluster become 'post-mitotic', until either dilution or migration occurs. In the control animals dilution is predicted between 2 and 5 days, therefore, the decrease in cluster size between 6 hours and day 2 is due to migration rather than dilution, and the significant fall thereafter is due to both migration and dilution. The same BrdU cluster size profile is observed in the dentates of animals exposed to kainate injection, indicating that dilution should not have occurred before day 2 after kainate (**Fig 6.2C inset**). Further evidence to support migration as the cause of the decline in BrdU cluster size between 6 hours and 2 days, is the continued increase in BrdU cell counts between 6 hours and 2 days in all treatment conditions (**Fig 6.18**). If dilution were the cause of the decrease in cluster size between these points, BrdU cell counts would not increase but would tend to decrease.

Although the cluster analysis assumes a steady state model and kainate has already been demonstrated to cause a deviation from the steady state model dilution is still unlikely, because with the pulse labelling method employed the point at which dilution occurs should be synchronised in most cells that contain BrdU and a sharp significant change should be observed. Further points between day 2 and day 5 could be used to identify when BrdU becomes diluted, but this would involve a considerable cost in animals for

little gain. It is probable that dilution in kainate treated animals occurs between day 2 and day 3 after injection and between day 3 and day 4 in saline injected animals. Due to the predicted decrease in cell cycle time in the kainate animals.

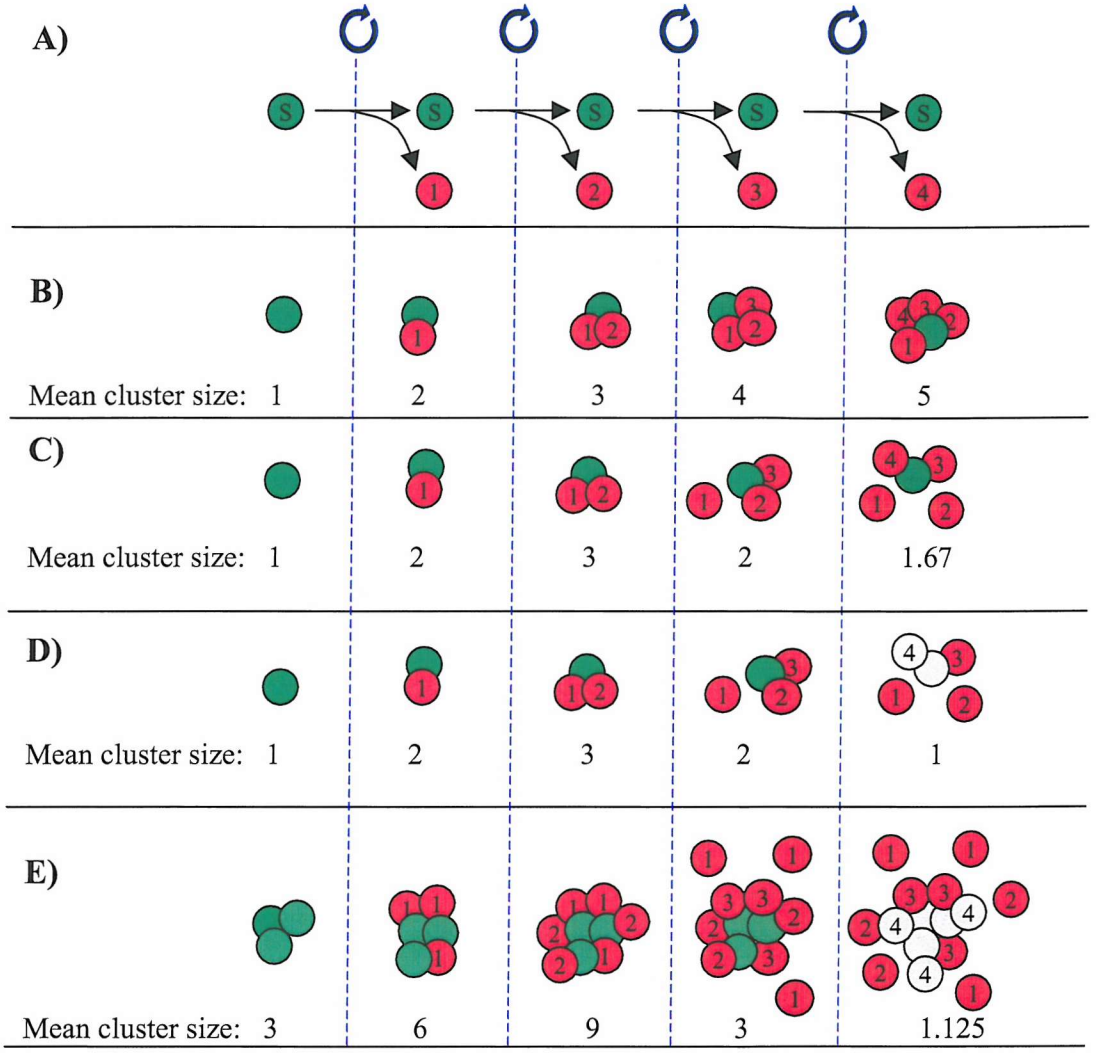

Fig 6.17: Changes in average sizes of BrdU 'clonal' clusters, caused by migration and dilution. A steady state cell division profile **(A)** with a BrdU labelled stem cell dividing repeatedly to produce a sequence of daughter cells , , etc. The average size of the cluster generated from a single dividing cell is traced, with no migration of cell or dilution of BrdU **(B)**, with migration 2 cell cycles after division but no dilution **(C)**, and with migration 2 cell cycles after division and dilution of BrdU label after 4 cell cycles **(D)**. Larger clusters are also seen in the tissue indicating groups of dividing cells, these can rapidly alter mean cluster size **(E)**.

6.4.12 Kainate induces a population, other than the 'clonal' cells, to proliferate.

Earlier it was stated that, 'only about 30% of the proliferation on day 2 in dentates ipsilateral to a kainate injection is derived from the pre-labelled population, significantly less than the 42% of proliferation in saline injected controls at the same time'. However, differences in rates of BrdU dilution could render this observation misleading. We established differences in the rate of BrdU dilution between the saline and kainate injected animals are probable, this dilution does not occur until after the day 2 point, and so is not a factor. It is therefore reasonable to conclude another population, other than the 'clonally' labelled cells, is responding to the kainate injection by dividing, since the PCNA only (i.e. non-'clonal' dividing cells) cell counts are significantly increased on day 2 after kainate.

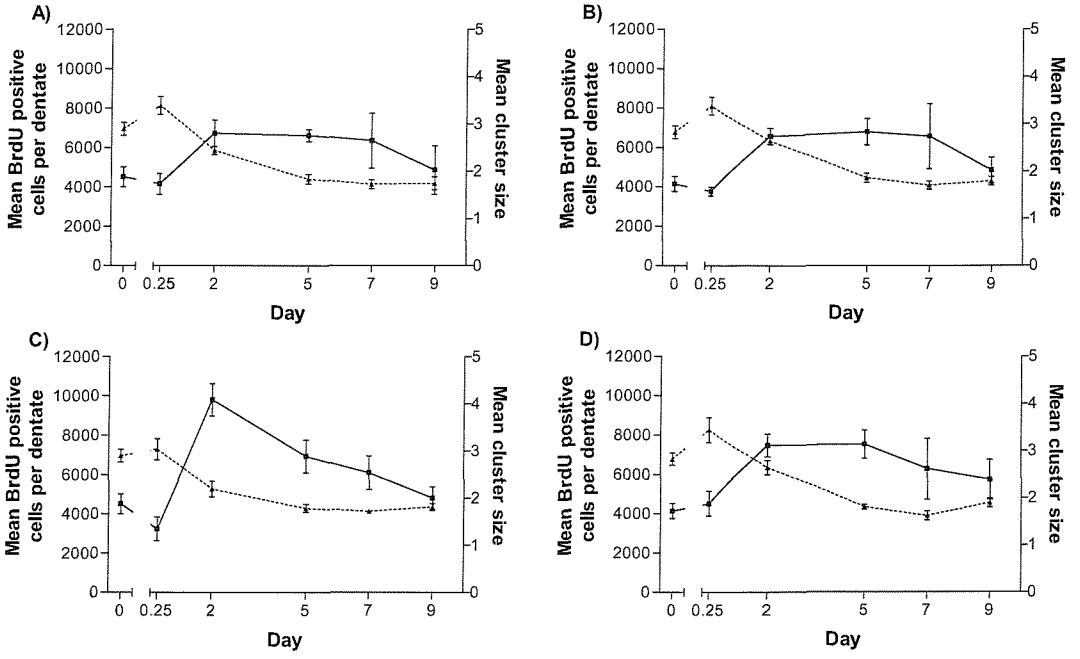

Fig 6.18: Profiles of BrdU labelled cells (solid lines) and average BrdU cluster sizes (dotted lines) in dentates of animals receiving unilateral i.c.v. injections of either saline (A+B) or kainate (C+D), and BrdU labelling of day 0 un-operated control data. Showing the profile of BrdU labelling (solid lines) in ipsilateral (A+C) and contralateral (B+D) dentates after saline injection **(A+B)** and after kainate injection **(C+D)**. The profile of BrdU cluster size (dotted lines) in ipsilateral (A+C) and contralateral (B+D) dentates after saline injection **(A+B)** and after kainate injection **(C+D)**. All values are expressed as mean ± SEM, taken from 4-6 animals per treatment with 6 sections systematically sampled from each animal, BrdU cell counts are scaled by the inter section interval.

6.4.13 Increased Neurogenesis is induced by kainate, ipsilateral to its injection.

In addition to the increased proliferation, we also observed increased neurogenesis. The increase in neurogenesis determined by Dcx staining, did not occur until day 5 and persisted to day 7 (**Fig 6.4**). This is later than increases in proliferation detected by PCNA immunohistochemistry. The reasons for this are two-fold; Dcx expression is not detected in putative neuroblasts until up to 2 days after their formation (Cooper-Kuhn and Kuhn, 2002), and expression persists for 7-10 days once detectable (Kempermann, Gast et al., 2003). This means newly generated Dcx positive cells are derived from the PCNA positive cells from up to 2 days previously, and they are being added to a large pool of cells, which will buffer any changes for a period. The PCNA and Dcx data obtained from dentates ipsilateral to kainate injection can be related. If a delay of 2 days between PCNA expression and Dcx expression is assumed, with Dcx expressed for 7 days, then the total number of new neurons added between day 0 and day 5 will form five-sevenths of Dcx count on day 7. Based on the PCNA data, with a cell cycle time of 24 hours, and 40 % of PCNA positive cells becoming Dcx positive (the proportion observed in controls) this would produce an increase in the number of Dcx positive cells of approximately 140%. The observed increase from saline injected control Dcx expression on day 7 is approximately 200%. However, the BrdU labelling protocol predicted a decrease in the length of cell cycle, if the decrease is from 24 hours (control length) to 16 hours (the minimum reported time) the number of new cells generated from the PCNA labelling would be 50% greater – approximately 210%, and very similar to the observed increase in Dcx. If Dcx expression persists for longer than 7 days, the predicted increase from PCNA labelling becomes reduced. Although these calculations are very approximate and based on several assumptions they do suggest that alteration in cell cycle time after kainate could be important in generating the observed changes in neurogenesis.

6.4.14 Cell death is induced by kainate, ipsilateral to its injection.

The principle areas of the hippocampal formation lesioned by an ICV kainate injection are the CA3 and CA4 pyramidal cell layer. Nadler et al. identified that infusion of kainate via an ICV injection over a period of 30 minute generated a unilateral partial

lesion of the CA3 region from doses as low as 0.5nmol, a dose of 3.8nmol is sufficient to destroy 90% of CA3 pyramidal cells, with little to no loss of cells in the contralateral dentate (Nadler, Perry et al., 1978). The dose of kainate we used (0.5μg ≈ 2.35nmol) was therefore sufficient to induce an extensive unilateral lesion, and seizure with a comparatively low mortality (LD_{50}=5.2nmol). Nadler reported "*no obvious depletion of granule cells ...[at concentrations] up to 26nmol.*"(Nadler, Perry et al., 1978), however the results in this experiment demonstrated significant FJB labelling in one animal 6 hours after kainate injection, this could be as a result of the reduced infusion time we used. Nadler also reported that by administering very high doses of kainate intra-hippocampally some granule cell death could be achieved, this could be a possibility in this case, however, no evidence of an intra-hippocampal injection tract was detected. It is also possible that the FJB stain is a more sensitive method of detecting cell death than the cresyl violet and Fink-Heimer stains used in the Nadler study. Cell death in the GCL has been previously reported, both immediately after seizures, and with a significant delay, and cell death has been postulated as an inducer of neurogenesis (Gould and Tanapat, 1997; Dong, Csernansky et al., 2003). We observed dentate granule cell death in some, but not all, animals after seizure, however the high cell death did not correspond to a different pattern of clonal proliferation compared with seizure animals that did not demonstrate FJB staining (**Fig 6.12 B**). An increased proliferation after cell death on day 9 post seizure may not be detected due to the BrdU dilution effect already discussed, however dilution is not a factor on day 2 and thus it is unlikely that in this model cell death is linked to increased neurogenesis. Additionally, Ekdahl et al. established that many of the newly generated cells die shortly after birth, and this results in a significant increase in cell death (Ekdahl, Mohapel et al., 2001). Although the death quantified by that study was apoptotic, it is not inconceivable that a necrotic elements of cell death could also be present, thus the cell death we detected at longer post seizure survival times may be newly generated cells that are not required and are dying.

6.4.15 Granule cell death does not induce changes in 'clonal' cell proliferation

The previous chapter identified an early phase of cell death in immature tissue, localised principally to the inside of the GCL (closest to the hilus) that includes the SGZ, leading

us to speculate as to whether the increase in proliferation observed after seizures was due to specific loss of progenitor cells. These experiments cannot eliminate cell death as a causative factor in the proliferative response to the seizures, as a substantial lesion to the CA3 and CA4 pyramidal cell layers was present in all kainate treated animals. However, the lack of a correlation between granule cell death, identified by FJB staining, and 'clonal' proliferation, identified by BrdU labelling, indicates that the increased proliferation of existing progenitor cells in response to kainate application is not direct response to progenitor cell death in the young adult rat.

6.4.16 Contralateral effects

Gray and Sundstrom reported increased neurogenesis in the 7 days after a unilateral ICV kainate injection, in the SGZ of dentates both ipsilateral and contralateral to the injection. However, the increases are not of the same magnitude, the ipsilateral increase is significantly greater (Gray and Sundstrom, 1998). These experiments demonstrated the same phenomenon, total PCNA labelling (point proliferation) in contralateral dentates of animals receiving ICV kainate was significantly increased compared with saline injected controls, but this increase is significantly smaller than the increase in corresponding dentates ipsilateral to the kainate injection (**Fig 6.8C and Fig 6.10C**).

The number of clonal proliferating cells tends to increase in dentates contralateral to the kainate injection, however this increase is predominantly in the number of post mitotic cells generated, and not in the number cells that continue to divide, when compared with dentates contralateral to a saline injection. This suggests that in the contralateral dentate kainate induces a decrease cell cycle time, generating more post-mitotic cells, but does not alter the model of proliferation which describes the cell divisions.

The fact that clonal proliferation is not producing the increase in point proliferation, also implicates activation of another proliferating population. Although the difference between the proportional contributions of the BrdU pre-labelled cells to the increased point proliferation in contralateral dentates is not significant after kainate or saline injection, the magnitude of the drop in this proportion between 6 hours and 2 days is significant in dentates contralateral to the kainate injection (**Fig 6.10F**). Additionally, the

contralateral decrease between 6 hours and day 2 is of a similar magnitude to the drop in the ipsilateral dentates (ipsilateral 43% → 30%, and contralateral 49% → 33%; **Fig 6.8F**), and the proportion in ipsilateral dentates is significantly less than in saline controls on day 2 (**Fig 6.9F**).

While neurogenesis (determined by Dcx staining) is not significantly greater, contralaterally, in the kainate animals than the salines, it does demonstrate a trend for increase, and failure to observe a significant change might be due to the low number of sections sampled per animal in this analysis, as the BrdU only labelling indicated an increase in post-mitotic cells.

The major difference between ipsilateral and contralateral hippocampal formations is the absence of detectable cell death contralateral to an ICV kainate injection. This particular difference between the ipsilateral and contralateral hippocampi of animals receiving unilateral kainate injection, allows us to speculate that cell death activates the existing progenitor cell population to divide in a different manner, moving away from a steady-state model of proliferation. While another factor or factors induce a change in cell cycle time, and induce activation of a 'quiescent' or slowly dividing population of cells to divide rapidly.

Chapter 7
Seizures induce proliferation of subgranular zone radial glia-like astrocytes in the adult dentate gyrus

7.1 Introduction

It is now well established that hippocampal neurogenesis occurs in adult mammals (Eriksson, Perfilieva et al., 1998; Biebl, Cooper et al., 2000; Fuchs and Gould, 2000; Cameron and McKay, 2001; Hastings, Tanapat et al., 2001), and is modulated by among other things seizures (Parent, Yu et al., 1997; Gray and Sundstrom, 1998; Covolan, Ribeiro et al., 2000). In spite of the evidence for the existence of postnatal hippocampal neurogenesis, the population(s) of cells from which these new neurons are generated has yet to be definitively identified. The ICV saline and kainate injection experiments described in the previous chapter both fit a model of proliferation with two types of dividing cell, one slowly dividing and the other rapidly dividing. Differences between the proliferation profiles are probably due to kainate inducing changes in the cell cycle kinetics and the mode of division of both the dividing cell populations. The results obtained under control conditions add further weight to the current evidence documenting adult proliferation and neurogenesis, but shed no light on the potential identities of these dividing cells. Neurons themselves are not responsible as they are terminally differentiated and thus incapable of further division. However at least 2 populations of cells have been proposed as potential progenitor / stem cell populations

7.1.1 Stem cell candidates in the subgranular zone.

Palmer has offered evidence that in the dentate gyrus stem cells may be of endothelial origin, a 2 hour pulse of BrdU results in 37% of BrdU labelled cells expressing an endothelial marker (Palmer, Willhoite et al., 2000). Many of these clusters of BrdU positive cells were closely associated with small capillaries, and Palmer hypothesised that the processes of angiogenesis and neurogenesis in the SGZ could be closely linked. Other work has subsequently identified a subpopulation of astroglial cells as stem/precursor cells. In the developing rat, radial glial cells give rise to the cells that form the cerebral cortex (Malatesta, Hartfuss et al., 2000; Heins, Malatesta et al., 2002; Malatesta, Hack et al., 2003). A cell phenotype that has similar morphology to the radial glial cells and expresses the same phenotypic markers, has recently been described as dividing to generate neurons, via an intermediate, in the adult subventricular zone (SVZ) (Doetsch, Caille et al., 1999; Doetsch, Garcia-Verdugo et al., 1999) and the SGZ of the dentate gyrus (Seri, Garcia-Verdugo et al., 2001; Seri and Alvarez-Buylla, 2002).

7.1.2 Problems associated with identifying stem cells

Identifying either the endothelial cells or the radial glial cells as neural stem cells is difficult, since debate over the specificity of markers is intense, although recently candidate genes for stem cells have been identified using genomics (Ivanova, Dimos et al., 2002; Ramalho-Santos, Yoon et al., 2002). Nestin, an intermediate filament protein expressed on cells that produce neurons and glia, is widely used as a progenitor cell marker (Lendahl, Zimmerman et al., 1990). However, after kainate-induced seizures most reactive astrocytes in the hilus express nestin (Clarke, Shetty et al., 1994), it is also not reported as being expressed in the SGZ (Yagita, Kitagawa et al., 2002), making it inappropriate for use as a marker in our experiments. Other markers of stem cells are being identified but are not yet well characterized such as Musashi1 (Yagita, Kitagawa et al., 2002), shkA (Conti, Sipione et al., 2001), and Lewis-X (Capela and Temple, 2002). Of these, Lewis-X is a promising candidate; it is detected in the neurogenic regions of the adult brain, it can be found in a small subpopulation of GFAP positive astrocytes, and it is often found in close association with blood vessels (Capela and Temple, 2002).

Another problem associated with the identification of stem cells is demonstrating that a specific stem cell has produced a specific neuron; therefore, the ability to mark a cells heritage is critical for identifying stem cell. BrdU pulse labelling techniques, similar to the method used in the pre-labelling experiments where progenitor cells were identified by tagging them with BrdU before the seizure, are only of limited value in identifying cell heritage. The BrdU marks a cell as a dividing cell or the product of a dividing cell, however it does not itself encode any information about the phenotype of the cell or that of its heritage (parent cell). Additional methods of marking the dividing cells are therefore required.

7.1.3 Transgenic techniques applied to cell phenotyping

The fact that GFAP positive cells with a radial glial morphology, that is "extending a process, radially, deep into the granule cell layer", may be stem cells (Alvarez-Buylla, Seri et al., 2002) makes these cells a candidate for the effectors of the proliferative response to seizures. However, GFAP immunostaining shows its distribution is

highly restricted in the cell, only staining processes and not the cell body, this makes identification of proliferating (BrdU positive), GFAP positive cells difficult to identify as BrdU incorporation is restricted to the nucleus. The use of transgenic technology can potentially over come this problem. A recent study used a transgenic mouse expressing Enhanced Green Fluorescent Protein (EGFP) under the promoter for nestin to identify nestin positive cells, overcoming the antibody specificity problems associated with cross reactivity of nestin antibodies with endothelial cells (Filippov, Kronenberg et al., 2003). Nolte et al., have developed a transgenic mouse in which, EGFP expression is under control of the hGFAP promoter (Nolte, Matyash et al., 2001). In these animals, EGFP freely diffuses in the cells it is expressed in marking both processes and the cell body, permitting evaluation of colocaisation between BrdU and EGFP. The EGFP cells have been characterised both morphologically and electrophysiologically throughout the brain. In the dentate gyrus, Nolte identified several subpopulations of astrocytes, including radial glial cells, and found no evidence for EGFP in oligodendrocytes or in mature neurons identified by myelin-associated glycoprotein (MAG) and NeuN respectively (Nolte, Matyash et al., 2001). Another advantage of the EGFP technique is the possibility of it persisting after the cell has ceased to express GFAP, thus it could potentially mark neurons that have had an astrocytic heritage, overcoming the problem described above. The reported variation in the intensity of EGFP fluorescence the cells of the hippocampus could support this hypothesis and is defiantly worth further investigation. In general, the characteristics of this model suggest it could be useful for studying the effects of seizures on specific populations of astrocytes, by combining it with immunochemistry for BrdU possible changes in astrocytic proliferation after seizure can be elucidated. Additionally although a high degree of co-localization between the EGFP cells and GFAP positive cells has been demonstrated (Nolte, Matyash et al., 2001), comparisons between this population and that of cells expressing other astrocytic markers for example s100b have not been considered.

7.1.4 Questions to be addressed

The identification of stem and progenitor cells in the adult dentate gryus has proved difficult. The aim of these experiments is therefore to investigate the hypothesis that the stem/progenitor cells reside in the astroglial cell lineage, and the proliferative

activity of these cells increases in response to seizures. The transgenic mouse with hGFAP promoter controlled EGFP-expression will be used to clearly identify an astrocytic population, and diffusion of the EGFP throughout the entire cell will also permit subdivision of this population based on morphology, additionally immunostaining for another astrocytic marker s100b will be used confirm phenotype. As in many of the previous experiments, proliferating cells will be identified with a pulse of BrdU. Intraperitoneal kainate injection will be used to induce seizures. The phenotypic distribution of dividing cells between the two treatments can then be compared. The initial increase in proliferation is detected by day 3 after seizure, the BrdU pulse will be applied at this time to increase the probability of labelling stem/progenitor cells, rather than the later generated neurons.

7.2 Methods

Animal experiments were carried out in the lab of Prof Steinhauser, Bonn university Germany in accordance with the EU directive of 24th November 1986 (86/89 EEC), and all attempts were made to reduce the numbers of animals and degree of suffering. Ten, Fifty-day-old transgenic mice (25g) were used in this experiment; these mice expressed enhanced Green Fluorescent Protein (EGFP) under the GFAP promoter. Five of the mice received an intraperitoneal (IP) injection of kainate (20mg/kg dissolved in sterile PBS), five control mice received a vehicle only IP injection. Animals were observed for 1 hour after the injection and seizure severity was recorded according to the Racine scale. One of the kainate treated animals failed to achieve a seizure level of 4 and so was excluded from the analysis. 72 hours after the initial IP injection all mice received a second IP injection, this time, of BrdU (50mg/kg, dissolved in PBS and filtered through a 2.2μm Millipore membrane; Boehringer Mannheim GmbH, Mannheim, Germany) to label cells at the time of the initial rise in proliferation (Nakagawa, Aimi et al., 2000).
Animals were then sacrificed 2 hours after this second injection, to prevent cells completing the mitotic cycle, thus cells incorporating BrdU are stem/progenitor cells and not their progeny. Sacrifice was by administration of a terminal dose of phentobarbitone, and was followed by transcardiac perfusion with 25mls 0.9% saline followed by 25mls 4% paraformaldehyde pH6.8, brains were then removed and post fixed in 4% paraformaldehyde and stored at 4°C. Sections were produced for immunochemistry on a vibrotome cutting in the coronal plane from the dorsal hippocampus at a thickness of 20μm, 80 serial sections were collected from each brain, encompassing the dorsal and mid hippocampus. Collecting the sections in order allowed reconstruction of the dentate to be carried out by sampling sections at a known separation; in the epifluorescence experiments, every 16th section was sampled starting from a randomly selected section in the first 16 sections containing dentate gyrus.

7.2.1 Immunochemistry

Both single and double-labelled fluorescent immunochemistry was carried out on free floating 20μm coronal sections, producing sections requiring two and three channel analysis respectively as EGFP occupies the green channel (Abs 470nm, Em 508nm)

in all sections. Single immunofluorescent antibody staining for BrdU was carried out on five sections per animal sampled at an interval of 320μm. For DNA denaturation, sections were first washed in Tris buffered saline (TBS) 0.05M, pH 7.4 and then incubated in 2N HCl at 37°C for 30 minutes. Sections were rinsed in Boric acid (0.1M pH 8.5; 10 min), followed by multiple washes in TBS, and incubation in 0.05 M TBS-TS (pH 7.6; Tris-buffered saline with 0.1% triton and 0.05% Bovine serum albumin) with primary antibody to BrdU (rat monoclonal, 1:1000; Harlan Sera-Lab) overnight at 4°C. After multiple washes in TBS sections were then incubated with a Cy3-conjugated Donkey anti-rat secondary antibody (1:200; Jackson Immunoresearch; Abs 555nm, Em 570 nm) in TBS-TS for 2 hours. Repeat washes were performed before sections were mounted on gelatinised slides in Moviol , cover-slipped and the edges varnished.

Single immunofluorescent antibody staining for TUC-4 and PSA-NCAM was performed on one 20μm section each. TUC-4 staining was obtained by washing free floating sections for 15 minutes in 0.1M TBS-TS (pH 7.6) twice, this was followed by 1 hour in 10% donkey serum in 0.1M TBS-TS (pH 7.6). Sections were subsequently incubated with the rabbit anti-TUC-4 (1:500; Chemicon) in 0.1M TBS-TS (pH 7.6) for 36 hours at 4°C. After multiple washes in 0.1M tris buffer (pH 7.6) sections were then incubated with a Cy5-conjugated Donkey anti-rabbit secondary antibody (1:200; Jackson Immunoresearch; Abs 650nm, Em 670nm) in 0.1M TBS-TS (pH 7.6) for 2 hours. Repeat washes were performed before sections were mounted on gelatinised slides in Moviol, cover-slipped and the edges varnished. A similar process was used for PSA-NCAM staining; briefly, multiple short washes in 0.1M PBS (pH 7.4; Phosphate Buffered Saline) were followed with 1 hour in 5% Donkey serum in 0.1 M PBS-TS (pH7.4; PBS supplemented with 0.1% Triton and 0.05% BSA), overnight incubation with mouse anti-PSA-NCAM (1:1000; gift from Dr. G.Rougon, University of Marseilles, France) at 4°C, further washes in PBS, 2 hour incubation with a Cy5-conjugated Donkey anti-mouse secondary antibody (1:200; Jackson Immunoresearch) in PBS-TS. A final set of washes in PBS preceded mounting as described above.

Double immunofluorescent staining included combinations of BrdU, s100b, GFAP and β-Tubulin. Sections for BrdU staining were acid treated as above and then all sections were processed in solutions made up in 0.05M TBS (pH 7.6), in a similar manner to the BrdU single labelling protocol, with both primary antibodies added simultaneously at the following dilutions rat anti-BrdU (1:1000; Harlan-Sera), rabbit

anti-s100b (1:5000; Swant), mouse anti-type III β-Tubulin (Tuj1 clone, 1:500; Covance) and mouse anti-GFAP (1:400; Sigma) or rabbit anti-GFAP (1:1000; gift from P. Steart) overnight at 4°C. A cocktail of secondary antibodies was also used, all raised in donkey, having specificity for rat, mouse or rabbit as appropriate, and conjugated to Cy3 or Cy5 (all 1:200; Jackson Immunoresearch) for 2 hours.

7.2.2 Cell counting

Cell counts were performed with both epifluorescence and confocal microscopes, in all subsequent analysis the examiner was blinded to the treatment the tissue had received.

7.2.3 Epifluorescence imaging

Epifluorescence counts were obtained on a Dialux 22 microscope (Leitz) with green (I3; Ex: 450-490nm, Em: 520nm) and red (N2.1; Ex: 540-560nm, Em: 570nm) filter blocks fitted, at 40x magnification. Every 16th section was sampled starting from a randomly selected section in the first 16 sections containing dentate gyrus; this systematic sampling permits estimation of the number of cells present in the dorsal dentate rather than just the cells present per slice. The sampling paradigm resulted in five sections per animal being examined; in each section, counts were made in both dentates, along the entire length of the sub granular zone. In all experiments, the counter was blinded as to the nature of the IP injection. Cells that were positive for BrdU (red), EGFP positive cells (green), EGFP positive cells that had radial Glial morphology and cells co-localizing green and red fluorescence were recorded.

7.2.4 Confocal Imaging

Two confocal z-stacks with a separation of 1μm between images at 40x magnification on a Leica SP2 confocal laser-scanning microscope were obtained from three sections per animal at a separation of 520μm, while this spacing is larger than that used in the epifluorescence experiments it retains the systematic approach to examining the entire dorsal hippocampus, while not requiring as much processing as a larger section sample, (one per dentate) for s100b (Cy5; Ex: 650nm, Em: 670nm) and EGFP (Ex: 492nm, Em: 510nm) co-localization, scanning of both channels was simultaneous as 'crosstalk' is unlikely due to the separation of the spectra. All images were from the same area, where the internal and external blades of the Granule cell layer meet, and

cell count taken from the whole of each image. EGFP (Ex: 492nm, Em: 510nm), BrdU (Ex: 555nm, Em: 570nm) and s100b (Ex: 650nm, Em: 670nm) z-stacked images were obtained from one section per animal. These images were from the same area as above, however sequential scanning was used in combination with tight filter bands centred on the peak emissions of EGFP, Cy3 and Cy5 to prevent 'cross-talk' between channels. 'Cross-talk' occurs when stimulation at a specific excitation wavelength of one fluorescent marker produces an emission at another wavelength that excites a second fluorescent marker causing a second emission spectrum from a species that was not directly excited. This can lead to identifying co-localization in cells where one of the markers is not really present, or a false positive. Using sequential scanning only one wavelength is excited at a time, reducing the probability of 'cross-talk', and combining this with tight filter bands means only emission wavelengths close to the expected maxima of the fluorophore being imaged are collected, effectively eliminating 'cross-talk'. Images were Z stacked into 3D projections and exported in TIF format to Photoshop (Adobe Photoshop v5.1), which was used for analysing all confocal images.

7.2.5 Statistical Analysis

At all times the counter was blinded as to the nature of the IP injection. Analyses of the results obtained using epifluorescent imaging are presented as estimates of cell counts in the dorsal hippocampus, and values expressed as mean ± standard deviation. Variances between groups were compared with an F-test, and the appropriate unpaired two-tailed students t-test. Variance within groups was examined using a one-way AVOVA with Tukey's post hoc test.

Analyses of the results obtained using confocal imaging are expressed as mean ± standard deviation per animal. Where cell numbers permitted the variance between groups was compared with an F-test, and the appropriate unpaired two-tailed students t-test used for comparisons. When cell numbers were insufficient to establish the data formed a Gaussian distribution Fisher's exact test was used for comparisons. Additionally, after the slide coding had been broken, the lengths of subgranular zone examined in the control and kainate groups were compared, to ensure equal sampling from both groups, by unpaired two-tailed students t-test to prevent the introduction of a bias into the cell counts obtained from each image.

7.3 Results

7.3.1 Increases in EGFP positive cells after seizures

Cell counts obtained from 5 sections per animal each separated by 320μm imaged with an epifluorescence microscope were used to obtain estimates of the number of EGFP positive cells, and BrdU positive cells in the granule cell layer of the whole dentate from the transgenic mice used. The dentate gyrus of control animals contained significantly less EGFP positive cells, (3792±571 cells per dentate) than kainate treated animals (5266±719 cells per dentate; $p<0.05$, unpaired two-tailed students t-test; Fig 7.1). The sampling used for the epifluorescence analysis also permitted investigation of the distribution of cells rostro-caudally. The most rostral section had significantly fewer EGFP positive cells (51.8±13.8 cells) than any of the other sections in the kainate treated animal (closest other mean 67.6±9.0 cells, $p<0.05$, one-way ANOVA with Tukey's post hoc comparison; Fig 7.3). There was no change in the distribution of EGFP positive cells in control animals, and although the sections taken from the most rostral extent of each group were not significantly different ($p=0.088$), the trend for increased EGFP expression was preserved. At all other points kainate induced a statistically significant increase in EGFP expression, (71.3±18.4 cells compared with 51.0±14.2 cells in controls in the mid section analysed where the difference was smallest, $p<0.05$, unpaired two-tailed students t-test with equal variance; Fig 7.4).

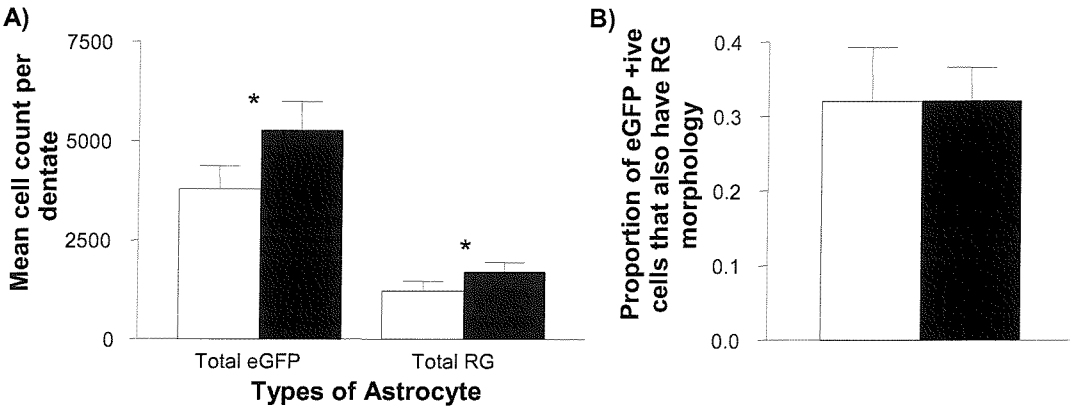

Fig 7.1: Comparison of abundance of types of astrocyte in the sub granular layer of the dentate gyrus of transgenic mice, expressing eGFP under the GFAP promoter. Animals were either exposed to i.p. kainate ■ (50mg/kg) or i.p. saline as a control □ and cell counts made using an epifluorescence microscope at 40x magnification on five 20μm sections per animal at a separation of 320μm, counting two dentates per section from 4/5 animals in the kainate and control groups respectively. Showing Total counts for eGFP positive cells, and a subset of those cells that also have radial glial (RG) morphology (A), and the proportion of eGFP positive cells that have radial glial morphology (B). Values are expressed as mean ± SD. *Asterisks* denote a significant difference at $p<0.05$, determined by unpaired two-tailed students t-test assuming equal variance.

7.3.2 Increases in Radial glia like, EGFP positive cells after seizure

Similarly the numbers of a subpopulation of these cells that have the morphology (defined by Nacher as 'a cell with a triangular body in the subgranular cell layer with a thin radial process extending up into the granule cell layer'(Nacher, Rosell et al., 2001); Fig 7.2) of radial glial (RG) cells and are EGFP positive (RG-EGFP) increases significantly after seizure, from 1221±231 cells per dentate in controls to 1704±238 cells per dentate after kainate ($p<0.05$, unpaired two-tailed students t-test with equal variance; Fig 7.1). As with the EGFP positive cells, in the control group there was no change in the number of RG-EGFP positive cells observed across the dentate sampled. In the kainate group the most rostral section (15.8±5.7 cells) examined had significantly fewer RG-EGFP cells than 3 of the other 4 sections (22.8±7.4 to 23.3±3.7 cells; Fig 7.3) and in three of the 5 positions examined the kainates contained significantly more RG-EGFP cells than corresponding controls. The remaining sections followed the same trend but missed statistical significance (Fig 7.4).

The relative increases in these two populations of cells are the same, as the proportion of EGFP positive cells that have radial glial morphology is unchanged (control 32.1±7.2% vs 32.2±4.5% in kainate; Fig 7.1).

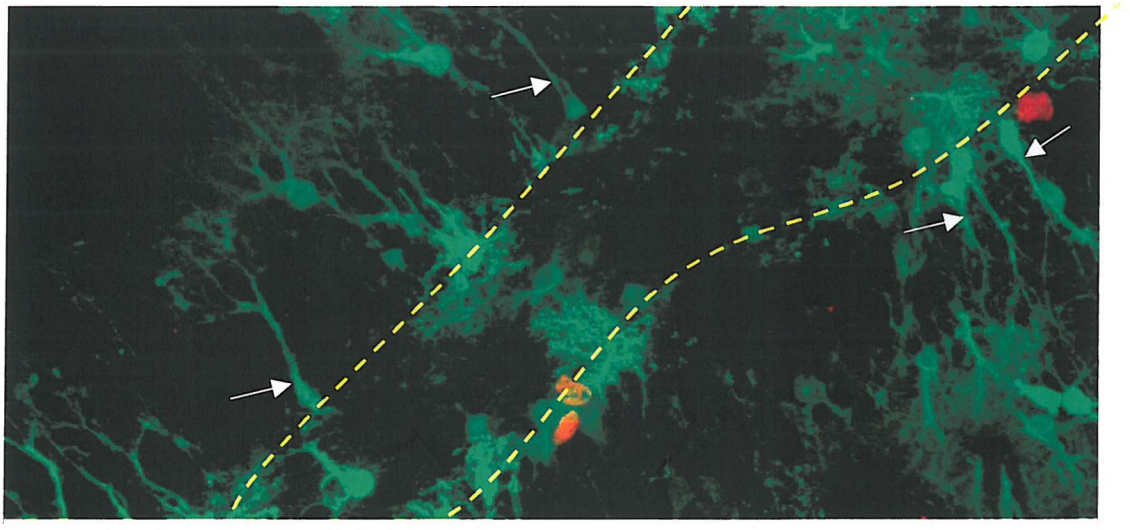

Fig 7.2: EGFP expressing cells in the dentate gyrus, including Radial glial cells. Cells incorporating BrdU are red. Arrows indicate the radial processes used to define radial glial morphology. It is also interesting to note the different intensities of EGFP fluorescence observed in the SGZ. The yellow dotted line indicates the approximate location of the SGZ. Image is at 40x magnification.

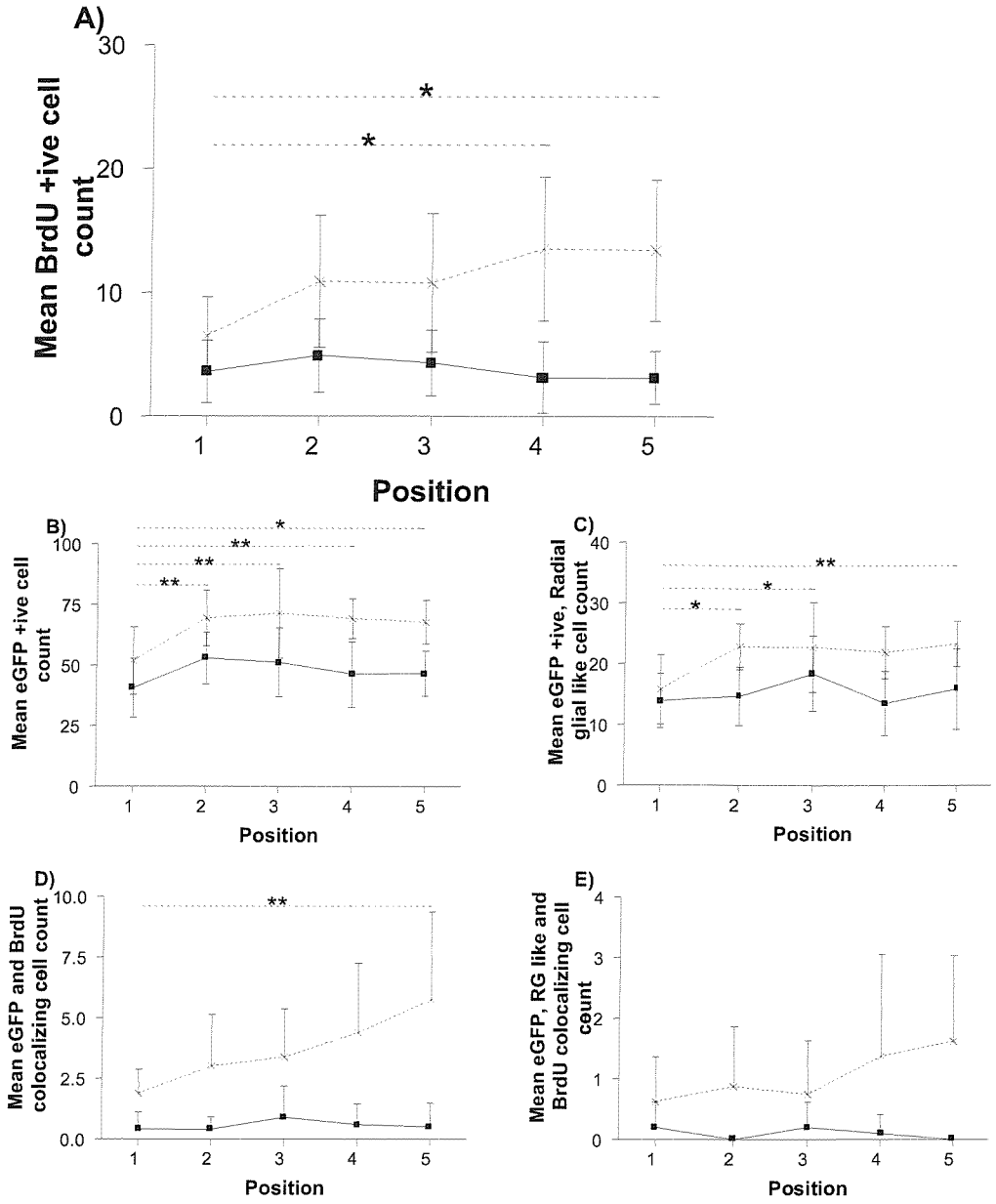

Fig 7.3: Comparison of cell counts in the sub granular layer of the dentate gyrus from 20µm thick coronal sections from transgenic mice, expressing eGFP under the GFAP promoter. Animals were either exposed to i.p. kainate (50mg/kg;broken line) or i.p. saline as a control (unbroken line) and cell counts made using an epifluorescence microscope at 40x magnification. Position refers to the sections location within the hippocampus, with position 1 being dorsal and 5 being ventral. Counts are from two dentates per section and from 4 or 5 animals in the kainate and control groups respectively. Showing BrdU incorporation, a measure of cell proliferation (A), cells containing eGFP indicating an astrocytic heritage (B), cells that in addition to expressing eGFP have the morphology of Radial glial cells, extending a single process into the granule cell layer (C), and cells co-localizing both eGFP and BrdU (D), or cell with the morphology of radial glial cells and co-localizing eGFP and BrdU (E). Values are expressed as mean ± SD. Bars identify significant differences, with the broken bars referring to kainate values unbroken bars to control values, with *Asterisks* denoting the level determined by repeated measures ANOVA and tukey's pos hoc comparisson (* $p<0.05$, ** $p<0.01$, *** $p<0.001$).

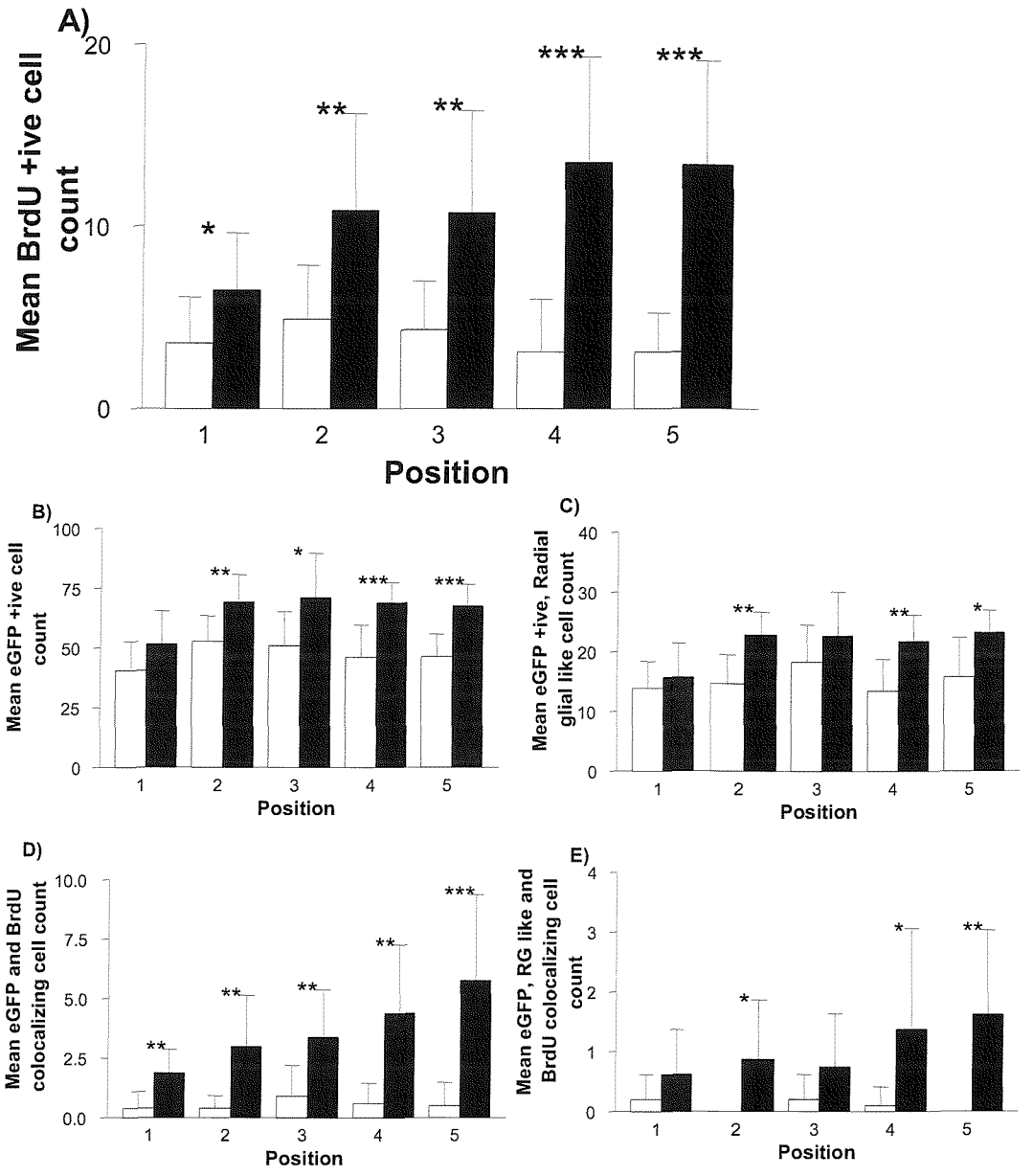

Fig 7.4: Comparison of cell counts in the sub granular layer of the dentate gyrus of transgenic mice, expressing eGFP under the GFAP promoter, treated with either saline or kainate. Measurements are made from 20μm coronal sections. Animals were either exposed to i.p. kainate ■ (50mg/kg) or i.p. saline as a control □ and cell counts made using an epifluorescence microscope at 40x magnification. Position refers to the sections location within the hippocampus, with position 1 being dorsal and 5 being ventral. Counts are from two dentates per section and from 4 or 5 animals in the kainate and control groups respectively. Showing BrdU incorporation, a measure of cell proliferation (A), cells containing eGFP indicating an astrocytic heritage (B), cells that in addition to expressing eGFP have the morphology of Radial glial cells, extending a single process into the granule cell layer (C), and cells co-localizing both eGFP and BrdU (D), or cell with the morphology of radial glial cells and co-localizing eGFP and BrdU (E). Values are expressed as mean ± SD. *Asterisks* denote significant differences determined by unpaired two-tailed students t-test with the assumption of equal variance (* $p<0.05$, ** $p<0.01$, *** $p<0.001$).

7.3.3 Kainate causes an increase in proliferating EGFP positive cells in the dentate gryus

BrdU pulse labelling allowed quantification of proliferative activity in the SGZ 3 days after an IP injection of kainate or saline. The number of proliferating cells increased significantly with kainate treatment (880±256 cells per dentate) compared with controls (304±75 cells per dentate, $p<0.05$ unpaired two-tailed students t-test with unequal variance; Fig 7.6). This increase is observed at all Rostro-Caudal points sampled (Fig 7.4), however there is a trend for increased proliferation in the more caudal sections of the kainate treated animals (13.5±5.8 and 13.4±5.7 cells per section) compared with the most rostral (6.5±3.1 cells per section, both $p<0.05$, one way ANOVA with tukey's post hoc comparison; Fig 7.3). Variation across the rostro-caudal dentate in controls is not significant.

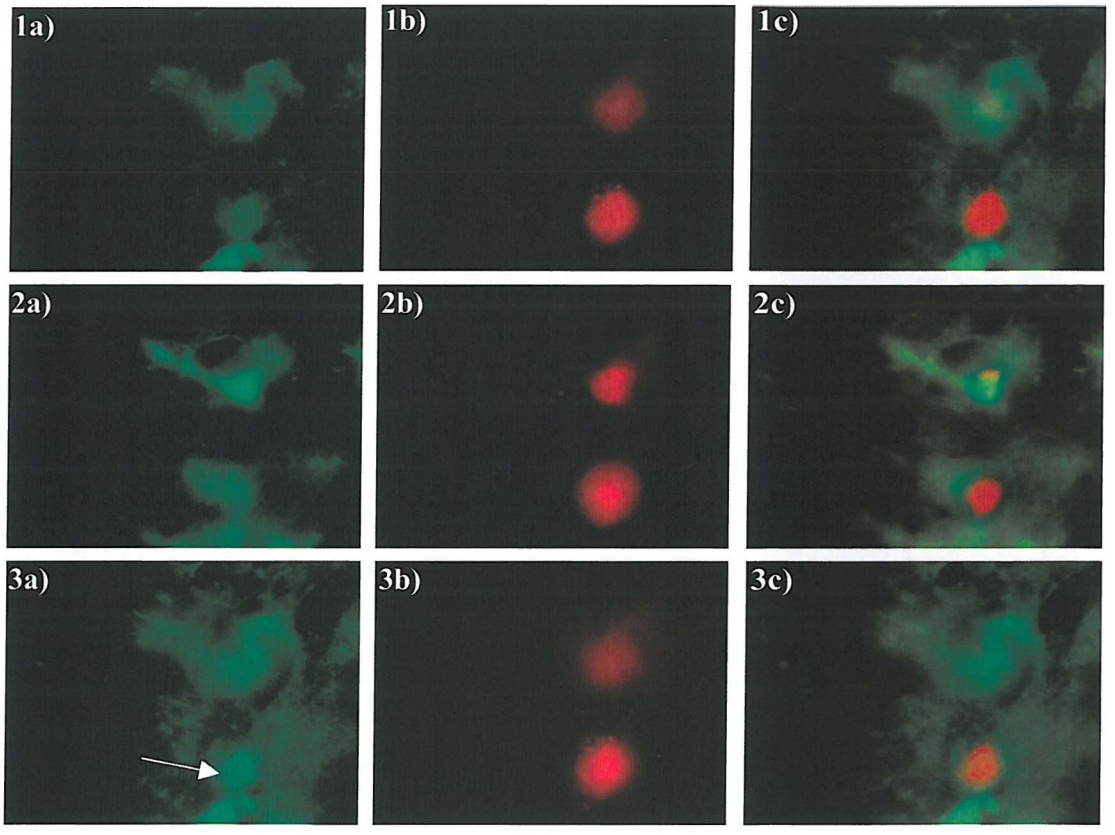

Fig 7.5: BrdU and EGFP colocalization as seen using epifluorescence microscopy. Images were obtained at three different focal points in the tissue **(1,2 and 3)**, using a 100x objective. EGFP positve cells **(a)**, BrdU positive cells **(b)** and colocalizing cells **(c)** can all clearly be seen. There is also some slight bleed through or cross-talk from **(3b)** to **(3a)** (arrow).

The number of EGFP positive cells that immunostain for BrdU is significantly increased 3 days after IP kainate, with co-localizing cell counts rising from 45±22 cells per dentate in controls to 294±105 cells per dentate ($p<0.05$, unpaired two-tailed students t-test with unequal variance; Fig 7.6). There is not a significant variation in control cell counts throughout the dorsal dentate. In kainate treated animals there is a trend for increased numbers of co-localizing cells in the more caudal dentate, with the most caudal section examined having significantly more co-localizing cells (5.8±3.6 cells) than the most rostral (1.9±1.0 cells, $p<0.05$, one way ANOVA with tukey's post hoc test; Fig 7.3). However this did not impinge on overall differences between the two groups, as the increase observed is statistically significant at all points (Fig 7.4).

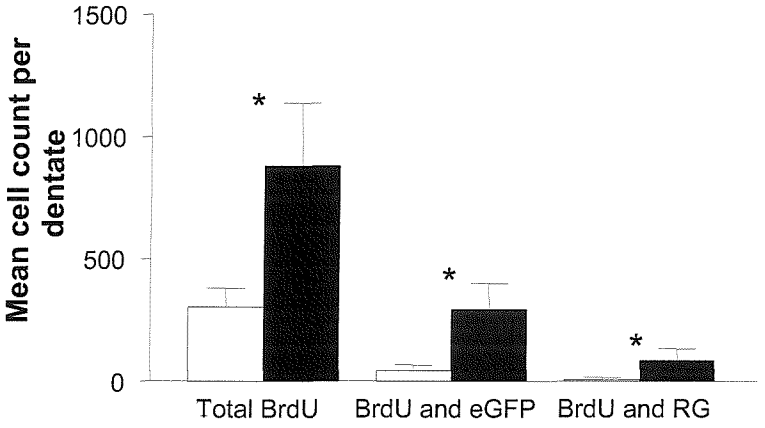

Fig 7.6: Comparison proliferation in the sub granular layer of the dentate gyrus of transgenic mice, expressing eGFP under the GFAP promoter. Animals were either exposed to i.p. kainate ■ (50mg/kg) or i.p. saline as a control □ and cell counts made using an epifluorescence microscope at 40x magnification on five 20μm sections per animal at a separation of 320μm, counting two dentates per section from 4/5 animals in the kainate and control groups respectively. Showing Total BrdU incorporation, cells colocalizing eGFP and BrdU and eGFP positive cells with radial glial (RG) morphology that colocalize BrdU. Values are expressed as mean ± SD. *Asterisks* denote significant differences determined by unpaired two-tailed students t-test with unequal variance as detemined using an F-test (* $p<0.05$, **$p<0.01$).

There is also a significant change in the proliferating population, in the kainate group approximately 34% of BrdU positive cells are EGFP positive compared with 14% in controls ($p<0.01$, unpaired two-tailed students t-test with equal variance; Fig 7.7). This increase in EGFP positive cell proliferation is also larger than the observed increase in EGFP positive cells, in controls approximately 1.2% of EGFP positive cells are also marked with BrdU, this rises significantly 3 days after kainate to 5.4% of EGFP positive cells ($p<0.01$, unpaired two-tailed students t-test with unequal variance; Fig 7.8).

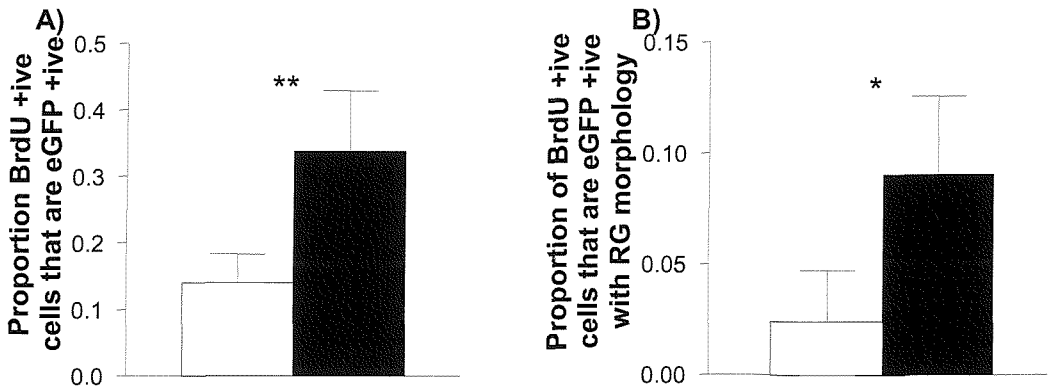

Fig 7.7: Proportions of proliferating cells that have specific astrocytic phenotypes in the sub granular layer of the dentate gyrus of transgenic mice, expressing eGFP under the GFAP promoter. Animals were either exposed to i.p. kainate ■ (50mg/kg) or i.p. saline as a control □ and cell counts made using an epifluorescence microscope at 40x magnification on five 20μm sections per animal at a separation of 320μm, counting two dentates per section from 4/5 animals in the kainate and control groups respectively. Showing proportion of BrdU positive cells that are also eGFP positive (A), and additionally have radial glial (RG) morphology (B) Values are expressed as mean ± SD. *Asterisks* denote a significant difference determined by unpaired two-tailed students t-test with equal variance (* $p<0.05$, ** $p<0.01$).

7.3.4 Kainate produces an increase in proliferating EGFP positive cells with radial Glial morphology in the dentate gryus

The coincidence of cells with radial glial morphology and containing EGFP (RG-EGFP) and BrdU positive cells shows the largest increase after kainate. This change is 10-fold, from 8±8 cells per dentate in controls to 84±48 cells per dentate in kainates (Fig 7.6). The change observed in the proportion of proliferating EGFP positive cells was duplicated with the RG-EGFP cells. Approximately 9.1% of BrdU positive cells are RG-EGFP cells compared with 2.4% in controls ($p<0.05$, unpaired two-tailed students t-test with equal variance; Fig 7.7). The increase in RG-EGFP cells that are proliferating is also larger than the observed increase in RG-EGFP positive cells, in controls approximately 0.6% of EGFP positive cells are also marked with BrdU, this rises significantly 3 days after kainate to 4.6% of RG-EGFP positive cells ($p<0.05$, unpaired two-tailed students t-test with unequal variance; Fig 7.8).

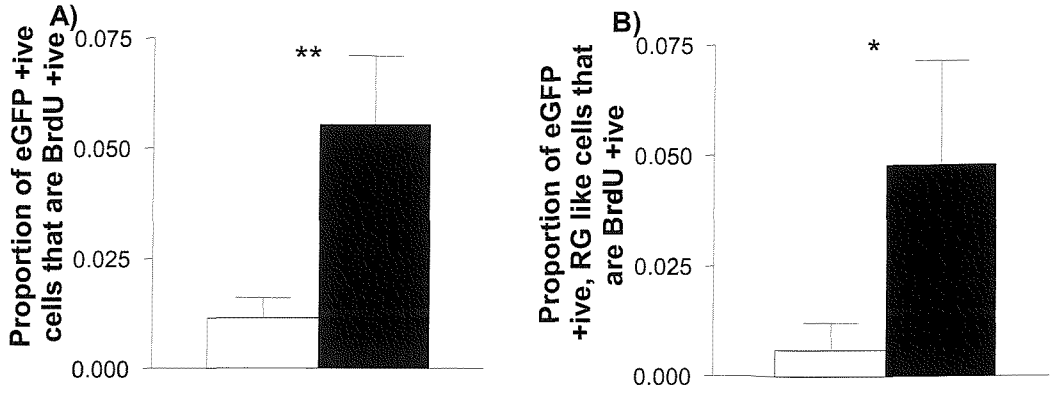

Fig 7.8: Proportions of astrocytes that are proliferating in the sub granular layer of the dentate gyrus of transgenic mice, expressing EGFP under the GFAP promoter. Animals were either exposed to i.p. kainate ■ (50mg/kg) or i.p. saline as a control □ and cell counts made using an epifluorescence microscope at 40x magnification on five 20μm sections per animal at a separation of 320μm, counting two dentates per section from 4/5 animals in the kainate and control groups respectively. Showing proportion of EGFP positive cells that are also BrdU positive (A), and the proportions of EGFP positive cells that have radial glial (RG) morphology and are also BrdU positive (B). Values are expressed as mean ± SD. *Asterisks* denote a significant difference determined by unpaired two-tailed students t-test with unequal variance (* $p<0.05$, ** $p<0.01$).

7.3.5 EGFP positive cells are a subpopulation of the astrocytes present in the SGZ of the dentate gyrus

Immunostaining against the astroglial marker s100b allowed three distinct astrocytic subtypes to be identified from confocal images. One population of cells was EGFP positive and s100b negative, a second population had the reverse staining pattern and the third population was positive for both EGFP and s100b. These observations, combined with the morphological definition of a radial glial cell as 'a cell with a triangular body in the SGZ with a thin radial process extending up into the GCL', allowed the identification of an additional sub-group of RG cells within each of the above astrocyte populations (Fig 7.9).

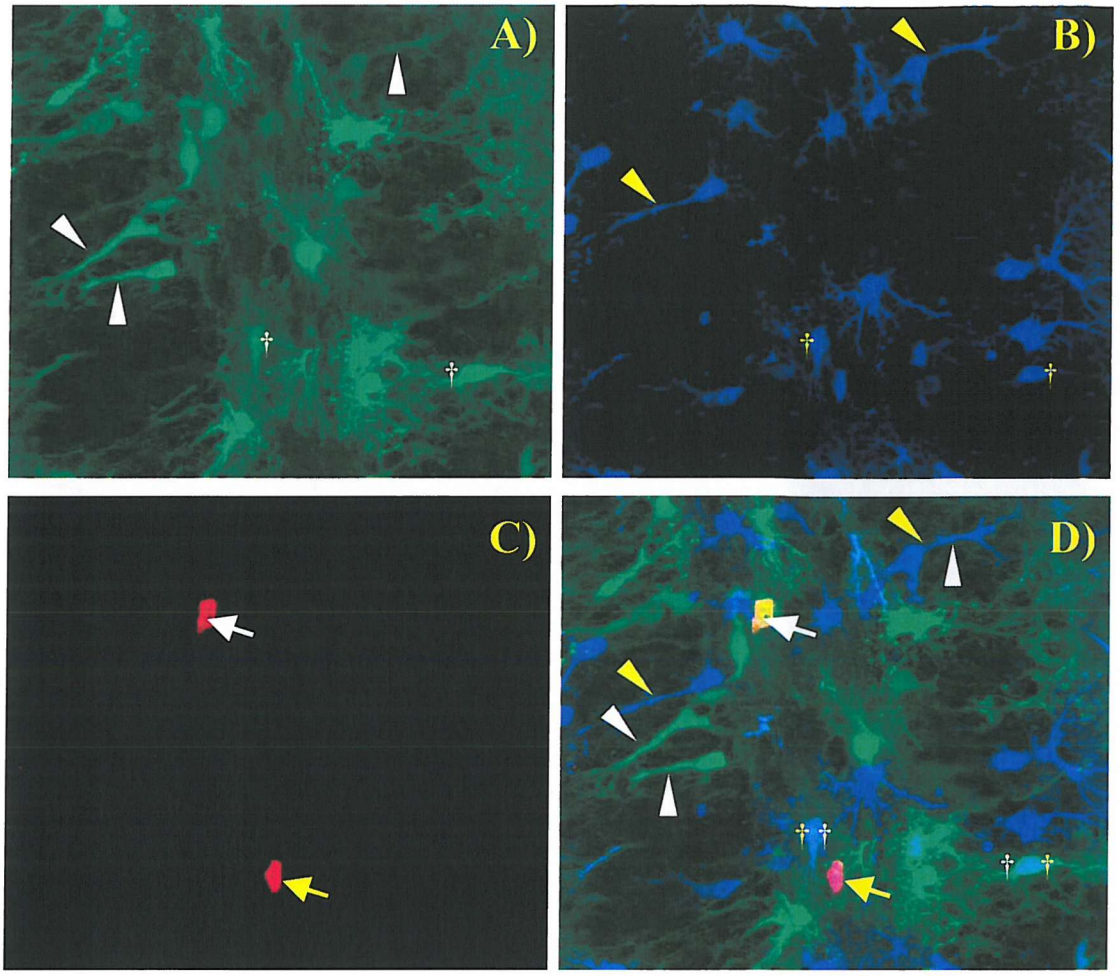

Fig 7.9: Several different astrocytic populations in the dentate gyrus. EGFP positive cells form one population of astrocytes **(A)**, and a sub population of this group are Radial Glial cells (white arrowheads), s100b positive cells are a second astroctyic population **(B)** again with a radial glial sub population (yellow arrowheads). Some of the cells express BrdU **(C)** . A composite image of all three channels **(D)** helps identify those cells that colocalize, including astrocytes expressing both EGFP and s100b (white and yellow crosses), proliferating EGFP positive astrocytes (white arrow) and proliferating s100b positive astrocytes (yellow arrow). All images are 40x magnification.

Confocal analysis from three sections per dentate at a separation of 520μm confirmed the epifluorescence observations. The number of EGFP positive cells was significantly increased from 137±22 cells in control tissue to 194±29 cells in kainate treated tissue ($p<0.05$, unpaired two-tailed students t-test with equal variance; Fig 7.10), and the number of RG-EGFP cells was also significantly increased (38±8 cells control vs. 55±12 cells kainate, $p<0.05$, unpaired two-tailed students t-test with equal variance; Fig 7.11). The proportion of EGFP cells that formed the RG-EGFP sub-population was also similar (28.1±4.4% in controls and 28.4±4.9% in kainates; Fig 7.14).

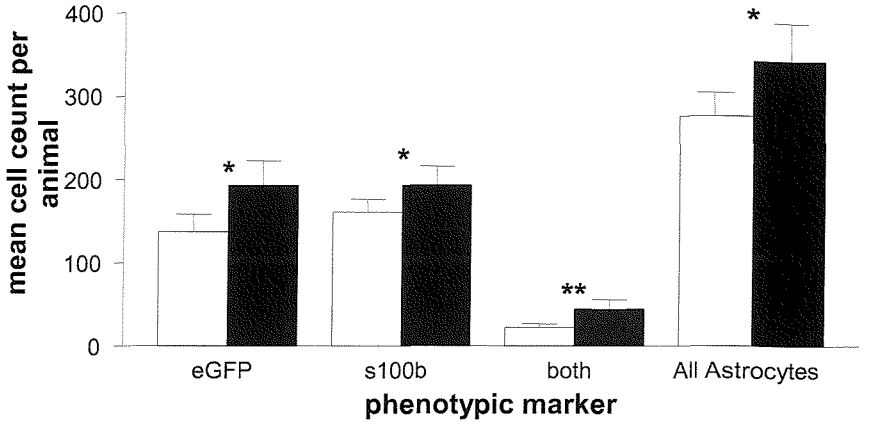

Fig 7.10: Cell counts of astrocytes in the sub granular layer of the dentate gyrus of transgenic mice, expressing eGFP under the GFAP promoter. Animals were either exposed to i.p. kainate ■ (50mg/kg) or i.p. saline as a control □ and cell counts made from single 40x confocal images of the hilar extreme of the gcl in three 20μm sections per animal at a separation of 520μm, counting two images per section from 4/5 animals in the kainate and control groups respectively, with counts expressed per mm to correct for differences in the length of hilus imaged. Showing eGFP positive cells, s100b positive cells, cells that colocalize both eGFP and s100b and the total number of astrocytes counted. Values are expressed as mean ± SD. *Asterisks* denote significant differences determined by unpaired two-tailed students t-test with equal variance established using an F-test (*$p<0.05$, **$p<0.01$).

EGFP positive astrocytes are not the only population of astrocytes that kainate increases. The number of s100b positive cells was significantly increased 3 days after kainate (194±22 cells) compared with controls (161±15 cells, $p<0.05$, unpaired two-tailed students t-test with equal variance; Fig 7.10). The sub population of s100b positive cells, exhibiting a radial glial morphology (RG-s100b) was also increased from18±3 cells in control tissue to 29±3 cells after kainate ($p<0.01$, unpaired two-tailed students t-test with equal variance; Fig 7.11). The proportion of s100b positive cells that had radial glial morphology was unchanged by IP kainate injection (approximately 11% control and 15% kainate).

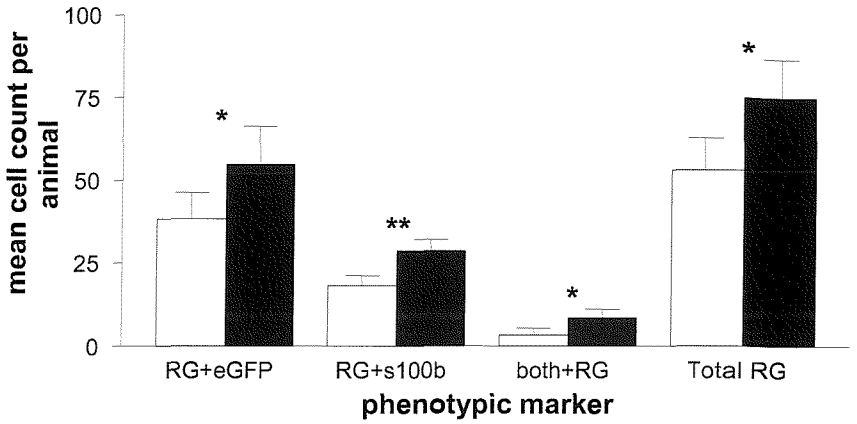

Fig 7.11: Counts of astrocytes having Radial Glial (RG) morphology in subgranular layer of the dentate gyrus of transgenic mice, expressing eGFP under the GFAP promoter. Animals were either exposed to i.p. kainate ■ (50mg/kg) or i.p. saline as a control □ and cell counts made from single 40x confocal images of the hilar extreme of the gcl in three 20μm sections per animal at a separation of 520μm, counting two images per section from 4/5 animals in the kainate and control groups respectively, with counts expressed per mm to correct for differences in the length of hilus imaged. Showing eGFP positive RG cells, s100b positive RG cells, RG cells that colocalize both eGFP and s100b and the total number of RG cells counted. Values are expressed as mean ± SD. *Asterisks* denote a significant difference at $p<0.05$ determined by unpaired two-tailed students t-test with equal variance, established using the F-test.

IP kainate injection also increased the numbers of cells staining for both EGFP and s100b (45±11 cells) compared with 22±5 cells in controls ($p<0.05$, unpaired two-tailed students t-test; Fig 7.10). This increase is not simply a result of increased EGFP or s100b expression as the proportion of the EGFP population that also labels with s100b increases after kainate (16% vs. 23%) as does the proportion of the s100b population that also labels with EGFP (14% vs. 23%) and the proportion of the total astrocyte population that express both EGFP and s100b (8% vs. 13%, all $p<0.05$, unpaired two-tailed students t-test with equal variance; Fig 7.12). The number of radial glial like cells that express both EGFP and s100b is significantly increased after seizure, with 3.4±1.9 cells observed in control animals and 8.5±2.5 cells observed after kainate. This increase is not proportionally different from the general increase cells co-labelling EGFP and s100b, (control 15% and kainate 20%).

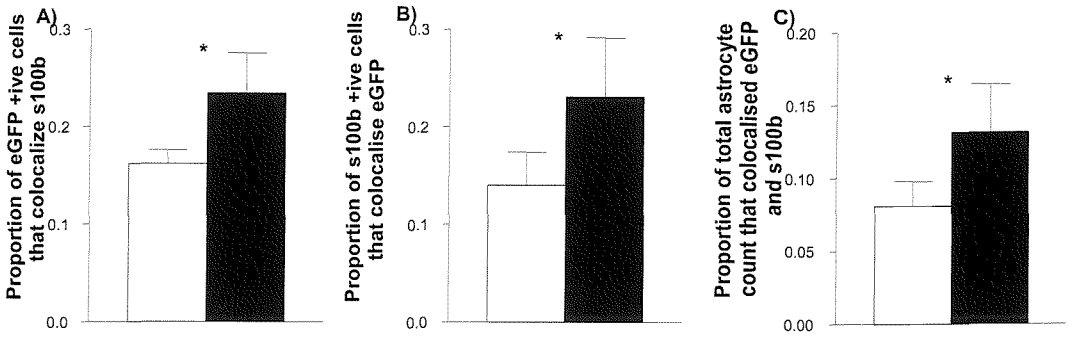

Fig 7.12: Relative proportions of astrocytes in the sub granular layer of the dentate gyrus of transgenic mice, expressing EGFP under the GFAP promoter. Animals were either exposed to i.p. kainate ■ (50mg/kg) or i.p. saline as a control □ and cell counts made from single 40x confocal images of the hilar extreme of the gcl in three 20μm sections per animal at a separation of 520μm, counting two images per section from 4/5 animals in the kainate and control groups respectively, with counts expressed per mm to correct for differences in the length of hilus imaged. Showing the proportions of: EGFP positive cells that colocalize with s100b positive cells (A), s100b positive cells that colocalize with EGFP positive cells (B) and the proportion of the observed astrocyte population that colocalizes EGFP and s100b (C). Values are expressed as mean ± SD. *Asterisks* denote a significant difference at $p<0.05$, determined by unpaired two-tailed students t-test assuming equal variance.

The total astrocyte population observed (i.e. cells expressing EGFP, s100b or both) is increased 3 days after seizure (343±46 cells vs. 276±29 cells in controls, $p<0.05$, unpaired two-tailed students t-test with equal variance; Fig 7.10). A corresponding increase is observed in the total number of RG cells, expressing EGFP, s100b or both, from 53±10 cells to 75±11 cells ($p<0.05$, unpaired two-tailed students t-test with equal variance; Fig 7.11), these increases are of a similar magnitude, with 19% of observed astrocytes being radial glial cells in the control group compared with 22% in the kainate group.

7.3.6 Analysis of proliferating Cell phenotypes

The overall increase in proliferation identified with the epi-fluorescence analysis is confirmed with the confocal analysis, BrdU labelling increases from 15 to 37 cells in sub granular zone of the eight 20μm thick images analysed in the control and kainate groups respectively ($p<0.05$, Fishers exact test; Fig 7.13).

Proliferation was observed in both EGFP positive astrocytes and s100b positive astrocytes, the numbers of these cells that co-localize BrdU are larger in kainate animals than controls (EGFP: kainate 9 cells, control 3 cells and s100b: kainate 4 cells, control 1 cell) although the numbers sampled are not sufficient for statistical analysis. A similar observation can be made for the total number of proliferating

astrocytes, which are EGFP or s100b positive, with the mean cell count increasing from 0.4±1.0 cells per dentate image to 1.6±1.1 cells per dentate ($p<0.05$, t-test). However, the observed values of 4 cells in control dentates and 13 cells in kainate animals do not reach statistical significance if the more appropriate Fischer's exact test is applied ($p>0.15$; Fig 7.13).

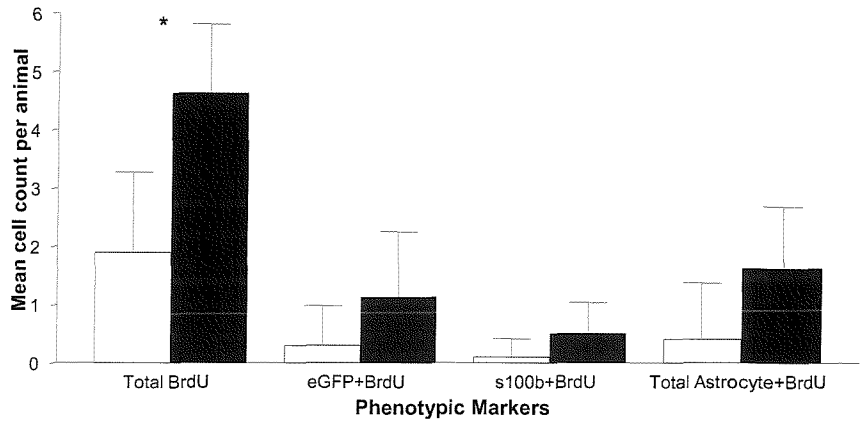

Fig 7.13: Counts of proliferating cells in the sub granular layer of the dentate gyrus of transgenic mice, expressing eGFP under the GFAP promoter. Animals were either exposed to i.p. kainate ■ (50mg/kg) or i.p. saline as a control □ and cell counts made from single 40x confocal images of the hilar tip of the gcl in one 20μm section per animal, counting two images per section from 4/5 animals in the kainate and control groups respectively, with counts expressed per mm to correct for differences in the length of hilus imaged. Showing total BrdU positive cells, BrdU positive cells colocalizing eGFP, s100b, and all astrocytes colocalizing with BrdU. Values are expressed as mean ± SD. *Asterisks* denote significant differences determined by Fisher's exact test (*$p<0.05$).

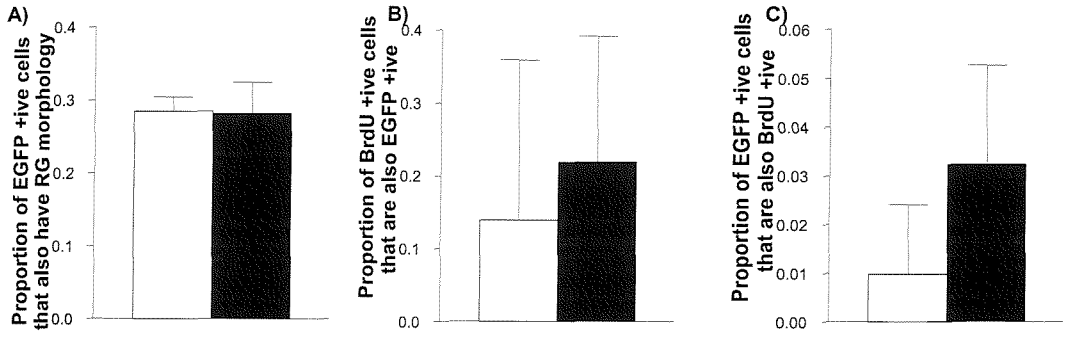

Fig 7.14: Relative proportions of astrocytes and proliferating astrocytes in the sub granular layer of the dentate gyrus of transgenic mice, expressing EGFP under the GFAP promoter. Animals were either exposed to i.p. kainate ■ (50mg/kg) or i.p. saline as a control □ and cell counts made from single 40x confocal images of the hilar extreme of the gcl in three 20μm sections per animal at a separation of 520μm **(A)** and one section **(B+C)**, counting two images per section from 4/5 animals in the kainate and control groups respectively. Showing the proportion of EGFP positive cells that have radial glial morphology **(A)**, the proportion of BrdU positive cells that are also EGFP positive **(B)** and the proportion of EGFP positive cells that are also BrdU positive **(C)**. Values are expressed as mean ± SD. Analysis with Fischer's exact test demonstrated no significant differences between groups.

7.3.7 Co-localization of EGFP and early neuronal markers

Seizures did not affect the numbers of cells expressing PSA-NCAM in control and kainate groups 26.3±5.2 and 29.3±8.7 cells per 40x confocal image respectively (Fig 7.15), neither did TUC-4 14.1±5.1 and 16.1±7.6 cells per image (Fig 7.16), at the time point examined – 3 days after kainate administration. However interestingly, there were cells that confocal analysis confirmed co-localized both EGFP and TUC-4 in both the control and kainate groups (Fig 7.18) of these 75% had radial Glial morphology. There were also cells that co-localized PSA-NCAM and EGFP in both groups, although less than 20% of these had radial glial morphology (Fig 7.17). There were no significant differences in the distributions of either of the neuronal markers between control and kainate treated animals.

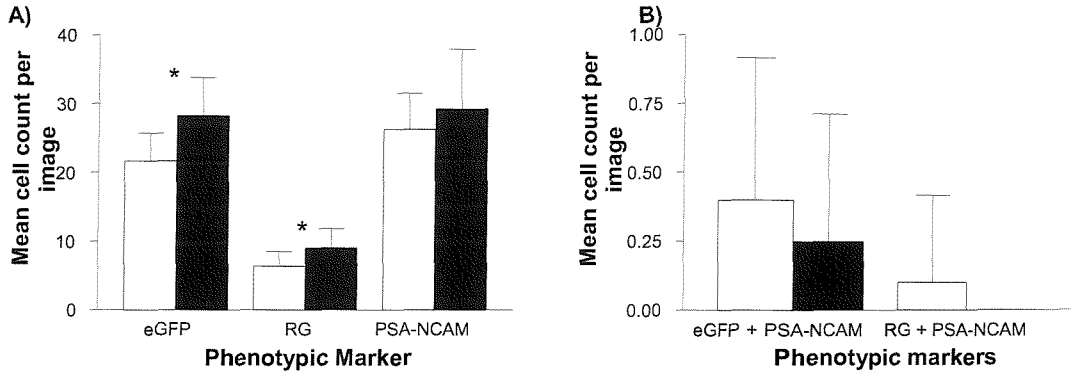

Fig 7.15: Counts of astrocytes and migrating neurons in the subgranular layer of the dentate gyrus of transgenic mice, expressing eGFP under the GFAP promoter. Animals were either exposed to i.p. kainate ■ (50mg/kg) or i.p. saline as a control □ and cell counts made from single 40x confocal images of the hilar tip of the gcl in one 20μm section per animal, counting two images per section from 4/5 animals in the kainate and control groups respectively, with counts expressed per mm to correct for differences in the length of hilus imaged. Showing total eGFP positive cells, eGFP positive cells that have radial glial (RG) morphology and PSA-NCAM, a marker for migrating neurons, positive cells (A) and PSA-NCAM positive cells that colocalise eGFP or have RG morphology and are eGFP positive (B). Values are expressed as mean± SD. *Asterisk* denotes a significant ($p<0.05$) determined using an unpaired two-tailled students t-test with equal variance identified using an F-test.

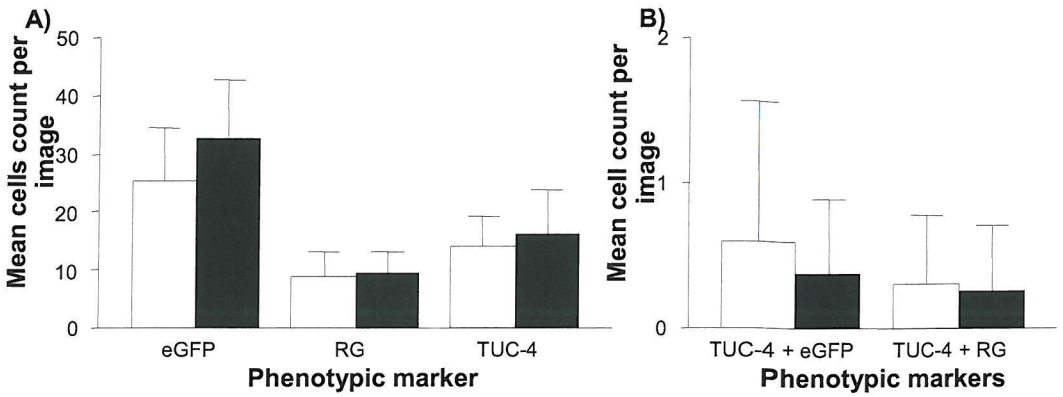

Fig 7.16: Counts of astrocytes and immature neurons in the sub granular layer of the dentate gyrus of transgenic mice, expressing eGFP under the GFAP promoter. Animals were either exposed to i.p. kainate ■ (50mg/kg) or i.p.saline as a control □ and cell counts made from single 40x confocal images of the hilar tip of the gcl in one 20µm section per animal, counting two images per section from 4/5 animals in the kainate and control groups respectively, with counts expressed per mm to correct for differences in the length of hilus imaged. Showing total eGFP positive cells, eGFP positive cells that have radial glial (RG) morphology and TUC-4, a marker for immature neurons, positive cells (A) and TUC-4 positive cells that colocalise eGFP or have RG morphology and are eGFP positive (B). Values are expressed as mean± SD.

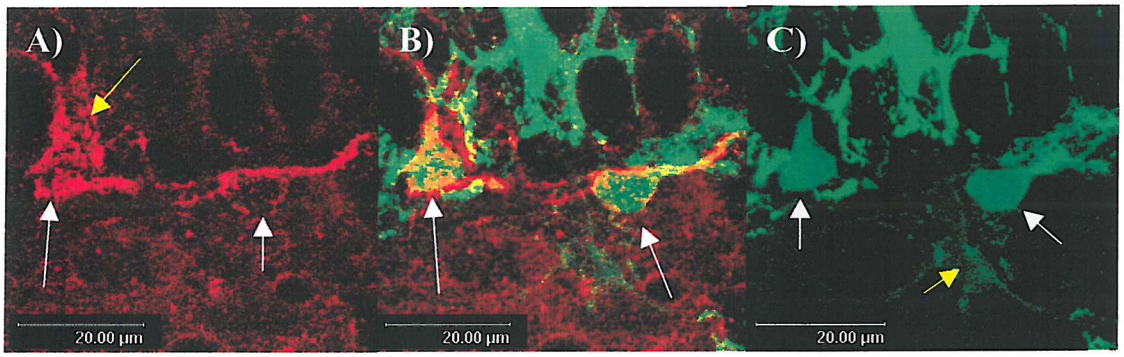

Fig 7.17: PSA-NCAM and EGFP confocal images obtained by sequential scanning at 100x magnification showing maximum projection (3D reconstruction) of the granule cell layer from a transgenic mouse expressing EGFP under the promoter of hGFAP. Showing cells expressing PSA-NCAM (Cy-3) in the red channel **(A)**, cells containing EGFP which are or have been astrocytes expressing GFAP in the green channel **(C)**, and co-localization of the two markers **(B)**.

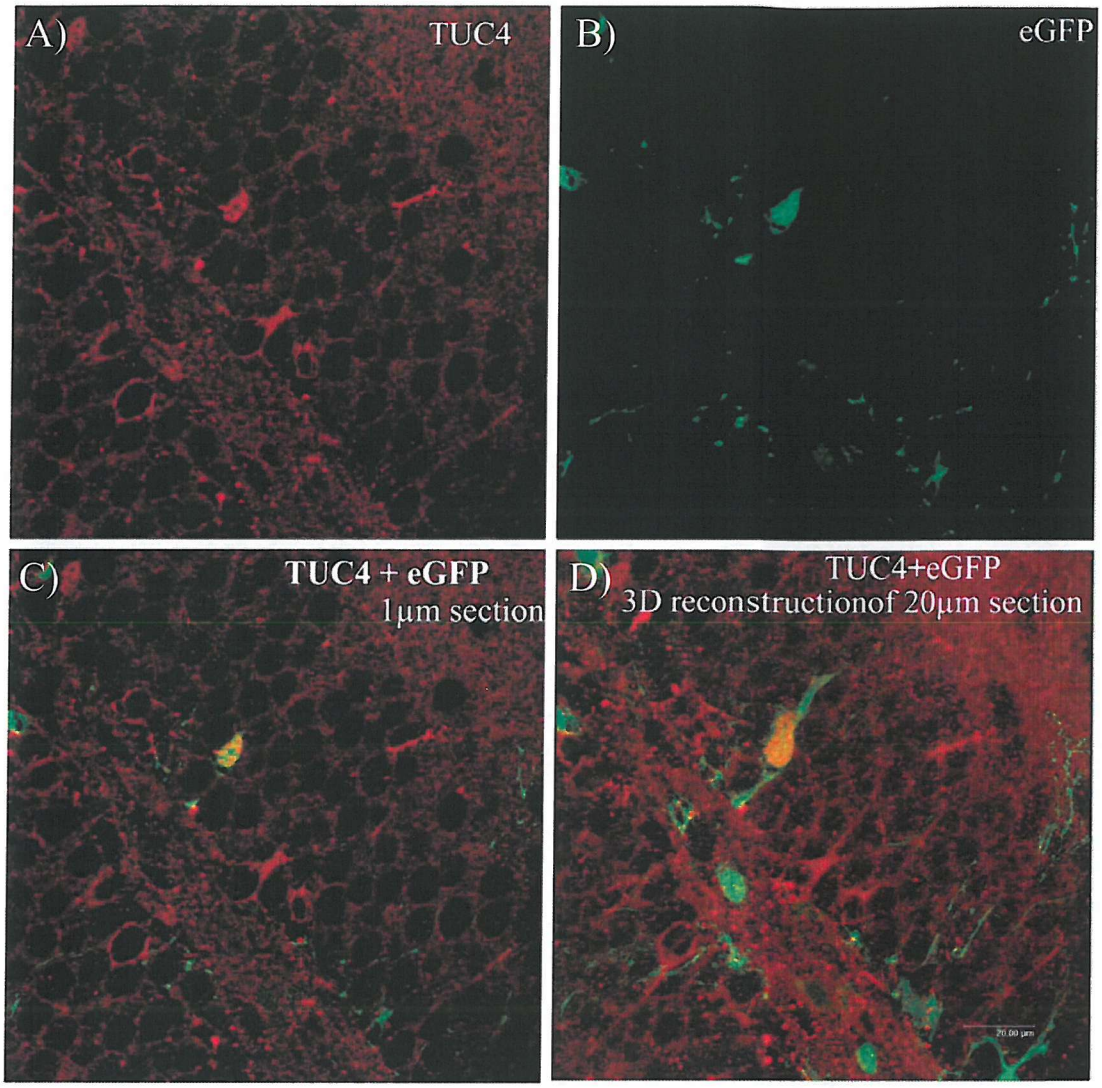

Fig 7.18: TUC-4 and EGFP confocal images obtained by sequential scanning at 100x magnification showing 1µm optical sections of the granule cell layer and hilus from a transgenic mouse expressing EGFP under the promoter of GFAP. Showing cells expressing the neuronal marker TUC-4 (Cy-3) in the red channel **(A)**, cells containing EGFP which are or have been astrocytes expressing GFAP in the green channel **(B)** and the co-localization of the neuronal marker TUC-4 (red) with the astrocytic marker EGFP-GFAP (green) **(C)**. The corresponding maximum projection (3D reconstruction) of the actual 20µm coronal section imaged **(D)** also shows clear colocalization between EGFP and TUC-4.

7.4 Discussion

The transgenic mouse model expressing EGFP under the promoter of GFAP has enabled us to examine the effects of seizures upon the proliferation of several populations of astrocytes. Among these cells identified are cells with radial glial morphology, which have previously been proposed as a stem/progenitor cell population in the sub granular zone of the dentate gyrus, capable of generating new neurons in adulthood (Seri, Garcia-Verdugo et al., 2001). Additionally images of immature neurons with an apparent astrocytic heritage have been obtained.

7.4.1 Kainate increases the abundance of several different astrocytic populations

During the experiments at as many points as were possible, the gross analysis of tissue using epifluorescence imaging has been corroborated with analysis of confocal images. This secondary analysis is important because the intensity of many of the EGFP positive cells is low (Nolte, Matyash et al., 2001). Some of these cells when examined using epifluorescence are not bright enough to be counted. However, the brightness of confocal images can be enhanced allowing all positive cells to be detected. Differences between the confocal results and the epifluorescence experiments could have indicated a shift in EGFP fluorescence intensity between control and kainate treated animals, rather than actual changes in cell number. Seizures produced an increase in both EGFP positive cells and in EGFP-RG cells at three days, these increases are of a similar magnitude as in both controls and kainates RG cells formed approximately 30% of the EGFP cell population. This effect was seen in both the confocal and epifluorescent experiments demonstrating a robust response that is independent of the analytical method used. Confocal imaging also allowed investigation of six different astrocyte populations. Three of these groups are RG cells expressing EGFP, s100b, or both. The other three groups identified are cells that express one or both of those markers and do not have radial glial morphology. Expression of all these cell types is significantly increased at three days after seizure, indicating astrocytic activation as a result of seizure.

7.4.2 An asymmetric increase in proliferation results in a astrocytic proliferation being disproportionately increased after kainate.

In this mouse model, 3 days after kainate an approximately 2.5 fold increase in proliferation was observed. This increase is of a similar magnitude to the increase observed contralaterally to an intracerebroventricular injection of kainate in the rat (Gray and Sundstrom, 1998). That study also examined the abundance of BrdU and GFAP positive cells in the dentates, finding no increase in the number of dividing astrocytes after seizures. However, the results described here show clear increases in proliferation in EGFP positive and RG-EGFP positive cells after seizure. These increases are six fold and ten fold respectively (Fig 7.6), and are proportionally larger than the overall increase in proliferation, indicating the differential up-regulation of astrocytic proliferation. The apparent inconsistencies between the studies could, in part, be due to the difficulty in confidently co-localising BrdU and GFAP immunostaining (discussed above, chapter 7.1.3). Additionally, the BrdU labelling profiles are different in the two experiments, in the study of Gray and Sundstrom marker co-localisation is examined on day 7 after seizures using a label and survive protocol, whereas in the above experiments co-localisation is examined on day 3 using a pulse labelling protocol. Since our hypothesis is that, the astrocytes form a stem/progenitor cell population that divide shortly after seizure to generate a later increase in neurons this difference between the experiments is not inexplicable.

7.4.3 Stem cell proliferation after seizures – the importance of radial glial cells

The largest increase in proliferation we detected after seizures, when grouped by phenotype is in RG-EGFP positive cells, which are the radial glial cell type that Alvarez-Buylla proposed as stem cells (Seri, Garcia-Verdugo et al., 2001). Recent work, using transgenic mice expressing EGFP under the nestin promoter and BrdU pulse labelling, identified two populations of nestin positive cells. 'Type 1' cells had radial glial morphology, expressed GFAP, were located in the SGZ, and were rarely dividing. 'Type 2' cells had were about half as abundant as type 1 cells, were generally GFAP negative, had small bodies without a radial process, were located in the SGZ and GCL, and were rapidly dividing. Neither 'type 1' or 'type 2' cells expressed s100b (Filippov, Kronenberg et al., 2003). Additionally, although the authors did not specifically refer to GFAP positive/ EGFP (nestin) negative cells with radial glial morphology these are also visible in some of their figures. Another group

examining primary cultures taken from 'germinal zones' demonstrated that the stem cells in these regions express GFAP in postnatal and adult tissue, but not in embryonic tissue. Furthermore, they describe three distinct phases of cell proliferation in these cultures as growth conditions were changed. Initially cultures grown in serum-based medium are GFAP positive and nestin negative, passage and transfer to serum free medium containing FGF2 resulted in nestin positive neurosphere development. Finally, withdrawal of FGF2 resulted in differentiation producing neurons, oligodendrocytes, and astrocytes (Imura, Kornblum et al., 2003). The work of Filippov and Imura, considered in combination with our observations, notably that shortly after seizure the largest increase in proliferation is in EGFP (GFAP) positive radial glial type cells, with a smaller, but still above average increase in EGFP positive cells that lack a radial process, permit the postulation of the phenotypic identities of the stem/progenitor cells residing in the SGZ in the model proposed by Alvarez-Buylla's group (Seri, Garcia-Verdugo et al., 2001).

7.4.4 A hypothesis modelling proliferation in the adult dentate gyrus

The EGFP positive cells that lack a radial process in our experiments probably equate to the rapidly dividing, transient 'D cells' of Alvarez-Buylla, the 'type 2' cells in Filippov's work. Although some of the 'type 2' cells did not express GFAP the continued identification of these cells with EGFP marker we used should be possible as the EGFP remains detectable in the cell for a short period after GFAP protein expression has ceased. Under normal conditions, some of the EGFP positive cells with radial glial morphology identified in our study probably equate to the slowly dividing B cells proposed by Alvarez-Buylla, and the 'type 1' cells in Filippov's experiments. Importantly, not all RG-EGFP cells are actively dividing 'B cells', some remain quiescent, possibly the fraction detected but not described by Filippov et al., which are GFAP positive and nestin negative. The presence of a population of proliferative cells, which can become quiescent, could be a part of the age related decrease in neurogenesis. Examining the proliferation in immature transgenic animals, possibly using the organotypic model detailed in chapter 5, could test this. After seizure induction, activation of the quiescent cells occurs, hence the greatest increase in RG-EGFP and BrdU positive cells. By day 3 these could also have generated more rapidly dividing non-radial EGFP positive 'D cells', a population in which is also differentially increased.

The 'D cells' are described as capable of a limited number of rapid divisions, what is the trigger for this final differentiation? Since some of the 'type 2' cells described by Filippov are not GFAP positive could the loss of GFAP expression be the trigger for terminal differentiation?

7.4.5 Observation of immature neurons derived from astrocytes

The co-localization of EGFP and PSA-NCAM (Fig 7.16) and EGFP and TUC-4 (Fig 7.16) are especially important observations. This demonstrates that cells that have recently synthesized EGFP, and were therefore of astroglial lineage have generated cells, which are committed to a neuronal fate. Ideally, these cells co-localize BrdU, showing that they are indeed newly generated cells. However, because cells were only permitted to survive for 2 hours after BrdU administration, the cell cycle has not been completed and so BrdU should not be co-localised with immature neuronal markers, as it is unlikely that even these early neuronal markers would be expressed in the cells showing BrdU incorporation. These experiments are also limited by practical constraints as PSA-NCAM and to a lesser extent TUC-4 are not stable in acid.

Chapter 8
General Discussion

The aim of this thesis is to investigate the control of dentate neurogenesis, especially, after seizures, and to identify the principle cells involved in these processes (Chapter 1.9). The results obtained when combined have led to the formulation of a hypothesis to describe the process of neurogenesis after kainate induced seizures, which may arguably be extended to describe the same phenomenon in many other types of brain injury.

My hypothesis is that Brain injury results in either death or inactivation of a progenitor cell population with consequent recruitment of either a quiescent or slowly dividing stem cell population which results in restoration of a functioning progenitor cell population with return to a normal or near normal proliferative state.

A direct consequence of this hypothesis is the requirement for at least two distinct types of precursor cells in the neurogenic SGZ. This is not the accepted view of dentate neurogenesis as reported by Nowakowski (Nowakowski, et al., 1989) who mathematically modelled SGZ proliferation as a single precursor population undergoing continuous asymmetric division to yield another precursor cell and a new granule cell neuron. This work assumed a steady state of division but did not show that models with two or more precursor cells were inferior; in fact they are equally valid (see discussion chapter 6). The clonal BrdU labelling studies (Chapter 6) found a subpopulation of BrdU pre-labelled cells that were still dividing 5 days after kainate and 6 days after BrdU injection, by which time BrdU should have been diluted below detection if a steady state of continually dividing cells was occurring (Hayes and Nowakowski, 2002). Even more significantly we found a population of cells (PCNA only staining) that were not BrdU pre-labelled but who contributed most to the seizure induced proliferation as compared to the dividing pre-labelled clone (BrdU + PCNA) on day two post kainate. This was reflected in the proportion of PCNA cells that were BrdU positive at this time point with no change in the ratio in saline animals compared to a decrease in the ratio in kainate treated animals. Dilution of the BrdU label was unlikely to be a significant factor at his time point because total BrdU counts in the kainate group peaked at day 2 post kainate (Day 3 after BrdU injection) implying that BrdU was still detectable in progeny despite multiple divisions up to this point. The only other study of a similar nature in adult rats claimed that BrdU dilution begins as early as one day (approx. 1 cell cycle) after addition (Dayer, et al., 2003), and suggest that variable dilution between cells could be related to the duration

of an individual cells exposure to BrdU while in S-phase, with different concentrations of BrdU between cells defining detection. However, the BrdU and Ki-67 double labelling work of Dayer et al. used a fluorescent secondary antibody, with no amplification step, which means that the BrdU signal will dilute beyond detection faster than in our studies, where amplification was used for primary antibody detection, and indeed initial tests using un-amplified fluorescent labelling when determining the optimal conditions in our experiments appeared to identify fewer BrdU positive cells than the amplification technique detected (qualitative observation). Additionally, the work of Nowakowski's group using the same amplification technique as I used found dilution occurred after a similar number of cell cycles to my estimated dilution point. The time to dilution was different between the two experiments, as Nowakowski used adult mice, and these have a shorter cell cycle time than the adult rats I used, however the number of divisions a cell undergoes is the critical factor in failure to detect a dividing cell due to dilution, and the length of the cell cycle merely defines the time at which the dividing cell will cease to be detectable.

The clonal proliferation study relies on detecting BrdU tagged cells over time, and although considerable work was done to establish that this BrdU dilution did not occur until after day 2 post seizure, when the recruitment of a quiescent stem cell population was detected, the possibility of an earlier dilution point cannot be totally excluded. If subsequent experiments were to demonstrate a more rapid dilution of the BrdU label than I have predicted, the conclusion that a quiescent stem cell population is recruited might be questioned based solely on the clonal labelling experiments. However, the considerable evidence obtained from the clonal experiments in support of the hypothesized quiescent or slowly dividing stem cell population selectively recruited to division in response to seizure induction was confirmed by the subsequent EGFP studies. These EGFP studies in transgenic mice expressing EGFP on the hGFAP promoter showed that the number of radial glial GFAP positive cells increased 3 days post kainate and that this population of cells was selectively recruited to divide. Work by Alvarez-Buylla's group has shown that these astrocytes give rise to neurons in the dentate gyrus (Seri, and Alvarez-Buylla, 2002). Previously, Alvarez-Buylla's group had identified two types of dividing cell by their morphology and activity; small, simple, rapidly dividing cells (D cells) and larger, slowly dividing

cells with a radial process (B cells)(Seri, et al., 2001). By selectively killing mitotic cells, and then allowing cell division to return Seri found the SGZ astrocytes (B cells) were the first dividing cells to recommence division (after 2 days) and that D cell division resumed by about 4 days, with new neurons detected at 8 days. Detection of alkaline phosphatase activity in BrdU positive neurons of mice, where retroviral labelling had coupled alkaline phosphatase synthesis to the GFAP promoter supported the genesis of neurons from the SGZ astrocytes (B cells), although the involvement of the D cells could not be established in this paradigm (Seri, et al., 2001).
Using a different method, our transgenic mouse experiments confirmed Seri's findings, establishing that some cells with an astrocytic heritage also have neurogenic properties, by co-localising faintly EGFP positive cells markers for neuroblasts (TUC-4 and PSA-NCAM). This observation coupled with the detected increase in SGZ astrocyte proliferation after seizure strongly support the hypothesis that these are the quiescent or slowly dividing population of cells that the clonal labelling studies predicted would be activated by seizures.

The experiments carried out in the cultures also appear to concur with the experiments of Seri, who used cytosine-β-D-arabinofuranoside and procarbazol treatment to kill dividing cells, eliminating proliferation, and then observed a slow recovery when the anti-mitotic cocktail was removed. Our culture experiments were not specifically designed to eliminate dividing cells, however a rapid phase of cell death was induced by kainate, in the SGZ, where the where the progenitor cells are known to reside (Altman and Das, 1965) in our culture model. The cell death was followed by a significant attenuation of proliferation, and a later recovery to initial levels. Although our culture experiments fail to demonstrate a direct causative link between the cell death and the decreased proliferation the independent observation that selective loss of proliferating cells produces a similar drop in proliferation followed by a recovery along a similar timescale is a persuasive argument in support of this theory.

The difference in detected cell death between the *in vitro* and *in vivo* models used in the studies is important, and requires explanation, as all the seizure experiments described here used the same chemoconvulsant; kainate. The observed differences probably arise from a combination of two factors, the age of the tissue and the method

of application. In adult tissue, IP kainate injection causes some granule cell death, and ICV injection causes very little granule cell death (Nadler, 1981). Kainate administration to perinatal tissue can cause a brief phase of cell death with a subsequent desensitisation mediated by decreased kainate receptor density (Tandon, et al., 2002). The observations of Tandon agree well with our findings, where in the immature OHSC study cell death was detected early after seizure and then declined. The absence of detected cell death contralateral to unilateral ICV kainate injection also fits with the observations of Nadler, however we detected some cell death in the dentates ipsilateral to kainite injection in this study. Although Nadler reported some cell death this was not considered significant, the reasons for differences may lie in the different methods used to detect the cell death, our study involved measuring an area of fluorescence above threshold, and not counting cell bodies. At later times this could lead to over estimation of cell death due to detection of inputs into the granule cell layer from cells in the hilus, as FJB detects synapses and processes in addition to the soma of dead cells. However the slight decrease (not significant) in BrdU pre-labelled cell counts between time 0 controls and 6 hours post kainate could indicate a small contribution of cell progenitor cell death, similar to that observed in the cultures.

The reported and observed differences in cell death between adult and immature tissue in response to seizures also raises questions about the proliferative responses in these two tissue types. The immature SGZ is also a more actively proliferative environment than the adult SGZ, which might complicate comparison between the adult and neo-natal tissue. However, analysis of gene expression profiles during development and after seizure induction has identified a large numbers of genes, including Neuro D,with known neurogenic properties common to both groups, indicating that the proliferative machinery is conserved from young to aged animals (Elliott, et al., 2003). Basic fibroblast growth factor (FGF) is also among these genes, Yoshimura demonstrated that increased proliferation after seizures was significantly attenuated in adult mice lacking the FGF-2 gene, compared with wild-type littermates. This attenuation was reversed by FGF-2 gene transfer via a viral vector (Yoshimura, et al., 2001). Application of subcutaneous FGF increases proliferation in both adult and immature rats (Wagner, et al., 1999), further supporting conserved control mechanisms of cell proliferation from development through to adult life.

The existence of a quiescent stem cell population in the SGZ of the dentate gyrus is hinted at by several studies. Neurogenesis decreases with increasing age and Cameron et al. demonstrated that this age related decrease in neurogenesis could be abolished by adrenalectomy, with young and aged rats having significantly increased and similar levels of neurogenesis after the adrenalectomy (Cameron and McKay, 1999). Gray et al. found that while aged rats had significantly lower neurogenesis than young animals, after seizures both young and old animals demonstrated neurogenesis that had increased to the same level, with no difference between them (Gray, et al., 2002). However, a report by Seaberg and van Der Kooy appeared to indicate that true stem cells are not present in the dentate gyrus, postulating instead the presence of progenitor cells capable of only a limited number of divisions before terminal differentiation, since this could explain the decrease in neurogenesis observed with age (Seaberg and van Der, 2002). Seaberg's study was carried out on primary dissociated cell culture. In contrast, the studies of Gray et al., and Cameron and McKay were *in vivo*. Additionally, a separate study in primary dissociated cell culture demonstrated that a culture of GFAP positive cells can fulfil the requirements stipulated for definition as stem cells, they can self-replicate, produce intermediate partially fate specified neurospheres, which will then give rise to cells of multiple phenotypes, and interestingly the progress through these states is regulated by the extracellular milieu (Imura, et al., 2003).

Our study extends the results of a previous study (Nacher, et al., 2001) which showed a greater number of radial glia-like cells 7 and 21 days after NMDA receptor blockade-induced cell proliferation and neurogenesis, revealing that radial glia-like astrocytes proliferate earlier, before the newly generated cells express neuronal markers, further supporting their role as precursor cells Seri, et al., 2001). Due to their increased number, our data also indicate that these radial glia-like cells are initially recruited to divide symmetrically, early after seizure induction, although further experiments are needed to directly prove this assumption.

The "dedifferentiation" and proliferation of Muller Glia after neurotoxic damage has been reported in the chicken retina (Fischer and Reh, 2001) with the generation of new neurons and glia, although the majority of newly produced cells remain

undifferentiated. This has interesting parallels with our organotypic slice culture experiments and with our EGFP positive radial glia-like proliferation after kainate induced damage. The proliferative response of Muller Glia appears to be mediated by FGF2 and insulin (Fischer, et al., 2002). The control of radial glia like cell proliferation in the dentate gyrus remains unknown but as noted above, FGF2 and Insulin are both important growth factors for SGZ proliferation and neurogenesis. Future work will concentrate on identifying the salient growth factors for radial glia-like cell proliferation. We identified three subpopulations of cells with radial glial like morphology and expressing astrocytic markers based on GFAP-(EGFP) and S100β staining. The EGFP and S100β positive cells appeared largely separate but the interesting phenomenon was the increase in EGFP + S100β co-localised radial glia like cells after kainate induced seizures/damage. Filippov et al have identified nestin positive cells with radial glia like morphology in the dentate SGZ, a proportion of which expressed sodium channels and membrane current patterns of an immature neuronal phenotype (Filippov, et al., 2003). Although we did not stain for nestin after kainate as kainate is known to induce nestin expression in hippocampal astrocytes, it is intriguing to speculate that radial glial like cells expressing astrocytic markers are not a homogenous population and their differing immunohistochemical signatures may reflect different stages in neuronal and or proliferative commitment.

In conclusion, the work presented here has provided evidence to confirm the identity of a previously reported slowly dividing stem cell population in the dentate gyrus, and established that these cells are central to the increased neurogenesis observed in response to kainate induced seizures.

References

Aberg MA, Aberg ND, Hedbacker H, Oscarsson J, and Eriksson PS. 2000. Peripheral infusion of IGF-I selectively induces neurogenesis in the adult rat hippocampus. J Neurosci 20:2896-2903.

Abrous DN, Adriani W, Montaron MF, Aurousseau C, Rougon G, Le Moal M, and Piazza PV. 2002. Nicotine self-administration impairs hippocampal plasticity. J Neurosci 22:3656-3662.

Abrous DN, Montaron MF, Petry KG, Rougon G, Darnaudery M, Le Moal M, and Mayo W. 1997. Decrease in highly polysialylated neuronal cell adhesion molecules and in spatial learning during ageing are not correlated. Brain Research 744:285-292.

Adamchik Y, Frantseva MV, Weisspapir M, Carlen PL, and Perez Velazquez JL. 2000. Methods to induce primary and secondary traumatic damage in organotypic hippocampal slice cultures. Brain Res Brain Res Protoc 5:153-158.

Albensi BC. 2001. Models of brain injury and alterations in synaptic plasticity. J Neurosci Res 65:279-283.

Altman J and Bayer SA. 1990a. Migration and distribution of two populations of hippocampal granule cell precursors during the perinatal and postnatal periods. J Comp Neurol 301:365-381.

Altman J and Bayer SA. 1990b. Mosaic organization of the hippocampal neuroepithelium and the multiple germinal sources of dentate granule cells. J Comp Neurol 301:325-342.

Altman J and Bayer SA. 1990c. Prolonged sojourn of developing pyramidal cells in the intermediate zone of the hippocampus and their settling in the stratum pyramidale. J Comp Neurol 301:343-364.

Altman J and Das GD. 1965. Post-natal origin of microneurones in the rat brain. Nature 207:953-956.

Alvarez-Buylla A, Seri B, and Doetsch F. 2002. Identification of neural stem cells in the adult vertebrate brain. Brain Res Bull 57:751-758.

Arvidsson A, Kokaia Z, and Lindvall O. 2001. N-methyl-D-aspartate receptor-mediated increase of neurogenesis in adult rat dentate gyrus following stroke. Eur J Neurosci 14:10-18.

Banasr M, Hery M, Brezun JM, and Daszuta A. 2001. Serotonin mediates oestrogen stimulation of cell proliferation in the adult dentate gyrus. Eur J Neurosci 14:1417-1424.

Barnea A and Nottebohm F. 1994. Seasonal Recruitment of Hippocampal Neurons in Adult Free-Ranging Black-Capped Chickadees. PNAS 91:11217-11221.

Bayer SA. 1980. Development of the hippocampal region in the rat. I. Neurogenesis examined with 3H-thymidine autoradiography. J Comp Neurol 190:87-114.

Bengzon J, Kokaia Z, Elmer E, Nanobashvili A, Kokaia M, and Lindvall O. 1997. Apoptosis and proliferation of dentate gyrus neurons after single and intermittent limbic seizures. Proc Natl Acad Sci U S A 94:10432-10437.

Bennett DA, Lehmann J, Bernard PS, Liebman JM, Williams M, Wood PL, Boast CA, and Hutchison AJ. 1990. CGS 19755: a novel competitive N-methyl-D-aspartate (NMDA) receptor antagonist with anticonvulsant, anxiolytic and anti-ischemic properties. Prog Clin Biol Res 361:519-524.

Best N, Mitchell J, Baimbridge KG, and Wheal HV. 1993. Changes in parvalbumin-immunoreactive neurons in the rat hippocampus following a kainic acid lesion. Neurosci Lett 155:1-6.

Best N, Sundstrom LE, Mitchell J, and Wheal HV. 1996. Pre-exposure to subtoxic levels prevents kainic acid lesions in organotypic hippocampal slice cultures: effects of kainic acid on parvalbumin-immunoreactive neurons and expression of heat shock protein 72 following the induction of tolerance. Eur J Neurosci 8:1209-1219.

Biebl M, Cooper CM, Winkler J, and Kuhn HG. 2000. Analysis of neurogenesis and programmed cell death reveals a self- renewing capacity in the adult rat brain. Neurosci Lett 291:17-20.

Blumcke I, Schewe JC, Normann S, Brustle O, Schramm J, Elger CE, and Wiestler OD. 2001. Increase of nestin-immunoreactive neural precursor cells in the dentate gyrus of pediatric patients with early-onset temporal lobe epilepsy. Hippocampus 11:311-321.

Bonfoco E, Krainc D, Ankarcrona M, Nicotera P, and Lipton SA. 1995. Apoptosis and necrosis: two distinct events induced, respectively, by mild and intense insults with N-methyl-D-aspartate or nitric oxide/superoxide in cortical cell cultures. Proc Natl Acad Sci U S A 92:7162-7166.

Bouilleret V, Ridoux V, Depaulis A, Marescaux C, Nehlig A, and Gal La Salle G. 1999. Recurrent seizures and hippocampal sclerosis following intrahippocampal kainate injection in adult mice: electroencephalography, histopathology and synaptic reorganization similar to mesial temporal lobe epilepsy. Neuroscience 89:717-729.

Brewer GJ. 1995. Serum-free B27/neurobasal medium supports differentiated growth of neurons from the striatum, substantia nigra, septum, cerebral cortex, cerebellum, and dentate gyrus. J Neurosci Res 42:674-683.

Brewer GJ. 1997. Isolation and culture of adult rat hippocampal neurons. J Neurosci Methods 71:143-155.

Brewer GJ, Torricelli JR, Evege EK, and Price PJ. 1993. Optimized survival of hippocampal neurons in B27-supplemented Neurobasal, a new serum-free medium combination. J Neurosci Res 35:567-576.

Brezun JM and Daszuta A. 1999. Depletion in serotonin decreases neurogenesis in the dentate gyrus and the subventricular zone of adult rats. Neuroscience 89:999-1002.

Brezun JM and Daszuta A. 2000. Serotonin may stimulate granule cell proliferation in the adult hippocampus, as observed in rats grafted with foetal raphe neurons. Eur J Neurosci 12:391-396.

Brott DA, Alvey JD, Bleavins MR, de la Iglesia FA, and Lalwani ND. 1993. Cell cycle dependent distribution of proliferating cell nuclear antigen/cyclin and cdc2-kinase in mouse T-lymphoma cells. J Cell Biochem 52:362-372.

Cameron HA, McEwen BS, and Gould E. 1995. Regulation of adult neurogenesis by excitatory input and NMDA receptor activation in the dentate gyrus. J Neurosci 15:4687-4692.

Cameron HA and McKay RD. 1999. Restoring production of hippocampal neurons in old age. Nat Neurosci 2:894-897.

Cameron HA and McKay RD. 2001. Adult neurogenesis produces a large pool of new granule cells in the dentate gyrus. J Comp Neurol 435:406-417.

Cameron HA, Woolley CS, McEwen BS, and Gould E. 1993. Differentiation of newly born neurons and glia in the dentate gyrus of the adult rat. Neuroscience 56:337-344.

Capela A and Temple S. 2002. LeX/ssea-1 is expressed by adult mouse CNS stem cells, identifying them as nonependymal. Neuron 35:865-875.

Cater HL, Benham CD, and Sundstrom LE. 2001. Neuroprotective role of monocarboxylate transport during glucose deprivation in slice cultures of rat hippocampus. J Physiol 531:459-466.

Chirumamilla S, Sun D, Bullock MR, and Colello RJ. 2002. Traumatic brain injury induced cell proliferation in the adult mammalian central nervous system. J Neurotrauma 19:693-703.

Clarke SR, Shetty AK, Bradley JL, and Turner DA. 1994. Reactive astrocytes express the embryonic intermediate neurofilament nestin. Neuroreport 5:1885-1888.

Conti L, Sipione S, Magrassi L, Bonfanti L, Rigamonti D, Pettirossi V, Peschanski M, Haddad B, Pelicci P, Milanesi G, Pelicci G, and Cattaneo E. 2001. Shc signaling in differentiating neural progenitor cells. Nat Neurosci 4:579-586.

Cooper-Kuhn CM and Georg Kuhn H. 2002. Is it all DNA repair?: Methodological considerations for detecting neurogenesis in the adult brain. Developmental Brain Research 134:13-21.

Corbo JC, Deuel TA, Long JM, LaPorte P, Tsai E, Wynshaw-Boris A, and Walsh CA. 2002. Doublecortin Is Required in Mice for Lamination of the Hippocampus But Not the Neocortex. J Neurosci 22:7548.

Covolan L, Ribeiro LT, Longo BM, and Mello LE. 2000. Cell damage and neurogenesis in the dentate granule cell layer of adult rats after pilocarpine- or kainate-induced status epilepticus. Hippocampus 10:169-180.

Covolan L, Smith RL, and Mello LE. 2000. Ultrastructural identification of dentate granule cell death from pilocarpine-induced seizures. Epilepsy Res 41:9-21.

Crespel A, Coubes P, Rousset MC, Brana C, Rougier A, Rondouin G, Bockaert J, Baldy-Moulinier M, and Lerner-Natoli M. 2002. Inflammatory reactions in human medial temporal lobe epilepsy with hippocampal sclerosis. Brain Research 952:159-169.

D'Sa-Eipper C, Leonard JR, Putcha G, Zheng TS, Flavell RA, Rakic P, Kuida K, and Roth KA. 2001. DNA damage-induced neural precursor cell apoptosis requires p53 and caspase 9 but neither Bax nor caspase 3. Development 128:137-146.

Dash PK, Mach SA, and Moore AN. 2001. Enhanced neurogenesis in the rodent hippocampus following traumatic brain injury. J Neurosci Res 63:313-319.

Dayer AG, Ford AA, Cleaver KM, Yassaee M, and Cameron HA. 2003. Short-term and long-term survival of new neurons in the rat dentate gyrus. J Comp Neurol 460:563-572.

Del Bigio MR. 1999. Proliferative status of cells in adult human dentate gyrus. Microsc Res Tech 45:353-358.

Del Rio JA, Heimrich B, Soriano E, Schwegler H, and Frotscher M. 1991. Proliferation and differentiation of glial fibrillary acidic protein- immunoreactive glial cells in organotypic slice cultures of rat hippocampus. Neuroscience 43:335-347.

Delatour B and Witter MP. 2002. Projections from the parahippocampal region to the prefrontal cortex in the rat: evidence of multiple pathways. Eur J Neurosci 15:1400-1407.

Derrick BE, York AD, and Martinez JL, Jr. 2000. Increased granule cell neurogenesis in the adult dentate gyrus following mossy fiber stimulation sufficient to induce long-term potentiation. Brain Res 857:300-307.

Des P, V, Pinard JM, Billuart P, Vinet MC, Koulakoff A, Carrie A, Gelot A, Dupuis E, Motte J, Berwald-Netter Y, Catala M, Kahn A, Beldjord C, and Chelly J. 1998. A novel CNS gene required for neuronal migration and involved in X- linked subcortical laminar heterotopia and lissencephaly syndrome. Cell 92:51-61.

Dikranian K, Ishimaru MJ, Tenkova T, Labruyere J, Qin YQ, Ikonomidou C, and Olney JW. 2001. Apoptosis in the in vivo mammalian forebrain. Neurobiol Dis 8:359-379.

Doetsch F, Caille I, Lim DA, Garcia-Verdugo JM, and Alvarez-Buylla A. 1999. Subventricular zone astrocytes are neural stem cells in the adult mammalian brain. Cell 97:703-716.

Doetsch F, Garcia-Verdugo JM, and Alvarez-Buylla A. 1999. Regeneration of a germinal layer in the adult mammalian brain. Proc Natl Acad Sci U S A 96:11619-11624.

Doetsch F, Petreanu L, Caille I, Garcia-Verdugo JM, and Alvarez-Buylla A. 2002. EGF converts transit-amplifying neurogenic precursors in the adult brain into multipotent stem cells. Neuron 19;36:1021-1034.

Donato R. 1999. Functional roles of S100 proteins, calcium-binding proteins of the EF- hand type. Biochim Biophys Acta 1450:191-231.

Dong H, Csernansky CA, Goico B, and Csernansky JG. 2003. Hippocampal Neurogenesis Follows Kainic Acid-Induced Apoptosis in Neonatal Rats. J Neurosci 23:1742.

Duman RS, Heninger GR, and Nestler EJ. 1997. A molecular and cellular theory of depression. Arch Gen Psychiatry 54:597-606.

During MJ and Spencer DD. 1993. Extracellular hippocampal glutamate and spontaneous seizure in the conscious human brain. Lancet 341:1607-1610.

Earnshaw WC, Martins LM, and Kaufmann SH. 1999. MAMMALIAN CASPASES: Structure, Activation, Substrates, and Functions During Apoptosis. Annu Rev Biochem 68:383.

Ekdahl CT, Mohapel P, Elmer E, and Lindvall O. 2001. Caspase inhibitors increase short-term survival of progenitor-cell progeny in the adult rat dentate gyrus following status epilepticus. Eur J Neurosci 14:937-945.

Elliott RC, Miles MF, and Lowenstein DH. 2003. Overlapping Microarray Profiles of Dentate Gyrus Gene Expression during Development- and Epilepsy-Associated Neurogenesis and Axon Outgrowth. J Neurosci 23:2218.

Eriksson PS, Perfilieva E, Bjork-Eriksson T, Alborn AM, Nordborg C, Peterson DA, and Gage FH. 1998. Neurogenesis in the adult human hippocampus. Nat Med 4:1313-1317.

Fanarraga ML, Avila J, and Zabala JC. 1999. Expression of unphosphorylated class III beta-tubulin isotype in neuroepithelial cells demonstrates neuroblast commitment and differentiation. Eur J Neurosci 11:517-527.

Filippov V, Kronenberg G, Pivneva T, Reuter K, Steiner B, Wang LP, Yamaguchi M, Kettenmann H, and Kempermann G. 2003. Subpopulation of nestin-expressing progenitor cells in the adult murine hippocampus shows electrophysiological and morphological characteristics of astrocytes. Molecular and Cellular Neuroscience 23:373-382.

Fuchs E and Gould E. 2000. Mini-review: in vivo neurogenesis in the adult brain: regulation and functional implications. Eur J Neurosci 12:2211-2214.

Fujikawa DG, Shinmei SS, and Cai B. 2000. Kainic acid-induced seizures produce necrotic, not apoptotic, neurons with internucleosomal DNA cleavage: implications for programmed cell death mechanisms. Neuroscience 98:41-53.

Fischer AJ, McGuire CR, Dierks BD, and Reh TA. 2002. Insulin and Fibroblast Growth Factor 2 Activate a Neurogenic Program in Müller Glia of the Chicken Retina J Neurosci 22:9387-9398.

Fischer AJ, Reh TA. 2001. Muller glia are a potential source of neural regeneration in the postnatal chicken retina. Nat Neurosci 4:247-52.

Gahwiler BH, Capogna M, Debanne D, McKinney RA, and Thompson SM. 1997. Organotypic slice cultures: a technique has come of age. Trends in Neurosciences 20:471-477.

Gatherer M and Sundstrom LE. 1998. Mossy fibre innervation is not required for the development of kainic acid toxicity in organotypic hippocampal slice cultures. Neurosci Lett 253:119-122.

Goldman SA. 1998. Adult neurogenesis: from canaries to the clinic. J Neurobiol 36:267-286.

Gould E, Beylin A, Tanapat P, Reeves A, and Shors TJ. 1999. Learning enhances adult neurogenesis in the hippocampal formation. Nat Neurosci 2:260-265.

Gould E, Cameron HA, and McEwen BS. 1994. Blockade of NMDA receptors increases cell death and birth in the developing rat dentate gyrus. J Comp Neurol 340:551-565.

Gould E and Tanapat P. 1997. Lesion-induced proliferation of neuronal progenitors in the dentate gyrus of the adult rat. Neuroscience 80:427-436.

Gould E, Tanapat P, Rydel T, and Hastings N. 2000. Regulation of hippocampal neurogenesis in adulthood. Biol Psychiatry 48:715-720.

Gould E and Tanapat P. 1999. Stress and hippocampal neurogenesis. Biological Psychiatry 46:1472-1479.

Gould E, Tanapat P, McEwen BS, Flugge G, and Fuchs E. 1998. Proliferation of granule cell precursors in the dentate gyrus of adult monkeys is diminished by stress. PNAS 95:3168-3171.

Gould E. 2002. Federation of European Neuroscience Societies Conference abstract.

Gray WP, May K, and Sundstrom LE. 2002. Seizure induced dentate neurogenesis does not diminish with age in rats. Neuroscience Letters 330:235-238.

Gray WP and Sundstrom LE. 1998. Kainic acid increases the proliferation of granule cell progenitors in the dentate gyrus of the adult rat. Brain Res 790:52-59.

Guillery RW and Herrup K. 1997. Quantification without pontification: choosing a method for counting objects in sectioned tissues. J Comp Neurol 386:2-7.

Hailer NP, Grampp A, and Nitsch R. 1999. Proliferation of microglia and astrocytes in the dentate gyrus following entorhinal cortex lesion: a quantitative bromodeoxyuridine- labelling study. Eur J Neurosci 11:3359-3364.

Hastings NB, Tanapat P, and Gould E. 2001. Neurogenesis in the adult mammalian brain. Clinical Neuroscience Research 1:175-182.

Haydar TF, Bambrick LL, Krueger BK, and Rakic P. 1999. Organotypic slice cultures for analysis of proliferation, cell death, and migration in the embryonic neocortex. Brain Research Protocols 4:425-437.

Hayes NL and Nowakowski RS. 2002. Dynamics of cell proliferation in the adult dentate gyrus of two inbred strains of mice. Developmental Brain Research 134:77-85.

Heins N, Malatesta P, Cecconi F, Nakafuku M, Tucker KL, Hack MA, Chapouton P, Barde YA, and Gotz M. 2002. Glial cells generate neurons: the role of the transcription factor Pax6. Nat Neurosci 5:308-315.

Hidalgo A, Barami K, Iversen K, and Goldman SA. 1995. Estrogens and non-estrogenic ovarian influences combine to promote the recruitment and decrease the turnover of new neurons in the adult female canary brain. J Neurobiol 27:470-487.

Hopkins KJ, Wang GJ, and Schmued LC. 2000. Temporal progression of kainic acid induced neuronal and myelin degeneration in the rat forebrain. Brain Research 864:69-80.

Houser CR. 1990. Granule cell dispersion in the dentate gyrus of humans with temporal lobe epilepsy. Brain Research 535:195-204.

Imura T, Kornblum HI, and Sofroniew MV. 2003. The predominant neural stem cell isolated from postnatal and adult forebrain but not early embryonic forebrain expresses GFAP. J Neurosci 23:2824-2832.

Ivanova NB, Dimos JT, Schaniel C, Hackney JA, Moore KA, and Lemischka IR. 2002. A Stem Cell Molecular Signature. Science1073823.

Jin K, Minami M, Lan JQ, Mao XO, Batteur S, Simon RP, and Greenberg DA. 2001. Neurogenesis in dentate subgranular zone and rostral subventricular zone after focal cerebral ischemia in the rat. Proc Natl Acad Sci U S A 98:4710-4715.

Kee N, Sivalingam S, Boonstra R, and Wojtowicz JM. 2002. The utility of Ki-67 and BrdU as proliferative markers of adult neurogenesis. J Neurosci Methods 115:97-105.

Kempermann G and Gage FH. 2002. Genetic determinants of adult hippocampal neurogenesis correlate with acquisition, but not probe trial performance, in the water maze task. Eur J Neurosci 16:129-136.

Kempermann G, Kuhn HG, and Gage FH. 1997. More hippocampal neurons in adult mice living in an enriched environment. Nature 386:493-495.

Kempermann G, Kuhn HG, and Gage FH. 1998. Experience-induced neurogenesis in the senescent dentate gyrus. J Neurosci 18:3206-3212.

Kempermann G, Gast D, Kronenberg G, Yamaguchi M, and Gage FH. 2003. Early determination and long-term persistence of adult-generated new neurons in the hippocampus of mice. Development 130:391-399.

Kernie SG, Erwin TM, and Parada LF. 2001. Brain remodeling due to neuronal and astrocytic proliferation after controlled cortical injury in mice. J Neurosci Res 66:317-326.

Kondratyev A, Sahibzada N, and Gale K. 2001. Electroconvulsive shock exposure prevents neuronal apoptosis after kainic acid-evoked status epilepticus. Brain Res Mol Brain Res 91:1-13.

Kornack DR and Rakic P. 1999. Continuation of neurogenesis in the hippocampus of the adult macaque monkey. PNAS 96:5768-5773.

Kristian T and Siesjo BK. 1998. Calcium in ischemic cell death. Stroke 29:705-718.

Kuan CY, Roth KA, Flavell RA, and Rakic P. 2000. Mechanisms of programmed cell death in the developing brain. Trends Neurosci 23:291-297.

Kuhn HG, Dickinson-Anson H, and Gage FH. 1996. Neurogenesis in the dentate gyrus of the adult rat: age-related decrease of neuronal progenitor proliferation. J Neurosci 16:2027-2033.

Lee MK, Rebhun LI, and Frankfurter A. 1990. Posttranslational Modification of Class III {beta}-Tubulin. PNAS 87:7195.

Leite JP, Garcia-Cairasco N, and Cavalheiro EA. 2002. New insights from the use of pilocarpine and kainate models. Epilepsy Research 50:93-103.

Lemaire V, Koehl M, Le Moal M, and Abrous DN. 2000. Prenatal stress produces learning deficits associated with an inhibition of neurogenesis in the hippocampus. Proc Natl Acad Sci U S A 97:11032-11037.

Lendahl U, Zimmerman LB, and McKay RD. 1990. CNS stem cells express a new class of intermediate filament protein. Cell 60:585-595.

Lewis PD. 1978. Kinetics of cell proliferation in the postnatal rat dentate gyrus. Neuropathol Appl Neurobiol 4:191-195.

Li M, Pevny L, Lovell-Badge R, and Smith A. 1998. Generation of purified neural precursors from embryonic stem cells by lineage selection. Curr Biol 8:971-974.

Lin RCS and Matesic DF. 1994. Immunohistochemical demonstration of neuron-specific enolase and microtubule-associated protein 2 in reactive astrocytes after injury in the adult forebrain. Neuroscience 60:11-16.

Lipton SA and Nicotera P. 1998. Calcium, free radicals and excitotoxins in neuronal apoptosis. Cell Calcium 23:165-171.

Liu J, Solway K, Messing RO, and Sharp FR. 1998. Increased neurogenesis in the dentate gyrus after transient global ischemia in gerbils. J Neurosci 18:7768-7778.

Liu M, Pleasure SJ, Collins AE, Noebels JL, Naya FJ, Tsai MJ, and Lowenstein DH. 2000. Loss of BETA2/NeuroD leads to malformation of the dentate gyrus and epilepsy. PNAS 97:865.

Lowenstein DH and Arsenault L. 1996. The effects of growth factors on the survival and differentiation of cultured dentate gyrus neurons. J Neurosci 16:1759-1769.

Lukaszewicz A, Savatier P, Cortay V, Kennedy H, and Dehay C. 2002. Contrasting Effects of Basic Fibroblast Growth Factor and Neurotrophin 3 on Cell Cycle Kinetics of Mouse Cortical Stem Cells. J Neurosci 22:6610-6622.

Lurton D, El Bahh B, Sundstrom L, and Rougier A. 1998. Granule cell dispersion is correlated with early epileptic events in human temporal lobe epilepsy. Journal of the Neurological Sciences 154:133-136.

Lurton D, Sundstrom L, Brana C, Bloch B, and Rougier A. 1997. Possible mechanisms inducing granule cell dispersion in humans with temporal lobe epilepsy. Epilepsy Research 26:351-361.

Madsen TM, Treschow A, Bengzon J, Bolwig TG, Lindvall O, and Tingstrom A. 2000. Increased neurogenesis in a model of electroconvulsive therapy. Biol Psychiatry 47:1043-1049.

Malatesta P, Hack MA, Hartfuss E, Kettenmann H, Klinkert W, Kirchhoff F, and Gotz M. 2003. Neuronal or glial progeny: regional differences in radial glia fate. Neuron 37:751-764.

Malatesta P, Hartfuss E, and Gotz M. 2000. Isolation of radial glial cells by fluorescent-activated cell sorting reveals a neuronal lineage. Development 127:5253-5263.

Malberg JE, Eisch AJ, Nestler EJ, and Duman RS. 2000. Chronic antidepressant treatment increases neurogenesis in adult rat hippocampus. J Neurosci 20:9104-9110.

Manabat C, Han BH, Wendland M, Derugin N, Fox CK, Choi J, Holtzman DM, Ferriero DM, and Vexler ZS. 2003. Reperfusion differentially induces caspase-3 activation in ischemic core and penumbra after stroke in immature brain. Stroke 34:207-213.

Mathern GW, Leiphart JL, De Vera A, Adelson PD, Seki T, Neder L, and Leite JP. 2002. Seizures decrease postnatal neurogenesis and granule cell development in the human fascia dentata. Epilepsia 43 Suppl 5:68-73.

McAdory BS, Van Eldik LJ, and Norden JJ. 1998. S100B, a neurotropic protein that modulates neuronal protein phosphorylation, is upregulated during lesion-induced collateral sprouting and reactive synaptogenesis. Brain Res 813:211-217.

McCabe BK, Silveira DC, Cilio MR, Cha BH, Liu X, Sogawa Y, and Holmes GL. 2001. Reduced Neurogenesis after Neonatal Seizures. J Neurosci 21:2094-2103.

McEwen BS. 1999. Stress and hippocampal plasticity. Annu Rev Neurosci 22:105-122.

McIntyre DC, Poulter MO, and Gilby K. 2002. Kindling: some old and some new. Epilepsy Research 50:79-92.

Mikkonen M, Soininen H, Kalvianen R, Tapiola T, Ylinen A, Vapalahti M, Paljarvi L, and Pitkanen A. 1998. Remodeling of neuronal circuitries in human temporal lobe epilepsy: increased expression of highly polysialylated neural cell adhesion molecule in the hippocampus and the entorhinal cortex. Ann Neurol 44:923-934.

Montaron MF, Petry KG, Rodriguez JJ, Marinelli M, Aurousseau C, Rougon G, Le Moal M, and Abrous DN. 1999. Adrenalectomy increases neurogenesis but not PSA-NCAM expression in aged dentate gyrus. Eur J Neurosci 11:1479-1485.

Moscovitch DA and McAndrews MP. 2002. Material-specific deficits in "remembering" in patients with unilateral temporal lobe epilepsy and excisions. Neuropsychologia 40:1335-1342.

Nacher J, Crespo C, and McEwen BS. 2001. Doublecortin expression in the adult rat telencephalon. Eur J Neurosci 14:629-644.

Nacher J, Rosell DR, Alonso-Llosa G, and McEwen BS. 2001. NMDA receptor antagonist treatment induces a long-lasting increase in the number of proliferating cells, PSA-NCAM-immunoreactive granule neurons and radial glia in the adult rat dentate gyrus. Eur J Neurosci 13:512-520.

Nadler JV. 1981. Minireview. Kainic acid as a tool for the study of temporal lobe epilepsy. Life Sci 29:2031-2042.

Nadler JV, Perry BW, and Cotman CW. 1978. Preferential vulnerability of hippocampus to intraventricular kainic acid. In McGeer EG, editor. Kainic acid as a tool in Neurobiology. New York: Raven Press. p 219-237.

Nadler JV, Shelton DL, Perry BW, and Cotman CW. 1980. Regional distribution of [3H]kainic acid after intraventricular injection. Life Sci 26:133-138.

Nagatomo I, Akasaki Y, Uchida M, Tominaga M, Hashiguchi W, Kuchiiwa S, Nakagawa S, and Takigawa M. 2000. Age-related alterations of nitric oxide production in the brains of seizure-susceptible EL mice. Brain Research Bulletin 53:301-306.

Nakagawa E, Aimi Y, Yasuhara O, Tooyama I, Shimada M, McGeer PL, and Kimura H. 2000. Enhancement of progenitor cell division in the dentate gyrus triggered by initial limbic seizures in rat models of epilepsy. Epilepsia 41:10-18.

Nakic M, Manahan-Vaughan D, Reymann KG, and Schachner M. 1998. Long-term potentiation in vivo increases rat hippocampal tenascin-C expression. J Neurobiol 37:393-404.

Nestor PJ, Graham KS, Bozeat S, Simons JS, and Hodges JR. 2002. Memory consolidation and the hippocampus: further evidence from studies of autobiographical memory in semantic dementia and frontal variant frontotemporal dementia. Neuropsychologia 40:633-654.

Nicotera P and Lipton SA. 1999. Excitotoxins in neuronal apoptosis and necrosis. J Cereb Blood Flow Metab 19:583-591.

Nijhawan D, Honarpour N, and Wang X. 2000. Apoptosis in neural development and disease. Annu Rev Neurosci 23:73-87.

Noctor SC, Flint AC, Weissman TA, Wong WS, Clinton BK, and Kriegstein AR. 2002. Dividing precursor cells of the embryonic cortical ventricular zone have morphological and molecular characteristics of radial glia. J Neurosci 22:3161-3173.

Nolte C, Matyash M, Pivneva T, Schipke CG, Ohlemeyer C, Hanisch UK, Kirchhoff F, and Kettenmann H. 2001. GFAP promoter-controlled EGFP-expressing transgenic mice: a tool to visualize astrocytes and astrogliosis in living brain tissue. Glia 33:72-86.

Nowakowski RS, Lewin SB, and Miller MW. 1989. Bromodeoxyuridine immunohistochemical determination of the lengths of the cell cycle and the DNA-synthetic phase for an anatomically defined population. J Neurocytol 18:311-318.

Nowakowski RS and Hayes NL. 2001. Stem Cells: The Promises and Pitfalls. Neuropsychopharmacology 25:799-804.

O'Farrell PH, Edgar BA, Lakich D, and Lehner CF. 1989. Directing Cell Division during Development. Science 246:635-640.

Palmer TD, Markakis EA, Willhoite AR, Safar F, and Gage FH. 1999. Fibroblast growth factor-2 activates a latent neurogenic program in neural stem cells from diverse regions of the adult CNS. J Neurosci 19:8487-8497.

Palmer TD, Willhoite AR, and Gage FH. 2000. Vascular niche for adult hippocampal neurogenesis. J Comp Neurol 425:479-494.

Parent JM, Tada E, Fike JR, and Lowenstein DH. 1999. Inhibition of dentate granule cell neurogenesis with brain irradiation does not prevent seizure-induced mossy fiber synaptic reorganization in the rat. J Neurosci 19:4508-4519.

Parent JM, Yu TW, Leibowitz RT, Geschwind DH, Sloviter RS, and Lowenstein DH. 1997. Dentate granule cell neurogenesis is increased by seizures and contributes to aberrant network reorganization in the adult rat hippocampus. J Neurosci 17:3727-3738.

Park C, Kang M, Kwon YK, Chung JH, Ahn H, and Huh Y. 2001. Inhibition of neuronal nitric oxide synthase enhances cell proliferation in the dentate gyrus of the adrenalectomized rat. Neuroscience Letters 309:9-12.

Pawlak R, Skrzypiec A, Sulkowski S, and Buczko W. 2002. Ethanol-induced neurotoxicity is counterbalanced by increased cell proliferation in mouse dentate gyrus. Neurosci Lett 327:83-86.

Paxinos G and Watson C. 1982. The rat brain in stereotaxic coordinates. Academic press,Inc.

Pleasure SJ, Collins AE, and Lowenstein DH. 2000. Unique Expression Patterns of Cell Fate Molecules Delineate Sequential Stages of Dentate Gyrus Development. J Neurosci 20:6095.

Pringle AK, Benham CD, Sim L, Kennedy J, Iannotti F, and Sundstrom LE. 1996. Selective N-type calcium channel antagonist omega conotoxin MVIIA is neuroprotective against hypoxic neurodegeneration in organotypic hippocampal-slice cultures. Stroke 27:2124-2130.

Pringle AK, Iannotti F, Wilde GJ, Chad JE, Seeley PJ, and Sundstrom LE. 1997. Neuroprotection by both NMDA and non-NMDA receptor antagonists in in vitro ischemia. Brain Res 755:36-46.

Quinn CC, Gray GE, and Hockfield S. 1999. A family of proteins implicated in axon guidance and outgrowth. J Neurobiol 41:158-164.

Ramalho-Santos M, Yoon S, Matsuzaki Y, Mulligan RC, and Melton DA. 2002. "Stemness": Transcriptional Profiling of Embryonic and Adult Stem Cells. Science1072530.

Rietze R, Poulin P, and Weiss S. 2000. Mitotically active cells that generate neurons and astrocytes are present in multiple regions of the adult mouse hippocampus. J Comp Neurol 424:397-408.

Rimvall K, Keller F, and Waser PG. 1987. Selective kainic acid lesions in cultured explants of rat hippocampus. Acta Neuropathol (Berl) 74:183-190.

Rivera S, Guillot S, Agassandian C, Ben Ari Y, and Khrestchatisky M. 1998. Serum deprivation-induced apoptosis in cultured hippocampi is prevented by kainate. Neuroreport 9:3949-3953.

Rodriguez JJ, Montaron MF, Petry KG, Aurousseau C, Marinelli M, Premier S, Rougon G, Le Moal M, and Abrous DN. 1998. Complex regulation of the expression of the polysialylated form of the neuronal cell adhesion molecule by glucocorticoids in the rat hippocampus. Eur J Neurosci 10:2994-3006.

Romcy-Pereira RN and Garcia-Cairasco N. 2003. Hippocampal cell proliferation and epileptogenesis after audiogenic kindling are not accompanied by mossy fiber sprouting or fluoro-jade staining. Neuroscience 119:533-546.

Rosenbaum RS, Winocur G, and Moscovitch M. 2001. New views on old memories: re-evaluating the role of the hippocampal complex. Behav Brain Res 127:183-197.

Routbort MJ, Bausch SB, and McNamara JO. 1999. Seizures, cell death, and mossy fiber sprouting in kainic acid-treated organotypic hippocampal cultures. Neuroscience 94:755-765.

Rutka JT, Murakami M, Dirks PB, Hubbard SL, Becker LE, Fukuyama K, Jung S, Tsugu A, and Matsuzawa K. 1997. Role of glial filaments in cells and tumors of glial origin: a review. Journal Of Neurosurgery 87:420-430.

Sakaguchi T, Okada M, and Kawasaki K. 1994. Sprouting of CA3 pyramidal neurons to the dentate gyrus in rat hippocampal organotypic cultures. Neurosci Res 20:157-164.

Sankar R, Shin DH, Liu H, Mazarati A, Pereira de Vasconcelos A, and Wasterlain CG. 1998. Patterns of Status Epilepticus-Induced Neuronal Injury during Development and Long-Term Consequences. J Neurosci 18:8382-8393.

Santarelli L, Saxe M, Gross C, Surget A, Battaglia F, Dulawa S, Weisstaub N, Lee J, Duman R, Arancio O, Belzung C, and Hen R. 2003. Requirement of hippocampal neurogenesis for the behavioral effects of antidepressants. Science 301:805-809.

Scharfman HE, Goodman JH, and Sollas AL. 2000. Granule-like neurons at the hilar/CA3 border after status epilepticus and their synchrony with area CA3 pyramidal cells: functional implications of seizure-induced neurogenesis. J Neurosci 20:6144-6158.

Schlessinger AR, Cowan WM, and Gottlieb DI. 1975. An autoradiographic study of the time of origin and the pattern of granule cell migration in the dentate gyrus of the rat. J Comp Neurol 159:149-175.

Schmued LC, Albertson C, and Slikker J. 1997. Fluoro-Jade: a novel fluorochrome for the sensitive and reliable histochemical localization of neuronal degeneration. Brain Research 751:37-46.

Scholzen T and Gerdes J. 2000. The Ki-67 protein: from the known and the unknown. Journal Of Cellular Physiology 182:311-322.

Schwab MH, Bartholomae A, Heimrich B, Feldmeyer D, Druffel-Augustin S, Goebbels S, Naya FJ, Zhao S, Frotscher M, Tsai MJ, and Nave KA. 2000. Neuronal basic helix-loop-helix proteins (NEX and BETA2/Neuro D) regulate terminal granule cell differentiation in the hippocampus. J Neurosci 20:3714-3724.

Seaberg RM and van Der KD. 2002. Adult rodent neurogenic regions: the ventricular subependyma contains neural stem cells, but the dentate gyrus contains restricted progenitors. J Neurosci 22:1784-1793.

Seki T. 2002a. Expression patterns of immature neuronal markers PSA-NCAM, CRMP-4 and NeuroD in the hippocampus of young adult and aged rodents. J Neurosci Res 70:327-334.

Seki T. 2002b. Hippocampal adult neurogenesis occurs in a microenvironment provided by PSA-NCAM-expressing immature neurons. J Neurosci Res 69:772-783.

Sensenbrenner M, Lucas M, and Deloulme JC. 1997. Expression of two neuronal markers, growth-associated protein 43 and neuron-specific enolase, in rat glial cells. J Mol Med 75:653-663.

Seri B, Garcia-Verdugo JM, McEwen BS, and Alvarez-Buylla A. 2001. Astrocytes give rise to new neurons in the adult mammalian hippocampus. J Neurosci 21:7153-7160.

Seri B and Alvarez-Buylla A. 2002. Neural stem cells and the regulation of neurogenesis in the adult hippocampus. Clinical Neuroscience Research 2:11-16.

Shetty AK and Turner DA. 1998. In vitro survival and differentiation of neurons derived from epidermal growth factor-responsive postnatal hippocampal stem cells: inducing effects of brain-derived neurotrophic factor. J Neurobiol 35:395-425.

Shneker BF and Fountain NB. 2003. Epilepsy. Dis Mon 49:426-478.

Shors TJ, Miesegaes G, Beylin A, Zhao M, Rydel T, and Gould E. 2001. Neurogenesis in the adult is involved in the formation of trace memories. Nature 410:372-376.

Sloviter RS, Dean E, Sollas AL, and Goodman JH. 1996. Apoptosis and necrosis induced in different hippocampal neuron populations by repetitive perforant path stimulation in the rat. J Comp Neurol 366:516-533.

Snyder JS, Kee N, and Wojtowicz JM. 2001. Effects of adult neurogenesis on synaptic plasticity in the rat dentate gyrus. J Neurophysiol 85:2423-2431.

Song HJ, Stevens CF, and Gage FH. 2002. Neural stem cells from adult hippocampus develop essential properties of functional CNS neurons. Nat Neurosci 5:438-445.

Stoppini L, Buchs PA, and Muller D. 1991. A simple method for organotypic cultures of nervous tissue. J Neurosci Methods 37:173-182.

Sundstrom LE, Mitchell J, and Wheal HV. 1993. Bilateral reorganisation of mossy fibres in the rat hippocampus after a unilateral intracerebroventricular kainic acid injection. Brain Res 609:321-326.

Tada E, Parent JM, Lowenstein DH, and Fike JR. 2000. X-irradiation causes a prolonged reduction in cell proliferation in the dentate gyrus of adult rats. Neuroscience 99:33-41.

Tanapat P, Hastings NB, Reeves AJ, and Gould E. 1999. Estrogen stimulates a transient increase in the number of new neurons in the dentate gyrus of the adult female rat. J Neurosci 19:5792-5801.

Tandon P, Yang Y, Stafstrom CE, and Holmes GL. 2002. Downregulation of kainate receptors in the hippocampus following repeated seizures in immature rats. Developmental Brain Research 136:145-150.

Temple S. 2001. The development of neural stem cells. Nature 414:112-117.

Temple S and Alvarez-Buylla A. 1999. Stem cells in the adult mammalian central nervous system. Curr Opin Neurobiol 9:135-141.

Uberti D, Piccioni L, Cadei M, Grigolato P, Rotter V, and Memo M. 2001. p53 is dispensable for apoptosis but controls neurogenesis of mouse dentate gyrus cells following [gamma]-irradiation. Molecular Brain Research 93:81-89.

van Lookeren CM, Lucassen PJ, Vermeulen JP, and Balazs R. 1995. NMDA and kainate induce internucleosomal DNA cleavage associated with both apoptotic and necrotic cell death in the neonatal rat brain. Eur J Neurosci 7:1627-1640.

van Praag H, Christie BR, Sejnowski TJ, and Gage FH. 1999. Running enhances neurogenesis, learning, and long-term potentiation in mice. Proc Natl Acad Sci U S A 96:13427-13431.

van Praag H, Schinder AF, Christie BR, Toni N, Palmer TD, and Gage FH. 2002. Functional neurogenesis in the adult hippocampus. Nature 415:1030-1034.

Vezzani A, Civenni G, Rizzi M, Monno A, Messali S, and Samanin R. 1994. Enhanced neuropeptide Y release in the hippocampus is associated with chronic seizure susceptibility in kainic acid treated rats. Brain Res 660:138-143.

Vornov JJ, Tasker RC, and Coyle JT. 1991. Direct observation of the agonist-specific regional vulnerability to glutamate, NMDA, and kainate neurotoxicity in organotypic hippocampal cultures. Exp Neurol 114:11-22.

Wagner AD. 2001. Synchronicity: when you're gone I'm lost without a trace? Nat Neurosci 4:1159-1160.

Wagner JP, Black IB, and DiCicco-Bloom E. 1999. Stimulation of neonatal and adult brain neurogenesis by subcutaneous injection of basic fibroblast growth factor. J Neurosci 19:6006-6016.

Wang KKW. 2000. Calpain and caspase: can you tell the difference? Trends in Neurosciences 23:20-26.

Wang S, Scott BW, and Wojtowicz JM. 2000. Heterogenous properties of dentate granule neurons in the adult rat. J Neurobiol 42:248-257.

Wasterlain CG, Niquet J, Thompson KW, Baldwin R, Liu H, Sankar R, Mazarati AM, Naylor D, Katsumori H, Suchomelova L, and Shirasaka Y. 2002. Seizure-induced neuronal death in the immature brain. Prog Brain Res 135:335-53.:335-353.

Wenzel HJ, Woolley CS, Robbins CA, and Schwartzkroin PA. 2000. Kainic acid-induced mossy fiber sprouting and synapse formation in the dentate gyrus of rats. Hippocampus 10:244-260.

West MJ, Slomianka L, and Gundersen HJ. 1991. Unbiased stereological estimation of the total number of neurons in thesubdivisions of the rat hippocampus using the optical fractionator. Anat Rec 231:482-497.

Wilde GJ, Sundstrom LE, and Iannotti F. 1994. Propidium iodide in vivo: an early marker of neuronal damage in rat hippocampus. Neurosci Lett 180:223-226.

Wolswijk G and Noble M. 1989. Identification of an adult-specific glial progenitor cell. Development 105:387-400.

Yagita Y, Kitagawa K, Sasaki T, Miyata T, Okano H, Hori M, and Matsumoto M. 2002. Differential expression of Musashi1 and nestin in the adult rat hippocampus after ischemia. J Neurosci Res 69:750-756.

Yan XX, Najbauer J, Woo CC, Dashtipour K, Ribak CE, and Leon M. 2001. Expression of active caspase-3 in mitotic and postmitotic cells of the rat forebrain. J Comp Neurol 433:4-22.

Yoshimura S, Takagi Y, Harada J, Teramoto T, Thomas SS, Waeber C, Bakowska JC, Breakefield XO, and Moskowitz MA. 2001. FGF-2 regulation of neurogenesis in adult hippocampus after brain injury. Proc Natl Acad Sci U S A 98:5874-5879.

Young D, Lawlor PA, Leone P, Dragunow M, and During MJ. 1999. Environmental enrichment inhibits spontaneous apoptosis, prevents seizures and is neuroprotective. Nat Med 5:448-453.

Zhang R, Zhang L, Zhang Z, Wang Y, Lu M, Lapointe M, and Chopp M. 2001. A nitric oxide donor induces neurogenesis and reduces functional deficits after stroke in rats. Ann Neurol 50:602-611.

Zhou R and Skalli O. 2000. TGF-[alpha] Differentially Regulates GFAP, Vimentin, and Nestin Gene Expression in U-373 MG Glioblastoma Cells: Correlation with Cell Shape and Motility. Experimental Cell Research 254:269-278.